Civil Engineering and Materials

ICCEM 2012

Edited by

Catalina Spataru

TRANS TECH PUBLICATIONS

Civil Engineering and Materials

Edited by
Catalina Spataru

Civil Engineering and Materials

Selected, peer reviewed papers from the
2012 International Conference on
Civil Engineering and Materials
(ICCEM 2012),
July 7-8, 2012, Paris, France

Edited by

Catalina Spataru

Trans Tech Publications Ltd
Kreuzstrasse 10
CH-8635 Durnten-Zurich
Switzerland
http://www.ttp.net

Volume 587 of
Advanced Materials Research
ISSN print 1022-6680
ISSN cd 1022-6680
ISSN web 1662-8985

Full text available online at *http://www.scientific.net*

***Distributed** worldwide by*

Trans Tech Publications Ltd
Kreuzstrasse 10
CH-8635 Durnten-Zurich
Switzerland

Fax: +41 (44) 922 10 33
e-mail: sales@ttp.net

and in the Americas by

Trans Tech Publications Inc.
PO Box 699, May Street
Enfield, NH 03748
USA

Phone: +1 (603) 632-7377
Fax: +1 (603) 632-5611
e-mail: sales-usa@ttp.net

PREFACE

Dear Distinguished Delegates and Guests,

The Organizing Committee warmly welcomes our distinguished delegates and guests to 2012 International Conference on Civil Engineering and Materials (ICCEM 2012) held during July 7-8, 2012 in Paris, France.

The conferences together report the results of research efforts in a broad range of Civil Engineering and Materials. These conferences are aimed at discussing with all of you the wide range of problems encountered in present and future high technologies. The ICCEM 2012 is organized to gather members of our international community scientists so that researchers around the world can present their leading-edge work, expanding our community's knowledge and insight into the significant challenges currently being addressed in that research.

This proceeding records the fully refereed papers presented at the conference. The main conference themes and tracks are Civil Engineering and Materials. The main goal of these events is to provide international scientific forums for exchange of new ideas in a number of fields that interact in-depth through discussions with their peers from around the world. Both inward research; core areas of Civil Engineering and Materials and outward research; multi-disciplinary, inter-disciplinary, and applications will be covered during these events.

The conference has solicited and gathered technical research submissions related to all aspects of major conference themes and tracks. All the submitted papers in the proceeding have been peer reviewed by the reviewers drawn from the scientific committee, external reviewers and editorial board depending on the subject matter of the paper. Reviewing and initial selection were undertaken electronically. After the rigorous peer-review process, the submitted papers were selected on the basis of originality, significance, and clarity for the purpose of the conference. The selected papers and additional late-breaking contributions to be presented as lectures will make an exciting technical program. The conference program is extremely rich, featuring high-impact presentations.

The high quality of the program – guaranteed by the presence of an unparalleled number of internationally recognized top experts – can be assessed when reading the contents of the program. The conference will therefore be a unique event, where attendees will be able to appreciate the latest results in their field of expertise, and to acquire additional knowledge in other fields. The program has been structured to favor interactions among attendees coming from many diverse horizons, scientifically, geographically, from academia and from industry. Included in this will to favor interactions are social events at prestigious sites.

We would like to thank the program chairs, organization staff, and the members of the program committee for their work. Thanks also go to Editors from TTP Press, for their wonderful editorial service to this proceeding. We are grateful to all those who have contributed to the success of ICCEM 2012. We hope that all participants and other interested readers benefit scientifically from the proceedings and also find it stimulating in the process. Finally, we would like to wish you success in your technical presentations and social networking.

We hope you have a unique, rewarding and enjoyable week at ICCEM 2012 in Paris of France.
With our warmest regards,

ICCEM 2012 Organizing Committees
July 7-8, 2012
Paris, France

Conference Chairs

Dr. Catalina Spataru, UCL Energy Institute, UK

Program Committee Chairs

Dr. Sa’ad P. Mansoor, School of Computer Science, College of Physical & Applied Sciences, Bangor University, UK

Prof. Ahmad K. Elshennawy, University of Central Florida, USA

Dr. Francisco Eduardo Rivera, Federal Aviation Administration, Dept. of Transportation, Air Traffic Organization, USA

Dr. Jinshan Tang, Michigan Technological University, USA

Dr. S M Sohel Murshed, University of Lisbon, Portugal

Dr. Risby Mohd Sohaimi, National Defence University Malaysia, Malaysia

Dr. S. Shantharam Patil, Manipal Institute of Technology Manipal University, India

Dr. M. Sreekumar, Indian Institute of Information Technology, India

Table of Contents

doi:10.4028/www.scientific.net/AMR.587.1

Thermodynamics of Advanced Alloys Modification by Exogenous Nanophases

Y.A.MINAEV

Russian Academy of Natural Science and National Research Technology University-MISiS Leninsky prt.4, Moscow 119049, Russia, E-mail: ymin36 mail.ru

Keywords: Nanophases solution. Thermodynamics of aggregation. Advanced nickel alloys.

Abstract. The thermodynamic analysis of a ceramic compound solubility was carried out for ceramic compounds which may be used for dispersion hardening of advanced nickel alloys. The thermodynamic description of stability conditions was completed for a disperse heterophase systems consists of metal melt – nanosize phases (NSP). For a thermodynamic criterion (K) of stability was selected the specific variation of a free energy of the process of a disperse system degradation (referred to change of unit of a surface phases contact). The analysis was executed in view of formation of thick and thin elastic wetting films and takes in account a disjoining pressure. The above definition of new thermodynamically rigorous criterions becomes physically real, if the isotherm of a disjoining pressure is measured. The derived criterions are simplified in the Young approximation. In this case the criterion are expressed through measurable interfacial performances - interfacial tension and wetting angles. The application of a stability condition gives a simple outcome: aggregation of NSP does not happen at a wetting angles $\leq 60^0$.
On a basis of own experimental data the evaluations are carried out for possibility of using of some compounds as exogenous modifiers of a nickel alloys. The example of dispersion hardening of high-temperature strength nickel alloy and improving its heat resisting properties is reduced.

Introduction

In an air building and space industry are widely applied advanced nickel alloys. The strength of foundry high-temperature nickel alloys increase at the expense of dispersion hardening by an intermetallic γ' phase. At the temperatures higher 800^0C the passage of this phase in a solid solution is happening and the high-temperature strength of alloys is sharp dropped [1]. To increase temperature of a threshold of high-temperature strength it is possible by a mode of introduction in an alloy of exogenous, dispersible NSP. The size of particles should not exceed sizes of the intermetallic hardening phase (30 - 1000 nm).

The problem of introduction of NSP and stabilization them in a melt consists of two parts. The first includes an evaluation of a possibility of dissolution of strengthening phases. The second is stabilization of a dispersible system NSP- liquid alloy. is provided

Application of Thermodynamics to the Problem Description

Thermodynamics of Nitrides Crystallization. The thermodynamic evaluation of a possibility of dissolution ceramic NSP in a liquid nickel alloys was carried out. An evaluation have executed on the basis of obtained equations of the Gibbs relative partial molar energy $\overline{G}_i^M$ (Table 1).

Table 1. Equations of the Gibbs relative partial molar energy.

Equation for $\overline{G}_i^M$ (metal % mass)	nanophase	alloy
- 165020 + 155.5T – 19.5T lg(%Nb)	NbN	Ni
- 216500 + 156.4T – 19.5T lg(%Ti)	TiN	Ni
- 239000 + 156.4T – 19.5T lg(%Ti)	TiN	Ni – 10%Cr
- 256200 + 156.4T – 19.5T lg(%Ti)	TiN	Ni – 20%Cr
- 272750 + 157 T – 19.5T lg(%Ti)	TiN	EI698
- 87800 + 82.9 T – 19.5T lg(%Zr)	ZrN	Ni

The data are a basis for estimations of temperatures of nitrides formation at residual pressure of nitrogen 1.33 Pa in function of a concentration of metal forming NSP (Table 2).

Table 2. Crystallization temperatures of nitrides in Ni and its alloys.

Ni					alloy Ni – 20%Cr				
[% mass] Nb	1	5	10		[% mass] Cr	1	3	5	10
T ^{0}K	1060	1160	1210		T ^{0}K	1650	1740	1820	1870
[% mass] Zr	1	3	5	8	alloy EI698				
T ^{0}K	1560	1650	1700	1750	[% mass] Ti	0.5	1	5	
[% mass] Ti	1	3	5	10	T ^{0}K	1680	1740	1900	
T ^{0}K	1300	1470	1520	1580					

As follows from the Table 2, generated by Ti or Zr solid nitrides can be presented in liquid nickel alloys at processing temperatures. There is a problem on stability of a dispersible system NSP in alloys.

Thermodynamics of Disperse Systems Stability. The possibility of NSP to aggregation in these conditions should be defined. The answer gives reviewing fundamental regularities of a thermodynamics and properties of surface films [2] in view of a surface forces and molecular interaction [3]. The existing common system of equations requires the additional thermodynamic analysis with the purpose of the definition of conditions of a realization of an equilibrium, stability and possibility of spontaneous processes of aggregating, integration of phases. The problem was already considered in a general, theoretical plan [4]. At introduction of NSP in a melt the smallness of sizes of particles ensures their driving with volumes of metal. Most probably is the mechanism of integration of particles owing to ortokinetic aggregation combined with a diffusio-foretical motion. The phenomena are described theoretically and are investigated experimentally for the high-temperature metallurgical systems [5].

Let's define a modification of the Helmholtz potential A of a system for two sequential equilibrium condition. The particles of NSP (α - phase with volume V_1^{α}) are in a liquid metal melt (γ - phase). Properties of the boundaries and gas phase not are taken into account, considering that the particles, going out on them, in an aggregation do not participate. In an initial condition each particle (adopted incompressible on a comparison with a dispersing medium) is under pressure P_1^{α}, has a surface of contact with metal $F_1^{\alpha\gamma}$ and interfacial tension $\sigma_1^{\alpha\gamma}$(the double indexes designate the boundaries of indicated phases). In the second condition we shall consider formation of an aggregate from two and three particles in a volume of metal.

In a part of description A_1 for a position NSP in a liquid metal melt it is possible to use the equations [4], considering a system partially open, where the term $(\Sigma\mu_i n_i)_1$ takes into account interchanging by components of an intersurface film (or an adsorption film) with a metal (with pressure P_1^{γ}):

$$A_1 = -P_1^{\alpha} V_1^{\alpha} - P_1^{\gamma} V_1^{\gamma} + \sigma_1^{\alpha\gamma} F_1^{\alpha\gamma} + (\Sigma\mu_i n_i)_1 \quad (1)$$

Further model representations vary and require the special analysis. Let's consider the process of particles aggregation in a melt in terms of a disjoining pressure Π (on Derjaguin B.V.) for an evaluation of influence of a formation of elastic wetting thin and thick films of liquid metal melts.
By taking for a basis the Eq.1 is written for one particle (radius $r_1^{\alpha\gamma}$) separately standing in a metal, we transform it on two $A_{1\,(2)}$ and three $A_{1\,(3)}$ such particles in view of known relations (for volumV_1^{α} and capillary pressure $2\sigma_1^{\alpha\gamma}/r_1^{\alpha\gamma}$):

$$V = V_1^{\alpha} + V_1^{\gamma},\ V_1^{\alpha} = (1/3)F_1^{\alpha\gamma} r_1^{\alpha\gamma},\ P_1^{\alpha} - P_1^{\gamma} = 2\sigma_1^{\alpha\gamma}/r_1^{\alpha\gamma},\ F_{1(3)}^{\alpha\gamma} = 3F_1^{\alpha\gamma} \quad (2)$$

$$A_{1(2)} = -P_1^{\gamma} V + (2/3)\sigma_1^{\alpha\gamma} F_1^{\alpha\gamma} + (\Sigma\mu_i n_i)_1;\ A_{1(3)} = -P_1^{\gamma} V + \sigma_1^{\alpha\gamma} F_1^{\alpha\gamma} + (\Sigma\mu_i n_i)_1 \quad (3)$$

Let's consider an aggregate from two or three particles with a film of metal with a tension σ_2^{L} in the field of contact (with an area of surface $F_{2(i)}^{L}$, where i - number of particles in an aggregate). The common surface on the boundary of contact NSP- metal, on comparison with separately standing

particles, is reduced to magnitude $F_2^{\alpha\gamma} - F_1^{\alpha\gamma} = - F_{2(i)}^{L}$. Therefore equation for a free energy of an aggregate from two ($A_{2\,(2)}$) or three particles ($A_{2\,(3)}$) is being written as follows:

$$A_{2(2)}= - P_2^{\gamma}V+ (2/3)\sigma_2^{\alpha\gamma}F_2^{\alpha\gamma} + \sigma_2^{L}F_{22}^{L} +(\Sigma\mu_i n_i)_2 \,;\; A_{2(3)}= - P_2^{\gamma}V+ \sigma_2^{\alpha\gamma}F_2^{\alpha\gamma} + \sigma_2^{L}F_{23}^{L} +(\Sigma\mu_i n_i)_2 \qquad (4)$$

The passage of NSP particles from a melt of metal in an aggregate under condition not change of an interfacial tension ($\sigma_2^{\alpha\gamma} = \sigma_1^{\alpha\gamma}$) reduces in a modification A_i on magnitude:

$$\left.\begin{aligned} \Delta A_2 &= - V(P_2^{\gamma} - P_1^{\gamma}) +(2/3)\sigma^{\alpha\gamma} (F_2^{\alpha\gamma} - F_1^{\alpha\gamma}) + \sigma_2^{L}F_{22}^{L} + (\Sigma\Delta\mu_i n_i); \\ \Delta A_3 &= - V(P_2^{\gamma} - P_1^{\gamma}) + \sigma^{\alpha\gamma} (F_2^{\alpha\gamma} - F_1^{\alpha\gamma}) + \sigma_2^{L}F_{23}^{L} + (\Sigma\Delta\mu_i n_i) \end{aligned}\right\} \qquad (5)$$

In view of an adopted approximation, that the particles do not exchange molecules with an environment, are homogeneous and are not compressible, and neglecting an adsorption, we can use a relation: $V(P_2^{\gamma} - P_1^{\gamma}) = (\Sigma\Delta\mu_i n_i)$ [5]. Simultaneously, for an elimination of indeterminacy at evaluations F_{2i}^{L}, we shall enter a thermodynamic criterion of the aggregation process is equal to a specific free energy on unit of square of a mutual contact of particles ($K_i = \Delta A_i / F_{2i}^{L}$):

$$K_2= \sigma_2^{L} - (2/3)\sigma^{\alpha\gamma};\;\; K_3= \sigma_2^{L} - \sigma^{\alpha\gamma} \qquad (6)$$

Aspect of the equation for σ_2^{L} we shall discover, using the definition of the Derjaguin disjoining pressure [3,6]: $\Pi = - \partial(\sigma^{L})/\partial L$. Counting a modification of an interfacial tension from a thick film ($\sigma^{L} = 2\,\sigma^{\alpha\gamma}$), for which $\Pi = 0$, it may be given in the form:

$$\sigma_2^{L} = 2\sigma_2^{\alpha\gamma} + \Pi L \qquad (7)$$

Below, assuming the applicability of Young's rule on equilibrium at the interface of an adjoining film to the meniscus of the bulk metal phase for each pair of particles, i.e., $2\sigma^{\alpha\gamma}\cos\theta^{\alpha\gamma} = \sigma_2^{L} = 2\sigma_2^{\alpha\gamma} + \Pi L$ the expression for Π is defined through experimentally measured parameters:

$$\Pi L = 2\sigma^{\alpha\gamma} (\cos\theta^{\alpha\gamma} - 1). \qquad (8)$$

For the considered process under isothermal conditions and after introducing the σ_2^{L} and ΠL values in Eq.6, we obtain the new criterion *Ki*, which can be used for characteristics of the equilibrium conditions, stability, and direction of aggregation:

$$K_2= (2\cos\theta^{\alpha\gamma} - 2/3)\sigma^{\alpha\gamma};\;\; K_3= (2\cos\theta^{\alpha\gamma} - 1)\sigma^{\alpha\gamma}. \qquad (9)$$

For further analysis let's to make use of the general Helmholtz energy criterion a spontaneous process occurring and equilibrium in systems: $dA_{T,P} \le 0$. This relation implies that a disperse system of NSP in a liquid metal is consequently stable if $K_3 \ge 0$. Assuming Eq.9, this inequality is transformed into the condition for the formation of thermodynamically stable suspension of NSP in a liquid metals:

$$\cos\theta^{\alpha\gamma} \ge 1/2 \text{ or } 60° \ge \theta^{\alpha\gamma} \ge 0 \qquad (10)$$

When finite contact angles form, it is equivalent to the condition for the formation of elastic thin films [7]. Mathematically, this condition can be written thus: $K_3 \le 0$ for all $\theta^{\alpha\gamma} \ge 60°$ (the system is unstable).

Let us also analyze the possibility of aggregation using K_3 from the more general Eq.6. NSP aggregation (in combinations of three particles) is impossible if $K_3 \ge 0$ or $\sigma_2^{L} \ge \sigma^{\alpha\gamma}$, that is equivalent Eq.10.

Experiment

Experimental determination of the characteristics of wetting was performed in helium or a vacuum of 10–5 mm Hg. The equilibrium boundary angels were measured according to the sessile drop method on solid plates obtained by sintering, hot pressing, or fusion from powders of chemically pure grade. All alloys were prepared by double melting in a resistance furnace with an argon atmosphere, and in a vacuum arc furnace from pressed metal powders with a total impurity content of less than 0.03 wt % (*O* <0.01%, *P* < 0.001%, and *S* < 0.0004%). The error in determining boundary angle θ is 1–2 deg. In all our experiments, the value of the boundary angle was determined after 30–60 min. The results from our study of wetting are given in Table 1.

Table1. Equilibrium boundary angles of wetting ($\theta^{\alpha\gamma}$) by a liquid nickel of solid plates obtained by a method of sintering at 1200 - 1400^{0}C within two hours.

alloy	Ni					EI437AL			
plates	TiO_2	$NdCrO_3$	Al_2O_3	ZrC	ZrN	Y_2O_3	TiO_2	ZrN	NbN
temperature[^{0}C]	1500	1500	1460	1500	1500	1460	1500	1410	1500
angels $\theta^{\alpha\gamma}$ [deg]	130	125	109	32	compl*	109	65	compl	compl

Note: * complete wetting.

In accordance with the criteria for the stability of suspension of NSP in liquid metal (Eqs.6, 9, 10), the suspensions of oxides represented in Table 1(with the exception of TiO_2) should form in a liquid metal unstable dispersion systems. These suspensions are inclined to the degradation by aggregate with consequent by separation. Carbides and nitrides can organize suspensions NSP in a liquid nickel and foundry nickel alloy steady to degradation, to separation (for them the angles of wetting are less 60^0). These materials can be used for a production of composite materials or modifying alloys on basis of nickel. The study of disperse systems formed NSP of $NdCrO_3$, TiO_2, ZrN, and NbN in a liquid nickel alloys were carried out. The micrographs of these modified alloys are represented on Fig.1. The particles $NdCrO_3$ form in the aggregates 5-30 grains (Fig.1 A). The powders ZrN and TiO_2 in the foundry nickel alloy are uniform and arrange the suspension steady to degradation (Fig.1 B, C).

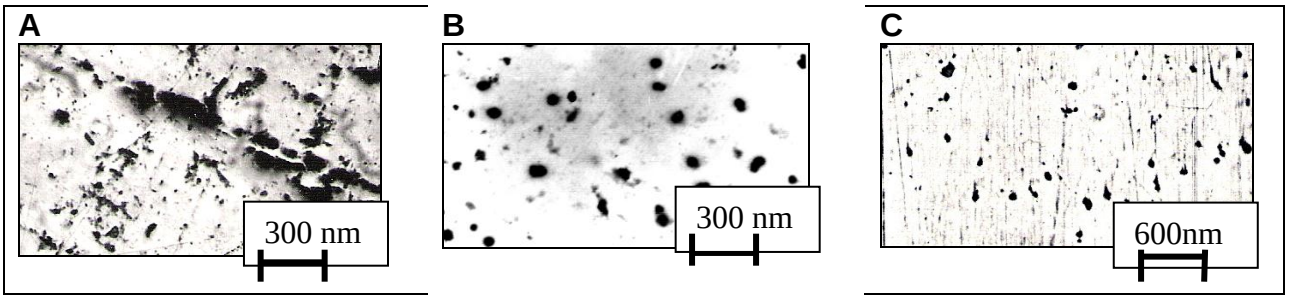

Fig.1. Micrographs of modified alloys: A – $NdCrO_3$ in Ni-Co (20%); B – ZrC and C – TiO_2 in foundry EI437AL alloy.

The trials for detection of comparative functionability of a hot-strength alloy EI437AL (standard and modified NSP of NbN) in a conditions of short-term overheating are carried out. The high-temperature creep at operation temperatures at 700^{0}C and after the short-term overheating up to 1100^{0}C down to destruction was determined at the basis of test from 1 minute till 1.5 hours (Fig.2).

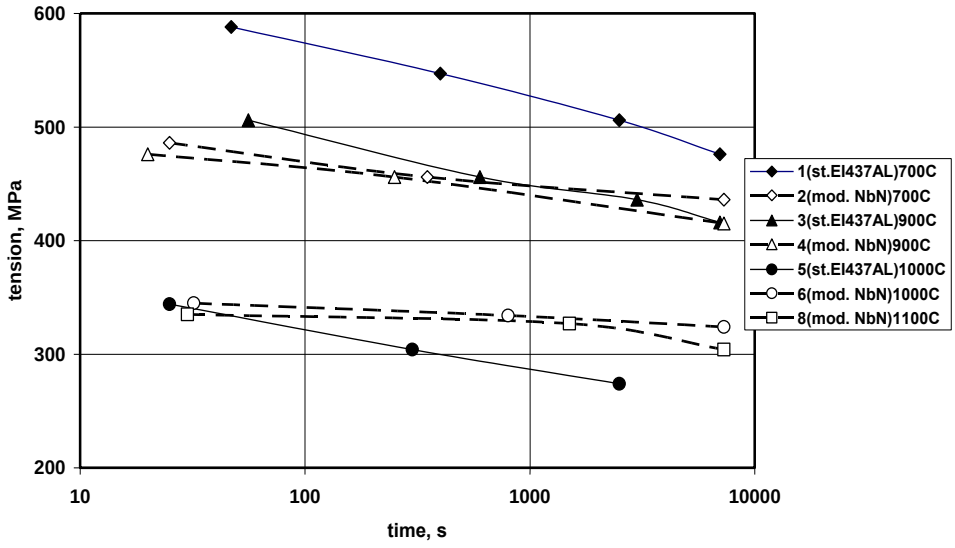

Fig.2. The high-temperature creep (σ_0, MPa) measured at 700^{0}C in a function of the overheating temperature.

The data Fig.2 characterize high-temperature strength of researched alloys in a function of temperature of a single overheating without fixed equalizing. The short-term overheating considerably descend high-temperature strength of standard alloys, that is stipulated by heavily dissolution of an intermetallic hardening γ' - phase. Modifying of alloy the refractory NSP (NbN) already at 900^0C ensures the 1.5 hours destruction at the higher value of a tension σ_0, and at 1000^0C makes 325 MPa (against 260 MPa at a standard alloy). At the overheating temperature 1100^0C the σ_0 for a modified alloy practically remains to constants (305 MPa), and the standard alloy fails before a one hour limit.

Summary

1. The carried out study of modified alloys are confirm of a possibility of prediction of the hardening components for high-temperature strength alloys on a complex of surface properties.

2. The thermodynamic stability criterion of disperse system NSP in metal melts is obtained. As a criterion the change of a specific free energy (referred to unit of a modification of a surface of contact of phases) of an aggregation process of disperse system particles is selected. The criterion takes into account appearances of formation of thick and thin elastic films and disjoining pressure on the boundary of contact of NSP particles of a disperse phase. The criterion is expressed through experimentally measured parameters - interfacial tension and boundary angles of wetting.

3. Using the general requirement for equilibrium gives the simply condition for the formation of thermodynamically stable suspension of NSP in liquid metals: the boundary angles of wetting NSP by metal should be less than 60^0.

4. The conclusion is confirmed experimentally. Improving of high-temperature strength properties is established at short-term overheating of alloy EI437AL, hardened of exogenous NSP of NbN.

References

[1] E.N Kablov: Cast blades of gas-turbine engines. Alloys. Process engineering. Cooating. (MISiS Ed., Moscow, 2001).

[2] A.I. Rusanov: Phase equilibrium and surface appearances (Chemistry, Leningrad 1967).

[3] B.V. Derjaguin, N.V. Churaev, V.M. Muller: Surface forces (Science, Moscow, 1987).

[4] Y.A. Minaev, A.I. Rusanov: Izv. ASci. USSR, Metals, № 5 (1971), p. 59.

[5] Y.A. Minaev, V.V. Jakovlev: Physical-chemistry in metallurgy. Thermodynamics. Hydrodynamics. Kinetics (MISiS Ed., Moscow, 2001).

[6] B.V. Derjaguin: Acta Physicochim. USSR, V.12, № 2 (1940), p.181.

[7] I.A. Minaev, in: Symposium Series S36, VII International Conference on Molten slags, fluxes and salts, SAIMM Publ., Johannesburg (2004), p. 763.

doi:10.4028/www.scientific.net/AMR.587.6

Hydromechanical properties of some mortars used in some ecologic construction techniques

Dashnor HOXHA[1, a], Vladimir Nicolae UNGUREANU [2,b] ,
Naima BELAYACHI[1,c] , Duc Phi DO[1, d] and Jean-Baptiste THEVARD [3,e]

[1]Laboratoire Pluridisiplinaire de Recherche en Ingenierie de Systèmes, Mécanique et Energie PRISME, Universite d'Orléans, 8 rue Léonard de Vinci, 45072 Orléans Cedex 2, FRANCE

[2]Université Technique "Gheorghe Asachi", Bd. Dimitrie Mangeron 43, 700050 Iasi, ROUMANIE

[3] Association pour la PROmotion et la Construction d'Habitations Ecologiques en Paille, APPROCHE-Paille, 11 rue de Lutèce - 45000 Orléans, FRANCE

[a]dashnor.hoxha@univ-orleans.fr , [b]vlad.nicolae.ungureanu@gmail.com
,[c]naima.belayachi@univ-orleans.fr, [d]Duc-Phi.Do@univ-orleans.fr, [e]jbthevard@approchepaille.fr

Keywords: Sawdust, mortar, GREB technique, straw bale construction, retention curve, water vapor permeability, uniaxial compression strength.

Abstract. This paper presents results of hydromechanical characterization tests performed on some mortars used in eco-construction practice. Typically, such mortars could be found in buildings constructed following so called GREB technique that uses straw bales as structural and insulating elements in addition to a wood frame. The full experimental program includes thermal, mechanical and hydraulic – hygroscopic tests. Mechanical tests, including uniaxial compression test and three point bending test and hydraulic tests including water and vapor water permeability, retention curve and unsaturated water permeability have been performed on three earth-cement mortars with sawdust additive. Tests were performed in age of 7, 14, 28 and 120 days. For retention curve and so called relative permeability a simple method has been used based on measurements of masse variations of samples on a controlled humidity environment and an inverse problem approach. Using of sawdust improves hydraulic properties of these mortars but the early age strength of these mortars has to be improved by cement additives.

Introduction

In relation with the global efforts to minimize the anthropologic impact on the nature, the eco-constructing nowadays has become a major issue in constructing practice [1]. More and more, in artisanal and industrial practices the objectives in terms of overall impact are formulated nnot only on final thermal efficiency of buildings but also in so-called gray energy used in materials used for constructions. This justifies the increasing interest on straw bale based constructions, initially used for their low economic cost in rural regions [1, 2, 3, 4].

The GREB technique [2, 5] initially developed by Ecologic Research Group of Baie (*G*roupe de *R*echerches *E*cologiques de la *B*aie, *GREB*, Canada) uses a wood frame as principal structural element and adds straw bales along with well positioned staples and metallic meshes in order to obtain a solid structure and an efficient insulating envelope. The finishes of such constructions are usually made by clay plasters with addition of sawdust or alternatively by earth cemented mortars enriched by various fibers such as chopped straw, hemp fiber, nylon fiber, and animal hair. The objective of finishes is to provide mechanical and fire protection of the bales, to restrict the passage of air through the bales, and to protect them from weather. While various studies on mechanical and thermal properties of straw bale walls [3, 4, 6] confirm the suitability of such construction techniques for low ecologic impact buildings, the main concerns about them is the durability, hydrous state and moisture permeability in order to avoid fungus formation [6, 7].

In this paper various formulations of finishes mortars used in GREB techniques are tested mechanically and hydraulically in order to obtain their characteristics in terms of mechanic and hydraulic resistance. These characteristics could be used on numerical simulations in order to assess the hydrous state of straw bale walls in given regional climatic conditions and to evaluate the risks of fungus apparition if any. Only experimental program of mechanical and hydraulic characterization of mortars is presented here. After a short description of materials studied in this work, laboratory techniques are presented briefly followed by results and a short discussion.

Description of materials

Three mortars that differ to each other from rapport of cement used in their formulas are used in this study. Firstly, a traditional mortar used in GREB construction is studied (referenced hereafter as F0 formulation): it is constituted by 4 sawdust parts (in volume), 3 parts of sand, 1 part of lime and 1 part of Ordinary Portland Cement (OPC). This standard traditional formulation is compared with two other formulas in which the contribution of OPS is initially reduced at 50% (F1 formulation) and finally has completely dropped from formulas (F2 formulation). The samples for F0 formulation have been prepared directly in a building site, while for two others formulations samples were prepared in laboratory. In order to keep as much as possible a homogeneous material from one sample to another one, for each formulation the samples were prepared from a single mixing apparatus. Each sample obtained an identification number and then introduced in the testing schedule. All samples were kept in atmospheric conditions of laboratory during all the period preceding testing.

Laboratory setups and test conditions

Mechanical tests were performed using a classical procedure and devices at different ages of samples: 7, 14, 28 and 120 days, respectively, following European standards (EN 196-1). The axial load is applied by a servo-controlled actuator and the normal displacements are measured by a LVDT sensor. For the three points bending tests, prismatic square-bases samples with standard dimensions (40mm x 40mm x 100 mm) were used and the same loading device is used as for compression tests. It is then possible, knowing applied force (when the macroscopic failure of samples is observed), to calculate tensile stress at failure known as bending strength.

The water permeability tests are performed on saturated cylindrical tests using a classical cell and standard steady conditions: maintaining a pressure difference between two bases of cylindrical sample one measures the water flow out and then calculates water permeability using Darcy's law. Knowing temperature of test and water viscosity it is then possible to access to the intrinsic permeability of tested sample.

For the vegetal-fibered walls, most often is more important to characterize the liquid water transfer and condensing capacity of a wall then water vapor permeability, which of course is always interesting to know. As mentioned by many authors, obtaining the full retention curve and water permeability in unsaturated conditions is a time-consuming process. In order to accelerate it, in this work a method suggested in [9] has been used. Following this method, instead of steady state measurements commonly used in practice, we use transient response of materials in terms of masse variation of samples and identify the permeability with the helps of a numerical inverse problem approach. Practically wise, we measure the mass taking (losing) of a sample when it is put in an atmosphere of controlled relative humidity (RH). The relative humidity is maintained during a test by the help of salt solutions technique: one puts a sample in a closed, isothermal cell communicating with a reservoir of an oversaturated salt. The salt solution through exchanges with the closed atmosphere of the cell and sample creates a constant relative humidity in the cell. Measuring the mass taking (losing) of as sample as a function of time allows in one hand identifying the relative permeability (see [9]) and in the other hand constructing of retention curve. The salt solutions used in this study and their equilibrium relative humidity are given in table 1. In our tests, in order to create appropriate conditions for interpretation, thin cylindrical samples, with know base surface were

isolated on laterals, so that the hygroscopic exchanges with the cell atmosphere are possible only through the bases of the sample and the problem of water transfer becomes 1D, which considerably simplifies the inverse problem. The theoretical bases of inverse problem and relative permeability identification are not detailed here (the interested reader could find details in [9] and references cited therein)

Table 1 : Salt solutions used in study and their equilibrium relative humidity

Level test	Salt Solution	Relative Humidity at equilibrium [%]
1	$MgCl_2$	33.07 %+/-0.18%
2	$Mg(NO_3)_2$	54.38 %+/-0.23%
3	NaCl	75.47 %+/- 0.14%
4	KCl	85.11 % +/-0.29 %
5	KNO_3	94.62 % +/- 0.66%
6	K_2SO_4	97.59 % +/- 0.53%

Principal results

Mechanical tests. Typical failure patterns of samples after uniaxial compression tests are given in the Fig. 1.a, while three point bending device is shown in the Fig. 1.b. As a general rule the failure of sample is of ductile type whatever cement content is. As expected, the strength of samples, deduced by uniaxial compression tests, increases with the age of samples and with fraction OPC used t. However as shown in Fig. 2, the differences are far more important between F0 (reference) and F1 (cement content reduced by 50% as compared to F0), than between F1 and F2 (no cement at all).

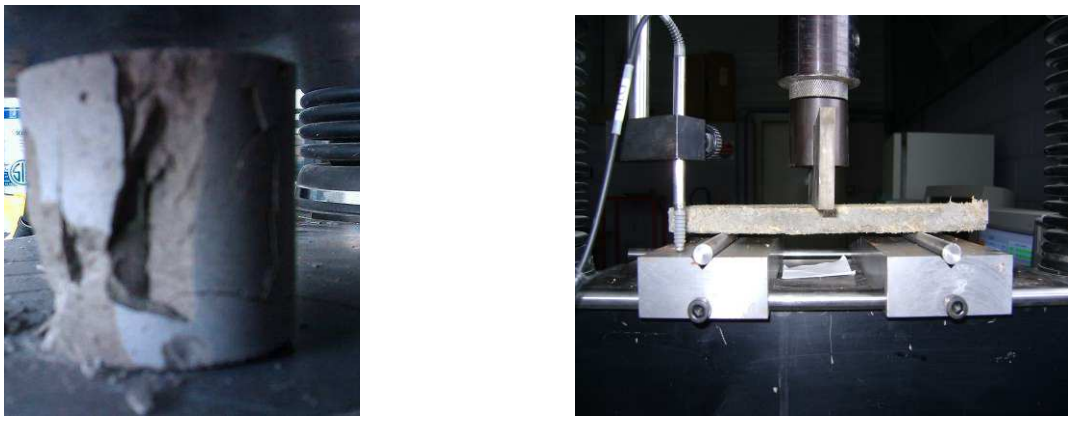

Figure 1: Pattern failure of samples under uniaxial compression and three points bending tests device

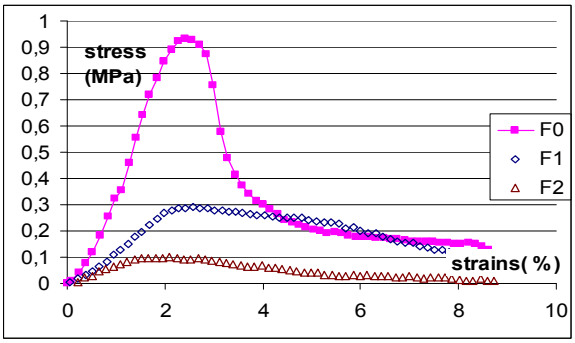

Figure 2.a : Stress-strains curves form uniaxial compressions tests (t=120 days)

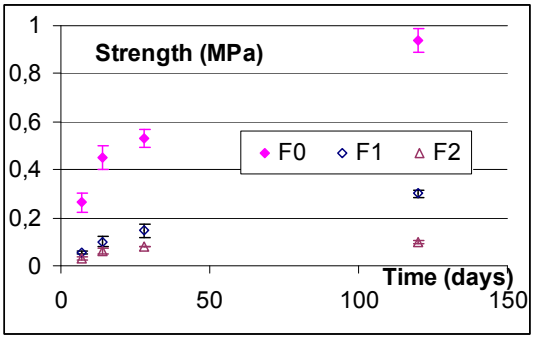

Figure 2.b : Evolution of compression strength with the age of samples

In the Fig. 3.a is shown a typical result from three points bending tests, while in figure 3.b is presented the evolution of bending strength as a function of the age of tasted samples. Again, no substantial differences are observed in behavior of F1 and F2 samples, while F0 samples clearly demonstrates a better mechanical resistance, especially in bending.

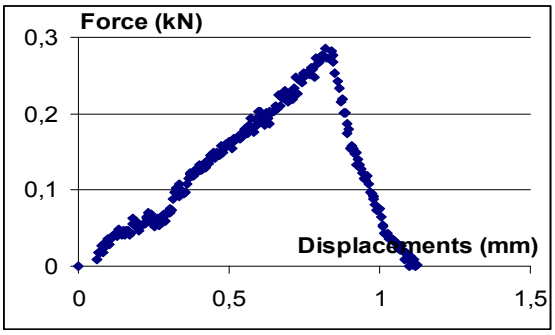

Figure 3.a Example force displacement curve from three points bending test

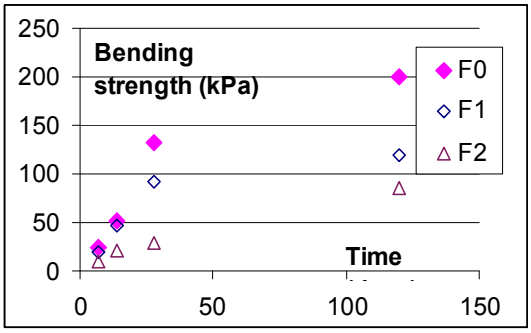

Figure 3.b : Evolution of bending strength with the age of samples

Hydraulic and hygroscopic tests. There were technical difficulties in measuring water-saturated permeability of all samples. These difficulties were due to the swelling of samples once saturated and some forms of decohesion of sawdust when fully saturated in water. So, all necessary precautions have to be taken in the interpretation of obtained values. Following these results water-saturated permeability decreases when the cement content increases going from 2.2 10^{-15} m^2 for reference samples to 5.4 10^{-15} m^2 for F1 samples and 1.2 10^{-14} m^2 for F2 samples.

Typical results of masse evolution of samples as a function of time are presented in the Fig. 4.a. As already mentioned a test of mass taking (loosing) is performed for each salt-solution-regulated relative humidity, so that a set of 18 graphics similar to that shown in Fig. 4.a is obtained and treated. Taking into account the measured porosity of each sample and numerical procedure indicated in [9], values of unsaturated permeability are calculated for each sample and results are presented in Tab 2.

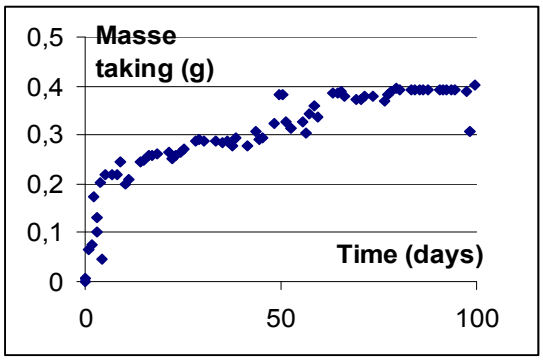

Figure 4.a : Masse evolution of sample #5F0 during hygroscopic equilibration (level 4 to 5)

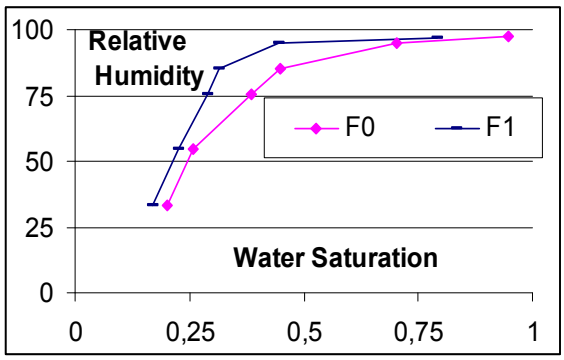

Figure 4.b : Retention curve from masse variation tests for two of mortars

Table 2 : Unsaturated effective water permeability deduced from mass variation tests

Masse variation curve used in identification of water permeability		Permeability of samples from [m^2]		
		Mortar F0	Mortar F1	Mortar F2
From RH=33%	To RH=54%	3.56 10^{-18}	4.53 10^{-18}	0.11 10^{-17}
From RH=54%	To RH=76%	1.14 10^{-17}	1.44 10^{-17}	1.36 10^{-17}
From RH=76%	To RH=85%	7.83 10^{-17}	1.66 10^{-16}	7.42 10^{-17}
From RH=85%	To RH=95%	1.45 10^{-16}	1.27 10^{-16}	1.68 10^{-16}
From RH=95%	To RH=97%	0.71 10^{-15}	0.42 10^{-15}	0.52 10^{-15}

Considering the mass of samples at equilibrium for a given Hr it is possible to finally construct the retention curve of each formulation (Fig. 4.b)

Discussion and concluding remarks

While the presence of cement in mortar formulation seems quite useful to give them the necessary strength, especially in the very first days, even if the cement maintains a high capillary capacity and significant water liquid permeability. The compromise found empirically in the practice of GREB construction to use cement at about 10% of inert constituents seems to be quite close to the optimum. In fact for smaller percentages of cement the mechanical properties decreases drastically. It particular the presence of the cement seems to influence the relative permeability for law capillary pressure, close to full saturated state. As discussed by several authors the problem of humidity in the buildings is above all a problem of capillary liquid water transfer. From this point of view it seems that F0 (reference mortar) is the worst protector among studied mortar. As shown in Tab. 2 liquid water permeability for reference formulation (with maximum cement) is smaller for the smaller capillary pressure which implies that it has the higher resistance to water vapor, but it is this mortar that could transfer by capillarity more humidity when slight unsaturated. Shifting towards a mortar with less cement would not only be more ecologic (since less cement means less grey energy) but also would be more appropriate for moisture transfer. For that, the problem of mechanical stability of mortar should be resolved beforehand and recent ongoing researches aims at obtaining an optimized mortar from thermal, hydraulic and mechanical properties point of view.

References

[1] J.C. Morel, A. Mesbah, M. Oggero, P. Walker, Building houses with local materials: means to drastically reduce the environmental impact of construction. *Building and environment,* Volume 36, Issue 12, Pages 1119–1126, (2001)

[2] V. BROSSAMAIN, J.B THÉVARD, *Construire sa maison en paille selon la technique du GREB* (2006)

[3] U.S. Department of Energy, *Energy Efficiency and Renewable Energy,* April 1995, www.eere.energy.gov/buildings/info/components/envelope/framing/strawbale.html

[4] The Federal Ministry of Traffic, Innovation and Technology (Department for Energy and Environmental Technologies) and the Austrian Energy Agency, *Wall systems made of renewable resources: Testing and optimising post and beam straw bale constructions*, http://energytech.at/architektur/publikationen/results/id1777.html.

[5] C. de la ROSA, *Contribution aux mesures mécaniques sur la construction paille selon la technique du GREB* Master Dissertation (in French) (2008),

[6] Steve Goodhew, Richard Griffiths, Tom Woolley, An investigation of the moisture content in the walls of a straw-bale building, *Building and environment,* Volume 39, Issue 12, Pages 1443-1451 (2004)

[7] Jim Carfrae, Pieter De Wilde, John Littlewood, Steve Goodhew, Peter Walker Development of a cost effective probe for the long term monitoring of straw bale buildings, *Building and Environment*, Volume 46, Issue 1, January 2011, Pages 156-164

[8] V. Ungureanu Characterization of mortars used in GREB technique, Master Dissertation of University of Orleans, July 2010

[9] Homand F., Giraud A., Escoffier S., Koriche A. & Hoxha D. - Permeability determination of a deep argillite in saturated and partially saturated conditions - *International Journal of Heat and Mass Transfer*. Volume 47, Issues 14-16 , pp. 3517-3531 (2004)

doi:10.4028/www.scientific.net/AMR.587.11

Finite Element Modeling For Prediction Of Stress – Strain At Several Feed Rates And Cutting Speeds For Titanium (Ti-6Al-4V) Alloy

Moaz H. Ali[1, a], Basim A. Khidhir[1, b], Bashir Mohamed[1, c]

[1]Department of Mechanical Engineering, Universiti Tenaga Nasional, Putra Jaya, Malaysia

[a]muezhm@hotmail.com, [b]basim_ak@yahoo.com, [c]bashir@uniten.edu.my

Keywords: Finite element modeling, Stress and Strain, Cutting parameters, Titanium alloy.

Abstract. Titanium (Ti-6Al-4V) alloy is a desirable material for the aircraft industry because of their excellent properties behaves of high specific strength, fracture resistant characteristics, lightweight and general corrosion resistance. This paper presents a study on a two-dimensional orthogonal cutting process by using a face-milling operation through ABAQUS/EXPLICIT finite-element software. Several tests were performed at various feed rates and cutting speeds while the depth of cut remains constant. The results led to the conclusion that the stress components at integration points (Von - Mises) and the equivalent strain (PEEQ) were increased with increasing the feed rate and cutting speed during the machining process.

Introduction

Titanium (Ti-6Al-4V) alloy is widely used in the aerospace industry due to the good compromise between mechanical resistance and tenacity, together with its excellent corrosion resistance and low density. However, this material is known to be difficult to machine. One of the reasons is due to its low thermal conductivity, which gives rise to high pressure, and temperatures at the tool–chip interface, a plastic instability localized in adiabatic shear bands, and tool wear by thermal fatigue and diffusion [1].

Researchers are focusing on modeling and simulation techniques to predict and optimize certain machining parameters such as cutting forces, temperature, roughness and residual stresses. These techniques do not need to perform many experimental tests that will take a long time and cost more money [2]. Therefore, a correct simulation enables good predictions in feed rate, cutting speed and strain and stress distribution. This will contribute to cost reductions for the machining process optimization that is still experimentally done and thus expensive [1].

The aim of this research work is to study characterize of the stress and strain at several feed rates and cutting speeds while the depth of cut remains constant. The titanium (Ti–6Al–4V) alloy is very important in the study of mach-inability due to it is the most widely used in industry and has been the subject of many experiments and modeling including the study of characterization of chip formation during orthogonal cutting [3].

In this work, in order to predict the effect of several cutting speeds and feed rates on the stress components at integration points (Von - Mises) and the equivalent strain (PEEQ) during the machining process. Besides that, the prediction by using finite-element modeling analysis can contribute in reducing together the cost of manufacturing in terms of prolongs the machining time saving and cutting tool life.

Finite Element Modeling

The FEM is the firstly dominant technique in structural mechanics. The FEM analysis obtains the stress and strain, cutting forces, or other desired unknown parameters. A typical finite element analysis in a software system requires the following procedures:

Material and Tool Modeling. The two-dimensional orthogonal cutting process is carried out by using face-milling operation through ABAQUS/EXPLICIT finite-element software [4]. The work-piece material is designed by using a dimension of 50 mm x 100 mm with various machining

parameters such as depth of cut (d), feed rate (f) and cutting speed (vc) as shown in Table 1. On the other hand, the tool of geometry is modeled with the assumption that it is mechanically rigid. Thermo-physical material is used for the cemented carbide inserts as shown in Table 1.

Table 1 Machining parameters modeling.

Cutting Parameters				
Rake angle, γ (deg)	Clearance angle, α (deg)	Depth of cut, d (mm)	Feed rate, (f) (mm/tooth)	Cutting speed, (v_c) (m/min)
6	21	1	0.1	70
			0.2	100

Contact and Failure Modeling. During this investigation, Titanium (Ti-6Al-4V) alloy is modeled with the Johnson–Cook plasticity technique of Eq. 1 as follow:

$$\sigma = (A + B\,\varepsilon_p^{\,n})\,(1 + C\,ln\,(\varepsilon/\varepsilon_0))\,(1 - (T\text{-}\,Tr/Tm - Tr\,)\text{^}m) \quad (1)$$

Where: σ is flow stress, ε_ρ and ε are strain and strain rate, ε_0 is the reference strain rate (*1/s*) and *n, m, A, B* and *C* are constant parameters for Johnson-Cook material model as shown in Table 2.

On the other hand, the failure criterion material is incorporated in the material model to simulate material removal during the orthogonal machining of titanium (Ti-6Al-4V) alloy. The failure parameters *d1* to *d5* are acquired from R. Lesuer [5] where: *d1*= -0.09, *d2*= 0.25, *d3*= -0.5, *d4*= 0.014 and *d5*= 3.87. Material failure of strain ε_f is expressed by Eq. 2 as follow:

$$\varepsilon_f = (\,d1 + d2\,e^{d3(\sigma_p/\sigma_e)})(1 + d4\,ln\,(\,\varepsilon_p/\varepsilon_0)) * (1 + d5\,(\,T - Tr\,/\,Tm - Tr\,)) \quad (2)$$

Where: σ is flow stress, ε_p and ε are strain and strain rate, ε_0 is the reference strain rate (*1/s*) and *n, m, A, B* and *C* are constant parameters for Johnson-Cook material model as shown in Table 2. The $\varepsilon_p/\varepsilon_0$ is the function of non-dimensional plastic strain, σ_p/σ_e is the dimensionless deviatoric-pressure stress ratio (where σ_p is the pressure stress and σ_e is the (Von-Mises stress)), *T* is the computed or modeled work-piece temperature, *Tr* is the room temperature, and *Tm* is the melting temperature [6].

Table 2 Constant parameters for Johnson-Cook material model of (Ti-6Al-4V) [7].

Cutting constant	Values
A (MPa)	987.8
B (MPa)	761.5
n	0.41433
m	1.516
C	0.01516
Reference strain rate	2000
Young's modulus (GPa)	113.8
Poisson's Ratio	0.342
Melting Temp. °*C*	1605
Density (kg/m^3)	4428

Meshing Elements. As shown in Fig. 1, the mesh generator starts by creating elements along the boundary of the work-piece material and the cutting of tool geometry. The meshing elements and assembly parts are used at the contact surface between the cutting of tool edge and work-piece material.

This is because the primary and secondary shear deformation zone was created there and then configures chip formation. The total number of elements is used with approximately about 1250 and the number of nodes is 1311. However, the number of elements at the contact surface between cutting edge of the tool and the work-piece material was meshed with the minimum element size of 2 μm. That has led to improving the predicting of machining parameters during cutting test.

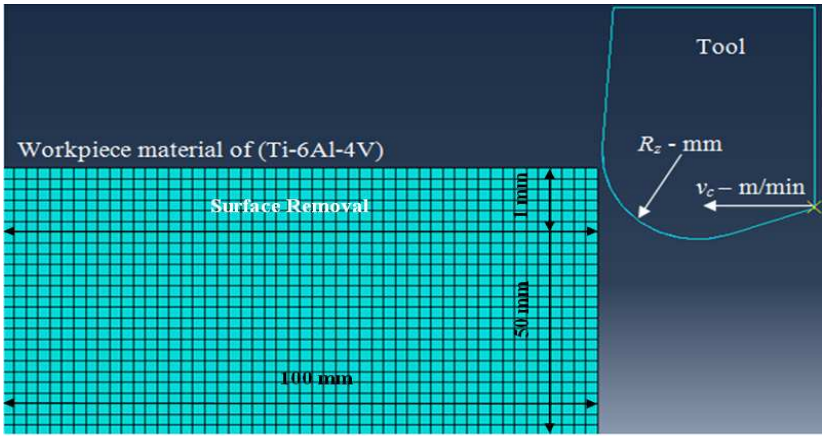

Fig. 1 Meshing elements and assembly parts along the boundary of the work-piece and tool.

Result and Discussion

Finite element modeling is used to determine the machining parameters such as stress components at integration points (Von – Mises) and the equivalent strain (PEEQ) by the designed tests as shown in Table 3.

Table 3 Test design whiles for the stress components.

Machining cutting test	Depth of cut, (d) = 1 mm was held as constant.			
	Test 1	Test 2	Test 3	Test 4
Stress – Mises N/mm^2	Feed rate (f) = 0.1 mm/tooth & Cutting speed (v_c) = 70 m/min	Feed rate (f) = 0.1 mm/tooth & Cutting speed (v_c) = 100 m/min	Feed rate (f) = 0.2 mm/tooth & Cutting speed (v_c) = 70 m/min	Feed rate (f) = 0.2 mm/tooth & Cutting speed (v_c) = 100 m/min
Plastic strain - PEEQ				

From the resultant tests as shown in Fig. 3 and Fig. 4, it could be seen that the values of the stress (Von – Mises) and equivalent strain (PEEQ) were increased with increasing of the feed rate and cutting speed. Therefore, the highest value of the cutting test measured for the stress (Von – Mises) was 1456 N/mm^2 at T2. Besides that, the stress (Von – Mises) at T4 is considered stable, convergent and harmonic more than another test due to the increasing of both cutting speed and feed rate. Therefore, the effect of the cutting speed on the stress was more obvious than the effect of the feed rate during the machining cutting test as shown in Fig. 3. On the other hand, the highest value of the cutting test measured for equivalent strain (PEEQ) was 0.941208 at T3. However, the equivalent strain (PEEQ) remains stable for T4 as convergent and harmonic more than another test. Hence, the effect of feed rate on the strain (PEEQ) was more obvious than the effect of cutting speed as shown in Fig. 4. Thus, it is clear that the cutting speed and feed rate are affected by stress and strain but in a different from the other. Therefore, high-speed machining process is growing industry interest and it is not only because they allow for larger material removal rates, but also because they may positively influence the properties of the finished work-piece [8, 9]. Besides that, the increase in cutting speed and feed rate led to their values of stress and strain to become more convergence and harmony.

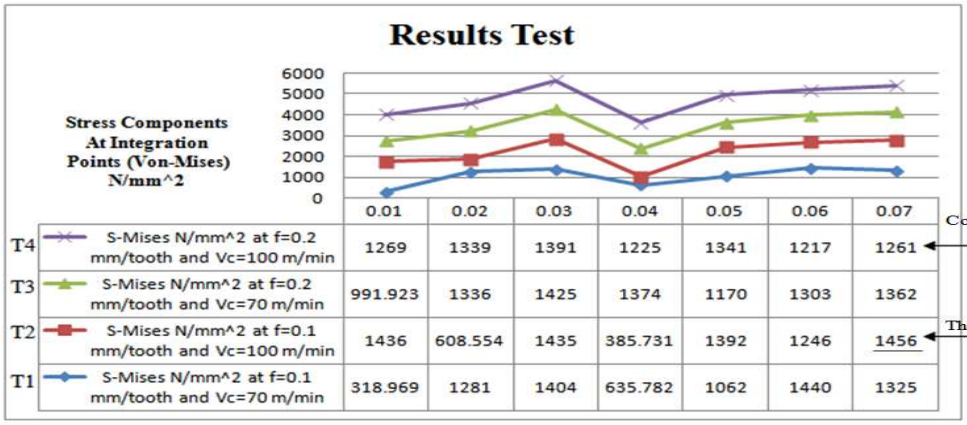

Fig. 3 Diagram of the stress (Von – Mises) (N/mm2) for titanium (Ti-6Al-4V) alloy.

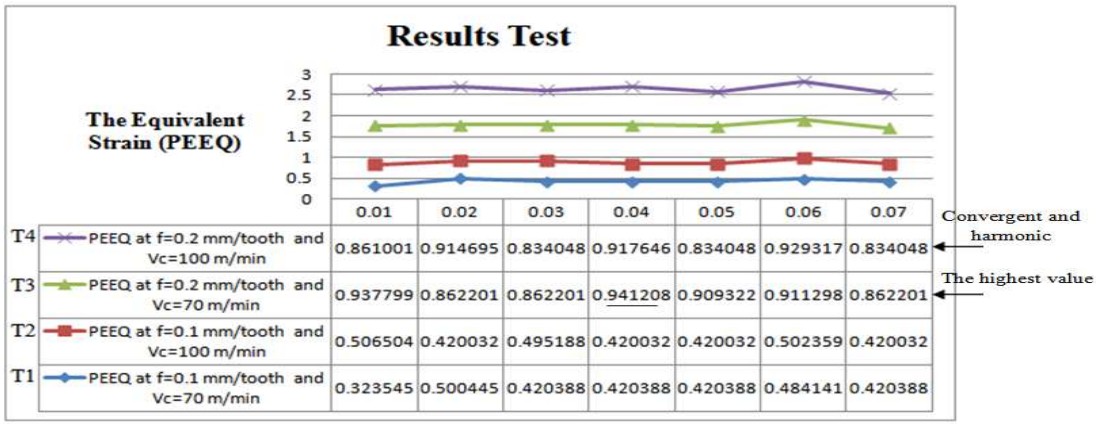

Fig. 4 Diagram of the plastic strain (PEEQ) for titanium (Ti-6Al-4V) alloy.

Conclusion

From the obtained results, the conclusion can be drawn as follows:

- Stress (Von – Mises) and plastic strain (PEEQ) increase with increasing the feed rate and cutting speed on titanium (Ti–6Al–4V) alloy.
- The effect of cutting speed on stress was more obvious than the effect of feed rate during the machining of titanium (Ti–6Al–4V) alloy.
- The effect of feed rate on strain was more obvious than the effect of cutting speed during the tests.
- Increasing the values of the cutting speed and feed rate led the stress and strain to become more convergence and harmony with each other and this will positively influence more on the machining process of titanium (Ti–6Al–4V) alloy.

Acknowledgment

The authors would like to acknowledge the support given by Universiti Tenaga Nasional in carrying out this research work.

References

[1] Madalina Calamaz, Dominique Coupard, Franck Girot, A new material model for 2D numerical simulation of serrated chip formation when machining titanium alloy Ti–6Al–4V, International Journal of Machine Tools & Manufacture 48 (2008) 275–288.

[2] HAMED SADEGHINIA, M.R.RAZFAR, JAFAR TAKABI, 2D finite element modeling of face milling with damage effects, 3rd WSEAS International Conference on APPLIED and THEORETICAL MECHANICS, Spain, December 14-16, 2007.

[3] Matthew Cotterell, Gerry Byrne. Characterisation of chip formation during orthogonal cutting of titanium alloy Ti–6Al–4V. CIRP Journal of Manufacturing Science and Technology 1 (2008) 81–85.

[4] HKS Inc., USA ABAQUS/Standard User's Manual, Version 5.8, 1998.

[5] Donald R. Lesuer, EXPERIMENTAL INVESTIGATIONS OF MATERIAL MODELS FOR Ti-6Al-4V TITANIUM AND 2024-T3 ALUMINUM, U.S. Department of Transportation Federal Aviation Administration Final Report Office of Aviation Research Washington, DC 20591.

[6] M.S. ElTobgy*, E. Ng, M.A. Elbestawi, Finite element modeling of erosive wear, International Journal of Machine Tools & Manufacture 45 (2005) 1337–1346.

[7] T. Ozel, Y. Karpat, Identification of constitutive material model parameters for high strain rate metal cutting conditions using evolutionary computational algorithms, Mater. Manuf. Process. 22 (5e6) (2007) 659e667.

[8] H. Schulz (Ed.), Scientific Fundamentals of HSC, Carl Hanser Verlag, M¨unchen, 2001.

[9] H.-K. T¨onshoff, F. Hollmann (Eds.), Spanen Metallischer Werkstoffe bei hohen Geschwindigkeiten, Deutsche Forschungsgemeinschaft, Bonn, 2000.

doi:10.4028/www.scientific.net/AMR.587.16

USING BIOMASS ASHES IN CONCRETES EXPOSED TO SALTED WATER AND FRESHWATER: MECHANICAL AND CHEMICAL PROPERTIES

RUI BARBOSA[a], DIOGO DIAS[b], NUNO LAPA[c], BENILDE MENDES[d]

[1] Universidade Nova de Lisboa, Faculdade de Ciências e Tecnologia, Departamento de Ciências e Tecnologia da Biomassa, Campus da Caparica, Ed. Departamental, Piso 3, gab. 364, 2829-516 Caparica, Portugal

[a] rfb@fct.unl.pt, [b] da.dias@campus.fct.unl.pt, [c] ncsn@fct.unl.pt, [d] bm@fct.unl.pt

Keywords: Biomass ashes, concrete, mechanical properties, leachability, chemical behaviour.

Abstract. The main aim of this work was to assess the possibility of using biomass ashes as substitutes for cement and natural aggregates in concretes without compromising their mechanical and chemical properties. Thirteen concrete formulations were prepared with different percentages of bottom and fly ashes produced at a forest biomass power plant. These formulations were submitted to mechanical compressive strength assays, after 28, 60 and 90 days of maturation. The reference formulation F1 that was produced without biomass ashes and one formulation incorporating fly and bottom ashes, F4, were selected for further characterization. After 90 days of maturation, the selected formulations were submitted to the leaching test described in the European Standard EN12457-2 (L/S ratio of 10 L/kg, in a batch extraction cycle of 24h) by using two different leaching agents: a synthetic marine medium (ASPM medium) and a synthetic freshwater medium (ISO 6341 medium). The eluates produced were submitted to chemical characterization which comprised a set of metals (As, Sb, Se, Cu, Zn, Ba, Hg, Cd, Mo, Pb, Ni, Cr, Cr VI, Al, Fe, Mg, Na, K and Ca), pH, SO42-, F-, dissolved organic carbon, chlorides, phenolic compounds and total dissolved solids. The substitution of 10% cement by fly ashes has not promoted the reduction of the compressive strength of concrete. The new formulation F4 has presented emission levels of chemical species similar or even lower to those observed for the reference formulation F1.

Introduction

The production of electric energy by using forest residues is one of the possible ways to increase the production of renewable energy and to promote the sustainable development [1]. Moreover, the valorization of forest residues allows to control the forest fires and to reduce the direct emission of greenhouse gases associated to the energetic sector.

A considerable amount of biomass received by pulp and paper industries is not appropriate for pulp and paper production. This biomass is considered a residue that can be valorized. The most common valorization route of these forest residues is their thermal valorization through combustion, since the energy content is high enough for energy recovery [2,3,4,5]. In the Portuguese pulp and paper sector, the thermal valorization of forest residues through combustion is widely used. Nevertheless, the combustion of biomass produces ashes that need to have an adequate management strategy. The type of ashes produced depends on the characteristics of the boiler and the treatment system of the exhaustion gases. Usually, two types of ashes are produced: bottom and fly ashes. The former are collected at the bottom of the boilers, while the latter are collected in the treatment systems of the exhaustion gases. The management strategy of ashes adopted by pulp and paper sector has been up to now to use them as soil conditioner or sending them to cement industries. The first destiny has some limitations imposed by European legislation, since it restricts the application of ashes in soil, due to the high content of alkali and alkali-earth metals. On the other way, the cement industries are not able to receive all fly ashes produced by pulp and paper industry. Therefore, it is necessary to find new applications for biomass ashes.

Concrete incorporating biomass ashes is a potential solution for coastal protection and embankment reinforcement of inland water flow systems [6,7]. Moreover, the use of concrete in the shore can reduce the eroding action of waves and also promote the development of high quality waves for surf practice. The main aim of this work was to produce concrete formulations containing biomass ashes as substitutes for cement and natural aggregates, without compromising their mechanical and chemical properties.

Materials and Methods

Origin of biomass ashes. The fly and bottom ashes were produced in a Portuguese biomass boiler of a pulp and paper industry. This industry produces electricity through the combustion of eucalyptus and pine bark in a Bubbling Fluidized Bed Combustor (BFBC). Bottom ashes were collected at the bottom of the BFBC and the fly ashes were collected in the electrostatic precipitator. The BFBC uses sand as fluidizing agent. The ashes were stored in air-tight polypropylene containers and maintained at a temperature of 4±1ºC, in the absence of light, to prevent their weathering and carbonation.

Concrete formulations. Thirteen formulations of concrete were prepared (Table 1). The reference formulation (F1), which was adopted from other work [8], was constituted by reference materials: cement, sand, 10 mm calcareous gravel and water. The formulations F2 to F13 were prepared with bottom and fly ashes. Three levels of cement substitution by fly ashes were used: 10% (F2 to F5), 20% (F6 to F9) and 30% (F10 to F13). In each of these formulations, four percentages of substitution of aggregates (sand and gravel) by bottom ashes were applied: 0% (F2, F6, F10), 9% (F3, F7, F11), 18% (F4, F8, F12), 36% (F5, F9, F13). The fresh concrete was prepared in a concrete mixer (Matest B025-SP), and then was placed in cylindrical plastic molds with 80 mm height and a diameter of 70 mm. Each mold containing the fresh concrete was submitted to a vibration process, with an amplitude of 0.3 mm, in a mechanical vibrator (Retsch AS 200 digit), in order to remove air bubbles. The molds were then capped and stored at 20±1ºC on the absence of light.

Table 1. Composition of the thirteen formulations of concrete [% wb]

Code	Cementitous materials		Aggregates			Water
	Fly ashes	Cement - CEM IV/A(V) 32,5N	Bottom ashes	Sand	Calcareous gravel - 10 mm	
F1 (ref.)	0.0	26.9	0.0	21.7	39.3	12.1
F2	2.7	24.2	0.0	21.7	39.3	12.1
F3	2.7	24.2	5.4	17.4	38.2	12.1
F4	2.7	24.2	10.9	13.0	37.1	12.1
F5	2.7	24.2	21.7	4.3	35.0	12.1
F6	5.4	21.5	0.0	21.7	39.3	12.1
F7	5.4	21.5	5.4	17.4	38.2	12.1
F8	5.4	21.5	10.9	13.0	37.1	12.1
F9	5.4	21.5	21.7	4.3	35.0	12.1
F10	8.1	18.8	0.0	21.7	39.3	12.1
F11	8.1	18.8	5.4	17.4	38.2	12.1
F12	8.1	18.8	10.9	13.0	37.1	12.1
F13	8.1	18.8	21.7	4.3	35.0	12.1

Compressive strength test. The concrete formulations were submitted to a maturation period of 28, 60 and 90 days, in the absence of light, at 20±1ºC, and in plastic molds to avoid air contact. In each of these maturation periods, the formulations were submitted to a compressive strength test in a Form+Test Digimess-M10, according to NP EN 12390-3. After 90 days of maturation, two formulations were selected for further characterization: the reference formulation (F1) and one new formulation of the set F2 to F13. The criteria for the selection of the new formulation were the

following: 1) selection of two formulations that had presented the highest compressive strength; 2) among the two formulations identified in item 1), the formulation containing the highest percentage of substitution of cement by ashes was selected for further characterization.

Leaching tests. The selected formulations were submitted to two different leaching tests after 90 days of maturation: a) leaching test with a liquid to solid ratio (L/S) of 10 L/kg (according to European Standard EN 12457-2) and using synthetic freshwater medium as leaching agent (ISO 6341, 1996); b) leaching test with L/S ratio of 10 L/kg and using synthetic marine water as leaching agent (ASPM medium, based on ISO 10253). The eluates produced in both leaching tests were submitted to a chemical characterization that comprised the following parameters: pH, phenolic compounds, F^-, dissolved organic carbon (DOC), SO_4^{2-}, total dissolved solids (TDS), Cl^-, Sb, Hg, As, Se, Cd, Cu, Cr, Cr VI, Ni, Zn, Pb, Mo, Ba, Na, K, Fe, Al, Ca and Mg.

Results and Discussion

Compressive strength data. Figure 1 shows the results of the compressive strength test after 28, 60 and 90 days of maturation of the reference formulation (F1) and of the formulations containing 10% of fly ashes (formulations F2, F3, F4 and F5).

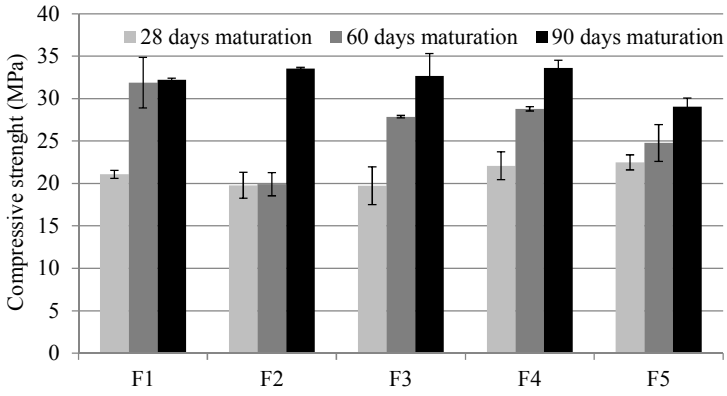

Figure 1. Compressive strength values of the reference formulation (F1) and of the formulations F2, F3, F4 and F5, after 28, 60 and 90 days maturation (±SD, 2 repl.)

The compressive strength values have generally increased with the increase of maturation period. The compressive strength of the reference formulation was very similar at 60 and 90 days of maturation (~32 MPa), while in the new formulations it was observed a tendency for the gradual increase of the compressive strength values throughout the maturation periods. After a period of 90 days of maturation, the compressive strength of F1 formulation was similar to or even lower than those observed for the new formulations containing 0%, 9% and 18% of bottom ashes.

Figure 2 shows the results of the compressive strength test after 28, 60 and 90 days of maturation for the formulations containing 20% of fly ashes (formulations F6, F7, F8 and F9) and again for F1. The compressive strength values of the new formulations have gradually increased with the increase of the maturation periods. After a 90 days maturation period, the compressive strength of F1 formulation was slightly higher than those observed for the new formulation. The new formulation containing 18% of bottom ashes (F8) has presented the highest compressive strength value among the new formulations.

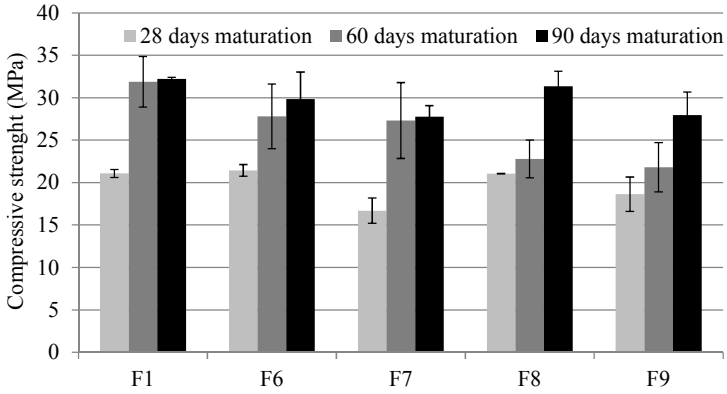

Figure 2. Compressive strength values of the reference formulation (F1) and of the formulations F6, F7, F8 and F9, after 28, 60 and 90 days maturation (±SD, 2 repl.)

Figure 3 shows the results of the compressive strength test after 28, 60 and 90 days of maturation for the reference formulation (F1) and for the formulations containing 30% of fly ashes (formulations F10, F11, F12 and F13).

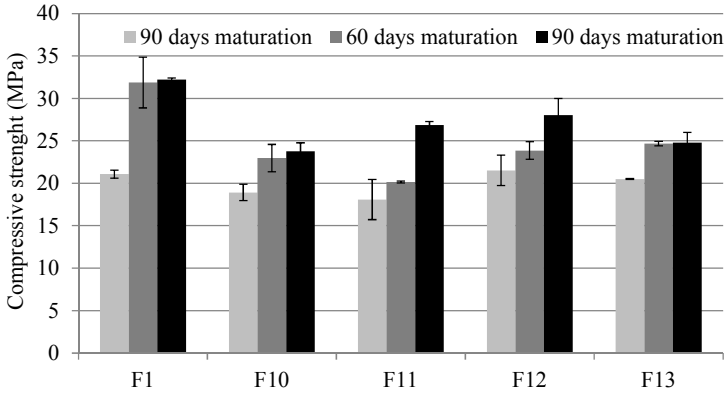

Figure 3. Compressive strength values of the reference formulation (F1) and the formulations F10, F11, F12 and F13, after 28, 60 and 90 days maturation (±SD, 2 repl.)

The compressive strength values of the new formulations have generally increased with the increase of maturation period. Nevertheless, after a period of 90 days of maturation, the compressive strength of the reference formulation F1 was much higher than those registered for the new concrete formulations. The new formulation containing 18% of bottom ashes (F12) has presented the highest compressive strength value among the new formulations.

The overall analyses of the formulations revealed a tendency for the reduction of the compressive strength with the increasing substitution of cement by fly ashes. Only the lowest substitution of cement by fly ashes (10%) has produced concretes with compressive strength values similar or slightly higher than that obtained for the reference material F1. In the new formulations containing a substitution level of 20 and 30% of cement by fly ashes, the highest compressive strength results were obtained in the formulations containing a percentage of substitution of natural aggregates by bottom ashes of 18% (F8 and F12).

Chemical characterization of eluates. Table 2 shows the chemical characterization of the eluates of concretes, after a maturarion period of 90 days. The concentrations of phenolic compounds, F^-, DOC, Al, Fe, Mg, Cu, Zn, Ba, Cd, Mo, Pb, Ni, Cr, As, Hg, Se and Sb are not shown because they were below the quantification limits.

The pH values produced by the freshwater eluates were higher to those produced by the marine eluates. The highest pH values observed in the freshwater eluates may indicate the release of oxides from the formulations. Nevertheless, it was not observed any significant difference between the reference material and the new formulation F4.

Table 2. Chemical characterization of the selected formulations of concrete (mg/kg db ±SD, except CrVI in μg/kg db and pH in Sorensen scale)

Parameter	Freshwater eluates		Marine eluates	
	F1	F4	F1	F4
pH	10.3 (±0.1)	10.4 (±0.2)	8.04 (±0.20)	8.14 (±0.08)
SO_4^{2-}	49.0 (±5.1)	38.7 (±4.8)	36.1 (±2.5)	51.1 (±5.3)
TDS	1175 (±184)	597 (±94)	1796 (±111)	1033 (±129)
Cl^-	547 (±54)	438 (< 1)	505 (±31)	617 (±36)
Na	24.0 (±0.2)	10.1 (±1.3)	58.5 (±9.3)	24.8 (±0.78)
K	67.0 (±0.7)	83.9 (±1.3)	131 (±13)	109 (±15)
Ca	271 (±51)	215 (±17)	772 (±105)	511 (±52)
Cr VI	1.98 (±0.11)	1.66 (±0.20)	0.26 (< 0.01)	0.35 (±0.01)

From the set of the alkali and alkali-earth elements only Ca, Na and K have presented concentrations above the detection limit. Generally, the release of these elements was lower in formulation F4 than in the reference concrete. The concentrations of all heavy metals analysed, except Cr VI, were below the detection limit, which indicate a leaching rate quite reduced. In the freshwater eluates, the concentration of Cr VI was lower in the formulation F4 than in the reference one. In what concerns the marine eluates, the concentration of CrVI was higher in formulation F4 (0.35 μg/kg) than in F1 formulation (0.26 μg/kg).

Conclusions

The concrete formulations prepared with ashes produced during the combustions of forestry biomass residues have presented similar to slightly higher compression strength of the reference concrete. The substitution of 10% cement by fly ashes (F2, F3, F4, F5) has not promoted the reduction of the compressive strength of the concrete. The substitution level of 18% of aggregates by bottom ashes (F4, F8 and F12) seems to have promoted the highest compressive strength values among the new formulations. The formulations F1 and F4 have presented very low emissions levels of chemical pollutants in both leaching scenarios (marine and freshwater). The new formulation F4 has presented emissions levels similar or lower to those observed for the reference formulation F1.

References

[1] J. Morais, R. Barbosa, N. Lapa, B. Mendes, I. Gulyurtlu: Resources Conservation and Recycling Vol 55 (2011), p. 1109

[2] M. Sami, K. Annamalai, M. Wooldridge: Progress on Energy Combustion Science Vol 27 (2011), p. 171

[3] H.H. Acma: Energy Conversion Management Vol 44 (2003), p. 155

[4] A. Al-Kassir, J. Gañán-Gómez, A.A. Mohamad, E.M. Cuerda-Correa: Energy Vol 35 (2010), p. 382

[5] J.F. González, B. Ledesma, A. Alkassir, J. González: Biomass and Bioenergy (In Press)

[6] R.E Melchers, C.Q. Lib: Cement and Concrete Research Vol 39 (2009), p. 1068

[7] S.-W. Pack, M.-S. Jung, H.-W. Song, S.-H. Kim, K.Y. Ann: Cement and Concrete Research Vol 40 (2010), p. 302

[8] E. Nawy, in: Concrete Construction Engineering Handbook. Taylor & Francis Group, 2nd Edition, New York, USA (2008).

doi:10.4028/www.scientific.net/AMR.587.21

A Study on Hardened State Properties of SCC using Fly Ash and Blended Fine Aggregate

Brabha H Nagaratnam[1, a], ME Rahman[1,b] and MA Mannan[2,c]

[1]Curtin University, Sarawak, 98009 Malaysia

[2]University Malaysia Sabah 88400 Malaysia

[a]brabhahari@curtin.edu.my, [b]merahman@curtin.edu.my, [c]mannan@ums.edu.my

Keywords: Self Compacting, Concrete; Low calcium, Fly ash; Mechanical properties, Compressive strength, Tensile strength, Absorption, Chloride penetration, Sorptivity.

Abstract. The aim of this research is to investigate hardened state properties of Self Compacting Concrete (SCC) containing low calcium based fly ash. The mixtures were prepared using various proportions of Class F fly ash ranging from 0% to 30% cement replacement. Water to powder ratio is 0.38 – 0.39 and powder content was kept constant at 540 kg/m3. Properties investigated were strength properties (compressive strength and splitting tensile strength), and durability properties (complete immersion water absorption, apparent volume of permeable voids (AVPV), sorptivity, and RCIPT tests. These tests were done at various days. Results showed that fly ash replacement of up to 30% gave acceptable strength and durability properties for medium strength SCC.

Introduction

SCC is seen worldwide as one of the most important developments in concrete materials technology. The main advantage of SCC is that it eliminates the need for the time consuming, labour-intensive, traditional methods of compaction. SCC can flow under its own weight, even through dense and congested reinforcement, filling formwork without any segregation or bleeding [1]. This is usually done by high content of cement, fines and sand with addition of superplasticizer. The high cement content is usually reduced by using supplementary cementitious material like fly ash, ground blast-furnace slag and silica fume. The replacement of cement with fly ash, while improves workability, it also aids in lowering the carbon footprint associated with concrete production and reduces the overall costs of construction material.

Details on Material for Testing

Cement. Ordinary Portland Cement (OPC) grade 42.5 based on ASTM C150 was used in the concrete as cementitious material. It also conforms to the Malaysian standard MS 522: Part 1 - 2007 while fulfilling the ISO 9001 and 14001 quality requirements. The particle density of the cement is 2950kg/m3.

Fly Ash. Low calcium fly ash, Class F as per ASTM C618 [2], was obtained from Sejingkat Coal Fired Power Station in Sejingkat, Kuching. The chemical composition of the fly ash, as determined by X-Ray Fluorescence (XRF) analysis is given in Table 1.

Table 1 Chemical Composition of Fly Ash and Cement [%]

Compound	*Fly ash*	*Cement*
SiO_2	57.8	20.0
Al_2O_3	20.0	5.20
Fe_2O_3	11.7	3.30
SO_3	0.08	2.40
MgO	1.95	0.80
CaO	3.28	63.2
K_2O	3.88	-
TiO_2	2.02	-
Na_2O	0.30	-
SO_3	-	2.40
Loss on igntion	0.32	2.50

Course Aggregate. 10mm nominal size coarse aggregate (crushed quartzite) was used in this research. It is composed of particles within the range of 5mm to 10mm. Sieve analysis of 2000 gram sample showed that the entire sample (100%) passed through 9.5mm sieve while only 5% passed the 4.75mm sieve (i.e. 95% retained on 4.75mm sieve). The aggregates fulfill the requirements in AS 2758.1 [3] for 10mm single sized aggregate.

Fine Aggregate. Fine Aggregate S 2758.1-1998 [3] categorizes aggregates with particles finer than 4.75mm as fine aggregates for concrete mix design. After several mix trials using various proportions and grades of fine aggregates, two types was finalized. The first category was a nominal size of 5.0mm with particles coarser than 600µm (crushed quartzite). The other category had a nominal size of 600µm (uncrushed river sand) with the presence of some micro-fines (particles of size less than 75µm). Characteristics of both types are shown in Table 2 & Table 3.

Table 2 River Sand gradation

Sieve Size (µm)	% Finer	AS 2758.1 Requirements
600	100	15 -100
300	58	5-50
150	10	0 -20

Table 3 Crushed Quartzite gradation

Sieve Size	% Finer	AS 2758.1 Requirements
4.75mm	99	90 -100
2.36mm	50	60 -100
1.18mm	20	30 -100
600µm	2	15 - 80

The fineness modulus of the local river sand is 1.32 and the fineness modulus of crushed quartzite is 4.29.

Admixtures. The super-plasticizer used in this research was supplied by Sika Kimia Sdn Bhd. The trade name of the high range water reducing admixture is Sikament®-NN and conforms to the requirements of ASTM C494 Type F [3] while the chemical base of the dark brown liquid is Naphthalene Formaldehyde Sulphonate. It is a dual action liquid for producing free flowing concrete or as a substantial water-reducing agent.

Mix Proportions. The main objective of this research is to develop a fly ash based normal strength (less than 60MPa) SCC. Four concrete mixes were designed and the dosages of fly ash are limited to 0%, 10%, 20%, & 30% by mass of the total cementitious material. Crushed quartzite was mixed with river sand to increase its fineness modulus. The maximum size of the coarse aggregate is limited to 10mm. The mix proportions of SCC are summarized in Table 4.

Table 4 Mix Proportions of SCC

Mix Material	***FA0***	***FA10***	***FA20***	***FA30***
Water to powder ratio	0.38	0.38	0.39	0.39
Cement by weight of powder (kg/m^3)	540	486	432	378
Fly ash by weight of powder (kg/m^3)	0	54	108	162
Fine aggregate 0/600µm (kg/m^3)	230	240	240	245
Fine aggregate 600µm/5mm (kg/m^3)	630	630	630	630
Coarse aggregate 5/10mm (kg/m^3)	690	690	690	690
Superplasticizer (kg/m^3) & (% by powder weight)	9.72 (1.8%)	9.72 (1.8%)	9.18 (1.7%)	9.18 (1.7%)
Total density of concrete (kg/m^3)	2305	2315	2320	2325

Due to the poorly graded aggregates used in this study, a specific mix procedure had to be followed for optimal mixing outcomes. The mixer used was a 0.5m^3 capacity 'forced action cylindrical pan mixer' with a vertical axis of rotation.

All the aggregates were first put into the pan and run for a minute. The powders (fly ash and cement) were then added and run for another minute. About 60% of the required water was added slowly and the mixer run for another minute. 30% of the water and 90% of the super plasticizer was mixed in a bucket and slowly added to the pan and run for about 3 minutes. The consistency of the resulting mixes was observed and the remaining 10% of water and 10% of super plasticizer (mixed together) was used to adjust the mix. The resulting mixture was then allowed to rest for not less than 2.5 minutes (for air dissipation), and remixed for 20 to 30 seconds. Workability tests [1] were done to investigate the fresh properties and finally the samples are casted in various moulds.

Tests on Hardened State SCC for Strength. Cylindrical specimens casted were tested for compressive and tensile strengths (indirect tensile strength by splitting tests) using a Universal Testing Machine, as per AS1012.9. Compression tests were carried out after 03, 07, 14, 28, 56 and 84 days of curing while splitting tests were carried out after 14, 28, 56 and 84 days .

Tests on Hardened State SCC for Durability. As per standard requirements, initially casted 200mm long cylinders were sliced into four pieces (of each 50mm long) for durability tests. All tests were carried out at 14, 28, 56 and 84 days after curing except for rapid chloride ion penetration test (RCIPT) which was carried out at 28 and 84 days only.

Complete immersion water absorption (AS 1012.21) was measured by first noting the oven dry weight, immersing in water for 48 hours and then calculating the weight gain as a percentage of the oven dry weight. For apparent volume of permeable voids (AVPV) test, samples were oven dried (noting dry mass as OD), boiled in water for 5 hours and let to cool down for 14 hours (noting surface dry mass as MSD) and then weighing the specimen while being suspended in water (noted as MA). The expression 100 x (MSD-MO)/(MSD-MA) was used to calculate AVPV (AS 1012.21). Sorptivity test measures water uptake though bottom surface of a specimen (other surfaces sealed) by capillary suction (ASTM C1585) and determined as the slope of regression lines obtained by plotting graphs of the water uptake per unit area (kg/m^2), versus the square roof of time at which uptake was recorded. RCIPT tests (ASTM C1202) were carried out by first conditioning specimens (curved surfaces coated with silicone) in a vacuum desiccator for 3 hours and then measuring the current passing through the specimen for 6 hours (at 30 minute intervals). Voltage cell was made of one NaCl negative terminal and one NaOH positive terminal, between which the specimens were clamped and a potential difference of 60V created. The total charge (coulombs) passed was calculated using the equation; $Q = 900 \times (I0 + 2I30 + \ldots + 2I330 + I360)$.

Results and Discussions

Strength of Hardened SCC. Figure 1 indicates that **t**he compressive strengths decrease with increase in fly ash content. Similar observations were reported by Sonebi [5] and Liu [6]. At 28 days, strengths of FA0, FA10 and FA20 are almost the same, indicating that fly ash becomes active with time (i.e. fly ash reacts slowly thus reducing early age strength as observed at 03, 07 and 14 days). Beyond 56 days, FA10 achieved strengths higher than FA0 confirming the fact that fly-ash contributes to long term strength gain and is attributed to the late hydration reactions in fly ash. This is because fly ash undergoes pozzolanic reactions beyond 28 days making the concrete matrix denser i.e. internal voids gets filled and interfacial bonds intensify as curing duration increases.

Table 5 shows that tensile strength decreases with increase in fly ash content. At 28 days, FA10 achieved the same strength as FA0 and exceeds FA0 beyond 56 days. The late tensile strength gain is more intensive than compressive strength implying that the improvements in interfacial bonds due to fly ash reactions, improves tensile strength more. This is because tensile strength entirely depends on how well particles in concrete are held together. If particles are held loosely, the ‘pulling effect’ imposed on specimens during tensile loading would easily lead to failure.

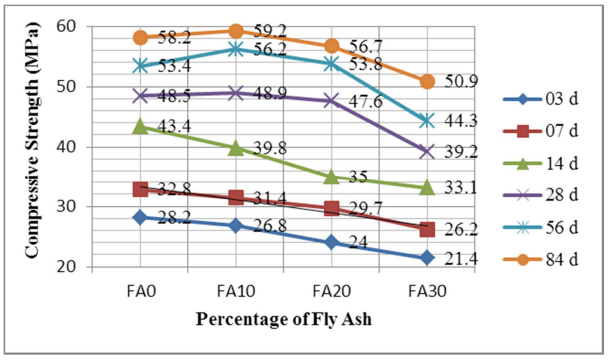

Fig. 1 Variation of Compressive Strength

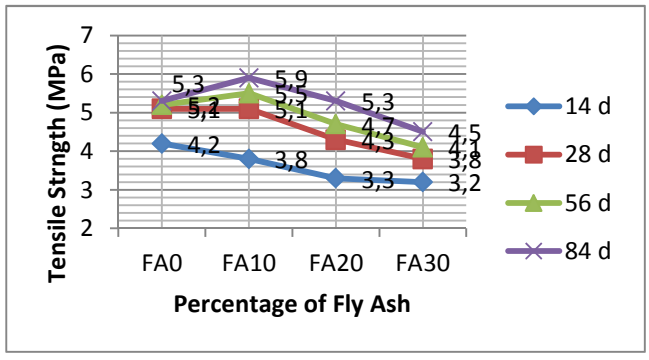

Fig. 2 Variation of Tensile Strength

Durability of Hardened SCC

Immersed water abosorption. Figure 3 shows that at 14 days, absorption level is highest with no significant trend (almost constant) with varying fly ash content as the concrete matrix is too porous at this early stage. Absorption decreases significantly between 14 and 84 days for same cement replacement levels, while the rate of decrease is faster for fly ash containing mixes. This is because with curing time, reactions intensify with fly ash leading to a finer pore structure which reduces absorption.

Apparent volume of permeable voids. Figure 4 shows that the trend in variation of AVPV with fly ash is similar to water absorption. Boiling reduces the ability of fly ash to resist water intake. Hence for the same fly ash content, boiled permeability is higher than simple water absorption.

Sorptivity. Figure 5 shows that sorptivity (water absorption by capillary suction) remains almost constant up to FA30 earlier than 28 days while a slight improvement is seen at 56 and 84 days.

Rapid chloride ion penetration. From Figure 6 it is evident that at same test age, all fly ash containing mixes show better resistance to chloride penetration (low charge passed) than FA0 while increase in fly ash reduces the resistance. Furthermore, 84 day penetrability is much lower than at 28 days. Note that this timely improvement caused by pore structure densification is smallest for FA0. As per ASTM C1202 criteria (Q <1000), all the fly ash containing mixes in this research, at 84 days, fall under 'very low' penetrability category [7]. It can hence be concluded that fly ash incorporation in SCC improves its resistance to chloride penetration.

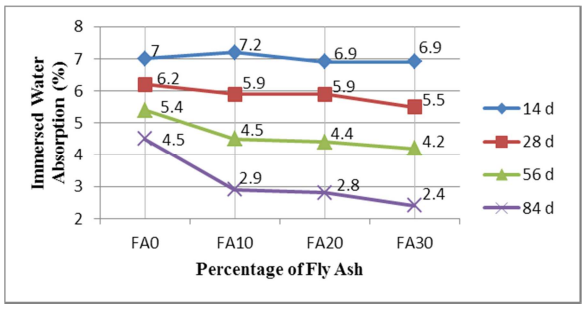

Fig. 3 Immersed Water Absorption Values

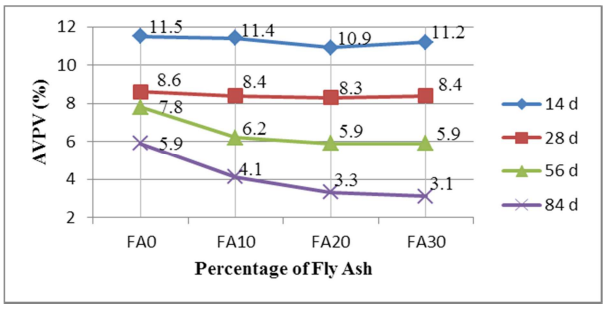

Fig. 4 Variation of AVPV

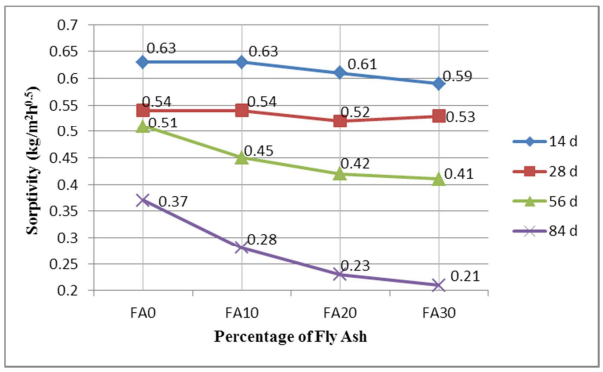

Fig. 5 Variation of Sorptivity

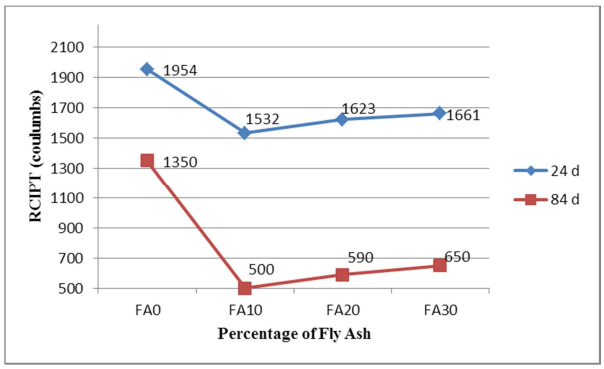

Fig. 6 Variation of RCIPT

Summary

Incorporation of fly ash in SCC reduces both compressive and tensile strengths however strength gain is faster in the long term. At low fly ash level, mixes can even be stronger than non-fly ash SCCs in the long term. Immersed water absorption, AVPV and Sorptivity decreases over long term. Any amount of fly ash improves resistance to chloride ion penetration significantly and is better at 84 days.

References

[1] N. Brabha, M. E Rahman, M.A Mannan, A. Faheem: *Investigation on Workability of SCC Using Low Calcium Based Fly ash*, 3rd CUTSE International Conference, 8-9 Nov., Sarawak, Malaysia.

[2] ASTM C 618-85, Standard Specification for Fly Ash and Raw Calcined Natural Pozzolan for Use as a Mineral Admixture in Portland Cement Concrete (1985), p. 385 – 388

[3] AS 2758.1-1998 Aggregates and rock for engineering purposes – Concrete aggregates

[4] ASTM C494 / C494M – 11, Standard Specification for Chemical Admixtures for Concrete.

[5] M.Sonebi: Cement and Concrete Research 34 (2003), p. 1199–1208.

[6] M. Liu, in: Wider Application of Additions in Self-compacting Concrete, PhD Thesis, University College London.

[7] ASTM C1202, Standard Test Method for Electrical Indication of Concrete's Ability to Resist Chloride Ion Penetration.

doi:10.4028/www.scientific.net/AMR.587.26

The Usability of Fly Ash for the Construction of Embankment Dams

Vít Černý[a], Rostislav Drochytka[b] and Jan Jandora[c]

Brno University of Technology, Faculty of Civil Engineering, Institute of Technology of Building Materials and Components, Veveří 331/95, 602 00 Brno, Czech Republic

[a]cerny.v@fce.vutbr.cz, [b]drochytka.r@fce.vutbr.cz, [c]jandora.j@fce.vutbr.cz

Keywords: Fly ash, dikes, embankment, dams, injection.

Abstract. Power supplying industry in the Czech Republic is still dependent on thermal power plants. Due to the on-going and completed renovation of the existing power plant units, it is expected that they will be serviceable for the following 30 years. It is therefore necessary to look for suitable use of the by-products of these plants.

Using the energy by-products during construction of dikes is currently limited to creation of little protective dikes on unloading yards of fly ash stabilizers. Here we can take advantage of the binding abilities of the energy by-product to stabilize the unloading yards and protect the environment. This method is technologically less effective for constructions of anti-flood dikes. Therefore we use the soils from the vicinity of the building area. A suitable method of using fly ash in water building industry lies in repairs of existing earth dams by using fly-ash and clay grouting that increase homogeneity, stability and impermeability of the dam.

This paper deals with laboratory verification of suitability of different types of fly-ash in the mixture with special sealing clay. It also deals with designing optimal recipes for "on-site" testing. Results of the tests clearly recommend classical fly ash as the most suitable raw material. On the other hand, the bedding ash marked is not suitable for this technology.

Introduction

Dikes are amongst the world's oldest hydro engineering structures. Their history began many thousands of years ago, which can be proved by the remains found in all centres of ancient culture, especially in China, India, Egypt and Mesopotamia. This fact often leads to the erroneous supposition that the long history of this type of construction contributes to progress in this particular field of civil engineering, which should logically have certain superiority over other younger branches of the science, for example, hydroelectric works. However, a thorough study of the present state of the design and construction of dikes persuades us that the reverse is true.

This unfavourable situation is evidenced in the fact that modern scientific knowledge about soil mechanics, hydro-geology and hydrology, nor even experience in modern construction technology, have been taken sufficiently into account when designing dikes. If we consider the profiles of dikes planned or constructed over the last twenty years, we see that new gains in our knowledge of the functional properties of soils commonly used in earth dams, are ignored both from the point of view of stability and from the possibilities of seepage and uplift control in embankment sub-soils.

Drawing knowledge from dam engineering leads, as with most problems, to an excessively perfectionist view of their solution; this results in a substantial increase in construction costs.

With regard to the inevitability of a reappraisal of our knowledge, we shall concern ourselves fairly thoroughly with the theory of seepage and calculations of stability, and also with examining the difficult geological conditions in the actual subsoil of dikes, not only in completely ideal conditions. From this standpoint, we also wish to analyse sealing methods and dikes-building technology, but without losing sight of the fact that our main concern is with the correct evaluation of dimensions, and solutions to the problems of dikes in unfavourable and changing geological conditions.

Rehabilitation of earth dams

One of the economically and technologically advantageous methods of dam repairing works consists in use of injection technologies which are used for example during implementation of micro piles, rock anchors, sealing walls, etc., when foundation soils characteristics are improved.

During works on injection of frictional rocks, the injection mixture fills the pores between grains of the rock. The mixture binds the pores, thereby creating artificial rock geo-composite. Such injected frictional (incoherent) rock has better mechanical characteristics and reduced permeability [1].

The technology is particularly suitable for repairs of such parts of the dams in which there is an excessive amount of cavities, inhomogeneity, increased groundwater flow, etc. It means the cases with threat of losing strength and breaking. These places can be located for example by using ground radars. Then later these places are verified by creating a so-called inspection drill-hole or shaft (Fig. 1).

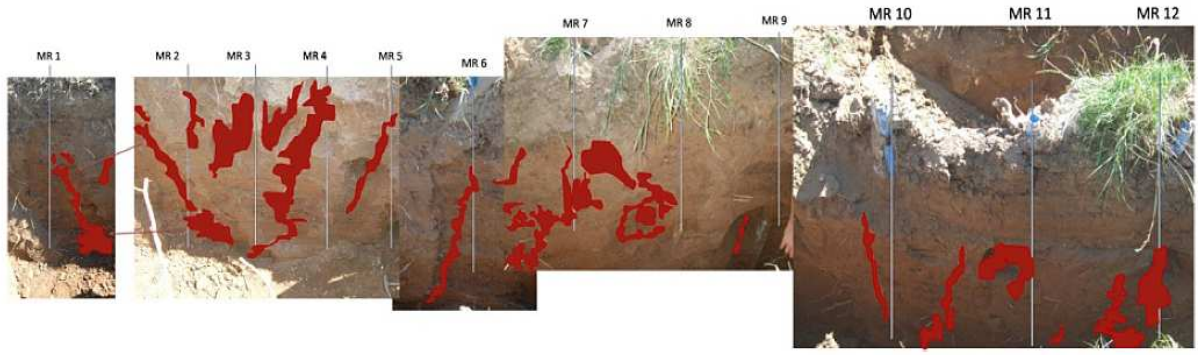

Fig. 1 Inspection shaft with marked cavities

In the next stage, there are the area designed for repair, the average value of individual drill-holes, their depth and spacing. Then there is subsequent process of grouting in the area by using clay mixture with the help of special technology (Fig. 2 and Fig 3). Sample cases in the pictures were made by Sächsische Bau GmbH by using the technology without direct grouting through the hollow axis of the drilling equipment, there was the additional pressure method instead [1].

Fig. 2 Making boreholes

Fig. 3 Pressure filling of the holes using clay mixtures [1]

Experimental verification of the basic recipes of ash-clay mixtures

Regarding the permanently high production of energy by-products in the Czech Republic, it is appropriate to address the experimental verification of their suitability for repairs of protective dikes. There were three fly-ashes selected from the classical method of burning (PR, PC, LE) and two from fluidized combustion (LEF-filter and LEB-bottom). These secondary raw materials will subsequently be used for partial substitution of high-quality clay of Ge which had already been used before to seal the dams. The basic parameters which are evaluated in the input raw materials, include granulometry, limit of fluidity, plasticity, maximum volume weight (Proctor Standard), coefficient of hydraulic conductivity.

Determination of granulometry

One of the basic parameters related to raw materials used for sealing the dam is granularity which should meet the requirements of the standard ČSN 75 2410 (grain line is located in area No. 2, or No. 1, Fig. 5).

Figure No. 5 shows the granularity curves of the various raw materials intended for using in the grouting technology. To assess the suitability, there are the boundary curves dividing the space into 3 main areas according to ČSN 75 2410. Suitable soils for sealing parts of the dam, according to this standard mentioned in Section 7.3.4, are identified as those whose line of granularity lies in the area of 2, or also in the area of 1. It is obvious from the graph shown in Fig. 5 that in terms of granularity the best results are expected when using high-temperature ash fly marked PC and LE whose granulometry curve does not lie in the minimum prescribed area No. 2 just in the very little part. Looking at the granularity curve of the tested clay of Ge, it is apparent that it contains more than 70 % of particles of size lower than 1 μm, which is an excellent assumption for very low values of filtration coefficient.

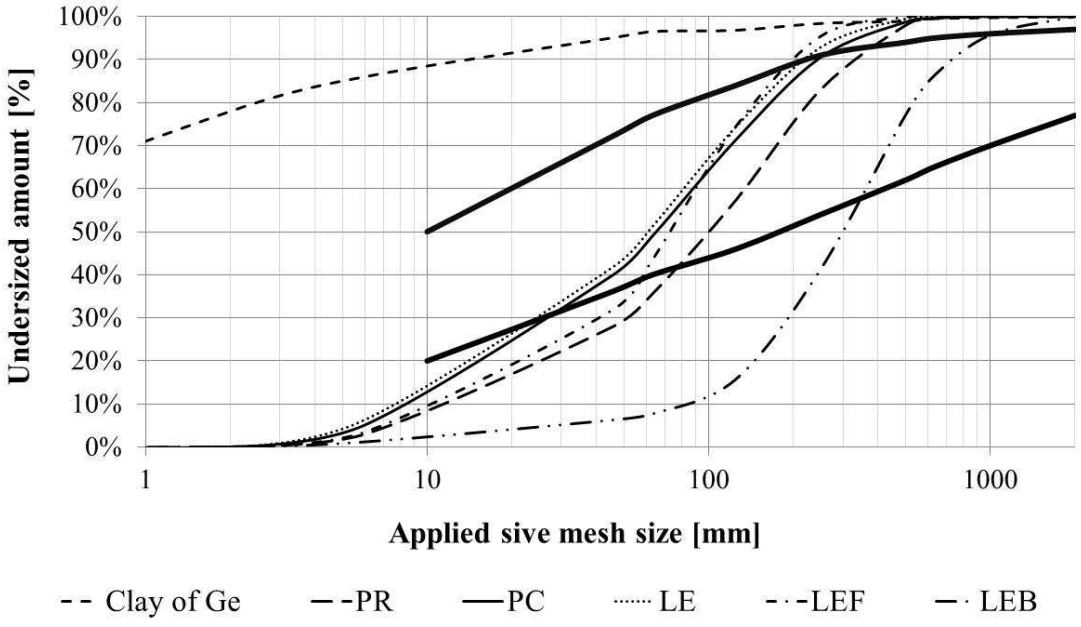

Fig. 5 Cumulative undersize distribution of material particles

Proctor test of maximum volume weight

To classify the soil according to ČSN 75 2410, it is necessary to determine the maximum volume weight value by using the Proctor test. For this phase, it has been necessary to create test mixtures of clay with secondary raw materials. The mixing ratios were determined to 25: 75 and 50: 50 (energy by-product: clay).

The test procedure is defined by the standard of ČSN EN 13286-2. The Proctor test of the maximum volume weight density $\rho_{d\max}$ [kg.m^{-3}] specifies the method of laboratory determination of dependency between moisture and volume weight of the soil which can be achieved by standardized compaction working of the soil in the normative mortar, using normative rammer, according Proctor standard test. Compactness of the soils is expressed by the maximum volume weight of dry soil at the optimal moisture of w_{opt} [%].

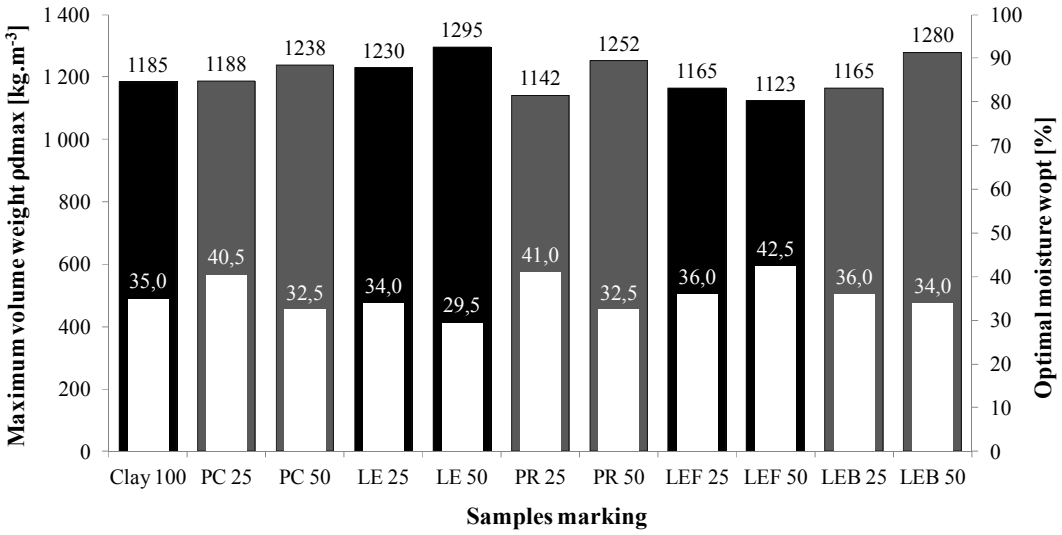

Fig. 5 Graphical representation of results related to determination of the maximum volume weight

With the reference to the standard of ČSN 75 2410, the results approach the values (ρ= 1330–1400 Kg.m^{-3}, w = 33–35 %) of the group marked as MH with which it is possible to approximately achieve the values of the coefficient of hydraulic conductivity $k = 8.10^{-9}$ to 1.10^{-10} m.s^{-1}.

Determination of hydraulic conductivity coefficient

The coefficient of hydraulic conductivity was determined by the test with a release-meter having constant slope in accordance with the valid standard of ČSN CEN ISO/TS 17892-11 "Geotechnical research and testing - Laboratory testing of soils - Part 11: Determination of permeability of soils at constant and variable slope".

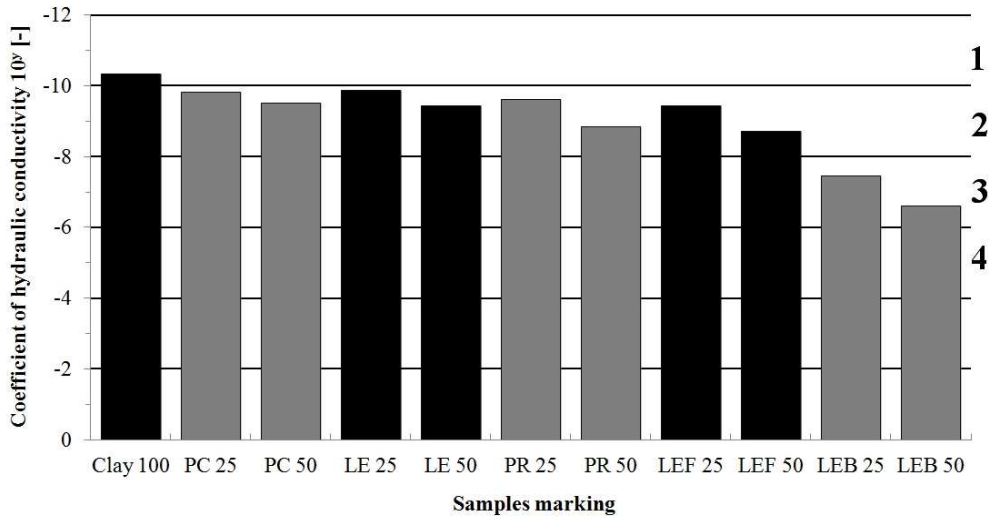

Fig. 6 Graphical representation of hydraulic conductivity

Legend:		
1 - very impermeable	$<10^{-10}$	Clay with high level of plasticity
2 - impermeable	10^{-8} ------ 10^{-10}	Medium-plastic, sandy and argillaceous clays
3 - low permeability	10^{-6} ------ 10^{-8}	Argillaceous sands and clay gravels
4 - permeable	10^{-4} ------ 10^{-6}	Sands and gravels with soils

Figure No. 6 shows results of the hydraulic conductivity coefficient determination, including the limit boundaries for each area of permeability, according to ČSN 75 2310. The results of the hydraulic conductivity coefficient determination confirmed previous assumptions. They showed high-temperature fly ash marked PC and LE as the most suitable alternative raw materials to replace montmorillonitic clay of Ge, mainly due to the high proportion of fine fraction and the amorphous phase. High-temperature fly ash marked PR and fluidized fly marked LEF are also meant as a suitable alternative. They also maintained the value of hydraulic conductivity coefficient at the level of impermeable soils, even with the 50 % replacement of clay. Due to its nature and low proportion of fine fraction, the bedding ash cannot be recommended for this purpose.

An interesting finding was observed when measuring permeability of the samples mixed with high-temperature fly ash during which considerable swelling of montmorillonitic clay of Ge was maintained. Some test results reached the values of hydraulic conductivity coefficient at the levels of 10^{-12}; whereas it took up to 7 days to wait until the sample started to leak water. This finding offers the very suitable use of clay-ash mixtures during repairs of the protective dikes. Using this method, they are able to remain for a long time without leakage when flooded.

Summary

Results of the tests clearly recommend classical fly ash marked PC, LE and PR as the most suitable raw material. These ashes excellently substitute primary raw material thanks to their high proportion of fine fractions. The high sealing effect was achieved even at the level of fifty per cent replacement of the highly plastic clay. On the other hand, the bedding ash marked LEB is not suitable for this technology, mainly because of the very low proportion of fraction sized under 0.063 mm.

It can be stated that the use of energy by-product to repair existing earth dams by using the technology of mixture injection based on clays has great potential, especially in the current situation in which there is a large number of small dams which no longer fulfill their original function very effectively.

Acknowledgement

The paper was developed thanks to the financial support from the national budget via the Ministry of Industry and Trade under the project entitled *New Progressive Rehabilitation Technologies of Dikes and Embankment Dams*, project code FR—TI4/335.

References

[1] http://www.wiebe.de/de/saechsische-bau/referenzen/index.php

[2] ČSN 75 2410 (752410) Small water reservoirs

[3] ČSN 75 2310 (752310) earth dams

[4] ČSN CEN ISO/TS 17892-11 Geotechnical investigation and testing - Laboratory testing of soil - Part 11: Determination of permeability by constant and falling head

doi:10.4028/www.scientific.net/AMR.587.31

Development and study of the possibilities to use natural materials for thermal-insulation systems of ETICS

Hroudová Jitka[1, a], Zach Jiří[2, b]

[1,2]Brno University of Technology, Faculty of Civil Engineering, Institute of Technology of Building Materials and Components, Veveří 331/95, 602 00 Brno, Czech Republic

[a]hroudova.j@fce.vutbr.cz, [b]zach.j@fce.vutbr.cz,

Keywords: insulation materials, easy renewable natural resources (technical hemp, flax), external thermal insulation composite systems ETICS.

Abstract. Thermal insulation systems of ETICS are now mostly solved in the building industry, whether in terms of insulating the structures, choices of materials and subsequent recycling after the end of their life period. From the environmental point of view and also in the perspective of sustainable development, it is essential to look for other suitable material bases which relate only to easily renewable sources of raw materials or to industrial wastes which have long been available in sufficient quantity and quality. It is important that production of the insulation systems is energetically efficient modest in terms of manufacturing facilities. The aim of this paper is to verify the possibility of using natural insulation materials for thermal insulation systems ETICS. This paper describes the results of studies of key properties of insulations based on industrial hemp and flax and the results of computational simulations of the behavior of these insulations incorporated in the real systems ETICS.

Introduction

Energy savings in the building industry and ensuring of maximum comfort for people at minimum cost. These are questions which have been asked by the people since the immemorial times. Traces of this issue can be found at each stage of development related to the building industry. There has been significant technological development in the field of using insulation building materials for thermal insulation of building structures and insulation technologies in the recent years. At present, this is the method of contact thermal insulation of external walls from the exterior mostly used during thermal insulation works on buildings. The undeniable advantage of this oldest method of thermal insulation lies in increasing the thermal insulating properties and thermal stability of the outer perimeter walls of the building structures. We can every year see the growing demand for affordable thermal insulation materials with high utility characteristics. The materials which would be suitable alternatives to the currently most manufactured thermal insulations based on mineral wool and foam polystyrene. In terms of possible use of other alternative insulating materials for exterior contact thermal insulation systems of ETICS, there were materials based on natural raw materials originating from the field of agriculture, designed on the basis of research works in the Faculty of Civil Engineering of Technical University in Brno. That was about materials based on technical hemp and flax. The materials were produced by using residues of crops and wastes generated during cultivation and processing of these technical crops. Composition of natural insulation materials taken from the individual input components were as follows, see Figure 1, 2. [1, 2]

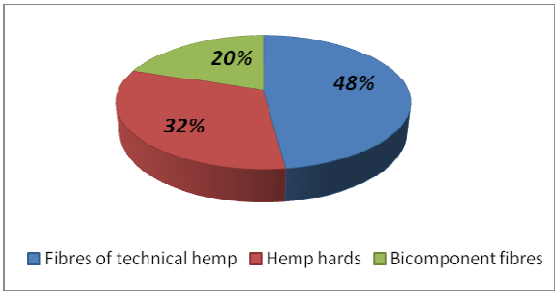

Fig. 1 Composition of samples of hemp insulation

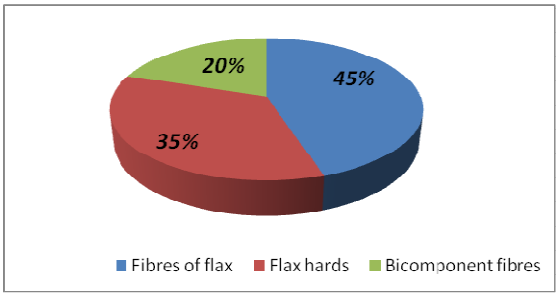

Fig. 2 Composition of samples of flax insulation

Fig. 3 Diagram of natural insulation materials

Production of natural insulations materials took place in a modern production line in Czech Republic, it was in a company called Canabest s.r.o. (Ltd.) in Břeclav-Poštorná. The above-mentioned production line allows processing of natural fibre materials. The waste-free manufacturing process is described in Figure 3. From the point of the view related to the use thermal insulation materials in the thermal insulation systems, some physical and mechanical parameters are meant as crucial. As for the perspective of normative requirements, it is especially necessary to take into account the requirements according to the following standards and regulations: EN 13499, EN 13500, EN 13162, EN 13163, ETAG 004 and CUAP Factory-made thermal insulation material and or acoustic insulation material made of vegetable or animal fibres. The natural materials were tested according to the above-mentioned legislation requirements. [1, 2]

Fig. 4 Photography of test sample (Flax board)

Fig. 5 Photography of test samples (Hemp boards)

Results of the measurement

The results of individual measurements are shown in Table 1. On the basis of the measurements, there were simulations of behavior of these natural materials in practice carried out by using the WUFI calculation program which allows calculating the real calculation of dynamic behavior of heat and moisture in the multilayer building structures subjected to external environmental conditions. [3, 4, 5, 6, 7, 8, 9, 10, 11, 12, 13]

Table 1: Overview of testing results

N.	Properties	Testing standards	Hemp board	Flax board
1	Reaction to fire test [-]	EN 13501-1, EN ISO 11925-2	E	E
2	Thermal conductivity [$W.m^{-1}.K^{-1}$]	EN 12667, ISO 8301	0,0404	0,0415
3	Thickness [mm]	EN 823	61	61
4	Density [$kg.m^{-3}$]	EN 1602	102	107
5	Short term water absorption by partial immersion [$kg.m^{-2}$]	EN 1609	7,67	8,02
6	Tensile strength perpendicular to faces [kPa]	EN 1607	12	16
7	Compressive stress at 10 % relative deformation [kPa]	EN 826	26	30
8	Length; Width [mm]	EN 822	1000; 501	1000; 501
9	Deviation from flatness [mm]	EN 825	2	2
10	Deviation from squareness on length and width of boards [$mm.m^{-1}$]; Deviation from squareness on thickness of boards [mm]	EN 824	2; 1	2; 1
11	Factor of diffusion resistance [-]	EN 12086	1,85	1,90
12	Biological resistance [-]	CUAP supplement C; EN ISO 846	Class 0	Class 0

A study was conducted classical behavior of real structures insulated with insulation systems ETICS on the basis of flax, and the results were compared with the construction of a system ETICS insulated with mineral wool. Calculations were carried out in WUFI program for the calculation considering the spread of unsteady heat and moisture.

The calculation program WUFI was developed model structure consisting of layers of material below:

- 10 mm Internal Lime cement plaster
- 240 mm Ceramics blocks
- 60 mm Insulation (Flax Board, Mineral Wool)
- 5 mm Basic layer with reinforcement
- 3 mm Mineral external plaster

The results of the moisture behavior of natural insulation based on flax in the construction in the period from 1.1.2010 to 01.01.2012 is shown in Figure 6, was created to compare the structural model of mineral wool, see Figure 7. The results of simulations of the moisture behavior of natural insulation boards based on flax suggests that they are moisture-sensitive compared with mineral wool, but the moisture content of flax insulation is only about twice as high as mineral wool insulation and overall maximum moisture content is around 5 %. In terms of year-round operation of the insulation can be seen that the moisture content does not increase in a comparison between years.

The calculation program was developed model structure consisting of layers of material below:

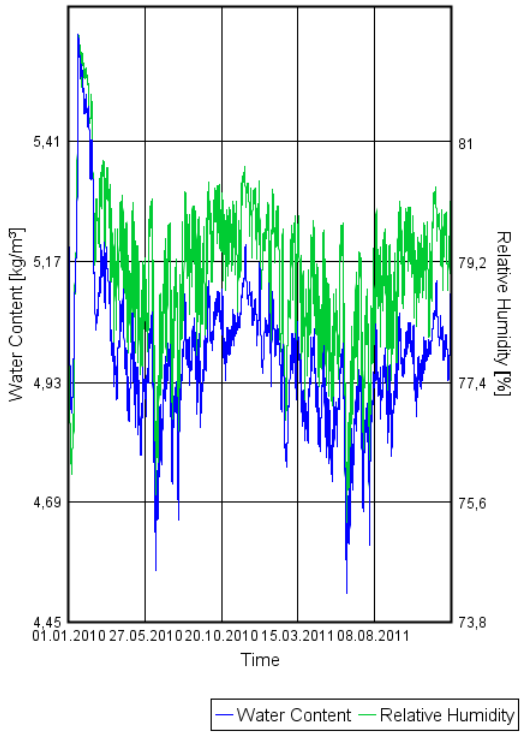

Fig. 6 Moisture behavior of flax insulation (dependence of water content on time)

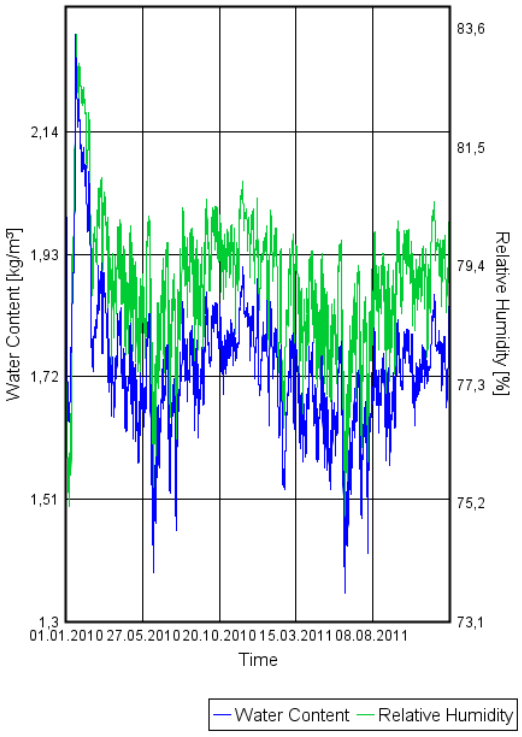

Fig. 7 Moisture behavior of mineral wool insulation (dependence of water content on time)

Currently, research is the realization of these natural materials in practice, where they will be regularly on a strict time intervals monitored thermal insulation and thermal-moisture characteristics of the construction and will be verified the possibility of application of these materials for external thermal insulation composite systems.

Conclusion

Based on the previously identified characteristics of natural insulation materials based on easily renewable, industrial crops (hemp, flax) can be stated that if these materials are properly incorporated in the insulation system to the building structure can be used as insulating materials suitable alternative to the currently used materials for thermal insulation of houses. It is necessary to resolve the issue, however, higher humidity sensitivity already in the system design to avoid increasing the moisture content in natural insulation, ie. degradation of thermal-insulating properties of the material and the function of the insulation system.

Acknowledgements

This paper was elaborated with the financial support of the project MPO FR-TI2/339.

References

[1] J. Hroudová; A. Korjenic; V. Petránek; J. Zach. Utilization of thermal insulating materials based on technical hemp for insulating of building structures. In Building Materials and Building Technology to Preserve the Built Heritage. Brno: Academic Publishing CERM, Ltd. p. 280-285. (2011)

[2] J. Zach; V. Petránek; J. Hroudová; A. Korjenic. Development and performance evaluation of natural thermal- insulation materials composed of renewable resources. In Energy and Buildings. Vol. 43, n. 9, p. 2518-2523. (2011)

[3] EN 13501-1 Fire classification of construction products and building elements - Part 1: Classification using test data from reaction

[4] EN 12667 Thermal performance of building materials and products - Determination of thermal resistance by means of guarded hot plate and heat flow meter methods - Products of high and medium thermal resistence

[5] EN 823 Thermal insulating products for building applications - Determination of thickness

[6] EN 1602 Thermal insulating products for building applications - Determination of the apparent density

[7] EN 1609 Thermal insulating products for building applications - Determination of short term water absorption by partial immersion

[8] EN 1607 Thermal insulating products for building applications - Determination of tensile strength perpendicular to faces

[9] EN 826 Thermal insulating products for building applications - Determination of compression behaviour

[10] EN 822 Thermal insulating products for building applications - Determination of length and width

[11] EN 825 Thermal insulating products for building applications - Determination of flatness

[12] EN 824 Thermal insulating products for building applications. Determination of squareness

[13] EN 12086 Thermal insulating products for building applications - Determination of water vapour transmission properties

doi:10.4028/www.scientific.net/AMR.587.36

Implication of Unbondedness in Reinforced Concrete Beams

S.F.A. Rafeeqi[a], S.U. Khan[b], N.S.Zafar[c] and T. Ayub[d]

NED University of Engg. & Tech., Karachi, Pakistan

[a]pvc2@neduet.edu.pk, [b]sadaqat@neduet.edu.pk, [c]najmsahar@neduet.edu.pk, [d]tehmina@neduet.edu.pk

Keywords: Unbonded rebar, Corrosion, Exposed reinforcement, Rehabilitation

Abstract. In this paper, behaviour of nine (09) RC beams (including two control beams) after unbonding and exposing flexural reinforcement has been studied which were intentionally designed and detailed to observe flexural and shear failure. Beams have been divided into three groups based on failure mode and unbounded and exposed reinforcement. Beams have been tested under two-point loading up to failure. Experimental results are compared in terms of beam behaviour with respect to flexural capacity and failure mode which revealed that the exposed reinforcement does not altered flexural capacity significantly and unbondedness positively influences shear strength; however, serviceability performance of beams with unbonded and exposed reinforcement is less.

Introduction

The usefulness of reinforced concrete as a structural material is a resultant of the blending of concrete that is strong in compression with rebar that is strong in tension. By maintaining bond between concrete and steel, transfer of load from concrete to steel is ensured. It is idealized that bond develops along the length of beam in vicinity of the steel-concrete. As far as the bond is present between concrete and steel, the assumption of plane section remains plane hold true [1]. Corrosion of steel, honeycombing in concrete along the rebar and improper bond due to use of rusty rebars are few causes resulting in affecting the composite action of concrete and steel in RC beams. Corrosion of rebar is one of the major causes of debonding of steel from concrete. At the initial stages of corrosion, concrete is repaired to improve passive environment around rebar before significant loss of steel cross section. Temporary support/ props are provided to such beams till new concrete is hardened, but in numerous cases, it is difficult to provide supports and beams has to withstand with unbonded or exposed reinforcement for considerable time during repair process.

Investigation have been done to understand the effects of loss of cover and flexural bond on flexural strength of RC beams [2], the load carrying capacity of RC beams with exposed tension rebar [8], effects of varying the debonded length of rebar on flexural strength of RC beams [9]. Based on these investigations it has been found that the loss of cover and flexural bond influence the flexural strength but it depends on the length of bond loss [2, 3] and it may be possible to debond the tension rebar over a significant length of span without causing significant reduction in flexural strength [3, 4]. For practical use, a simpler method has also been developed to estimate the length of bar that may be exposed without significant loss of strength [3]. This paper emphasises on the effect of unbonded rebar on flexural strength, mode of failure and shear capacity with varying length of the unbonded rebar. The experimental study conducted to check the behaviour of reinforced concrete beam and also validate the existing model [1].

Material and Their Mechanical Properties

Concrete. Ordinary Portland cement, sand (passing through 3.125 mm ASTM sieve), course aggregate (passing through 12.5 mm and retained on 4.75 mm ASTM sieves) have been used to prepare concrete with a mix proportion of 1:2:4 and water cement ratio of 0.5.

Steel. Deformed steel bars of 12 mm diameter (f_y = 504 MPa) has been used as flexural reinforcement and plain mild steel bars of 6 mm diameter (f_y = 330 MPa) has been used for hanger and transverse shear reinforcement for all beams.

PVC Pipe. PVC pipe has been used to wrap rebars before pouring of concrete so that the flexural bars remain unbonded after casting of concrete.

Preparation of Specimens. Total of nine RC beams having concrete section of 150 mm x 200 mm and total length of 1800 mm have been cast. The test spans of all the beams have been kept as 1650 mm with constant shear span to depth (*a/d*) ratio of 3.3. All beams have been designed and detailed keeping in view the intended mode of failure. Steel percentage of 0.968 has been used in all beams. Typical reinforcement details for all the beams have been shown in Fig. 1.

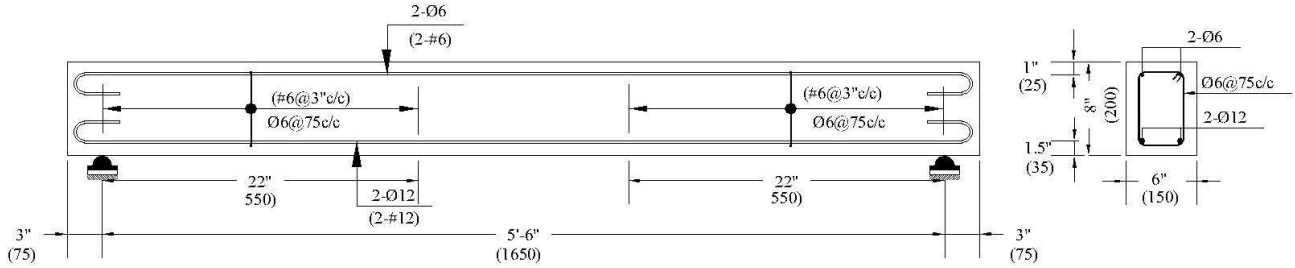

Beam Detail for Flexure Mode of Failure

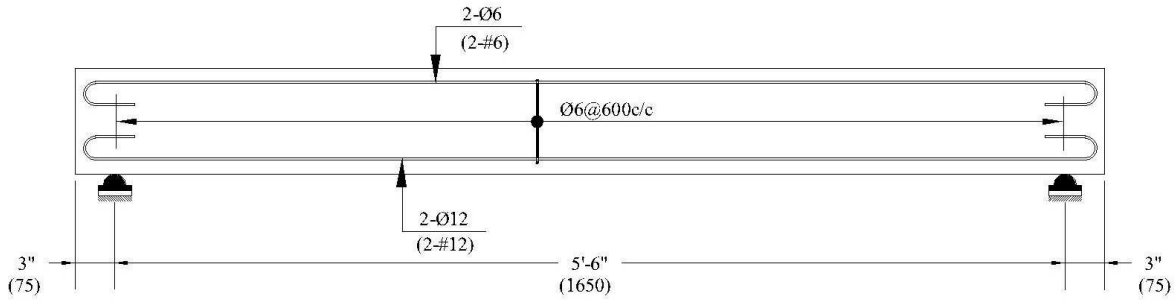

Beam Detail for Shear Mode of Failure

Fig. 1 Typical Reinforcement Detail for RC Beam

Each beam has been cast along with three cylinders of 150mm x 300mm to evaluate the compressive strength (f'_c) of concrete. Beams have been divided into groups 'A', 'B' and 'C'. Group 'A' comprised of four (04) beams which have been unbonded using PVC pipe and intended failure mode is flexure. Group 'B' also comprised of four (04) beams which have been unbonded using PVC pipe but intended failure mode is shear. Group 'C' comprised of one (01) beam which has been cast with Exposed reinforcement and intended failure mode is flexure. The detail of beam of group 'C' has been shown in Fig. 2.

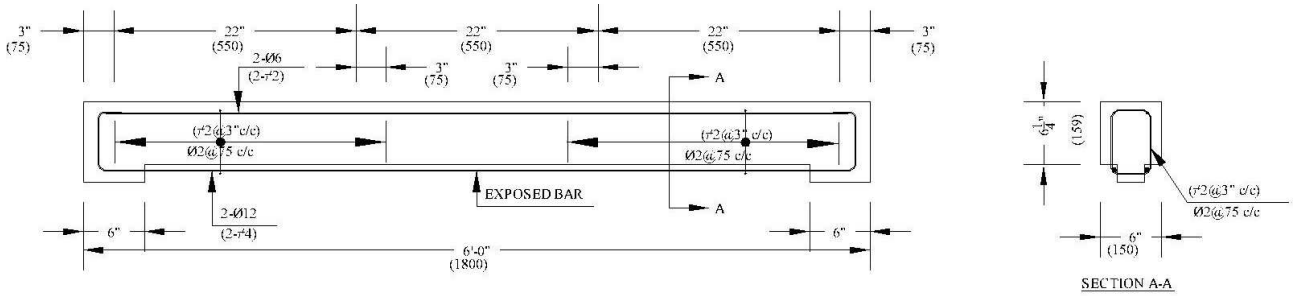

Fig. 2 Detail of Beam "CEi"

Beam of group 'C' is detailed to validate the exposed length for retaining at least 90% of fully bonded strength in flexure mode of failure under two point load of simply supported beam [1]. For beam of span 1650 mm (5'-6"); the breakout length is less or equal to 678mm (26.69") from the centre of the beam to either side. Beam CEi of group 'C' has been tested with exposed length equal to 750mm (30") from the centre of the beam to either side to validate the retaining of at least 90% of fully bonded strength in flexure. Detailed experimental program based on failure mode and unbonded or exposed length is described in Fig. 3.

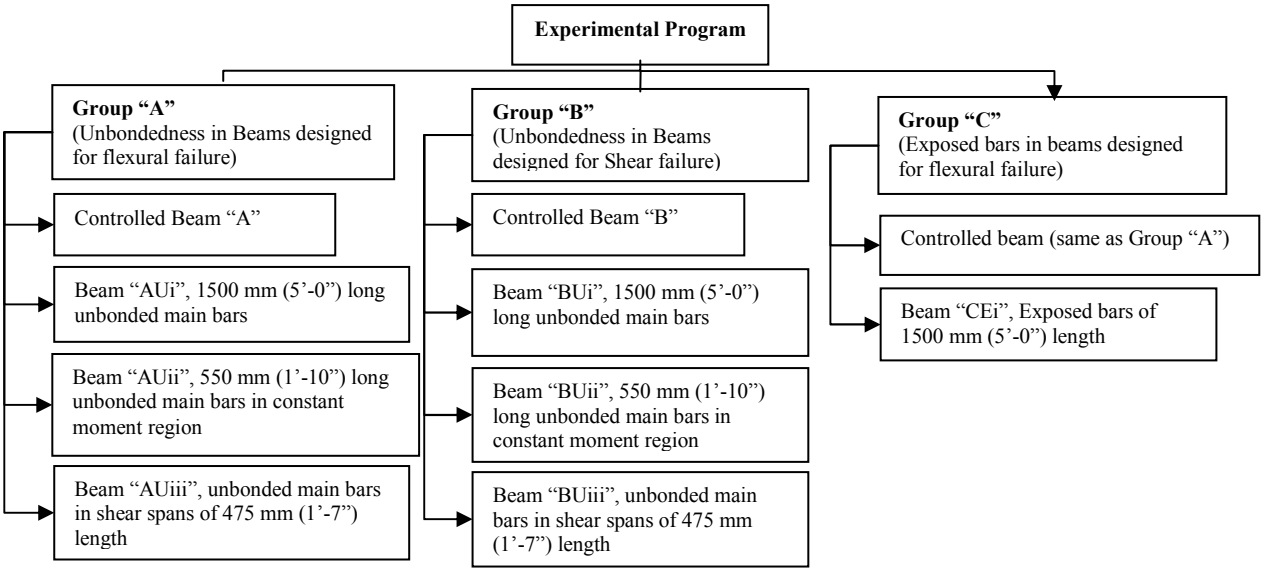

Fig. 3 Experimental Program

Testing Procedure

All beams of group "A", group "B" and group "C" have been tested to failure under third point loading.

Measurement of Surface Strains and Crack Width. In order to measure surface strains, demec buttons 200 mm apart have been installed on front side of the beam. Overall, 10 demec buttons have been fixed using epoxy after white wash of beams. Surface strains have been measured at each load increment of 5 kN till failure. Crack widths within the span have also been recorded. Cracks have been marked at each loading increment with markers.

Deflection. Deflections of the tested beams have been measured using two deflectometers, which has been installed under beams at mid span and under point load.

Test Results and implication

Test results have been presented in Table 1 and Table 2. Experimental results are compared within and across each group with respect to flexural capacity and failure mode, while other parameters have also been studied including stiffness, ductility and crack patterns.

Effect of Unbondedness on Flexural Capacity. In Group 'A' the unbondedness of the tension rebar of length 1500 mm of the span of RC beam (AUi) showed about 10.7% reduction in the flexural capacity and in beam (AUii) having unbonded rebar in constant moment region of length 550 mm showed 6.7% reduction in flexural capacity. There is no reduction in flexural capacity in beam (AUiii) having unbonded rebar in constant shear region of length 475 mm establishing that unbondedness in constant shear region is not affecting flexural capacity. In Group 'B' the unbondedness of the tension rebar of length 1500 mm of the span of RC beam (BUi) showed about 5.7% increase in the flexural capacity while 4.3% and 1.4% reduction in flexural capacity are demonstrated by the beams (BUii, BUiii) having unbonded rebar in constant moment region and constant shear region respectively. In Group 'C' the reduction in flexural capacity due to exposed reinforcement over full length of the span is 13.3%.

On an average 5.8% reduction has been observed in flexural capacity of the beams of Group 'A' and 0 % reduction has been observed in flexural capacity of the beams of Group 'B' whereas the lone specimen of Group 'C' gave the 13.3% decrease in flexural capacity.

Effect of Unbondedness on Failure Mode. Beams of Group 'A' and Group 'C' failed in flexural mode. In Group 'B' beams (BUi and BUiii) have been failed in flexure mode while the Beam BUii failed in shear as shown in Fig. 5. Beams BUi and BUiii have been unbonded along the span of

length of 1500 mm and in constant moment region of length 550 mm respectively, therefore, it may infer that unbondedness in constant moment region caused the change in failure mode of Beams BUi and BUiii.

Mid span load-deflection results have been presented in graphical form in Fig. 6. Other Parameters evaluated have been described as under:

Table 1 Comparison of Moment capacity of Beams

Group	Nomenclature	Avg. Cylinder Strength MPa (Ksi)	M_{Exp} kN.m (lb.ft)	M_{Theo} kN.m (lb.ft)	M_{Exp}/M_{Theo}	% Deviation in experimental results as per Control beam	Remarks
Group 'A'	A	26.12 (3.79)	20.96 (15195.3)	19.47 (14361.7)	1.07	-	
	AUi	20.56 (2.98)	18.72 (13808.5)	[1]18.82 (13882.3)	0.99	-10.7%	
	AUii	21.5 (3.12)	20.56 (15112.3)	[1]18.95 (13978.2)	1.03	-1.9%	
	AUiii	21.79 (3.16)	20.96 (15195.3)	[2]18.99 (14007.7)	1.10	0.0	
Group 'B'	B	16.03 (2.33)	19.56 (14428.1)	13.31 (9817.9)	1.47	-	
	Bui	28.29 (4.1)	20.68 (15254.3)	[1]16.50 (12171)	1.25	+5.7%	
	Buii	15.66 (2.27)	18.12 (13367.8)	[1]13.19 (9729.4)	1.42	-7.3%	
	Buiii	23.86 (3.46)	19.28 (14221.6)	[2]15.44 (11389)	1.25	-1.4%	
Group 'C'	CEi	23.2 (3.37)	18.56 (13695.4)	[3]19.17 (14140.5)	0.95	-11.45%	Validating [5]

[1] Based on Reference [5]
[2] Bond lengths in constant moment region are sufficient to be treated as fully bonded for flexural capacity.
[3] Based on BS Code 8110

Table 2 Stiffness and Ductility

Group	Nomenclature	Stiffness before yielding P/Δ N/m	Δ_y mm.	Δ_u mm.	Ductility ratio = Δ_u/Δ_y
Group 'A'	A	5.75	9.288	22.024	2.37
	AUi	5.48	8.638	18.554	2.15
	AUii	4.10	8.963	20.289	2.26
	AUiii	5.25	10.24	23.982	2.34
Group 'B'	B	5.36	9.144	24.704	2.70
	Bui	4.52	11.22	24.18	2.15
	Buii	5.10	9.046	15.012	1.66
	Buiii	4.06	11.959	25.482	2.13
Group 'C'	CEi	3.35	14.102	32.368	2.29

* Δ_u = deflection of beams at failure (refer Fig. 5)
*Δ_y = deflection of beams at Yielding of steel (refer Fig. 5)

Effect of Unbondedness on Stiffness. Unbondedness caused decrease in the stiffness of beams of Group 'A', Group 'B' and Group 'C'. Overall least stiffness has been observed in beam of Group 'C'.

Effect of Unbondednesson Ductility. In all Groups, ductility has been reduced. Least ductility has been observed in beam 'Buii' of Group 'B' as shown in Table 2.

Effect of Unbondedness on Cracks Pattern. More widely spaced cracks have been observed in beams (AUi, BUi, CEi) may be because of full unbonded and exposed reinforcement along the span. While more number of cracks have been observed in a regions of bonded rebar in beams AUiii and BUiii as shown in Fig. 5.

From the above mentioned results, it seems that unbonded rebar contributes in altering failure mode. It has no substantial effect on ultimate flexural capacity; however it causes more deflection and reduction in ductility.

Beam A

Beam AUi

Beam AUii

Beam AUiii

Beam B

Beam Bui

Beam BUii

Beam BUiii

Beam CEi

Conclusions

Following conclusions may be drawn from this study:

1. The unbondedness in constant shear region does not affect the flexural capacity of beam significantly.
2. The unbondedness and exposed reinforcement in constant moment region influence the flexural capacity of beam.
3. The unbondedness in constant shear region cause flexural mode of failure in beam detailed to be failed in shear.
4. The serviceability performance of beams with unbonded and exposed reinforcement is less as initial stiffness is reduced.
5. It is possible especially in repair work to expose rebar up to significant length without affecting the flexural capacity of beam but need to prop/ support the beam during repair to avoid excessive deflections.
6. It may also conclude that loss of bond up to significant length due to corrosion of rebar cause serviceability problem without affecting the flexural capacity.

References

[1] J. Cairns, in: *Proc. Engineering Experimental Station Bulletin,* pp. 499-504, (1995).

[2] H. Sharaf and K. Soudki, in: *Proc. CSCE 30th Annual Conf., Canadian Society for Civil Engineering, Montréal,* (2002).

[3] J. Eyre and M. Nokhasteh, in: *Proc. ICE-Structures and Buildings,* vol. 94, pp. 197-203, (1992).

[4] ACI Committee, "Building code requirements for structural concrete (ACI 318-05) and commentary (ACI 318R-05)," (2005).

[5] J. Cairns and S. Rafeeqi, *Constr. Build. Mater.,* vol. 11, pp. 309-317, (1997).

doi:10.4028/www.scientific.net/AMR.587.42

Application of technical hemp into the structure of cement-chip boards

Šárka Keprdová[1, a], Jiří Bydžovský[2,b] and Tomáš Melichar[3,c]

[1] Brno University of Technology, Faculty of Civil Engineering, Institute of Technology of Building Materials and Components, Veveří 331/95, 602 00 Brno, Czech Republic

[2] Brno University of Technology, Faculty of Civil Engineering, Institute of Technology of Building Materials and Components, Veveří 331/95, 602 00 Brno, Czech Republic

[3] Brno University of Technology, Faculty of Civil Engineering, Institute of Technology of Building Materials and Components, Veveří 331/95, 602 00 Brno, Czech Republic

[a]Keprdova.s@fce.vutbr.cz, [b]Bydzovsky.j@fce.vutbr.cz, [c]Melichar.t@fce.vutbr.cz

Keywords: Technical hemp, cement-chip board, filler, wood, cement, secondary raw materials.

Abstract. Cement-chip boards are building elements that combine the advantageous properties of wood and cement. It is this synergistic effect which determines the versatile use in the building industry. The boards can be used in any place where the favourable properties of this construction material can fully be appreciated.

The disadvantage of the cement-chip boards remains in their relatively high price. Reduction of the price and possible improvement of physical and mechanical properties can be achieved by partial substitution of the raw materials. The basic ingredients of the cement-chip board include the binding material (cement) and filler (wood). The filling material may be partially replaced by secondary raw materials or completely replaced by other herbal sources, such as technical hemp. As the individual components mutually influence each other and, as their effects may not only be added up (additive effect), but also mutually reinforced (synergistic effect), it is not so easy to determine the optimal recipe as it may seem at first sight.

This article deals with the use of technical hemp shives as a replacement of filling component of the cement-chip boards. To evaluate the possibility of future use of the boards in building structures, the physical and mechanical properties were monitored. Special emphasis was placed on tests of flexural strength, modulus of elasticity and volume weight. The mixture must meet the technical parameters related to the cement-chip boards.

Introduction

Cement-chip boards have the good qualities of wood and the cement in common; their characteristics predetermine them to be used in many different cases, be it for the construction of walls, bars, lower ceilings, facades, floors etc. The disadvantage of cement-chip boards however is the high price, which reflects mainly the price of input materials. The main component, which forms the filler of the cement-chip boards, is wood. The wooden chips are derived from the stems of cut trees, which means, that the chips must be produced from the wooden mass first.

This part of the production can be partially or completely avoided using alternative fillers. Using alternative, quickly renewable raw-materials in construction materials creates the opportunity to decrease production costs and eliminate ecological burden. A great advantage of alternative fillers is in their fast growth:, their renewal period in this temperate climate is usually one year compared with wood, which grows for several tens of years. It must also be taken into account that wood can be used much more effectively in the building industry, i.e. in the form of timber, boards etc., where it cannot be substituted with other materials.

An interesting possibility to use alternative, quickly renewable sources is the application of technical hemp as the full or partial substitute for chips. Thanks to its very good mechanical features, technical hemp is a perspective solution in the building material production. It can be assumed that the technical hemp is a suitable renewable source of raw materials for the production of construction materials, which can compete with other commercial products using natural as well as secondary raw materials. [3]

This document considers the utilization of technical hemp as a quickly renewable source instead of chips as fillers in cement-chip boards. A most suitable mix composition was explored, namely from the view of various combinations of fractions and methods of pre-adjustments of hemp shives, the modification of the cement and mixing water amounts.

To evaluate the future utilization possibilities in building constructions, physical-mechanical characteristics were investigated, the stress being laid mainly on the bulk strength and elastic modulus firmness tests, depending on the proportion of individual components.

The mixture must fulfil the required technical parameters for the cement-chip boards; however, a decrease in the total price for the raw materials used during production must be achieved.

Cement-chip boards

Cement-chip boards belong to the group of fiber composites. They are made using the cement matrices, usually Portland cement, and stemmed chips, namely of pines and firs. The boards are pressed under 2 ~ 3 MPa to obtain the required thickness (ca. 1/3 of the apparent thickness). According to the shape of wooden parts and their bulk weight, the cement-chip boards can basically be divided into:

Boards from the excelsior with a low bulk weight (up to 400 $kg.m^{-3}$), they are used for the heat insulation of walls and ceilings, to produce bars, dividing walls etc. These boards are known under the name Heraklit.

Boards from heavy chips with medium bulk weight (400-800 $kg.m^{-3}$), they are produced from wooden particles with the thickness between 0,5 - 5 mm, width 2 - 10 mm, length 20 - 50 mm. The shape of wooden particles is not determining during the production of this type of boards; various unit wastes can be used, e.g. wood and heavier chips are used. Wooden particles are usually mineralized with potassium silicate, which at the same time decreases the absorbing power and increases the resistance of boards to pests and moulds. Boards with an additional insulation layer of foam polystyrene are used as a lost form during the production of enclosure walls, namely in the residential construction.

Boards from soft chips with a high bulk weight (over 800 $kg.m^{-3}$) are made from softer chips and contain a higher quantity of cement (25 % and more in weight) than the previous kinds. The usual production thickness is between 8 and 40 mm. They are trimmed to an exact size; they can be equipped with a pen and a fold.

Characteristics: the bulk weight of the cement-chip boards from the soft chips ranges from 1 000 to 1 500 $kg.m^{-3}$. The boards have a relatively high strength in tension in the bent (over 10 MPa), and according to the reactions to fire belong to the A2 group. Like all materials containing wooden mass rate, they have relatively high linear expandability depending on the humidity, therefore, the boards should be left to dilate. The cement binder increases the thermal conductivity to values around 0,3 $W.(m.K)^{-1}$. The boards also have excellent acoustic features (the airbone sound transmission loss is 30 - 35 dB), however they have a low sound absorbability. They are resistant to freeze, insect and mould. They resist dampness, therefore are generally used in exteriors; they practically do not expand, and are ecological and hygienic [1], [2].

The requirements for the features of cement-chip boards according to the ČSN EN 634-2 are:

- the bulk weight: min. 1000 $kg.m^{-3}$
- the bending strength: min. 9 $N.mm^{-2}$
- the modulus of elasticity: min. 4500 $N.mm^{-2}$ [4]

The use of the cement-chip boards is very broad, as they are a quality board material with extraordinary features. The boards can be used for floor systems, loft building, roof buildings, aerated facades, anti-fire applications, lower ceilings, walls and bars, garden fittings, forms and many others.

Technical hemp

Technical hemp (cannabis sativa) is an annual, thermopiles plant in the Cannabaceae family. It is a plant with a long and straight stem and little branching, which lignifies quickly, and with palmate, jagged leaves and small, oval fruits. The main stem can be up to 3 - 5 m long and 30 mm wide on

average. It is grown everywhere in the temperate zones, except where the soils are permanently wet or dry. The whole plant is used during processing, there is no waste. Cannabis is a valuable crop. It is important to realize that only the Cannabis sativa can be grown in this country, as its low content of THC (Tetrahydrocannabinols) – less than 0,3% - prevents its use as a narcotic. [3, 5]
Technical hemp used in the document
Fraction A, particle size to 8 mm, powder weight 133 $kg.m^{-3}$
Fraction B, particle size over 20 mm, powder weight 93 $kg.m^{-3}$

Fig. 1: Technical hemp: on the left, hemp shives fraction A; on the right, hemp shives fraction B

Work methodology

The research incorporated carrying out two types of modifying the composition of cement-bonded boards, the first of them being to find the optimal shives hemp (fraction shives A or B). The second was to test the influence of mineralization shives on the properties of boards. The composition of the reference mixture in the Figure 1. Below is a summary of each formula:

- mixture 1: reference mixture – made of filler wood;
- mixture 2: made of shives technical hemp “A”;
- mixture 3: made of shives technical hemp “A”, mineralization of the 14 % concentration of sodium water glass;
- mixture 4: made of shives technical hemp “A”, mineralization of the 10 % concentration of sodium water glass;
- mixture 5: made of shives technical hemp “B”;
- mixture 6: made of shives technical hemp “B”, mineralization of the 14 % concentration of sodium water glass;
- mixture 7: made of shives technical hemp “B”, mineralization of the 10 % concentration of sodium water glass;
- mixture 8: made of fraction shives “A + B” in the ratio of 1:1;
- mixture 9: made of fraction shives “A + B” in the ratio of 1:1, mineralization of the 14 % concentration of sodium water glass;
- mixture 10: made of fraction shives “A + B” in the ratio of 1:1, mineralization of the 14 % concentration of sodium water glass.

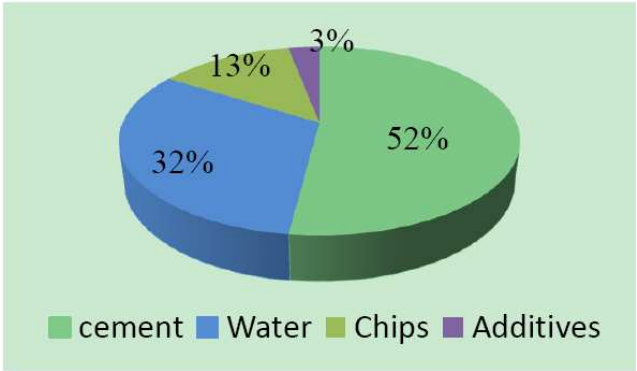

Fig. 2: The dosage of individual components of the reference mixture in% by weight.

Test results

Since this was the initial stage of research, experiments were carried out regarding the basic parameters, which specifically involved observing bending strength, modulus of elasticity and bulk weight.

The chart in Fig. 3 shows the values of mean bulk weight values for each mixture. The following chart provides a graphical comparison of the average bending strength (see Fig. 4). The values of mean modulus of elasticity are in the chart in Fig 5.

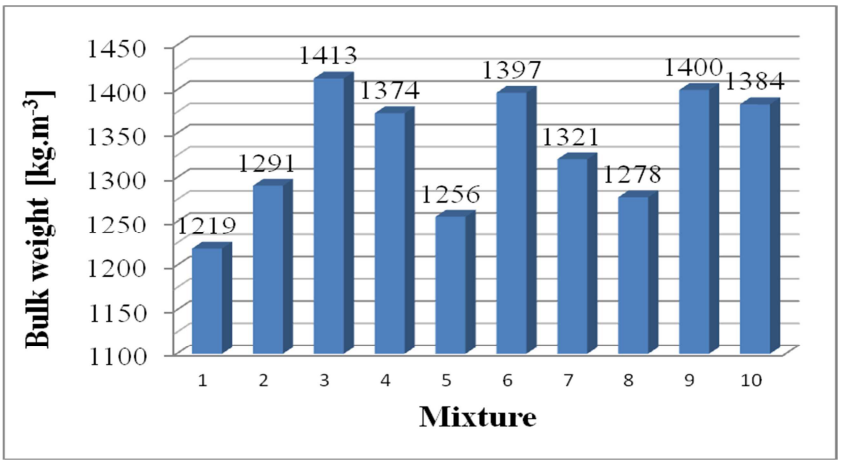

Fig. 3: Comparison of average bulk density values.

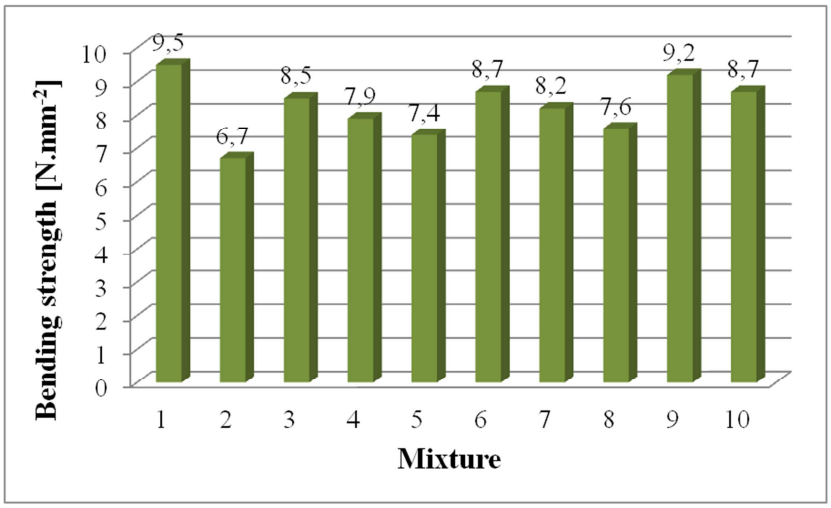

Fig. 4: Comparison of average bending tensile strength values.

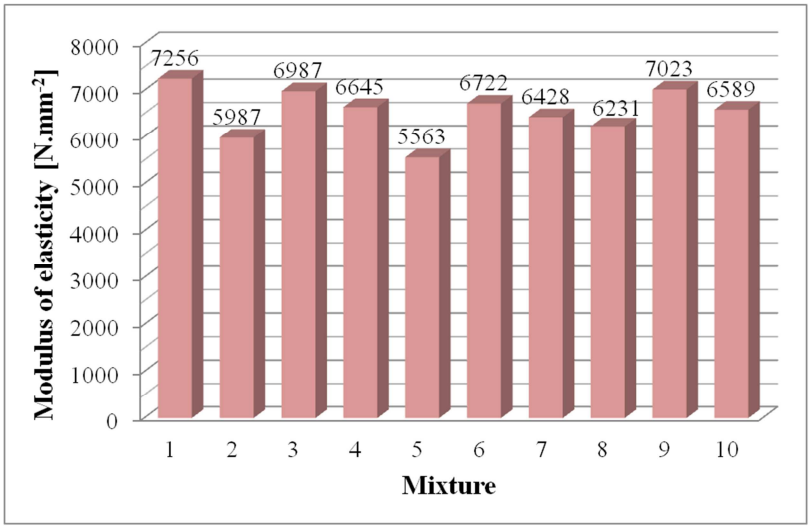

Fig. 5: Comparison of average modulus of elasticity values.

Summary

This work has focused on the optimization of the cement-chip board's characteristics using various combinations and adjustment of the initial materials. In a subjective appraisal of the appearance of cement-chip and cement-hemp boards, the cannabis boards had a clearly smoother surface and uniform colour comparing to the reference samples from the chips. This will be of an advantage for these boards, regarding not only the exposed applications.

Based on the test results we can say that: mineralization of shives technical hemp contributes to improving the strength characteristics of boards. However, the density increases. Size particle shives does not affect significantly characteristics of the resulting boards. The use of technical hemp in the structure of boards is possible.

The boards from cannabis were very similar to the boards made from chips. With regards to the low price of hemp (the wholesale price of cannabis is ca. 2,000 CZK/t, wholesale price of wood ca. 4,000 CZK/t), the cannabis boards could find their place on the market in the near future. There is no need for such great mechanization using cannabis, it is easy to dry and cut, it is quickly renewable and the yield of cannabis is up to 4 times higher than wood.

Acknowledgements

This result was realized with financial support from the state budget through the Ministry of Industry and Trade under the project FR-TI3/595 „Mixture composition innovation for production of cement-chip boards".

References

[1] Svoboda, L. and coll. (2005) Building materials Jaga group, s.r.o., Bratislava, ISBN 80-8076-007-1.

[2] Cetris - Basic information. [Seen 26th March 2012] <http://www.cetris.cz/>.

[3] Sladký, V. (2002) *Cannabis - the ancient cultural plant in Europe and the Czech Republic*. <http://biom.cz/index.shtml?x=62806>. ISSN: 1801-2655. [Seen 22th February 2012]

[4] ČSN EN 634-2: Cement-bonded particleboards - Specifications - Part 2: Requirements for OPC bonded particleboards for use in dry, humid and external conditions

[5] Konopa, o. s. – Everything about cannabis. [Seen 20th March 2012]. <http://www.konopa.cz/>.

doi:10.4028/www.scientific.net/AMR.587.47

Possibility of using the technical hemp as a filling component in external thermal-insulation composite systems

Šárka Keprdová[1, a], Jiří Bydžovský[2, b]

[1] Brno University of Technology, Faculty of Civil Engineering, Institute of Technology of Building Materials and Components, Veveří 331/95, 602 00 Brno, Czech Republic

[2] Brno University of Technology, Faculty of Civil Engineering, Institute of Technology of Building Materials and Components, Veveří 331/95, 602 00 Brno, Czech Republic

[a]Keprdova.s@fce.vutbr.cz, [b]Bydzovsky.j@fce.vutbr.cz

Keywords: Technical hemp, hemp insulation, binding component, cement, calcium hydroxide, fly-ash.

Abstract. Combining air or hydraulic binders with hemp shives, we can gain a set of new building materials. These products achieve excellent performance characteristics for durable, environmentally sustainable buildings. Being together, these products create natural composite building material that can be used to create insulating elements for walls, floors and roofs and also to create excellent thermal and acoustic properties of the buildings.
Hemp insulation material is created by connection of technical hemp shives with a binder consisting of cement and calcium hydroxide. The production process may vary depending on whether the hemp is mineralized or not. It can be generally said that dry components should be mixed at first (binder and shives) and then water should be added. During the production, all components of insulating material must be perfectly mixed. The paper deals with the proposal and testing of new hemp insulation composites. Tests of the hemp insulation described in this paper are not typical representatives of the tests of insulation materials. Due to the doubts about the insulating properties of the proposed material, there was testing carried out in such the ways as if it was the filling material based on lightweight concretes.

Introduction

The use of rapidly renewable raw materials in the building industry is seen as very promising with regard not only to the environmental issues but also to its economic aspects. A number of producers, not only in this country, have been trying to replace fine construction materials with secondary raw materials or rapidly renewable ones. As an example, technical hemp is a very promising material due to its good mechanical and thermal insulation characteristics. One of the possibilities is its use as filling component for non-constructional filling materials.

Combining binders on the basis of non-hydraulic lime with hemp chaff yields a range of new construction materials. These products offer excellent work characteristics for permanent, environmentally sustainable buildings. These products as a whole form a natural composite construction material that can be used to build insulation walls, floor and roof insulation layers, and to obtain excellent heat and acoustic characteristics of buildings. [1]

Technical hemp

Technical hemp (cannabis sativa) is an annual, thermopiles plant in the Cannabaceae family. It is a plant with a long and straight stem and little branching, which lignifies quickly, and with palmate, jagged leaves and small, oval fruits. The main stem can be up to 3 - 5 m long and 30 mm wide on average. It is grown everywhere in the temperate zones, except where the soils are permanently wet or dry. The whole plant is used during processing, there is no waste. Cannabis is a valuable crop. It is important to realize that only the Cannabis sativa can be grown in this country, as its low content of THC (Tetrahydrocannabinols) – less than 0,3% - prevents its use as a narcotic. [2, 3, 4]
Shives technical hemp is a CHANVIBRAT: bulk weight 109 kg/m^3.

Fig. 1: Technical hemp: on the left, hemp in growth [5]; on the right, shives.

Designing and making mixtures

Hemp insulation is composed: 44 % binder, 15 % filler and 41 % water (in %weight.).
Binder composition:
Mixture **1 -** 44% cement
Mixture **2 -** 30 % cement + 14 % fly-ash Dětmarovice
Mixture **3 -** 30 % cement + 14 % fluid fly-ash Hodonín
Mixture **4 -** 10% cement + 34 % calcium hydroxide
Mixture **5 -** 10 % cement + 24 % calcium hydroxide + 10 % fly-ash Hodonín
Mixture **6** – 10 % cement + 24 % calcium hydroxide + 10 % fluid fly-ash Dětmarovice
Adjustment of technical hemp, identification of a mixture:
A – Clean shives
B – Mineralized hemp - milk of lime
C – Mineralized hemp **-** sodium water glass at a concentration of 12%
Labelling mixture: **1A, 1B, 1C, 2A, 2B, 2C, 3A, 3B, 3C, 4A, 4B, 4C, 5A, 5B, 5C, 6A, 6B, 6C**

Results of measurements

Individual powdery components of the given recipes are placed into a mixing container. Then the material is mixed with a mixer. Measured amount of water is added to the mixture during the process. The mixture further homogenizes. The well-blended mixture is poured into the three parts of the mould and then it is vibrated. They were made specimens with dimension 100 x 100 x 100 mm (see in Figure 2 - picture a), 100 x 100 x 400 mm (see in Figure 2 - picture b) and 300 x 300 x 50 mm (see in Figure 2 - picture c), which are used for the following laboratory tests: compressive strength, bending tensile strength and heat conductivity factor. Test specimens were tested after 28, 60 and 90 days of hardening. The test results are shown in Table 2 and 3. Values in the table are the average of the 3 of test specimens.

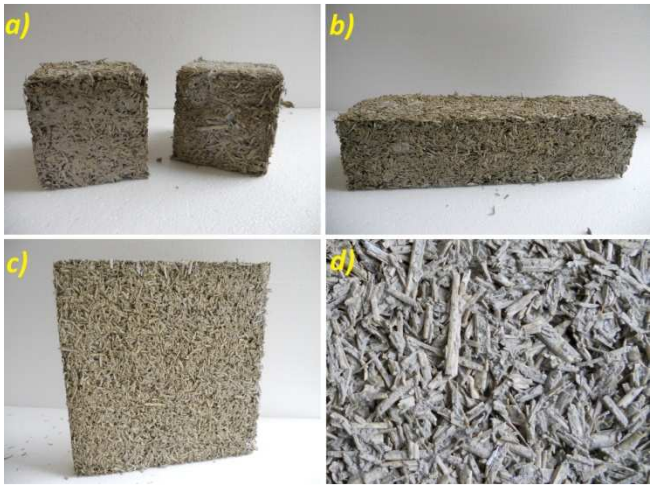

Fig. 2: Different types of test specimens (a - c) and structure of the material (d).

Tab. 1: Table of bulk weight and compressive strength.

Mixture	Bulk weight [kg.m^{-3}]				Compressive strength [N.mm^{-2}]		
	0 time	7 days	28 days	60 days	7 days	28 days	60 days
1A	902	856	768	724	0,88	1,08	1,21
1B	926	731	642	622	1,06	1,21	1,38
1C	987	839	764	721	**1,21**	**1,73**	**1,92**
2A	**864**	**573**	**518**	**451**	0,43	0,59	0,87
2B	869	785	698	553	0,51	0,84	1,09
2C	924	814	747	719	0,94	1,01	1,34
3A	893	754	601	498	0,49	0,67	0,83
3B	903	764	624	567	0,94	1,21	1,45
3C	867	704	632	526	0,76	0,89	1,29
4A	**864**	**749**	**538**	**464**	0,46	0,75	1,02
4B	873	658	598	487	0,64	0,87	1,12
4C	852	764	603	504	0,74	0,98	1,24
5A	864	647	567	489	0,91	1,14	1,21
5B	840	682	539	482	**1,02**	**1,16**	**1,38**
5C	876	803	769	637	0,98	1,09	1,35
6A	903	567	743	541	0,63	0,96	1,19
6B	869	792	637	562	0,73	0,87	1,13
6C	927	860	724	637	0,62	0,92	1,18

Tab. 2: Table of tensile strength in bending and heat conductivity factor - λ.

Mixture	Tensile strength in bending [N.mm^{-2}]			Heat conductivity factor -λ[W.(mK)$^{-1}$]
	7 days	28 days	60 days	
1A	0,45	0,58	0,95	0,094
1B	0,71	0,89	1,25	0,098
1C	**1,43**	**1,55**	**1,87**	0,100
2A	0,21	0,37	0,78	0,087
2B	0,42	0,75	0,83	**0,081**
2C	0,36	0,57	0,86	0,083
3A	0,65	0,72	0,86	0,076
3B	0,84	1,02	1,23	0,079
3C	1,15	1,24	1,56	0,087
4A	0,51	0,78	1,06	0,076
4B	0,36	0,73	0,98	**0,074**
4C	0,23	0,88	1,07	0,086
5A	0,51	0,86	0,92	0,082
5B	0,84	1,02	1,15	0,096
5C	**0,62**	**0,97**	**1,21**	0,084
6A	0,21	0,57	0,84	0,081
6B	0,63	0,91	1,06	0,087
6C	0,52	0,83	1,04	0,097

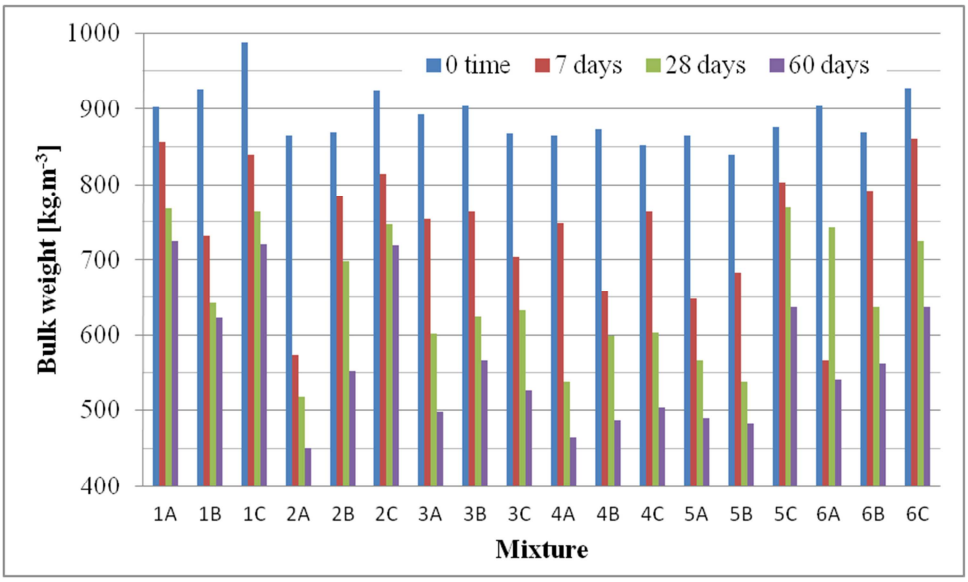

Fig. 3: Comparison of average bulk density values.

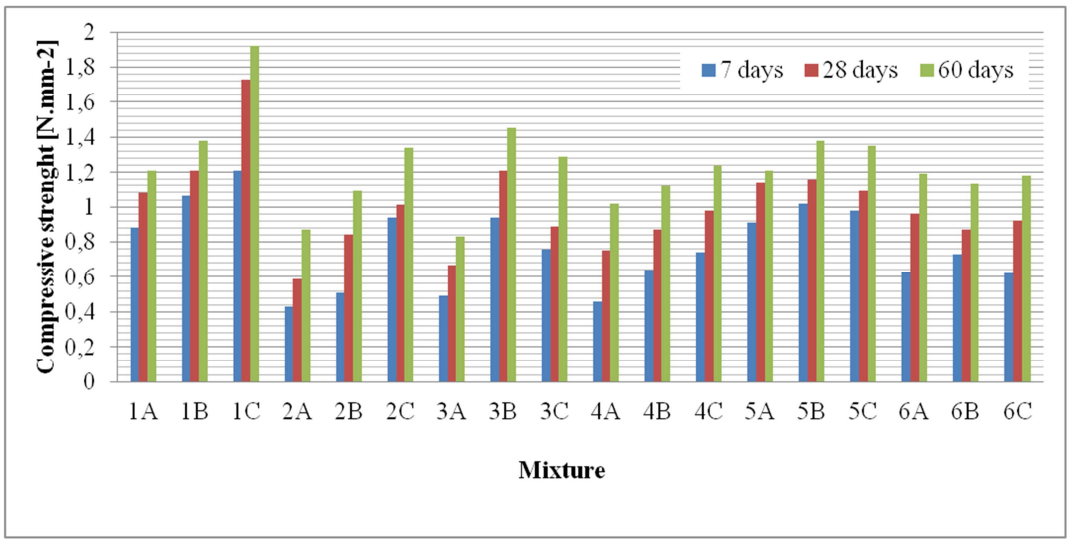

Fig. 4: Comparison of average compressive strength values.

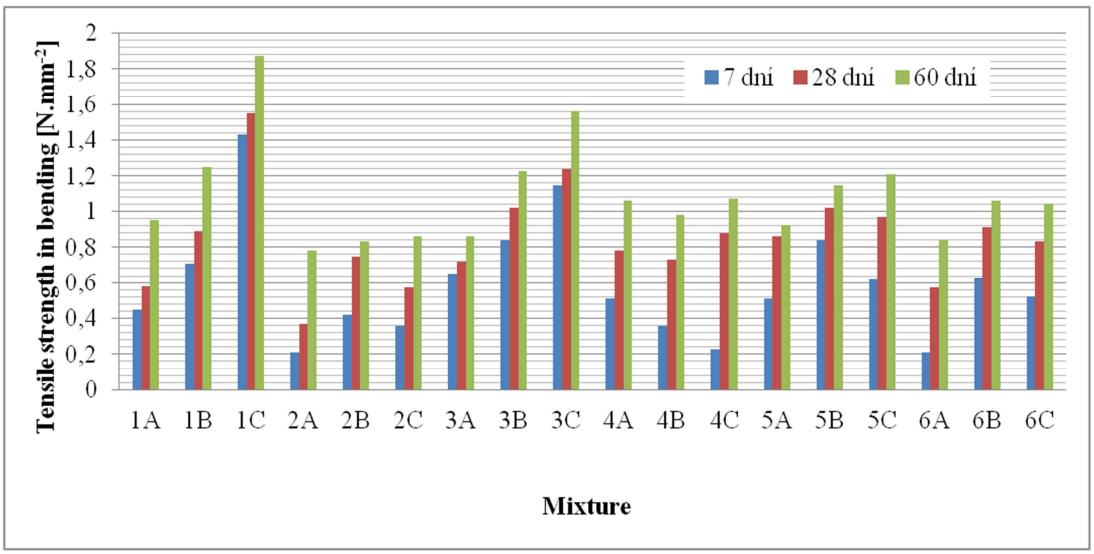

Fig. 5: Comparison of average tensile strength in bending values.

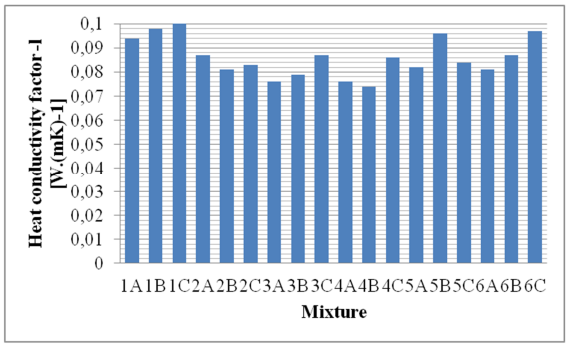

Fig. 6: Comparison of average heat conductivity factor - λ

Summary

Use of natural materials in construction is quite closely connected with the construction of low energy and passive houses. Use of natural materials in building construction has a major positive impact on the indoor environment, the more you can get a healthy organic living. Thermal insulating and acoustic properties of natural building materials are usually fully comparable with commonly used building materials, in some cases are even better. Easy renewable between natural raw material resources useful in the construction industry and we are one of the technical hemp, which provides a wide range of possible applications in various other industries. Technical hemp is rapidly renewable waste-free plant material that is becoming increasingly popular in many construction applications. Its physical-mechanical and thermal-mechanical characteristics are close to those of wood and it can be estimated that it will become an alternative to wood.

The paper describes the production and testing of hemp insulation based on technical hemp. Within the research were off to testing of 18 different mixtures insulations of the hemp. The difference was mainly used in binders and pre-treatment of hemp shives. Binders of different mainly using the basic raw materials and adding secondary materials. Adjustment consisted of mineralization shives lime milk or solution sodium water glass. Samples bonded with cement have good bending strength, but a high bulk weight and high thermal conductivity. Samples bonded with cement + lime hydrate reach of the average properties. Mineralization hemp improves the final properties of insulators (strength, thermal conductivity, durability, flammability, biological degradation), however, increases the bulk weight. The use of secondary raw materials leads to a drastic deterioration. Y057Isolation of hemp shives bonded hydraulic or air binders has a very good physic-mechanical and thermo-technical properties, but cannot yet compete with the used insulating materials. (The higher thermal conductivity compared to polystyrene and mineral wool.).

Acknowledgements

This result was realized with financial support from the state budget through the Ministry of Industry and Trade under the project TIP FR-TI 2/339 „External Thermal Insulation Composite Systems with Use of Alternative Raw Materials" and Project of Specified university-level research Brno University of Technology n. FAST-J-11-14/1240.

References

[1] Information on Tradical®, http://www.lhoist.co.uk/tradical/hemp-lime.html

[2] Sladký, V. (2002) *Cannabis - the ancient cultural plant in Europe and the Czech Republic*. <http://biom.cz/index.shtml?x=62806>. ISSN: 1801-2655.

[3] Information on Konopa, o. s. – Everything about cannabis. <http://www.konopa.cz/>.

[4] Svoboda, L. and coll. Building materials Jaga group, s.r.o., Bratislava, ISBN 80-8076-007-1.

[5] Information on http://www.urban-shop.cz/co-je-technicke-konopi/t-143/

doi:10.4028/www.scientific.net/AMR.587.52

Free Vibration of Simply Supported Piezolaminated Composite Plates using Finite Element Method

Kamal M. Bajoria[1,a] and Rajan L. Wankhade[2,b]

[1]Professor, Department of Civil Engineering, Indian Institute of Technology Bombay, Mumbai, Maharashtra, India-400076. Tel.: +91-22-2572-7332; fax: +91-22-2572-7302.

[2,]Research Scholar, Department of Civil Engineering, Indian Institute of Technology Bombay, Mumbai, Maharashtra, India-400076.

[a]kmb@iitb.ac.in, [b]rajan.wankhade@iitb.ac.in

Keywords: Piezolaminated plates, Finite element method, Free vibration

Abstract. Piezolaminated smart structures are becoming more popular as they can be used as light weight structures to control structural response in various structural applications. Piezoelectric materials have direct and converse piezoelectric effects which can be adequately employed to control the deflection, shape and vibration of the structure. A finite element methodology based on higher order shear deformation theory is developed for free vibration analysis of smart piezolaminated composite plates subjected to combined action of electrical and mechanical loading. To achieve the accurate prediction of the frequencies, a finite 2D isoparametric element for the mechanical displacement field is combined with an electric potential field. Numerical results are presented for free vibration analysis of simply supported piezolaminated composite plate considering different electric condition with varying thickness to span ratio.

Introduction

Smart material systems and structures have been adopted by engineering and research community over the last two decades. In the recent past theoretical as well as experimental investigations has been successfully carried out in the area of smart structures. The need of light weight structures in engineering applications has led to the gradual replacement of many isotropic materials with composites which provide both high stiffness and low weight. The coupled electromechanical properties of piezoelectric ceramics and their availability in the form of thin sheet makes them well suited for use as distributed sensors and actuators for controlling structural response.

Dhonthireddy and Chandrashekhara [1] carried out modeling and shape control of composite beams with embedded piezoelectric actuators. Eisenberger and Abramovich [2] studied shape control of non-symmetric piezolaminated composite beams. Nguyen et al. [3] presented evolutionary piezoelectric actuators design optimization for static shape control of smart plates. Mukherjee and Chaudhuri [4] presented analysis of piezolaminated beams with large deformations. Kulkarni and Bajoria [5] carried out large deformation analysis of piezolaminated smart structures using higher-order shear deformation theory. Thus in present work the free vibration problem of simply supported piezolaminated plate is examined considering electromechanical loading. Using the benefits of direct and converse piezoelectric effects, surface bonded integrated piezoelectric sensors and actuator layer may be employed to adequately suppress the transient vibration or to control the deflection, shape of the structures.

Finite Element Formulation

Fig. 1 shows a laminated composite plate provided with piezoelectric patches at top and bottom surface. As piezolaminated plate and shell are laminated composite structure, the effect of shear deformation will have to be considered. It cannot be ignored like in case of classical plate theory based on Kirchoffs hypothesis. In higher order shear deformation theory, higher order terms of

displacement field are incorporated to consider transverse shear deformation correctly. Thus the three dimensional elasticity problem is approximated to two dimensional formulation using Taylor series expansion for displacement components u, v and w.

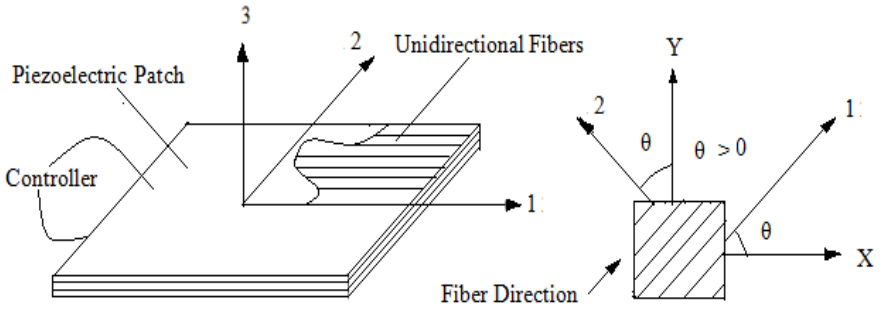

Figure 1 Laminated composite plate provided with piezoelectric patches at top and bottom surface.

Assuming the condition of zero shear stresses at the top and bottom surface of laminate, equations for HOST 9 are as following

$$u = u_0 + z\theta_x + z^2 u_0^* + z^3 \theta_x^*$$

$$v = v_0 + z\theta_y + z^2 v_0^* + z^3 \theta_y^*$$

$$w = w_0 \tag{1}$$

Where, $u(x,y,z)$, $v(x,y,z)$ and $w(x,y,z)$ are the displacement of any point in the plate domain in in x, y and z direction respectively. $u_0(x,y,z)$, $v_0(x,y,z)$ and $w_0(x,y,z)$ are the displacement of midpoint of normal. $\theta_x(x,y)$, $\theta_y(x,y)$ are the rotations of normal at the middle plane in x and y direction about y and x axis respectively. $u_0^*(x,y)$, $v_0^*(x,y)$, $w_0^*(x,y)$, $\theta_x^*(x,y)$ and $\theta_y^*(x,y)$ are higher order terms which accounts cubic variation of normal.

Displacement-strain relation

Strains are related with displacements as follows

$$\underbrace{\varepsilon} = B \underbrace{\delta_e} \tag{2}$$

And $\underbrace{\gamma} = B_s \underbrace{\delta_e}$ (3)

Electro-Mechanical Coupling

Due to the direct and converse piezoelectric effect there exists a coupling between electrical and mechanical loading in smart piezoelectric structures. Thus the piezoelectric equations can be decoupled resulting in electromechanical coupling. Variation of temperature effect is neglected in formulation. The constitutive equations of a piezoelectric material including the effect of electrical and mechanical expansion can be expressed as follows. Hence dielectric displacement vector in local coordinate field is given as, For the piezoelectric layer polarized in the thickness direction, the dielectric displacement vector using direct piezoelectric equation is,

$$\{D\} = [e]\{\varepsilon\} + [g]\{E^p\}$$

$$\{\sigma\} = [C]\{\varepsilon\} - [e]^t \{E^p\} \tag{4}$$

In all above equations, {D} is electric displacement vector, [e] is dielectric permittivity matrix, ε is the strain vector, $\{g\}$ is the dielectric matrix. $\{E^p\}$ is the electric field vector, $[\sigma]$ is the stress vector and [C] is the elastic matrix for constant electric field.

Electrical Potential Function

One electrical degree of freedom is adopted per node of an element. If $\phi_a^{'}$ *and* $\phi_s^{'}$ are the electric displacement at any point in the actuator and the sensor layers, respectively, the electrical potential functions in terms of the nodal potential vector are given by

$$\phi_a^{'} = [N_{pa}]\{\phi_a^e\}$$

$$\phi_s^{'} = [N_{ps}]\{\phi_s^e\} \tag{5}$$

Where, $\lfloor N_{pa} \rfloor$ and $\lfloor N_{ps} \rfloor$ are the shape function matrices for the actuator and sensor layers, respectively. $\{\phi_a^e\}$ and $\{\phi_s^e\}$are the nodal electric potential vector for the actuator and sensor layers, respectively and can be given as follow.

$$\{\phi_a^e\} = \{\phi_{a1}\ \phi_{a1}\ \phi_{a1}.....\phi_{a1}\}^T$$

$$\{\phi_s^e\} = \{\phi_{a1}\ \phi_{a1}\ \phi_{a1}.....\phi_{a1}\}^T \tag{6}$$

The electric field strength of an element in terms of the electrical potential of the actuator and sensor layers is expressed as

$$\{E_a^P\} = \begin{Bmatrix} E_x^P \\ E_y^P \\ E_z^P \end{Bmatrix}_a = -\begin{Bmatrix} \partial\phi_a/\partial x \\ \partial\phi_a/\partial y \\ \partial\phi_a/\partial z \end{Bmatrix} \quad \text{and} \quad \{E_s^P\} = \begin{Bmatrix} E_x^P \\ E_y^P \\ E_z^P \end{Bmatrix}_s = -\begin{Bmatrix} \partial\phi_s/\partial x \\ \partial\phi_s/\partial y \\ \partial\phi_s/\partial z \end{Bmatrix} \tag{7}$$

The electric field vector for the actuator and sensor layer can be modified as

$$\{E_a^P\} = -\sum_{i=1}^{n} B_{a(i)}\,\phi_{a(i)}^e = -[B_a]\{\phi_a^e\} \quad \text{and} \quad \{E_s^P\} = -\sum_{i=1}^{n} B_{s(i)}\,\phi_{s(i)}^e = -[B_s]\{\phi_s^e\} \tag{8}$$

Stiffness Matrix Equations

Element stiffness matrix can be written as,

$$[K^e]\{\delta^e\} + [K_\sigma^e]\{\delta^e\} = [F_1^e] + [F_{ac}^e] \tag{9}$$

In which

$$[K^e] = [K_d^e] + [K_{aa}^e]^{-1}[K_{aa}^e][K_{ad}^e] + [K_{ds}^e][K_{ss}^e]^{-1}[K_{sd}^e] \tag{10}$$

$$\{F_{ac}^e\} = [K_{da}^e][K_{aa}^e]^{-1}\{Q_a^e\} \tag{11}$$

Where,

$$[K_d^e] = \int_V [B]^T[C][B]dV\ ,[K_{da}^e] = [K_{ad}^e]^T = \int_{Va} [B]^T[e][B_a]dV\ ,[K_{aa}^e] = \int_{Va} [B_a]^T[g][B_a]dV\ ,$$

$$[K_{ds}^e] = [K_{sd}^e]^T = \int_{Vs} [B]^T[e][B_s]dV \text{ and } [K_{ss}^e] = \int_{Vs} [B_s]^T[g][B_s]dV \tag{12}$$

Vibration Criterion

For free vibration problems, the equations of motion can be expressed as the following eigenvalue problem form which natural frequency can be calculated:

$$\left(\left[K-\omega^2[M]\right]\right)\{\delta_E\}=\{0\} \tag{13}$$

Where, matrix [K] denotes the stiffness matrix and matrix [M], the mass matrix. After solving eigen value problem frequencies can be fount out.

Numerical Analysis

Free vibration analysis of piezoelectric laminated plate is carried out considering three layered cross-ply laminates with piezolayer attached at the top and bottom of the plate. Hence a square piezoelectric laminated plate of thickness of 0.01 m and side length 'a' is having simply supported boundary on all four edges. The laminate consists of a $(0^0/90^0/0^0)$ Graphite-Epoxy sublaminate provided with two PZT-4 attached on outer surfaces of the plate. Each piezoelectric layer has thickness of 0.1h, whereas each elastic layer has a thickness of 0.2h. The elastic and piezoelectric properties are given in Table 1. Whereas fundamental frequencies are found out for closed and open circuits for different a/h ratio and are presented in table 2.

Table 1. Elastic and piezoelectric properties

Elastic Properties			**Piezoelectric Properties**		
Properties	**Graphite-Epoxy**	**PZT-4**	**Properties**	**Graphite-Epoxy**	**PZT-4**
$E_{11}\,(Gpa)$	132.38	81.4	$e_{31}\,(C/m^2)$	0	-5.20
$E_{22}\,(Gpa)$	10.756	81.3	$e_{32}\,(C/m^2)$	0	-5.20
$E_{33}\,(Gpa)$	10.756	64.5	$e_{33}\,(C/m^2)$	0	15.08
$G_{12}\,(GPa)$	5.654	30.6	$e_{15}\,(C/m^2)$	0	12.72
$G_{23}\,(GPa)$	3.606	25.6	$e_{24}\,(C/m^2)$	0	12.72
$G_{32}\,(GPa)$	5.654	25.6	ε_{11}/t_0	3.5	1475
υ_{12}	0.24	0.329	ε_{11}/t_0	3.0	1475
υ_{23}	0.24	0.432	ε_{11}/t_0	3.0	1300
υ_{32}	0.49	0.432			

Table 2. Fundamental frequency ($\omega/100$ in rad/sec) of simply supported square laminated plate $(p/0^0/90^0/0^0/p)$

a/h		Closed	Open
4	Present	55.239	56.450
	Akhras et al. [8]	55.460	56.972
10	Present	12.671	13.860
	Akhras et al. [8]	12.908	13.522
50	Present	583.912	617.620
	Akhras et al. [8]	584.280	618.150

The comparision of fundamental frequencies for closed loop and open loop piezolaminated plates having different a/h ration has been done. The results of these fundamental frequencies shwos that piezoelectricity has little effect on the fundamental frequency of the laminates with closed-circuits. The incerase in fundamental frequency is found to be 2.14 %, 8.57% and 5.45% for open loop circuit than that of closed loop for a/h = 4,10 and 50 respectively.

Conclusions

A finite element methodology for free vibration analysis of piezolaminated composite plate is developed based on higher order shear deformation theory. It combines a finite 2D isoparametric element for the mechanical displacement field with an electric potential field to achieve the accurate prediction of the frequencies. With proper selection and placement of piezoelectric actuators, it is feasible to generate enough forces on a structure in order to control its response in vibration. It is observed that the maximum percentage variation in fundamental frequency is 8.57 % for PZT-4 for a/h=10. Hence the increase in stiffness due to piezoeffect can be considered with sufficient accuracy to control its response.

References

[1] P. Dhonthireddy, K. Chandrashekhara: Modeling and shape control of composite beams with embedded piezoelectric actuators, Composite Structures, Vol. 35 p. 237-244 (1996).

[2] M. Eisenberger, H. Abramovich: Shape control of non-symmetric piezolaminated composite beams, Composite Structures, Vol. 38 p. 565-571 (1997).

[3] Q. Nguyen, L. Tong, Y. Gu: Evolutionary piezoelectric actuators design optimization for static shape control of smart plates, Computer Methods in Applied Mechanics and Engineering, Vol. 197 p. 47–60 (2007).

[4] A. Mukherjee, A.S. Chaudhuri: Piezolaminated beams with large deformations, International Journal of Solids and Structures, Vol. 39 p. 4567–4582 (2002).

[5] S. Kulkarni, K.M. Bajoria: Large deformation analysis of piezolaminated smart structures using higher-order shear deformation theory, Smart Materials and Structures, Vol. 16 p. 1506-1516 (2007).

[6] S. Kulkarni, K.M. Bajoria: Finite element modeling of smart plates/shells using higher order shear deformation theory, Composite Structures, Vol. 62 (2003), p. 41-50

[7] R.K. Khare, T. Kant, A.K. Garg: Closed-form thermo-mechanical solutions of higher-order theories of cross-ply laminated shollow shells, Composite Structures, Vol. 59 (2003), p. 313-340

[8] G. Akhras, W. Li: Stability and free vibration analysis of thick piezoelectric composite plates using spline finite strip method, International journal of Mechanical Sciences, Vol. 53 p.575-584 (2011).

doi:10.4028/www.scientific.net/AMR.587.57

Laboratory Study on the Effect of Asphalt Emulsion as a Rejuvenator in Aged Asphalt Pavement

Rashid.Tanzadeh[a], Mahyar.Arabani[b]

University of Guilan, Dept. of Civil Engineering, I. R. Iran

[a]rashidtanzadeh@yahoo.com,[b]m_arbani@yahoo.com

Keywords: Asphalt Pavement, Aging, Modified Bitumen, Rejuvenator, Dynamic Test

Abstract. Modification of the asphalt binder is one approach taken to improve aged pavement performance. To make the most of maintenance budgets, many agencies have resorted to the use of asphalt rejuvenators as an alternative to revive aging and brittle asphalt pavements. The purpose of this study is laboratory research on the effect of asphalt emulsion in restoring the original properties of aged asphalt pavement. For this purpose, the repeated load axial test is carried out on conventional asphalt samples and aged asphalt samples containing rejuvenator agents in different stress and rejuvenator percentage. Bitumen aged with RTFO according to ASTM-D2872 and the optimum bitumen of 5.5% were considered. The softening point and penetration tests, to examine the effect of rejuvenator in asphalt mixtures modification, On the basic, aged and modified aged bitumen were performed. The results represent that asphalt emulsion as a rejuvenator material in aged asphalt samples because of suitable performance improve aged asphalt permanent deformation resistance and aged bitumen Rheological property.

1. Introduction

Pavement preservation is now on the mind of every agency charged with maintaining their inventory of asphalt pavements. The problem of asphalt is that it oxidizes with time and therefore its beneficial properties disappear [1].After some years of use, the stiffness of asphalt concrete increases while its relaxation capacity decreases, the binder becomes more brittle causing development of micro-cracks and ultimately cracking of the interface between aggregates and binder occurs. This mainly happens as a result of oxidation, which is the chemical reaction of the hydrocarbon compounds of bitumen with oxygen [2].Asphalt consists of two main fractions: asphaltenes and maltenes. The maltenes consist of sub fractions which are oily or resinous and chemically reactive [3].Chemical and physical properties of bitumen change in three stages:

1 . Operation and mixing time
2 . Distribution time on road surface and compression operation
3 . throughout the lifetime of the pavement.

At The first two, high mixing temperature cause bitumen exhaustion because high temperature due to the presence of oxygen beside the bitumen ,oxidation accelerate, Maltyn percent reduced and asphalt with little flexibility are prone to fatigue cracks [4].Numerous methods are being employed for asphalt pavement preservation, including rejuvenator emulsions, fog seals, and several different thin overlay technologies. Only the first method, rejuvenators, partially restores the original properties of the pavement. The most important goal of rejuvenator products is to restore the asphaltenes/maltenes ratio [1].An asphalt rejuvenator was introduced in 1960 by the Golden Bear Oil Company. That product was Reclamite and it has a history of use spanning 50 years. In an era of moderately low price asphalt products, the rejuvenator was ahead of its time. Thousands of laboratory tests and field trials have been performed to determine the best possible formula and procedures for applying an asphalt rejuvenator [2].In Japan, a research on the properties of recycled mixtures using recycling agents with different components was conducted. The results indicated that the aged binders could be recovered to a target penetration by using different rejuvenating agents if adequate amount is added. The purpose of this study is laboratory study on the effect of Asphalt Emulsion as a rejuvenator materials in restoring the original properties of asphalt pavement

that aged with rolling thin film oven. For this purpose, the repeated load axial test is carried out on the conventional asphalt samples and aged asphalt samples containing rejuvenator agents in different stress and rejuvenator percentage .The softening point and penetration tests, to examine the effect of rejuvenator in asphalt mixtures modification, were performed.

2. Materials and Test Program

2.1. Materials Used. The gradation of aggregates used in this study was the average range of the continuous gradation for HMA in the Topeka and Binder layer suggested in Issue 101 of the general and technical properties of roads (Iranian standard), which is presented in Table 1 .

Table 1: The gradation of aggregates used in this research

Sieve size	Passing Percentage	
	Binder	Topeka
1"	100	-
3/4"	95	100
1/2"	-	95
3/8"	68	-
#4	50	59
# 8	36	43
#50	12	13
#200	5	6

The bitumen (Penetration grade 60/70) used for this study was kindly supplied courtesy of refinery in Tehran. Engineering properties of the bitumen were presented in Table 2.

Table 2: Properties of bitumen used in this research

Specific gravity (at 25°C)	Penetration grade (mm/10)	Softening point (°C)	Ductility (cm)	Flash point (°C)	Loss on heating (%)	Purity grade (%)
1.02	67	51	112	262	0.75	99.6

The benefits of an asphalt rejuvenator are:
1. Increasing penetration value of the asphalt cement in the top portion of the pavement which extends the pavement's lifecycle
2. Sealing pavement against intrusion of air and water, thereby slowing oxidation, preventing stripping and raveling and protects the pavement in depth
3. Increasing the durability of the asphalt in the top portion of the pavement by improving the chemical composition of the asphalt cement.

These materials can be bitumen with high degree of influence (soft bitumen), bitumen emulsions or chemical compounds which have duty of lowering the viscosity and enhance penetration degree.

According to the definition, sustainable bitumen is the bitumen which the asphaltene is well resolved and spread homogeneously. Therefore Asphalt Emulsion was used as rejuvenators. Finally according to the performed RLA tests, using 10% of this material has been suggested as a rejuvenator. Properties of the rejuvenators were presented in Table 3.

Table 3: Properties of Asphalt Emulsion used as a Rejuvenator

Specific gravity (at 15.6°C)	Penetration grade (mm/10)	Viscosity (at 60°C)	Flash point (°C)	Purity grade (%)
0.966	188	513.75	60	99.8

2.2. Sample preparation. Marshal cylindrical asphaltic samples were produced. Bitumen aged with RTFO according to ASTM-D2872 and the optimum bitumen of 5.5% were considered for all of the mixtures. RLA test were conducted at two stresses (150 and 300 kPa) for virgin , aged and modified bitumen with three rejuvenators content (5 , 10 , 15) .

2.3. Laboratory Tests

2.3.1. Rolling Thin Film Oven (RTFO). In 1963 Hveem, Zube, and Skog introduced the RTFO test in specifications for the CALTRANS. Bell, 1989, summarized the test methods that have been used to simulate the short-term aging on asphalt binders. Initially, the Rolling Thin Film Oven (ASTM D 2872) and Thin Film Oven (ASTM D1754) tests were both being utilized for short-term aging in the Superpave asphalt binder specifications. In this study, new asphalt binder is placed in a cylindrical jar, which is then placed in a carousel inside a specially designed oven.

2.3.2. Penetration Test. The penetration test is performed on the virgin, aged and modified aged bitumen according to ASTM-D5 standard for evaluation the effect of rejuvenator in asphalt mixtures. Penetration grade (mm/10) of virgin bitumen was obtained 67, after being exhausted with the RTFO was obtained 51 and Penetration degree of modified bitumen, 10 hours after adding 10% the optimum amount of rejuvenator was obtained 65.

2.3.3. Softening point. This test covers the determination of the softening point of bitumen in the range from 30 to 157°C (86 to 315°F) according to ASTM-D36 using the ring-and-ball apparatus immersed in distilled water (30 to 80°C), USP glycerin (above 80 to 157°C), or ethylene glycol (30 to 110°C). Softening point of initial bitumen was obtained 50, after being exhausted with the RTFO was obtained 58 and softening point of modified bitumen 10 hours after adding 10% the optimum amount of rejuvenator was obtained 51.

2.3.4. RLA Test. Control stress version of RLA test was used for evaluation of the resistance to deformation of samples. Test was conducted using constant repeated stress of 150 and 300 KPa. In the RLA test, the strain percentage of a material is defined as the measure to distinguish the mixture permanent deformation resistance. In this test an unconfined cylindrical specimen is subjected to axial stress pulses of 1 second duration and specified stress value separated by 1 second rest periods. The test duration is normally 1000 load pulses and it is carried out at a constant temperature. The diameter and height of samples in RLA test was 101.4 and 70 mm, respectively.

3. Results and Discussions

3.1 The Rheological Test Result. According to the following table, with adding higher percentages of rejuvenators, Penetration grade of aged bitumen is increased and softening point of aged bitumen is decreased. As you can see, the optimum bitumen of 10 % rejuvenators, to restore the rheological properties of bitumen is sufficient and according to the following table, adding more, not desirable.

Table 4: The Rheological Test Result

Test	Virgin bitumen	Aged bitumen	rejuvenated bitumen
Penetration degree(mm/10)	67	51	65
Softening point(°C)	50	58	51

3.2. The RLA Tests Results. In this study, the repeated load axial test is carried out on conventional asphalt samples and aged asphalt samples containing rejuvenator agents in different stress and rejuvenator percentage. Fig1 shows the comparison of average axial strain percentage in RLA tests in virgin, aged and modified aged samples. The stress was 150 kpa with the constant temperature 25^0C .The strain values decrease 1.42 % in Topeka and 1.39 % in Binder classification when we aged, new bitumen. It is evident that Topeka classification because of dense aggregation and much bitumen, has less strain values than the Binder classification. By increasing the Rejuvenator percentage from 0 % in aged samples to 15 %, the average strain(For 1000 pulse), increase 1.47 % in Topeka ,1.43% in Binder classification. By increasing the Rejuvenator percentage from 10 % to 15 %, the strain values increase more than virgin(not aged) asphalt samples and in this situation the permanent deformation resistance, decrease. Finally, a mean value of the common contents, 10 % , with which all requirements were satisfied , was used as a design

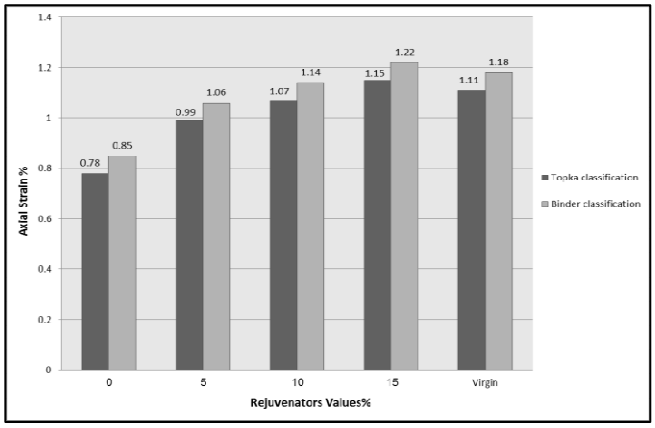

Fig. 1: Average axial Strain Percentage in RLA in virgin, aged and modified aged samples at stress 150 kPa and temp25^0C

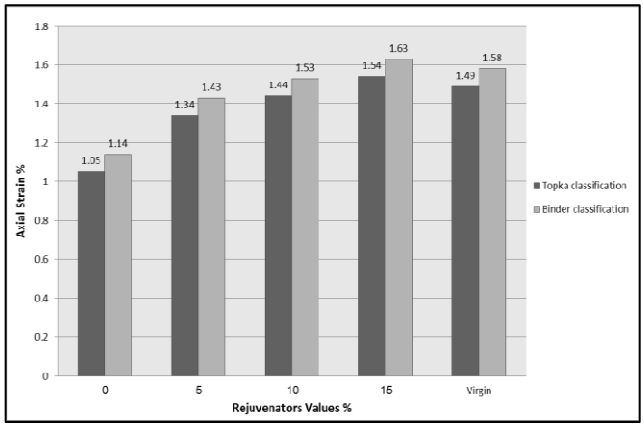

Fig. 2: Average axial Strain Percentage in RLA in virgin, aged and modified aged samples at stress 300 kPa and temp25^0C 25^0c

As is observed, with bitumen aging, axial strain because of brittle property in aged asphalt samples decrease and with bitumen modifying with Asphalt Emulsion, bitumen original property return to aged samples. For example in obtained figures ,with 10 % rejuvenator, we can reach the bitumen that has almost virgin bitumen property.

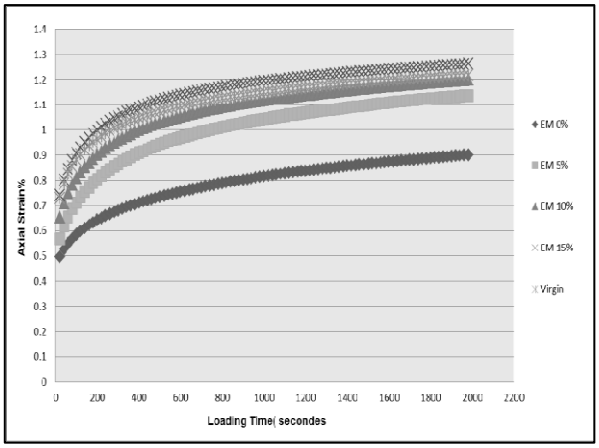

Fig. 3: Axial Strain Percentage with Loading Time at stress150 kPa and temp25^{0}c inTopeka classification

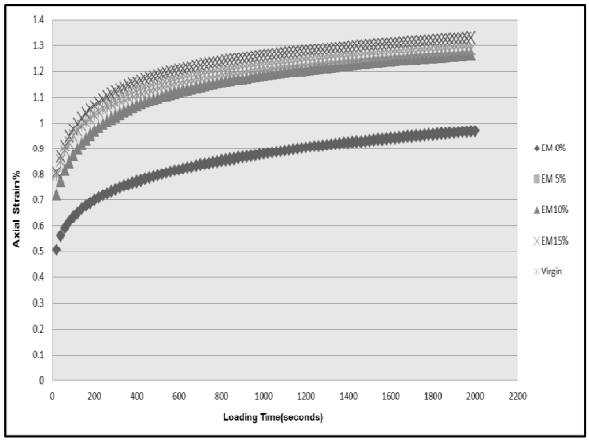

Fig. 4: Axial Strain Percentage with Loading Time at stress150 kPa and temp25^{0}c in Binder classification

It is clear that because of test location environmental conditions, the temperature considered 25^{0}C and we can understand that in the low loading time, the samples are in elastic and after loading time increasing, the samples reach to viscose mode.

4. Conclusion

The purpose of this study was laboratory research on the effect of rejuvenator materials in restoring the original properties of the asphalt pavement that aged by RTFO. For this purpose, the RLA test is carried out on the virgin asphalt samples and aged asphalt samples contains rejuvenator agent. The results express that:

- With adding higher percentages of Asphalt Emulsion as a rejuvenators, Penetration grade of aged bitumen is increased and softening point of aged bitumen is decreased
- Oxidation reaction in the bitumen content of asphalt samples in the rolling thin film oven reduces samples Maltyn content and the asphaltene content in the samples is increased
- With stress increasing, axial strain of asphalt specimens can be added. Due to the high sensitivity of the asphalt to stress changes, this lead to reduction of deformation resistance under repeated load
- With adding optimum percentage of Asphalt Emulsion as a rejuvenator in the aged samples the durability of the asphalt binder increase by improving the balance of chemical fractions of the asphalt binder and higher percentage, increase axial strain in the modified aged samples.

5. References

[1] Rostler, F.S., and White, R.M., Rejuvenation of Asphalt Pavements, Materials Research and Development, Inc., Oakland, California, under Air Force Systems Command Contract F29601-69-C-0129 - May 1970.

[2] Technical Report R690, Reclamite as a life Extender for Asphalt concrete pavements, Navy Facilities Engineering Command, Port Hueneme, California - August 1970.

[3] Value Engineering, Report on Reclamite Usage, Naval Weapons Center, China Lake, California, Navy Facilities Engineering Command - Western Division, San Bruno, California 94066 - August 1973.

[4] J. Shen, S. Amirkhanian, J.A. Miller, Effects of rejuvenating agents on superpave mixtures containing reclaimed asphalt pavement, J. Mater. Civil Eng. 19 (5) (2007) 376–384.

[5] ASTM. (1980). Recommended practice for classifying hot-mix recycling agents, Philadelphia

doi:10.4028/www.scientific.net/AMR.587.62

Application of Slow Curing Bitumen as a Rejuvenating Agent in Aged Bituminous Mixes

Amir.Kavussi[1,a], Rashid.Tanzadeh[2,b]

[1]Tarbiat Modares University, Faculty of Civil Engineering, Tehran, Iran

[2]Guilan University, Dept. of Civil Engineering, Rasht, Iran

[a]kavussia@modares.ac.ir,[b]rashidtanzadeh@yahoo.com

Keywords: Recycling,Aged Bitumen, Rejuvenating agent, Creep Test

Abstract.Recycling of bituminous mixes is extending worldwide with the aim of conserving natural resources and the environment. Rejuvenating agents are generally used in recycling processesin order to soften the aged binders in mixes.

Cutback bitumens have been used in Iran mainly in preparing conventional cold mixes. However, the long term good performance of these cold mixes in various parts of the country has shown less hardening of these mixes, compared with conventional HMA mixes.

In this research the application of a cutbackbitumen has been investigatedas a rejuvenating agent in mixes containing laboratory aged binders. A 60-70 penetration grade bitumen from Refinery of Tehran was aged under Thin Film Oven Testing (TFOT) conditions. Asphalt Concrete samples were prepared using TFOT aged and virgin binders. Additional samples were prepared using the aged binders together with various amounts of a slow curing SC-250 cutback bitumen from the above refinery. The compacted four inchdiameter samples were tested under static creep testing. The results showed promising effects of the cutback binder in rejuvenating the aged mixes. Based on the results of this study, a mix design criteria wasset for recycled mixes containing cutback bitumen as the rejuvenating agent.

1. Introduction

Asphalt concrete, a continuously graded mix that is prepared at high temperatures ($\sim 160^0$ C), is one of the commonly used mixes in pavement layers. These mixes, when properly compacted, are consisted of a mixture of asphalt binder (bitumen), aggregate particles and air voids. After some years of service under environmental and traffic conditions, their stiffness generally increases, while their flexibility reduces appreciably. In these conditions, mixes might become brittle, causing development of micro-cracks within the mix. Ultimately, cracking of the interface between aggregate particles and bitumen binder might occur. This mainly happens as a result of oxidation, which is the chemical reaction of hydrocarbon compounds of bitumen with oxygen [1]. This process begins at very early stages of the mix preparation (i.e. during hot-mix preparationin asphalt plants) and continues throughout the lifetime of the pavement. Asphalt binder components are usually simplified into two subdivisions: solid components, namedas asphaltenes; and liquid components named as maltenes [2]. Upon aging, the amounts of maltenes are reduced and those of asphaltenes are increased. This will finally results in brittleness of the binder. High mixing temperature causesearly hardening of bitumen which will later on results in cracking and loss of aggregates from the road surfaces.

With proven performance of asphalt rejuvenators to revive the aged asphalt layers, pavement engineers have effective and economical methods to extend the pavement service life. A study sponsored by Air Force Weapons Laboratory,entitled "Rejuvenation of Asphalt Pavement" consisted of a laboratory investigation of five rejuvenating agents[3]. Briquettemix samples were subjected to equal application rates of five rejuvenator products. These were then aged in the air till one-half of their volatile constituents wereevaporated. Subsequently, the briquettes were subjected to various testing methods, including permeability, depth of penetration, viscosity, and pellet abrasion testing. The conclusion of this study revealed that only two of the rejuvenating agents

performed well. In mixes containing these rejuvenators,the viscosity of asphalt binder was improved. In addition, in these mixes, loss of aggregates from the pellet abrasion testing was minimal[3].

The aim of this study wasto apply a slowcuring cutback bitumen as a rejuvenating agent to restore the original properties of asphalt mixes in those their binders were previously aged under standard Thin Film Oven Testing conditions. Static creep testingwas carried out on the conventional asphalt samples and those aged at the above conditions.

2. Materials and Testing Program

2.1.Materials Used. The gradation of aggregates used in this study (Table 1) was the average range of the continuous gradation of HMA in the top wearing and base course gradingsrecommended inIranianSpecifications [4]. Properties of the 60/70 penetration grade bitumen from Tehran Refinery is reported in Table 2.

Table 1: Gradation of aggregates used in this research

Sievesize	Passing Percentage	
	Surface Course	Base Course
1″	100	-
3/4″	95	100
1/2″	-	95
3/8″	68	-
#4	50	59
# 8	36	43
#50	12	13
#200	5	6

Table 2: Properties of bitumen used in the research

Specific gravity at 25°C (g/cm^3)	Penetration (mm/10)	Softening point (°C)	Ductility (cm)	Flash point (°C)	Loss on heating (%)	Purity (%)
1.02	67	51	112	262	0.75	99.6

Several categories of rejuvenating agents are used in HMA recycling processes. These could be softbitumens, bitumen emulsions, oils or chemical compounds. All will have the role of lowering the viscosity of the aged binders which can easily be shown by an increase in penetration of the rejuvenated binder. As for the definition,adurable bitumen is one inthatthe asphaltenecomponents are well dissolved and spread homogeneously[1].Hence, keeping with the above criteria in this research, a slow curing bitumen was used as the rejuvenating agent. Properties of this are reported in Table 3.

Table 3: Properties of the rejuvenating agent used

Specific gravity at 15.6°C (g/cm^3)	Penetration (mm/10)	Viscosity (at 60°C)	Flash point (°C)	Purity grade (%)
0.94	176	501.42	50	99.4

2.2.Sample preparation. Asphalt mixes were compacted upon applying 75 blows of Marshall hammer on each sides of the four inch diameter samples. The bitumen of the mix was previously aged under TFOT conditions in accordance with ASTM-D1754 standard testing method. The optimum binder content of mixes was determined to be 5.5%.Mix samples were prepared at four different rejuvenating agent contents of 5,10,15 and 20% of the weight of the binder. Creep testing was then performed at two stress levels of 150 and 300 kPa respectively.

2.3.Laboratory Testing

2.3.1. Thin Film Oven Test(TFOT): This test is associated with short-term aging of the bitumen in asphalt plants. Early in 1940s,Lewis and Welborn introduced TFO test for differentiating between volatility and hardening characteristics of asphalts [5]. The thin-film oven(TFO) test simulates short-term aging of binders by heating a thin film of asphalt binder in an oven for 5 hours at 163°C. The effects of heat and air conditioning are determined from changes that occur in physical properties of the binder (measured before and after the oven treatment) [6].

2.3.2. Penetration Test. Penetration test is an empirical testing method which measures the consistency (hardness) of a binder at a specified testing condition. It is performed on the virgin, aged and modified aged bitumen according to ASTM-D5 standard testing method. In this research, the penetration of the virgin bitumen was 67(mm/10). After being treated under TFOT condition, it was around 54(mm/10). In order to keep that close to the virgin binder, several percentages of the rejuvenating agent were added. Penetration testing was carried out and it resulted that 15% of rejuvenator (by weight of the binder), would be the optimum amounts to be added in the mix. In these conditions, after ten hours curing mixes in the air, penetration of the treated binder wasapproximately 65(mm/10).

2.3.3. Softening point. Ring and Ball Softening point test is used to determine the temperature at which the fluidity of asphalt cement begins. Determination of this temperature is of great importance, as it denotes an equi-viscous point for all asphalt cements. The softening point test was carried out in order to distinguish between the effects of the various rejuvenating agents. The result of this test for the virgin bitumen was 50^oC. After treating it under TFOT conditions, it resulted to be around 56^oC. Upon the addition of 15% rejuvenating agent and air curing the sample for ten hours it was around 51^oC.

2.3.4. Creep Test. Static creep testing was performed in order to determine the permanent deformation resistance of both virgin mix and mixes containing TOFT aged binders. In this study, the controlled stress version of creep testing was carried out in order to determine the resistance to permanent deformation of the samples. The tests were conducted applying constant stresses of 150 and 300 kPa separately. In creep testing, the strain percentages of a material are determined as a measure of permanent deformation resistance of a mix. The tests are performed at constant high ambient temperatures with the duration of normally 1000 seconds. The diameter and height of the samples in creep testing were 101.4 and 70 mm, respectively.

3.Results and Discussions

3.1 Rheological Properties. With reference to Table 4, it can be seen that the addition of the rejuvenating agent will result in increased penetration and decreased softening point values of the binders. As for the optimum amount of the rejuvenating agent, 15% by the weight of the binder was considered to be a sufficient amount to restore the original properties of the binder.

Table 4: The Rheological Test Results

Testing	Virgin bitumen	TFOT Aged bitumen	Rejuvenated bitumen
Penetration (mm/10)	67	54	65
Softening point(°C)	50	56	51

3.2. Deformation Resistance. Fig.2 shows the axial strains in creep testing of the virgin,aged and modified aged samples at 25^{o}C testing temperature. The applied stress was 150 kPaat constant temperature of 25^{0}C.The strain values were decreased by 3.96 % in the wearing course and by 3.55 % in the base course. The wearing course mix showed less strain values than the base course mix. By increasing percentagesof the rejuvenating agent from 0 to 20%in the aged samples, the average strain(in 1000 seconds testing) was increasedto 4.1% in the wearing course mix and 3.74% in the base course. Hence, it was confirmed that the value of 15%, determined in penetration and softening point testswas the optimum amount for the rejuvenating agent.

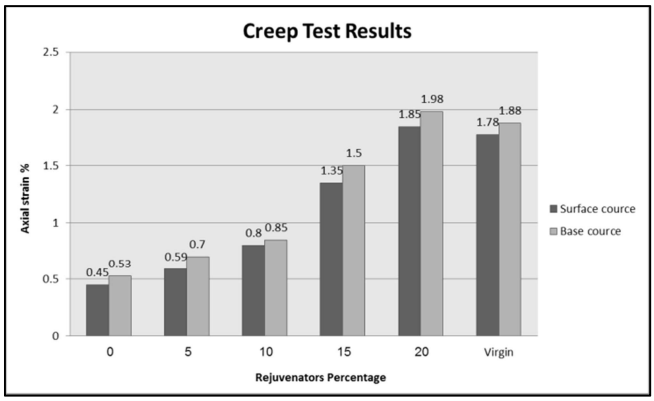

Fig. 1: Axial strains in creep testing at 150 kPastress level

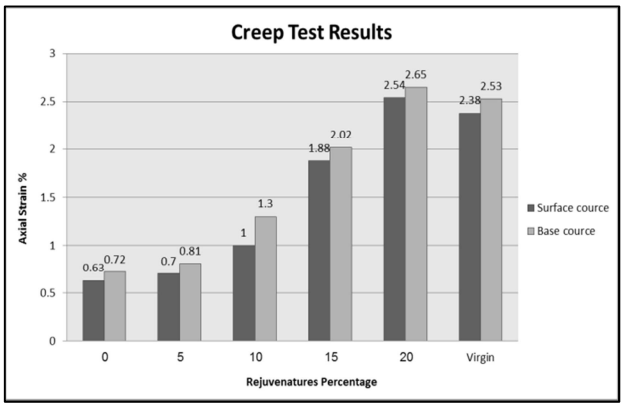

Fig. 2: Axial strains in creep testing at 300 kPastress level

With the addition of 10% rejuvenator agent, the axial strain values increased excessively. With the addition of 20%, the deformation resistance decreased again. Results of creep testing of the samples containing various amounts of rejuvenating agentare reported in Fig 4 and Fig 5.

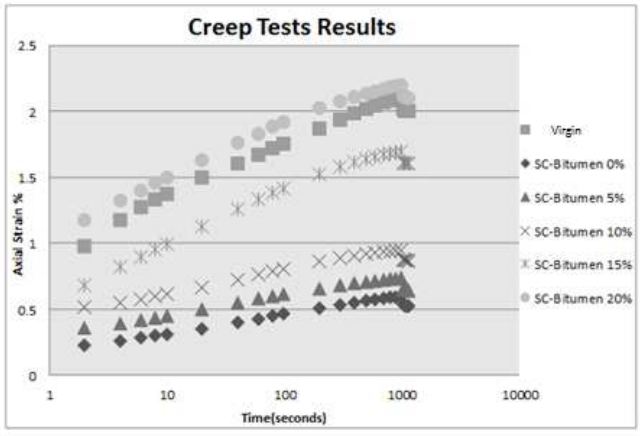

Fig. 3: Axial strains at various loading times at150 kPastress level

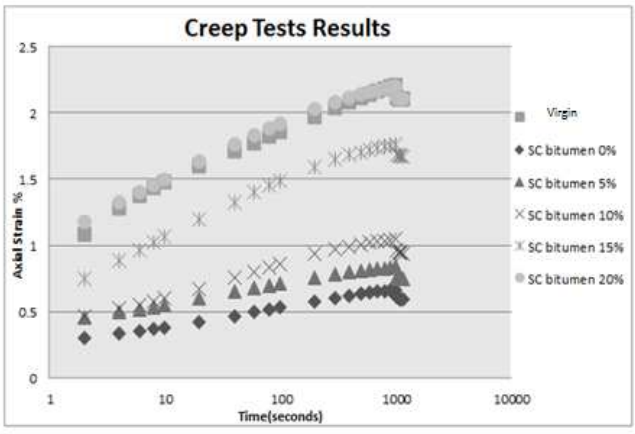

Fig. 4: Axial strains at various loading times at300kPastress level

4. Conclusions

The purpose of this study was to perform a laboratory research work so that to investigate the effects of a cutback bitumen as a rejuvenator in restoring the original properties of TFOT aged binders in mixes. For this purpose, creep testingwas carried out on virgin asphalt mix samples and TFOT binder aged samples. The main conclusions could be summarized as it follows:

- With the addition of the rejuvenating agent, penetration of the aged binder was increased and itssoftening point was decreased. The proper amount of the rejuvenator to be applied in a mix could be determined based on the required penetration and softening point values.
- Creep testing is a useful test in evaluating the effectiveness of cutback rejuvenators. As a result of this test, the optimum amount of the rejuvenator could be determined.
- The optimum amounts of the rejuvenator, determined both at binder studies with penetration and softening points and with creep testing matched reasonably. Hence, the procedure that was carried out in this research could be followed as a guideline for verification and optimizing purposes of the rejuvenating agents.

5. References

[1]Rostler, F.S., and White, R.M., Rejuvenation of Asphalt Pavements, Materials Research and Development, Inc., Oakland, California, under Air Force Systems Command Contract F29601-69-C-0129, May 1970.

[2] Technical Report R690, Reclamite as a Life Extender for Asphalt Concrete Pavements, Navy Facilities Engineering Command, Port Hueneme, California, USA, August 1970.

[3] Value Engineering, Report on Reclamite Usage, Naval Weapons Center, China Lake, California, Navy Facilities Engineering Command - Western Division, San Bruno, California 94066, USA, August 1973.

[4] Planning and Management Organization, Hot and Cold Mix Asphalt Recycling Methods, Transportation Division, Technical Affairs and Standards Bureau, Tehran, Iran, 2012.

[5] Lewis R. H. and Welborn J. Y., Properties of the Residues of 50-60 and 85-100 Penetration and Ductility at Plant Mix Temperatures", Proceedings of the Association of Asphalt Paving T echnologists, Vol. 12, 1940, p 14.

[6]J. Shen, S. Amirkhanian, J.A. Miller, Effects of Rejuvenating Agents on SuperpaveMixtures Containing Reclaimed Asphalt Pavement, J. Mater. Civil Eng. 19 (5), 2007, pp 376–384.

© (2012) Trans Tech Publications, Switzerland
doi:10.4028/www.scientific.net/AMR.587.67

THE EFFECT OF CHEMICALATTACK OF SOME ORGANIC ACIDIC SOLUTIONS TO SELF COMPACTING CONCRETE (SCC)

Jabbar Abbas. Jabir. Al Khafaji[1a], Najah Mahdi Lateef .Al-Maimuri[2b], and Abdul Hadi Meteab. HassanAL Sa'adi[3c],

[1,2,3]Babylon Tech. Inst., Iraq

[a]JabbarJabir64@yahoo.com,[b]Najahml@yahoo.com, [c]Alkhiljan@yahoo.com

Keywords: SCC : self-compacting Concrete, NCC: Conventional Concrete, Trichloroacetic acidic,salicycilic acidic

Abstract. A study of a mechanical performance(Compressive strength, flexural strength, and splitting tensile strength)of self-compacting (SCC) and conventional (NCC)concretemixes and some physical properties of the mixes made of Portland cement under the effect of acidic solution attackare made. Trichloroacetic and Salicycilic acids are selected and used in this study. It is found that the reduction percentage in compressive strength is about 6% and 3% under the effect of Trichloroacetic acidic solution whereas itisabout 8% under the effect the salicycilic acidic solution attackfor both SCC and NCC mixes after 62 days of treatment for bothSCC and NCC mixes respectively.

The reduction percentage in flexural strengthisabout 27% and 37% under the effect of the Trichloroacetic acidic solution attack whereas itis about 59% and 79% under the effect the salicycilic acidic solution attackfor both SCC and NCC mixes respectivelyafter 62 days of treatment.

The reduction percentage in splitting tensile strength is about 60% and 63% under the effect the Trichloroacetic acidic solution attack whereas it is 70% and 88% under the effect of the salicycilic acidic solution attack% for both SCC and NCC mixes after 62 days of treatment.

At the age 90 days, the SCC and NCC mixes have a reductionpercentage in the cubes weight of 3% and 4% whereas there is an increasing in volume of 0.3% and 0.4% respectively under the effect of salicyclic acid solution attack.It is observed that SCC mixes offer more resistant and less deterioration against acidic solutions attack.

Introduction

The costs associated with the provision and maintenance of drinking water and wastewaterinfrastructure represents a significant a financial worldwide demand. Maintenance costs aredisproportionately high, indicating a lack of adequate durability. There remains a lack ofconsensus on degradation mechanisms, the performance of various cement types, the role ofbacteria in the corrosion process associated with wastewater applications and testingmethodologiesConnell et al [1].It is estimated that the annual operation and maintenance costs associated with drinking water and wastewater infrastructure to be in excess of $31 billion and $25 billion respectively. Against this backdrop, it is surprising to note that the corrosion of water and wastewater infrastructure has been a topic of debate for decades, with little consensus on the methods for designing and specifying this infrastructure to optimally meet the harsh environmental demands it will meet in serviceAttiogbe [2], Beeldens et al [3],Monteny et al [4], Mori et al [5], Neville [6], and Yamanaka et al [7].

Evidence thus far has identified bacterial manifestation of the genus '*Thiobacillus'* as a major contributor to the deterioration process of concrete sewer pipelines Mori et al [5], andParker [8]. The product of their metabolism results in sulfuric acid being formed which attacks the cementitious matrix of the concrete causing loss of strength and cohesion. *Thiobacillus* however, plays only a part of a much broader and complicated corrosion process.Budiea et al [9] Illustrates the durability aspect of high strength concrete product using palm oil fuel ash (POFA) of different fineness when exposed to acidic environment. Two POFA concrete mixes with different fineness

termed (POFA 45 and POFA 10) at 20% replacement level by weight of cement. All the specimens are subjected to water curing for 28 days before immersion in a hydrochloric solution having pH 2 for 1800 hours. It is found that an increase in POFA fineness enhances the resistance of high strength POFA concrete towards acidattack.Dan [10] H_2SO_4 attacks concrete in two ways; as it has a dissolving effect and as a propulsive attack through the solidified waste product, i.e, the plaster that is created as a consequence of the chemical reaction. The ensuing crystal growth leads to an implosion within concrete. Cracks appear, the damaging acid can penetrate even deeper into the concrete and destruction is accelerated.Aimin et al [11] reports a review of the standard tests developed to date for sulfate attack, and how the test methods have evolved. He also reviews laboratory research that has been done on the mechanisms of sulfate attack.Turkel et al [12] proved experimentally that the acid resistance of mortars made of Portland cement is better than the pozzolanic cement incorporated samples after 120 days of acidic attack after 28 days of hardening and exposure to four different concentrations of hydrochloric, nitric, and sulfuric acid solutions. Bertron et al[13] studied the chemical elements of cement paste (Ca, Si, Al, Fe and Mg) submereged in organic acid solutions to compare the intensity of the chemical attack of acids produced by pesticides solutions with PH of 4. It is found that Si, Al, and Fe are favorable elements for binder to resist chemical attack, Ca should be limited. The results show that the four acids used;acetic, propionic, butyric, and iso-butyric are equally aggressive.Alexandra et al [14] investigated the effect of 6 organic acids through their pKa, poly-acidity and salts properties: acetic, succinic, malic, tartaric, oxalic and citric acids. The immersion of cement paste for 12 month in similar acidic concentrations shows there is aggressiveness effect of oxalic, tartaric, malic, acetic, succinic and citric acid whereas Calcium oxalate protects matrix.

Organic acids which attack concrete, acidic industrial wastes, silage, fruite juice, sour milk and some untreated water may also cause concrete deterioration. Most ammonium salts are destructive since in alkaline media of concrete, ammonium gas and hydrogen ions are released and replaced dissolving concrete calcium causing a leaching action similarto acidic attack. In this research two types of organic acids are used to evaluate their acidic impact on SCC mixes experimentally; they are trichloroacetic and Salicyclic acids.

Case Study and Cotemporaneous Problem

deteriorationof concrete and reinforcement corrosion in the saturated or unsaturated zone of organic acidic media such as kitchens, tanks or sewage pipes is a significant problem in the world wide and specially in Iraq due of habitual cooking and sewage style .This study is focused to investigate the physiochemical attack of such organicacidic solutionsonthe performanceof self-compactingconcrete mixes made of Portland Cement to recognize and accommodate SCC deterioration comparing with the NCC mixes.

Purpose of the Study

The purpose of current research is exerted to trace the physiochemical deterioration ofacid attack toSCC concrete mixes. Specifically, strength, weight, and volumetric deteriorations are the properties to be in the evaluation process.

Methodology of the Work

a) Acids

Two organic acids are used in this study;they are Trichloroacetic and Salicyclic acids to investigate their effects on some properties of SCC comparing with those of NCC . Trichloroacetic acid has a chemical symbol of CCL_3COOH and molecular weight(163.39) whereas Salicyclic acid has a chemical symbol $HOC_6H_4CO_2HC_7H_{603}$ with a molecular weight of (138.12). The acid of (5) gm powder is soluted in distilled water and the volume is completed to maintain a concentration of (5%) of acidic solution for this work.

b) Cement

Ordinary Portland cement has been employed in mixing proportions for it's more finely ground and lower tricalcium aluminates (C_3A) content. Table (1) shows the physiochemical properties of Ordinary Portland Cement.

Table 1 Physiochemical Properties ofOrdinary Portland Cement

Physical Analysis (According to IOS No.5/1984)		
Setting Time [min]		
Initial	135	≥45
Final	240	≤600
Fineness (Blaine) [m^2.kg]	280	≥230
Compressive Strength [MN/m2]		
At 3days	20	≥15
At 7days	30.5	≥23
Soundness (Auto Clave) %	0.028	≤0.8
Chemical Analysis		
Oxides	%by Weight	Allowable Limits
CaO	64.16	-
SiO_2	20.50	-
Al_2O_3	5.92	-
Fe_2O_3	3.28	-
MgO	2.20	≤4%
So_3	2.21	≤2.5% if C_3A <5% ≤2.8% if C_3A >5%
Free Lime	0.76	-
Loss on Ignition	0.8	≤4%
Insoluble Residue	1.75	≤1.5%
Allumina	%by Weight	
C_3S %	54.76	-
C_2S %	23.2	-
C_3A %	5.146	-
C_4AF%	9.97	-

Tested inBabylon Unv and Industry Ministry Contrapuntal laboratories, 2011

c) Coarse Aggregate

Once the request for coarse aggregate has been examined previously and its grading should be smooth with no gaps in between fine and coarse fractions. A maximum aggregate size of 10-14mm is usually preferred. The percentage passing by weight in the specification is used as shown in Table(2).

Table 2 Gradation of coarse Aggregate

Sieve Size [mm]	%Passing by Weight	Allowable Limits
37.5	100	100
20	97.5	95-100
10	52.5	35-70
5	2.5	0-5
Pan	0	-

Tested by the Researchers, 2011

Table (3) presents the results of specific gravity, Loss Angles (abrasion), and absorption tests for the white crushed gravel which are compared with corresponding values of the common black rounded gravel.

Table 3 Experimental Results of Coarse Aggregate.

	Max Allowable limits	Black Rounded Gravel
Specific Gravity Test	2.6 (Typical Value)	2.63
Loss Angles Test [%]	30	20
Absorption Test [%]	5	1.02

Tested by the Researchers,2011

d)Fine Aggregate Gradation

Fine aggregate should accurately be selected to reduce water requirement whereas the clay and silt content is kept minimum. It is obviously recognized that the selection of fine aggregate to increase workability and reduce segregation. The local type of Kerbala Sand has been carefully used for its rounded grains. Table (4) includes a typical grading of the used sand.

Table 4 Gradation of Fine Aggregate (Sand of Kerbala Queries)

Sieve Size [mm]	[%]Passing by Weight	Allowable Limits
10	100	100
4.75	95	90-100
2.36	87.5	75-100
1.18	77.5	55-100
0.6	47	35-59
0.3	30	8-30
0.15	19	0-10
Pan	0	-

Tested by the Researchers, 2011

e) Mix proportionandPreparation of specimens:

A laboratorial analysis begins with molding of conventional and SCC concrete mixes samples, microscopic testing for the samples sections before and after exposing to acidic solutions, and then testing the mechanical performance and strength properties before and after acidic exposing. In summary, the proportion of the current mixes is prepared and listed in Table (5).

Table 5 Mixes Proportion, kg Per [$1m^3$]

Item	SCC Mix	Conventional Mix
Cement	380	350
Filler	100	-
Water	160	140
Coarse Aggregate	800	1400
Fine Aggregate	750	700
Super Plasticizer	6 liters	-

It is designed by the Researchers, 2011

f)Testing procedure

After 28 days of curing, the specimens of both conventional and SCC mixes are dried in an oven at $105C^{o}$and the initial weights were measured. Then one set of specimensof both types of concretes are stored into solutions of the considered organic acidsand another set are stored in curing water.After the exposure to the acids, specimens are washed inorder to remove the porous disintegratedlayer such as soft and crystallized acidicmaterials. Then specimens are dried in an oven at $105C^{o}$. Loss in weightof the specimens is measured after four weeks during the testing period of 90 days. Compressivestrength of the control (non-exposed) specimens andthose specimens

subjected to solutions of acids with the concentrationof 0.5% at the ages of (28,56and 90)daysare determined. The compressivestrength values of specimens are calculated by using the original cross-sectionalarea of the original cubes.

Two types of acid solutions have been used to expose the manufactured cubes of concrete; they are:-

1- Trichloroaceticis preparedby the reaction of chlorine with acetic acid in the presence of a suitable catalyst:$CH_3COOH + 3\ Cl_2 \rightarrow CCl_3COOH + 3\ HCl$
2- Salicyclic Acid has the formula $C_6H_4(OH)COOH$

g)Sequential Exposure and Testing

1) Compressive Strength: Two sets of NCC and SCC cubes are exposed to Trichloroacetic Acid solution with age of (28)days and two sets of the foregoing two mixes are unexposed.A compressive strength test has been carried out for both types of exposure of the two types of concrete. The results are presented in the Fig.(1).The figureindicates that the strength is increased with ageprogressivefor both types of unexposed concretes; moreover SCC concrete records higher results than the corresponding NCC concrete due to better compaction comparing with NCC concrete. The strengthening process is accompanied with reducing of compressive strength values with age progressive due to theconsequences of acidic solutionexposure and the resulting deterioration of concrete. SCC mix stilloffershigher results and better resistance to Trichloraceticacidic attack than NCC mixes as presented in Fig.(1).

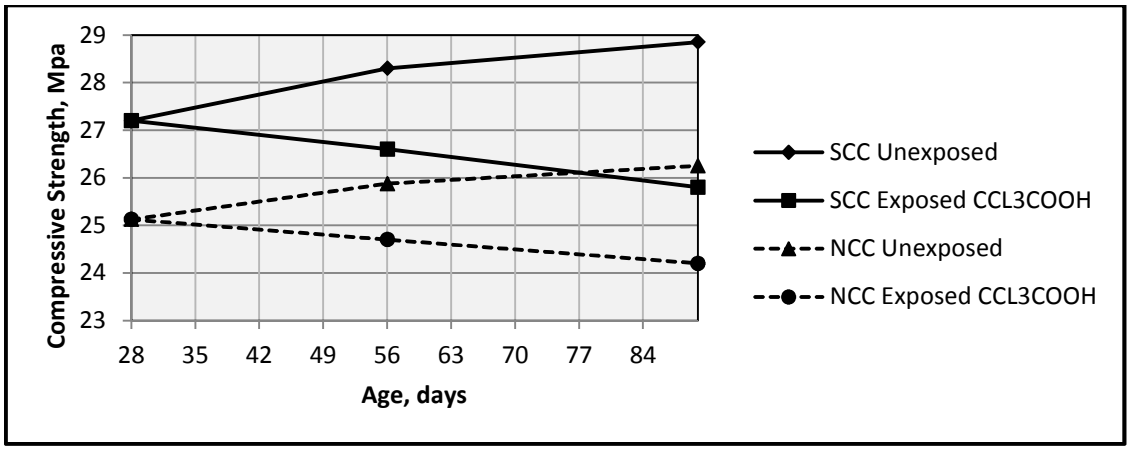

Fig.1Relation between Compressive Strength versus Age for SCC & NCCin Trichloacetic Acid Solution Exposure

2) Flexural Strength: A flexural rigidity test has been executed to an exposed and unexposed concrete specimens for 90 days period in trichloroacetic acid solution and the results are shown in Fig.(2).The results trends of both concrete types are similar to that of compressive strengthand SCC mixes also offer more resistant to the deterioration effect of acids due to its denser structure. The results also show that the deteriorative effectof acidic attack is relatively much more in the case of tensile stresses than compressive stresses for both SCC and NCC mixes.

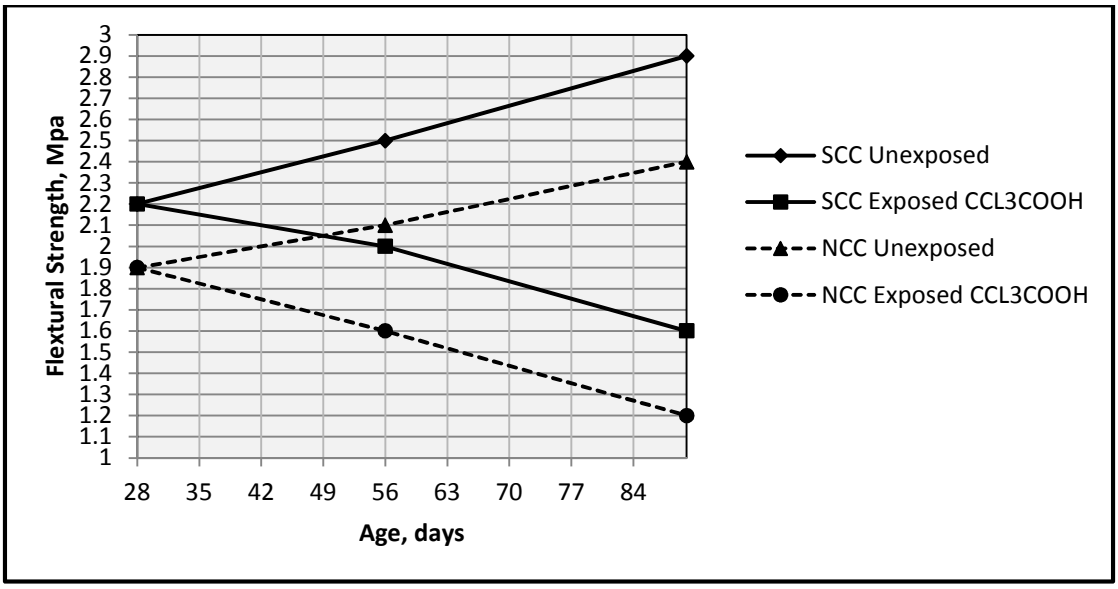

Fig 2 : Relation between Flexural Strength versus Age for SCC & NCC in Trichloroacetic Acid Solution Exposure

3) Splitting Strength:A splitting Tensile Strength Test is achieved on exposed and unexposed samples to Trichloroacetic acid solution and the results are shown inFig.(3).

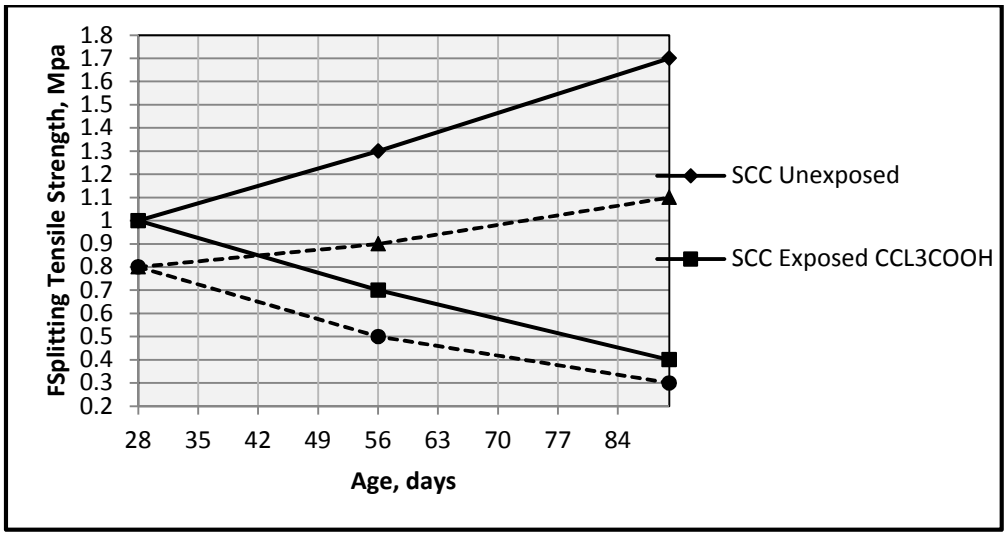

Fig. 3: Relations between Split Tensile Strength versus Age for SCC & NCCin Trichloroacetic Acid Solution Exposure

4) A series of compressive strength tests have been performed on sets of SCC &NCC exposed and unexposed samples to salicyclic acid solution. The results are presented in Fig.(4).

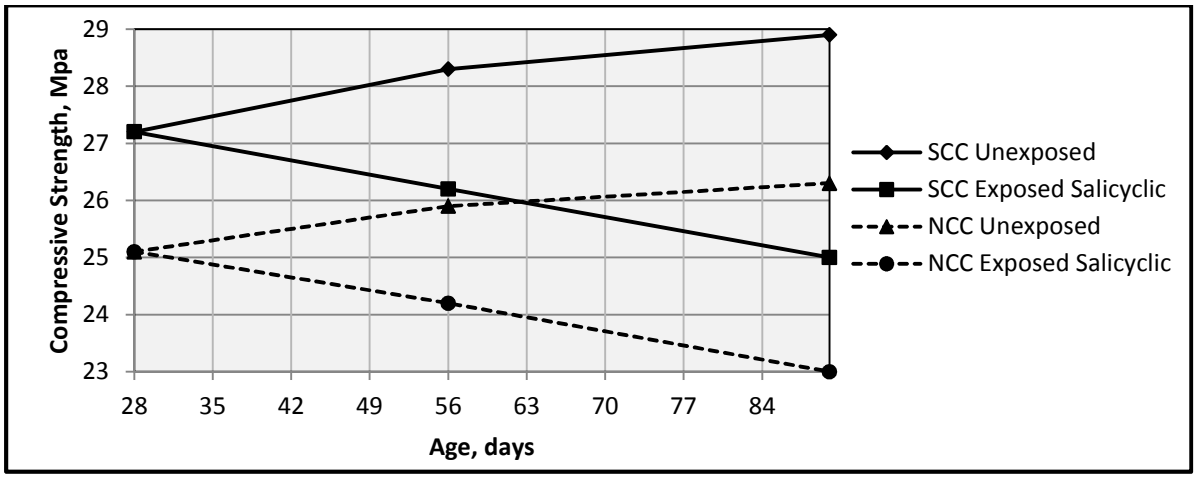

Fig.(4) : Relation between Compressive Strength versus Age for SCC & NCCin Salicyclic Acid Solution Exposure

5) A flexural rigidity test has been conducted to an exposed and unexposed concrete specimens for 90 days period in salicyclic acid solution and the results are shown in Fig.(5).The results shows that theSalicyclic acid is more destructive than Trichloroacetic acid as a result of a more reduction in ftextural rigidity values.

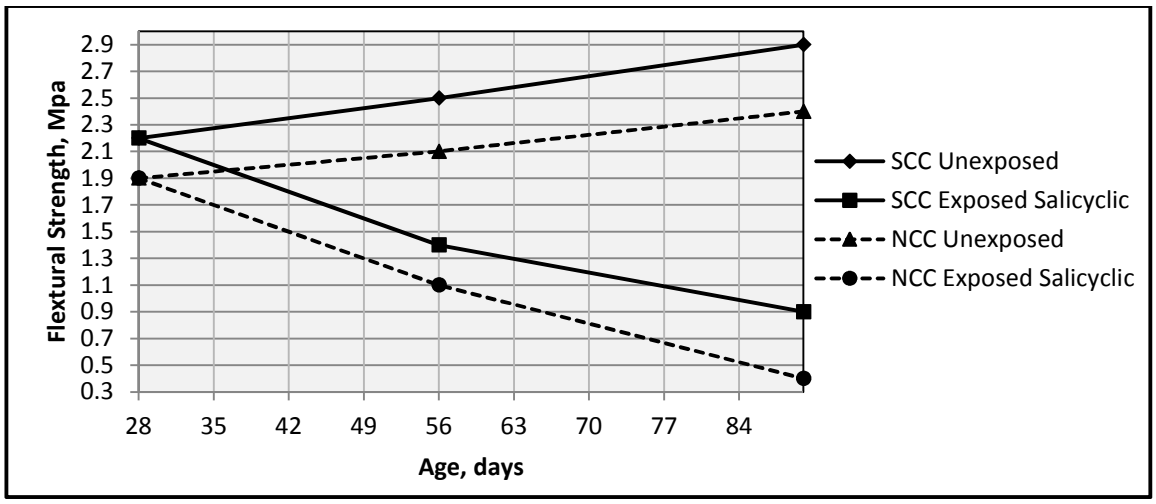

Fig. 5: Relation between Flexural Strength versus Age for SCC & NCCin Salicyclic Acid Solution Exposure

6) A splitting Tensile Strength Test is achieved on exposed and unexposed samples to Salicyclic acid solution and the results are shown in Fig.(6).

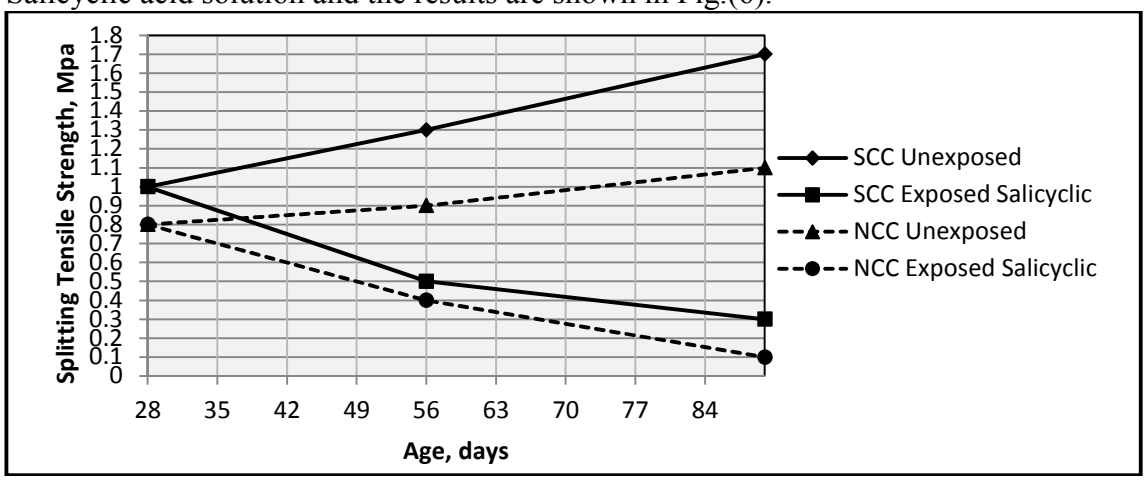

Fig. 6: Relation between Splitting Tensile Strength versus Age for SCC & NCCin Salicyclic Acid Solution Exposure

Weight Reduction

It is found that the treated cubes submerged insalicyclic acidic solution undergo a reduction in weight due to the corrosive process of the concrete due to exposure. The results are represented graphically in Fig.7

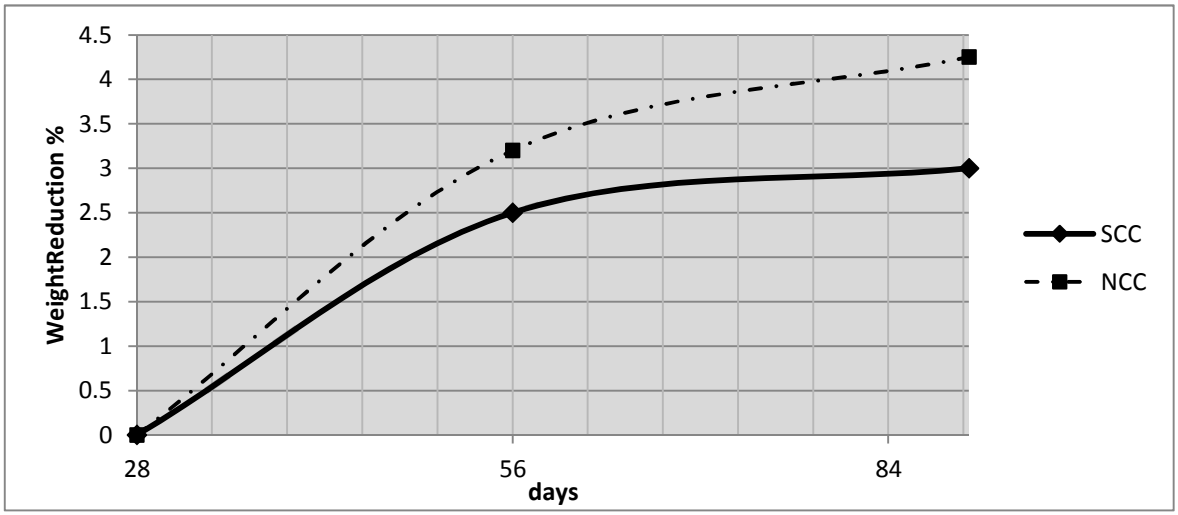

Fig.7: Weight ReductionPercentage Accompanied with Salicyclic Acid Solution

Volumetric Expansion

It is observed that the treated cubes with salicyclic solution characterized with a certain expansion with age under salicyclic acid solutions as shown in Fig.8.

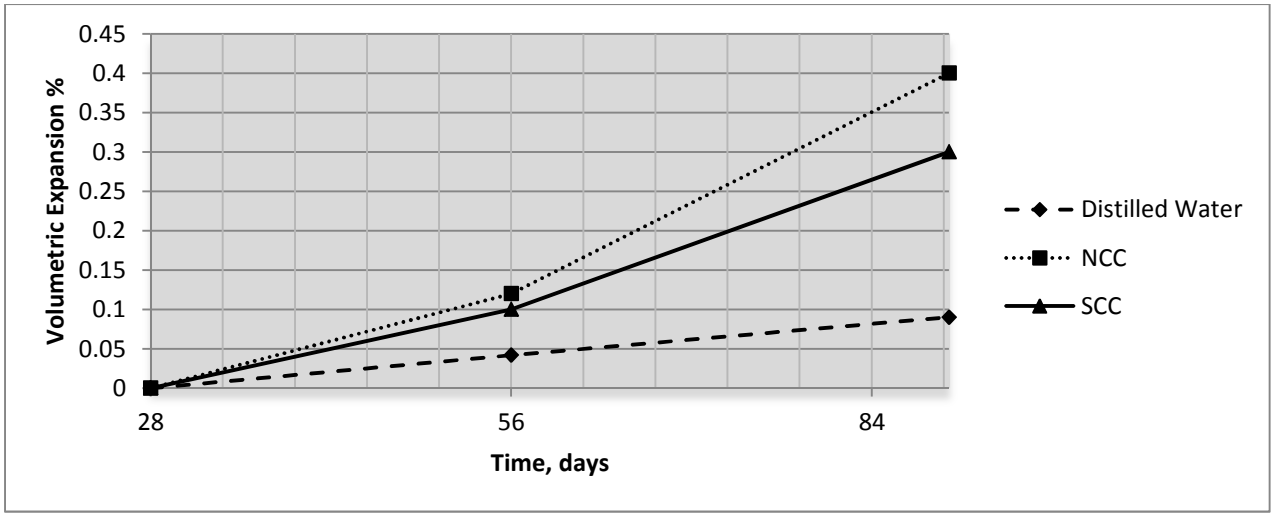

Fig. 8 Volumetric Expansion Percentage of Concrete Mixes Under the Effect of salicyclic Solution

Results and Discussion

Briefly, acidic solutions have many bad effects on the physical properties of concrete constituents and mechanical performance. They could be abbreviated as follows:

1- The reduction percentage in compressive strength is about 6% and 3% under the effect ofTrichloroacetic acidic solution attack whereas itis about 8% under the effect the salicycilic acidic solution attack for both SCC and NCC mixes respectively after 62 days of exposure as indicated in Fig.1 and Fig.4.

2- The reduction percentage in flexural strength is 27% and 37% under the effect the Trichloroacetic acidic solution attack whereas it is 59% and 79% under the effect of salicyclic acidic solution attackfor both SCC and NCC mixes respectively after 62 days of treatment as indicated in Fig.2 and Fig.5.

3- The reduction percentage in splitting tensile strength is 60% and 63% under the effect the Trichloroacetic acidic solution attack whereas it is 70% and 88% under the effect the salicyclic acidic solution attackfor both SCC and NCC mixes respectively after 62 days of treatment as indicated in Fig.3 and Fig.6.
4- At the age 90 days of Trichloroacetic acid solution attack, the SCC and NCC mixes have a reduction in the cubes weight of 3% and 4% respectively. This is attributed to the effect of the chemical reaction between the acid and the concrete mix constituents.
5- It is observed that after 90 days of the concrete cubes of treatment with the acidic solution; there are increasing in volume of 0.3% and 0.4% for both SCC and NCC mixes respectively.
6- It is observed that SCC mixes offer more resistant and less deterioration to the acidic solution attack if they are compared to the NCC mixes. This phenomenon may be attributed to high density and more compacted concrete constituents of SCC mixes which is produced by the fine materials (filler). The fines materials produce less porous structure of concrete samples which in-turn produces less bad effects of acids attack.

Conclusions

The current study reveals to the following conclusions:-

1- The self-compacting concrete(SCC) mixesPortland cement show more resistance and less deterioration to acidic solutions attack than the conventional mixes.
2- From the results of the mechanical performance (compressive strength, splitting tensile strength, and flexural strength) of SCC and NCC mixes, the two organic acids attacka hardened concrete identically with time with exception thatSalicyclic acid shows more viable effect and produces more deterioration to both SCC and NCC mixes as shown in Figs.1 to 6.

Recommendations

From this study, the followings are recommended:-

1- It is recommended to use SCC mixes for construction parts wherever and whenever an acidic mediums are expected to be occurred.
2- It is recommended to extend this study to comprise the effect of other organic acids attack on SCC mixes made of Portland cement.

REFERENCES

[1] O. M. Connell., C. McNally and M.G. Richardson: Biochemical Attack on Concrete in Wastewater Applications. School of Architecture, Landscape and Civil Engineering, University College Dublin, Newstead, Belfield, Dublin 4, Ireland, 2010.

[2] EK. Attiogbe, and SH. Rizkalla: Response of concrete to sulfuric acid attack. ACI Mater J; 84(6):481–488, 1988.

[3] A. Beeldens, J. Monteny, E. Vincke, N. De Belie, D. Van Gemert, L. Taerwe, and W. Verstraete: Resistance to biogenic sulfuric acid corrosion of polymer-modified mortars". Cem Concr Comp; 23(1):47-56,2001

[4] J. Monteny, E. Vincke,A. Beeldens, N. De Belie, L. Taerwe, D. Van Gemert, and W. Verstraete: Chemical, microbiological, and in situ test methods for biogenic sulfuric acid corrosion of concrete". Cem Concr Res; 30(4):623-634, 2000.`

[5] T. Mori, T. Nonaka, K. Tazaki, M. Koga,Y. Hikosaka, and S. Noda: Interactions of nutrients, moisture and pH on microbial corrosion of concrete sewer pipes.,Water Res; 26(1):29-37,1992.

[6] A. Neville: The confused world of sulfate attack on concrete., Cem Concr Res; 34(8):1275-1296,2004.

[7] T. Yamanaka, I. Aso, S. Togashi, M. Tanigawa, K. Shoji, T. Watanabe, N. Watanabe, K. Maki, and H. Suzuki: Corrosion by bacteria of concrete in sewerage systems and inhibitory effects of formats on their growth., Water Res; 36(10):2636-2642, 2002.

[8] CD. Parker: The isolation of a species of bacterium associated with the corrosion of concrete exposed to atmospheres containing hydrogen sulfide., Aust J Exp Biol Med Sci;23:81-90, 1945.

[9] A. Budiea, M.W. Hussin, K. Muthusamy,and M. E. Ismail: Performance of High Strength POFA Concrete in Acidic Environment.,Department of Structure and Material, Faculty of Civil Engineering, University Technology Malaysia, MALAYSIA.2009.

[10] Dan Babor and G. Micheal : Treated and Terminated Sulphuric Acid Attack., BuletinulInstitute Polytechnic Din Lasi Tomul LII (LVII), Fase, 3-4, 2007.

[11] Xu. Aimin, S. Ahmed, and B. Pud: Test methods for Sulfate Resistance of Concrete and Mechanisim of Sulfate Attack., Arrb Transport Research Ltd Review Report 5 September 1998.

[12]S. Turkel, B. Felekoglu, and S. Dulluc: Influence of Various Acids on the Physico-Mechanical Properties of Pozzolanic Mortars., Sadhana Journal Vol. 32, Part 6, December, PP.683-691, © Printed in India, 2007.

[13] A. Bertron, J. Duchesne, and G. Escadeillas,: Attack of Cement Paste Exposed to Organic Acids in Mature., Laboratoire Mate´riaux et Durabilite´ des Constructions, INSA-UPS, Complexe Scientifique de Rangueil, 31077 Toulouse, France, Cement & Concrete Composites 27 898–909, 2005.

[14] B. Alexandra, L. Steeves, and E. Gilles: Organic Acids Attack on Cementitious Materials., Mendeley Miscellaneous Papers, 2011.

doi:10.4028/www.scientific.net/AMR.587.77

Comparison of Field Performance between Bamboo-Geotextile Composite Embankment and High Strength Geotextile Embankment

Aminaton Marto[1], Bakhtiar Affandy Othman[1*], Fauziah Kasim[1] and Ismail Bakar[2]

[1] Department of Geotechnics and Transportations, Faculty of Civil Engineering, Universiti Teknologi Malaysia, 81310 UTM Skudai, Johore, Malaysia

[2] Research Centre for Soft Soils (RECESS), Faculty of Civil & Environmental Engineering, Universiti Tun Hussein Onn Malaysia, 86400 Parit Raja, Batu Pahat, Johore, Malaysia

*Corresponding Author : aminaton@utm.my, bakh_7@yahoo.com

Keywords: Trial embankment, field performance, geotechnical instrumentation, bamboo, geotextile.

Abstract. Trial embankment approximately 3 meters height, 10 meters of length, 16 meters width, and a slope of 1V: 2H was completed on soft clay site at RECESS, UTHM, Batu Pahat, Johor, Malaysia. Two embankments were respectively reinforced by a high strength geotextile (HSG) and the combination of bamboo and low strength geotextile or bamboo-geotextile composite (BGC) at the interface between embankment fill and foundation soil. Each embankment was installed with the same geotechnical instrumentation scheme for monitoring purposes. The purpose of this paper is to analyse the field performance for both embankments in terms of improving settlement embankment under the embankment. For this purpose, the settlement under the embankment, settlement at the surface of the embankment and the excess pore water pressure response were measured through geotechnical instrumentation for over 418 days. The results showed that the BGC system is more practical than HSG in terms of settlement and also in terms of cost, without compromising the quality of the embankment performance.

Introduction

Generally, the use of geotextile was widely applied on any construction projects today such as soil stabilization, earth dam, coastal protection works, road pavement and etc. Geotextiles is widely used in soil as separation, filtration, reinforcement, soil erosion control and drainage purposes. As filtration purpose, the geotextile allows the flow of water, gases, and fine particles but prevents the passage of large particles soil. Geotextiles placed below or beneath embankment is able to provide extra lateral forces to prevent embankment from failing or deformed caused by rotation and splitting [1]. Concern on environmental effect brings the geotechnical engineers to reduce the rely on the unrenewable materials such as geotextile and try to apply the natural resources like bamboo. It grows in abundance in the earths of subtropical, tropical and even in temperate countries. [2] reported that over 75 genera and 1250 species of bamboo exist in the world. The strength of the various of bamboo has been reported by [3], [4] and [5]. A few of researchers have published and reported the use of bamboo in construction (e.g. [6], [7], [8] and the findings show that the effectiveness of the usage of bamboo in construction.

This paper aimed to analyse the performance of the BGC system compared with HSG reinforcement of embankment with respect to the effectiveness of the used of bamboo. The construction of the embankment, location of installation of the instrumentations and the results from monitoring works are carried out in order to achieve the aims of this paper.

Field Embankments

There are three types of embankment constructed on soft foundation which are differentiated by different type of reinforcement installed at the soft clay foundation surface. But for this paper, only two embankments (BGC and HSG) are focused. The embankments are:

1. HSG Embankmnet - Using high strength geotextile (PEC100) laid at the interface between embankment and foundation soil.
2. BGC Embankment – Using bamboo with low strength geotextile (TS40) as separator laid at the top of bamboo arrangement (1 m x 1 m) square pattern installed at the interface between embankment and foundation soil.

In situ Measurement

For the purpose of collecting data from field monitoring works, various geotechnical instrumentations such as hydrostatic profiler, piezometers and surface settlement marker had been installed. Fig. 1 shows the locations of the installed geotechnical instrumentations for each embankment.

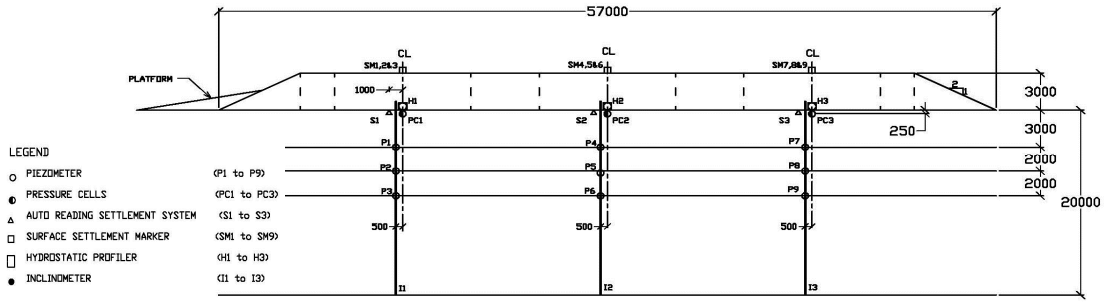

Fig. 1. The arrangement and the location of the instrumentations (Marto, 2010)

Hydrostatic Profiler

Settlement rate across each embankment was measured by hydrostatic profiler. The settlement rate were measured for every 1 m interval from the reference point (permanent concrete box) through excess tube using polyethylene (PE) tube with outer diameter (OD) of 75 mm Class 12. The excess tube was laid along below the embankment fill with the concrete box at the toe of the embankment as a reference level.

Surface Settlement Marker

The surface settlement markers had been used for monitoring the variations in height of the embankment with time. The settlements markers have been installed at the surface of the embankment with gap between the three settlement markers were 1.5 m.

Piezometer

The variation of excess pore water pressure developed start from construction of the embankment fill to end of monitoring works have been read out by piezometers installed. Three numbers of piezometers had been installed at different depth of 3 m , 5 m and 7 m from ground level for each embankment. This piezometers reading was logged automatically and saved in the attached data logger.

Results and Analysis

The fill height of the BGC embankment was close to the height of the HSG embankment, measured of 2.970 m and 2.968 m respectively at the end construction works (Fig. 2). During the construction of the embankment, the settlement at the base of the BGC embankment increased at rate 15.2 mm/day and 8.3 mm/day for HSG embankment until Day 17. At the end of the construction work, the BGC embankment showed higher settlement compared to that of HSG embankment where 258 mm and 141 mm respectively. This condition might be due by the inhomogenity of the soil layers. For the consolidation settlement monitored within 401 days, BGC embankment again showed the lowest value of 330 mm, while HSG embankment recorded 458 mm. The results show that as the BGC system retained the surcharge load and distributed only small load to the underlain clay soil, resulted in smaller consolidation settlement was obtained compared to HSG embankments.

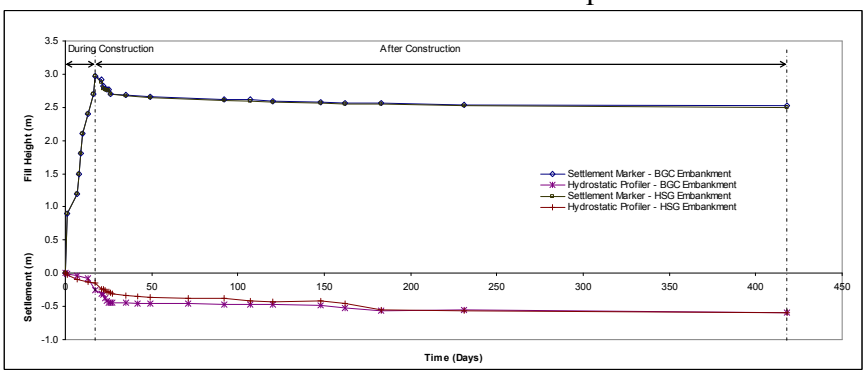

Fig. 2. Settlement results with time

Fig. 3 shows that during the 17 days of backfilling BGC embankment, the excess pore pressure increased rapidly with the embankment height. At the end of construction period, it achieved 20.98 kPa reading at 3 m depth. In general, during the construction phase, the excess pore pressure was observed to increase proportionally with the embankment height and after the construction, it decreased proportionally with time, but at a slower rate, until end of monitoring works on Day 418. The dissipation of excess pore water pressure was slow due to low permeability nature of the foundation soil. At the end of Day 418, the excess pore pressure was measured at 6.19 kPa.

In HSG embankment, for 17 days of construction period, the excess pore pressure had increased rapidly with embankment height and achieved the maximum excess pore pressure at 2.968 m height with 22.49 kPa. After the completion of embankment construction, the dissipation of pore pressure that occurred at 3 m below HSG embankment dissipated at different rate compared with BGC embankments. The excess pore pressure for HSG embankment had been recorded as 3.30 kPa at the end of monitoring works (418 Days). This condition occurred because the HSG embankment was using the same material (geotextile). However, the properties of geotextile using PEC 100 provide higher horizontal flow rate at $30x10^{-7}$ m^2/sec compared with TS 40 geotextile only $24.5x10^{-7}$ m^2/sec. On the other hand, the use of bamboo decreased the area of the geotextile for dissipation of the pore pressure due to the properties of bamboo which cannot act as drainage system. The same trend also occurred at 5 m depth of piezometer readings (Fig. 4).

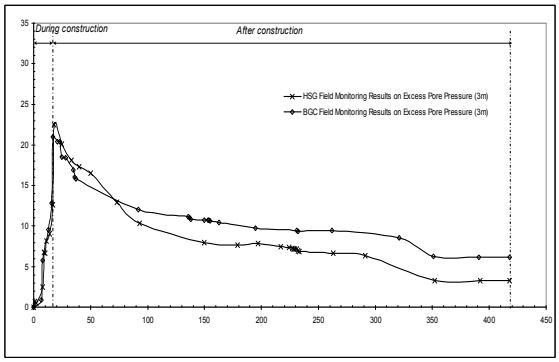

Fig. 3. Pore pressure response at 3 m depth

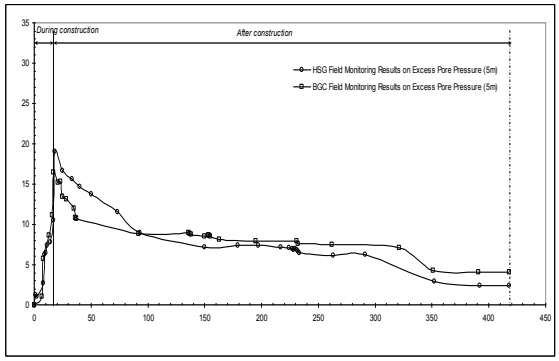

Fig. 4. Pore pressure response at 5m depth

Based on the finding by [7], the use of the BGC system in the construction of embankment on soft clay could save the construction cost of at least 46.4 % per square meters of area. BGC system is cheaper than any other product of the same category. This alternative green technology method could therefore be used as an effective soft clay improvement method in embankment construction.

Conclusion

The analysis and the results from these two embankments have shown that there are a big potential of the use of the BGC system for environmental impacts and cost effectiveness. The BGC system decreased the settlement in a long term compared to the HSG system. The results show that the BGC system could save a cost about 46.4 % per m^2 [7] and decreased the consolidation settlement about 28 % compared to HSG system. The use of bamboo as green material is not only decrease a rely on unrenewable materials but at the same time improves the quality of the available system in market. Therefore, the BGC system as a new soil reinforcement system can be used in construction embankment, especially for future buildings constructed on soft clay deposit.

Acknowledgement

The authors would like to thank to individual, groups of researchers and company involved in this research for their guidance and support. The appreciation is also addressed to Ministry of Higher Education (MOHE) of Malaysia and Universiti Teknologi Malaysia (UTM) through research project under the Research University Grant (RUG) Program, Vot No. Q.J130000.7122.00J22 for financial support.

References

[1] R.W. Sarsby. *Use of "Limited Life Geotextiles" (LLGs) For Basal Reinforcement of Embankment Built on Soft Clay*. Civil Engineering Section, SEBE, Wolverhampton University, Wolverhampton WVI ISB, UK. Elsevier Science Direct. (2007)

[2] S. Thammicha. *Bamboo*. Proceedings of A Workshop on Design and Manufacturing of Bamboo and Rattan furniture. Jakarta, Indonesia, pp. 1–12 (1989).

[3] S.C. Lakkad & J.M. Patel. Fiber Sci. Technol. 14: 319-322 (1980).

[4] K. Ghavami. *Bamboo as Reinforcement in Structural Concrete Elements*. Cement & Composites. 27.p.p 637-649 (2005).

[5] A. Marto and B. A. Othman. *The Potential Use of Bamboo as Green Material for Soft Clay Reinforcement System.* Published at IPCBEE vol.8 (2011) © (2011) IACSIT Press, Singapore.

[6] M. Irsyam, S. Krisnanto and S.P.R. Wardhani. *Instrumented Full Scale Test and Numerical Analysis to Investigate Performance of Bamboo Pile-Mattress System as Soil Reinforcement for Coastal Embankment on Soft Clay*. Geotechnical Engineering for Disaster Mitigation and Rehabilitation Liu, Deng and Chu (eds) 2008 Science Press Beijing and Springer-Verlag GmbH Berlin Heidelberg (2008).

[7] A.Marto, F. Kasim and B.A. Othman. *Bamboo-Geotextile Composite Soil Reinforcement System*. Slide presentation at Industrial Art and Technology Exhibition 2010 (INATEX 2010).

[8] A. Khatib. *Bearing Capacity of Granular Soil overlying Soft Clay Reinforced with Bamboo-Geotextile Composite at the Interface*. Ph.D Thesis, Universiti Teknologi Malaysia. (2009)

doi:10.4028/www.scientific.net/AMR.587.81

The Effect of Blast Furnace Slag on Foam concrete in terms of Compressive strength

Zaid Shaker Aljoumaily[1,a], Norizal Noordin[2,b], Hanizam Awang[3,c] and Mohammed Zuhear Almulali[4,d]

[1,2,3,4]School of Housing, Building and planning, Universiti Sains Malaysia 11800 Minden, Penang, Malaysia

[a]zsm10_hbp095@student.usm.my, [b]norizal@usm.my, [c]hanizam@usm.my, [d]mza11_hbp029@student.usm.my

Keywords: Foam concrete, Blast Furnace Slag, Compressive strength, Additive

Abstract. This study is a part of an on-going research studying the effect of blast furnace slag as a binder and filler replacement on the properties of fresh and hardened foam concrete. A mix having the density of 1300kg/m^3 with a proportion of (1 cement:2 sand), W/C ratio of 0.45, a commercially available additive (SP-1), class F fly ash and a unprocessed blast furnace slag was used. The results show that the mix containing the slag achieved a higher compressive strength (6.31MPa at 28 days) than that of the control mix at the same age (5.81MPa). In addition, combining both slag and fly ash as a cement replacement further enhanced the compressive strength achieving higher compressive strengths. Also, a more stable mix was achieved by the slag replacement when compared to the control mix. This result concludes that the unprocessed slag is a good pozzolanic material that can be used with foam concrete.

Introduction

Concrete is known to have a mix of cement, fine sand, coarse aggregate and water. In its simple form, it is the most consumed material on planet earth after water. However, its manufacturing is a large contributor to global warming. A single cubic metre of concrete produces 480kg of carbon dioxide emitted to the atmosphere. Cement is the largest (CO_2) emitter when manufactured. A tonne of (CO_2) is emitted due to the production of a single tonne of cement. Another environmental concern arises is the depletion of natural resources [1]. The construction industry is needed to be more environmentally considerate. This is achieved by the usage of energy saving materials and the utilisation of waste materials in the manufacture of the building components.The Malaysian industry sector produces more than 10 million tons of by-products per year and due to environmental concerns, more than 50% of the by-products can be utilized in the construction industry as pozzolanic materials [2]. The utilization of by-product materials as cementation materials is a common practice in concrete manufacturing, discovered many years ago, in order to enhance concrete properties. The most common supplementary cementitious materials (SCMs), used as a cement replacement material, are fly ash, silica fume and ground granulated blast furnace slag (GGBFS) [3]. The reason behind using the by-product materials in the construction industry is due to the boost of raw material costs and the increasing consumption of natural resources [4-5].Foam concrete, as a low weight material, is considered to be a green product since it uses less natural resources and to its ability of incorporating by-product or waste materials in its mix [6].Foam concrete is defined byWimpenny[7] as " a relatively light-weight, low strength material formed by entraining air in a sand-cement mortar. The air is entrained by the addition of either chemical admixture or preformed foam to the base mortar mix".However, foam concrete's structural properties have been gaining growing interest due to its low weight, material savings and further more its potential in incorporating high volumes of waste materials [8].There are many types of applications that utilize foam concrete varying from building components with higher density and strength to make it as filling material to fire protection and thermal insulator, like cast in-situ piles, soil backfill, fill the cavity wall in precast elements or insulator filler in wall [9].The type of

raw materials, equipment and the final product play a vital role in the cost of foam concrete. The normal patch of foam concrete is produced from Ordinary Portland Cement, fine sand and stable foam. The mix design and water content in the production of foam concrete is related to the cost and the strength of the product. The strength of the dry density foam concrete will decrease with the increasing amount of fine sand leading to the decrease of cost [6].This paper is a part of an on-going research focusing on the utilisation of Blast Furnace Slag in foam concrete. The research is dealing with the replacement of both binder and filler by this by-product. This paper, however, deals with the replacement of cement by raw slag (as received from the source) at a replacement level of 40% and its effect on the compressive strength.

Properties of blast furnace slag

As a by-product, blast furnace slag is produced during the process of iron manufacture. Slag is the siliceous and aluminous residue resulting from the merging of limestone flux with the ash from the coke [10]. Blast furnace slag is considered as a glassy material varying in colour from dark beige to off-white depending on the raw materials used in the iron manufacturing process. When compared to cement, blast furnace slag has a lower specific gravity but having a higher fineness [11]. Silicates and alumina-silicates of calcium and other bases are the main constituents of this by-product. Its pozzolanic properties are a result of its glassy nature. Its main chemical components are CaO, Al_2O_3, SiO_2 and MgO, which are the same as cement's components but in different proportions [10].Blast furnace slag as a partial cement replacement can result in a number of environmental benefits. Such benefits are the energy conservation, reducing CO_2 emissions andsaving natural resources from depletion. It also creates the opportunities of the incorporation of such a material in concrete manufacturing to replacement levels up to 80%[11]. The utilisation of slag has economical benefits also. The benefits are the reduction of concrete cost and it creates the opportunity to the steel manufacturers to redeem a financial benefit from their waste [12].

The effect of blast furnace slag on compressive strength

Many researchers have studied the effect of utilising blast furnace slag on the different types of concrete, mortars and cement paste. These studies used different replacement levels of blast furnace slag as a cement or filler replacement.Austin, et al. [13],studied the effect of replacing the cement in a conventional concrete mix having the proportions of (1:1.8:2.6 and W/C of 0.5) by slag at a replacement level of 50%. The researcher used more than one type of curing method, and the maximum strength gained from the polyethylene wrapping method was 39.1MPa at 28 days. Using a conventional concrete mix of (1:1.66:2.77) and a W/C ratio of 0.45, Mohd Shariq, et al.[14] used slag as a cement replacement at levels ranging from 20% to 60% and gained compressive strengths in the range of 38.4MPa to 31.1MPa (82% and 64% from the control mix's strength) respectively. R Siddique andKaur[15] also used slag as a cement replacement at levels of ranging from 20% to 60% in a normal concrete mix with proportions of (1:1.1:2.3) and W/C of 0.45 and superplasticizer at 1.1% by weight of binder. The compressive strength at 28 days obtained by the researcher for the replacement mixes was less than the control mix (34.5MPa) by 16.8% to 28.5%. In another study, a number of recycled materials such as cement-slag (grade 120), recycled concrete aggregate and crushed glass were used by different percentages in a conventional concrete mix having the proportions of (1:2.15:2.7), W/C of 0.4, High-Range Water-Reducing Admixture(HRWRA) and cured via water bath (23$\pm$2C°) at different percentages [3]. The maximum strength gained by Maier and Stephan [3] at 28 days (46MPa) was achieved by using a 50% replacement of all mix constituents by recycled materials when compared to the control mix's strength of 40.3MPa.

A study conducted by Bekir andTurhan[16] focused on the replacement of cement by blast furnace slag in a mortar. He also studied the effect of different fineness of slag (3500-4000m^2/kg), different replacement levels and the effect varying temperatures on strength. The mortar used had a proportion of (1:3) with a W/C of 0.5. The maximum strength gained by Bekir andTurhan[16] was 69.1MPa (the control mix had a compressive strength at 28 days of 39.4MPa) at a slag fineness of

4000m^2/kg and a replacement level of 30% of cement by slag by weight on 28 days at a temperature of 20C°. Thomas andBremner[17] used a concrete mix having lightweight aggregates with a size of 25mm and replacing the cement by slag at levels from 25% to 65% with densities ranging from 1940 to 1870kg/m^3, respectively. The concrete mix had a constituent ratio of (1:1.4:1.2) with nominal W/C ratio of 0.4. The samples were moisture cured and the obtained compressive strength of the control mix at 28 days was 36.5MPa; however, the compressive strength increased by 107% and 109% at replacement levels mentioned previously.Aguilar andDíaz[18] studied the effect of slag replacement on the properties of non-autoclaved aerated concrete. The researcher used the slag as filler in the mix and 100% metakoalin as cemintitous material. The mix proportions used was (1:1) and the samples were cured by cling film wrapping and stored at a isothermal chamber at a temperature of 20C°. The maximum strength gained from samples having a density of 1200kg/m^3 was 14.6MPa at an age of 28 days. In another study, Esmaily andNuranian[19] used the same type of concrete with the incorporation of alkali-activated slag. The maximum compressive strength gained was 15.3MPa from samples having a density of 1127kg/m^3. A 50% replacement level of cement by slag was used by Wee, et al. [20] in foamed cement slurry. Samples were cured by a fog room at a temperature of 30C°$\pm$2. The mix had a proportion of 1 batch of cement mixed with water at 0.3 by weight of binder. Obtained densities ranged from 600-1935kg/m^3 and the compressive strengths gained were in the range of 2.18 to 58.8MPa, respectively.

The studies mentioned above were chosen due to some similarities between them and this study, such as slag replacement levels, W/C ratio and curing method. From these studies, it is obvious that the utilisation of blast furnace slag obtained compressive strengths which either higher or nearer to the control mix's strength at the same age. This is due to the difference in the replacement levels, W/C ratio, type of curing, concrete additives and type concrete used.

Material and testing procedures

1- Materials. The cement used in this study, produced by Cement Industries of Malaysia Berhad (CIMA Group) classified as a type 1cement according to BSEN 196-1; 2005 [21]. The fine sand met the requirements of BS 812-103.1:1985 [22] for determination of distribution and particle size. The foaming agent used (NORAITE PA-1) is a protein-based agent, which was diluted in water at ratio of 1:33 for obtaining preformed foam having a density of 75- 80kg/m^3. By weight of binder, 1% was used in one mix and 1.5% SP-1 was used as an additive in the remaining mixes. The foaming agent (PA-1) and the additives (SP-1) are commercially available provided by DRN concrete resources company. The GGBFS was used as cement replacement at level 40% in one of the mixes. In another mix, slag was mixed with the fly ash (mix percentage of 50% slag and 50% fly ash) and the mixture was used as a cement replacement at a level of 40%. The slag was used withoutgrinding having the majority of its particles sized between 1.18mm and 0.15mmsieve size.Table 1 below shows the main chemical constituents of the used slag meeting the requirements of BS EN 15167-1:2006 [23]. The Fly ash used in this study was a class Fmeeting the specifications of ASTM C618 [24] and the chemical composition for the Fly ash is illustratedin Table 2. Both the GGBFS and the Fly ash are provided by the school of Housing, Building and planning, USM.

Table 1 Main chemical composition of GGBFS

SiO_2	CaO	Al_2O^3	MgO	MnO	TiO_2	S	TFe
38%	39%	12%	8.5%	0.6%	0.6%	0.5%	0.4%

Table 2 Main chemical composition of Fly Ash class F

SiO_2	Al_2O_3	Fe_2O_3	CaO	MgO	SO_3	K_2O	Na_2O	LOI
55.2%	25.5%	5.2%	5.5%	2.06%	1.4%	0.7%	0.37%	1.92%

2- Mixing procedure. The mass of each constituent was weighed and prepared formixing. The five mixes tested in this study had the same dry density of (1300kg/m^3) and a mix proportion of (1:2.0:0.45). Before mixing, the mixer should be wet; then the sand was put at first in the mixer along with one or two cups of the water. After being mixed properly, the cement was added and

also the rest of the water added with the additive gradually depending upon the mortar flow test. The constituents were left to mix in the mixer until a homogeneous mixture and the required target flow test was obtained. The density of the mixture was measured by filling a one- litre cup from the mix and weighed. After that, the foam weight was calculated from the actual mortar volume and the total volume. The foam was added according to the flow rate of the machine (litre/ sec) then waiting two minutes to let the foam mix properly with mortar then, measure the density of the concrete which is acceptable $\pm$2-3%from the wet density. The resultant mix was poured into cube steel moulds of (100x100x100mm). The cubes were demoulded after 24 hours and then wrapped with polythene film for curing until the day of testing. Table 3 below illustrates the amount of constituents for the five mixes per cubic meter.

Table 3: Mix Constituents

Mix No.	Mix Ref.	Target density [Kg]	Wet density [Kg]	Cement [Kg]	Sand [Kg]	Water [Kg]	Foam [m^3]	GGBFS [Kg]	Fly ash [Kg]	Additive [Kg]
1	CM	1300	1400	398	796	179	0.368	-	-	-
2	CM1	1300	1400	398	796	179	0.376	-	-	3.98
3	CM1.5	1300	1400	398	796	179	0.339	-	-	5.97
4	FS1.5	1300	1400	239	796	179	0.312	159	-	5.97
5	FAS1.5	1300	1400	239	796	179	0.385	79.5	79.5	5.97

Results and Discussion

The concrete cubes were oven dried before 24 hours from the date of testing. The compressive strength was taken as an average reading of three cubes at each age. The testing machine used is an ELE International with a capacity of 2000KN and a paste rate of 2.5KN/s. The tests were conducted at the ages of 7, 14 and 28 days. Tables 4shows the results of the compressive strengthsachieved by the five mixes.

Table 4: Compressive strength and oven drydensity for the mix samples

	CM		CM1		CM1.5		FS1.5		FAS1.5	
Age [days]	[N/mm^2]	[kg/m^3]	[N/mm^2]	[kg/m^3]	[N/mm^2]	[kg/m^3]	[N/mm^2]	[kg/m^3]	[N/mm^2]	[kg/m^3]
7	4.1	1226	5.57	1263	6.86	1269	5.5	1319	5.9	1293
14	5.68	1224	7.05	1272	7.5	1277	6.23	1308	8.09	1253
28	5.81	1225	7.6	1272	7.96	1274	6.31	1289	10.4	1261

This study obtained results that followed a similar trend to that of Thomas andBremner[17], achieving a higher compressive strength than that of the control mix. However, all five mixes achieved higher compressive strengths than those mentioned by Aldridge[25] although using a mix proportion of (1:2) when compared to Aldridge's (1:1) mix; however, the control mix achieved the same results of that mentioned by Hamidah, et al. [26].By looking at the table above, it is obvious that the strengths for all mixes have increased by age.When compared with the control mix (CM), it is obvious that mixes CM1 and CM1.5 obtained a higher compressive strength; where mix CM1.5 with an additive percentage of 1.5% achieved the highest compressive strength. This percentage of (SP-1) accelerated the hydration of cement; therefore, this percentage was chosen for the rest of the mixes. On the other hand, the addition of SP-1 also affected the density of the mixes achieving stable mixes than that of the control mix (CM).Mix FS1.5 contained a cement replacement by slag at a level of 40% with an addition of SP-1 at 1.5% by weight of binder. This mix achieved a compressive strength higher than that of the control mix by 109% at 28 days. However, the compressive strength of mix FS1.5 was lower than that of CM1.5 due to the reduction of cementitious material. On the other hand, mix FAS1.5 contained a mixture of both type F fly ash and slag at a (50:50) mixture replacing cement at a level of 40% with the addition of SP-1 at1.5% by weight of binder. This mix achieved the highest compressive strength at 28 days obtaining a

strength higher than the control mix (CM) by 179%,higher than mix CM1.5 by 130% and higher than mix FS1.5 by 165%. This increase in compressive strength is due to the addition of fly ash into the mix. Fly ash, due to its higher fineness, has helped to fill in the gaps within the concrete matrix; hence, obtaining a stronger and denser concrete mix.Figure 1 and 2 illustrates the development of strength and density for the five mixes with age.

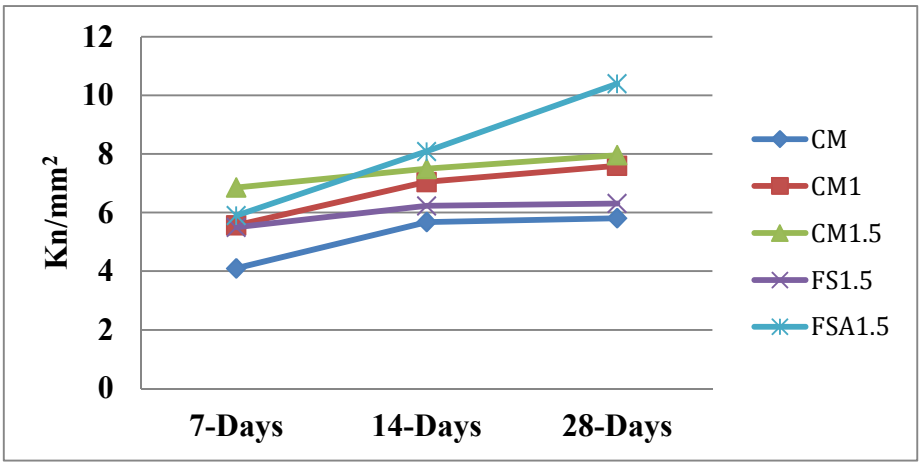

Figure 1: Strength Development with Age

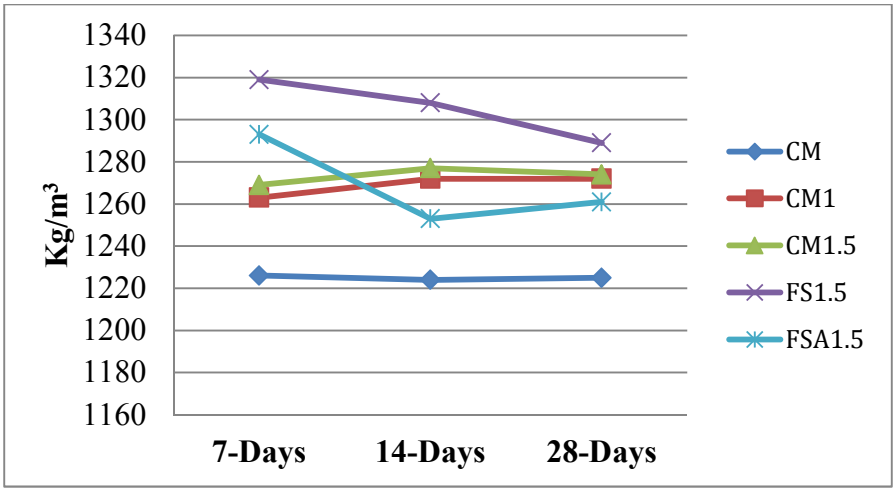

Figure 2: Density Development with Age

The compressive strength obtained by mix FSA1.5 can be compared to that of Zhihua, et al. [27]. Although using the same combination of fly ash and slag; however, this combination was used as filler with the addition of silica fume and not as a cement replacement. Also, the amount of cement used by the mentioned study is higher than this study by 163%. Another difference is that the slag and the fly ash used in Zhihua, et al. [27]study had an ultra fine fineness; where this study used the slag and fly ash as received from the source without any grinding.It is appropriate to say that this study has achieved a loadbearing concrete mix with a minimum amount of cement having incorporated unprocessed slag and class F fly ash.

Conclusion

This study used an unprocessed blast furnace slag for the replacement of cement in a foam concrete mix at a replacement level of 40%. The results show that the unprocessed slag not only reduced the price of concrete due to the high replacement level but also enhanced the compressive strength of the concrete at 28 days by 109%. In addition, combining both slag and class F fly ash has achieved

a stronger concrete mix higher than that of the control mix by 179%. Thus, slag replacement can enhance the strength of foam concrete when used as a cement replacement. Further enhancement can be achieved when combining both slag and class F fly ash as a cement replacement. In addition, a more stable concrete mix can be obtained when using slag as cement replacement.

References

[1] Bremner TW, Environmental Aspects of Concrete: Problems and Solutions,1st All-Russian Conference on Concrete and Reinforced Concrete, 9-14 September 2001, (2001). PP 1-14.

[2] Mohd Hilton Ahmad and Noor NM, Chemical Attack of Malaysian Pozzolans Concrete, journal of Science and Technology, (2009). PP 11-24

[3] Patrick L. Maier A and Stephan A. Durham, Beneficial use of recycled materials in concrete mixtures, Construction and Building Materials, (2012). PP 428-37

[4] Zaid Shaker Mahmood, Low-Medium Cost House "Design And Construction Two Storey House From Lightweight Concrete, Univesiti Sains Malaysia, (2010).

[5] AbdulkadirKan A. and RamazanDemirbog, A novel material for lightweight concrete production, cement and concrete composites, (2009). PP 489-95

[6] Noordin N and Awang H, Lightweight Foamed Concrete in Construction Industry,In International Conference on Construction and Real Estate Management ICCREM 2005, (2005).PP 1-6

[7] Wimpenny DE, in: Some Aspects of the Design and Production of Foamed Concrete, edited by R K Dhir, McCarthy MJ, in Concrete In The Service Of Mankind: Appropriate Concrete Technology πvolume E & FN Spon (1996). PP 243-253

[8] N. Narayanan and Ramamurthy K, Structure and properties of aerated concrete: a review, cement and concrete composites, (2000). PP 321-329

[9] Khalid. Ali. Mg, Mechanical and Physical Properties of Fly Ash Foamed Concrete, Master Thesis, University Tun Hussein Onn Malaysia, (2011).

[10] Lewis R, Sear L, Wainwright P and Ryle R, in:3 - Cementitious additions, edited by John N, Ban Seng C, Ban SengChooa - John Newman BSC, in Advanced Concrete Technology Set volume Butterworth-Heinemann (2003). PP 3-66

[11] Rafat Siddique and DeepinderKaur. Supplementary Cementing Materials. London, New York: Springer 2011. PP 121-173

[12] TeohCherh Yi, Performance Evaluation of Steel Slag as Natural Aggregates Replacement in Asphaltic Concrete, Master Thesis, Universiti Sains Malaysia, (2008).

[13] S. A. Austin, E J. Robins and A. Issaad, Influence of Curing Methods on the Strength and Permeability of GGBFS Concrete in a Simulated Arid Climate, cement and concrete composites, (1992). PP 157-67

[14] Mohd Shariq, Jagdish Prasad and AmjadMasood, Effect of GGBFS on time dependent compressive strength of concrete, Construction and Building Materials, (2010). PP 1469-78

[15] Rafat Siddique and DeepinderKaur, Properties of concrete containing ground granulated blast furnace slag (GGBFS) at elevated temperatures, journal of advanced research (2011). In press

[16] Topculker Bekir and BilirTurhan, Effects of slag fineness on durability of mortars, Journal of Zhejiang University SCIENCE A, (2007). PP 1725-30

[17] Michael Thomas and Theodore Bremner, Performance of lightweight aggregate concrete containing slag after 25 years in a harsh marine environment, cement and concrete composites, (2011). In press

[18] R. Arellano Aguilar, O. BurciagaDíaz and J.I. Escalante García, Lightweight concretes of activated metakaolin-fly ash binders, with blast furnace slag aggregates, Construction and Building Materials, (2010). PP 1166-75

[19] H. Esmaily and H. Nuranian, Non-autoclaved high strength cellular concrete from alkali activated slag Construction and Building Materials, (2012). PP 200-6

[20] Tiong-Huan Wee, DanetiSaradhiBabu, T. Tamilselvan and Hwee-Sin Lim, Air-Void System of Foamed Concrete and its Effect on Mechanical Properties, ACI material journal (2006). PP45-52

[21] Brithish Standard institute,Methods of testing cement 196-1, (2005).

[22] Brithish Standard institute,Testing aggregates 103.1, (1985).

[23] Brithish Standard institute,Ground granulated blast furnace slag for use in concrete, mortar and grout, 15167-1, (2006).

[24] The American Society for Testing Material,Standard Specification for Coal Fly Ash and Raw or Calicined Natural Pozzolan for use as a Mineral Admixture in Concrete, ASTM C618, (2004).

[25] Aldridge D, Introduction of foamed concrete: what, why, how?,Use of foamed concrete in construction (2005). PP 2-11

[26] M S Hamidah, I Azmi, M R A Ruslan and Kartini K, editors.Optimisation of foamed concrete mix of different sand-cement ratio and curing conditions Use of foamed concrete in construction 2005; Scotland, UK: Scotland, UK. 39-47

[27] Zhihua P, Hiromi F and Tionghuan W, Perpetration of High Performance Formed Concrete from Cement, Sand and Mineral Admixtures, Journal of Wuhan University of Technology-Mater, (2007). PP 295-298

doi:10.4028/www.scientific.net/AMR.587.88

An Investigation into the Optimum Carbonization Conditions for the Production of Porous Carbon from a Solid waste

Sara Kazemi Yazdi[1, a], Salman Masoudi Soltani[2, b], Soraya Hosseini[3, c]

[1,2]Department of Chemical and Environmental Engineering, The University of Nottingham (Malaysia Campus), Broga Road, 43500 Semenyih, Selangor, Malaysia

[3]Department of Chemical and Environmental Engineering, Universiti Putra Malaysia 43400, Selangor, Malaysia

[a]Sara.Yazdi@nottingham.edu.my, [b]keyx1smt@nottingham.edu.my, [c]Soraya@eng.ukm.my

Keywords: activated carbon, porous carbon, cigarette filter, carbonization

Abstract. Cellulosic materials and cellulose derivatives have been long used in the synthesis of numerous materials. These include various products such as papers, cigarette filters and sanitary pads. Cigarette filters, containing 95% cellulose acetate fibers, are responsible for one of the largest solid wastes generation today. In this work, a simple one-step carbonization of cigarette filters under various operational parameters is used in order to produce porous carbon. The effects of various pyrolysis parameters including carbonization temperature, heating rate and hold time on the final porous carbon product have been investigated. Adsorption-desorption isotherms, scanning electron microscopy (SEM), Energy-dispersive X-ray spectroscopy (EDX) as well as thermal gravimetric analysis (TGA) have been employed to characterize the pyrolyzed product. The optimum conditions for the production of porous carbon from cigarette filters in relation to its maximum specific surface area (637 m^2/g BET surface area) is understood to be at a heating rate of 5 °C/min at 900 °C for 1 hour.

Introduction

Porous carbons have been produced using numerous approaches including templating methods (soft and hard) and direct carbonization. These porous carbons could then be used in various industrial or scientific fields. They have been applied vastly in separation processes as adsorbents, catalysts and catalytic supports, as well as in electrical and energy storage devices. Amongst the production methods mentioned above, direct pyrolysis of a carbonaceous material is the most straight forward approach in the production of activated carbon. In the past few years the use of different polymeric materials as carbonaceous precursors to synthesize carbon materials, has led to the production of activated carbons with new or improved porosity characteristics [1].

As much as 766,571 metric tons of cigarette butts are littered every year worldwide [2]. The trillions of cigarette butts generated each year in the world raise a significant challenge for disposal regulations, primarily because there are millions of points of disposal. Along with the necessity to segregate, collect and dispose of butts in a safe manner, cigarette butts are considered to be of toxic, hazardous waste [3]. Numerous proposals have been made to prevent or mitigate cigarette butt pollution, but none has been effective; cigarette butts are consistently found to be the single most collected item in beach clean-ups and litter surveys [2]. Cigarette filters are made of 95% non-biodegradable cellulose acetate (a plastic), and the balance are made from papers and rayon. The cellulose acetate tow fibers are thinner than sewing thread, white and packed tightly together to create a filter; they can look like cotton. Cigarette butts contain fibrous matter. Spreading apart the matrix reveals more than 12,000 white fibers. Microscopically, they are Y shaped. Although they are mainly made of cellulose acetate, a plasticizer, triacetin (glycerol triacetate) is applied to bond the fibers [4].

To date, very few investigatetions have been made on recycling cigarette butts as porous carbon materials. Polars *et al*. [5] reported the synthesis of porous carbon from cigarette filters with a surface area of 262 m^2/g. However, they did not study the effects of carbonization duration nor the

heating rate effect on the resulted porous carbon. In this work, we have considered various operational parameters (heating rate, hold time and carbonization temperature) to investigate their effects on the pore surface area and surface morphology of the resulted carbon. The Brunauer, Emmet, and Teller (BET) surface area could be increased by almost 240% compared to the previous report. Doing so, carbon yield could also reach the maximum amount of 15% which is the highest possible value reported in the literature [6].

Materials and Methods

Freshly smoked cigarettes were collected, all belonging to the same cigarette manufacturer. The butts were then removed and unwrapped from within the cigarette paper. They were first placed into a ceramic furnace crucible and then inside a steel tube furnace (Carbolite Co.). N_2 gas flow was supplied from a nearby nitrogen capsule which was directly connected to a flow meter and then the furnace tube. Prior to any experiment, nitrogen was allowed to pass through the furnace for several minutes to make sure the furnace tube was free of any oxygen. Nitrogen flow rate was set to 100 cm^3/min in all experiments. Carbonization temperatures were set to 700, 800 and 900 and 1000 °C. Carbonization (hold) times were adjusted to 0.5, 1, 2 and 3 hours. The heating rates were controlled at 2, 5, 7 and 10 °C/min. To prevent any unwanted oxidation at elevated temperatures, before taking out the sample after its pyrolysis was complete, the furnace was left closed for several hours with the same nitrogen gas flow rate. This allowed the ambient temperature to be achieved. Then the sample was taken out. To characterize the synthesized carbon, adsorption-desorption isotherms were obtained using a Micromeritics Co. surface analyzer using liquid nitrogen at 77 K as the analysis gas. Prior to the analysis the samples were degassed for 6 hours at 300 °C at a heating rate of 5 °C/min to make sure no gas molecules or other impurities were trapped inside the pores. An FE-SEM (Quanta Co.) was used to study the surface morphology of the materials. Also, a METTLER TOELDO (Star System) Co. thermo gravimetric analyzer (TGA) was used to study the thermal decomposition of the smoked cigarette filters.

Results and Discussions

To study the effect of hold time, four experiments were first carried out. The optimum sample (and consequently, optimum hold time) corresponding to the maximum BET surface area was taken for the second round of experiments. At this stage, the effect of carbonization temperature was studied by varying the furnace temperature (700, 800, 900, 1000 °C) and keeping the optimum hold time and the heating rate (5 °C/min) constant. The optimum pyrolysis temperature was then selected according to the maximum BET surface area. In the last round of experiments, the effect of temperature ramping rate (2, 5, 7, 10 °C/min) was investigated by keeping the optimum temperature and hold time constant at the optimum values gained from round one and two of the experiments.

Adsorption-desorption experiments. A relative pressure range of 0.05 to 0.3 was selected to calculate the BET surface area [7]. However, it was found that the linear region of the range for the BET equation should be limited to 0.05 to around 0.18 p/°p to validate the calculated BET area for some samples. This is the total micro and meso porous surface area. According to the results, the optimum carbonization conditions were found to be carbonization at 900 °C at 5 °C/min for 1 hour. The adsorption-desorption isotherm of the optimum sample (900 °C, 5 °C/min, 1 hr) is illustrated in Fig. 1. The isotherm below clearly is a type IV isotherm which is obtained for solids containing pores in the mesopores range [7]. The section of the isotherm which is parallel to the pressure axis is attributed to filling of the larger pores by capillary condensation. The most important feature of type IV isotherms is the presence of hysteresis which means the amount adsorbed is always greater at any given relative pressure along the desorption branch than along the adsorption branch [7]. From the BET equation, a surface area of 637 m^2/g has been calculated. Also by the application of BJH method using the desorption branch of the isotherm, an average pore size of 3.3 nm was evaluated. Meanwhile, the single point adsorption total pore volume of pores is measured to be 0.35 cm^3/g at p/p°=0.984 from the isotherm data.

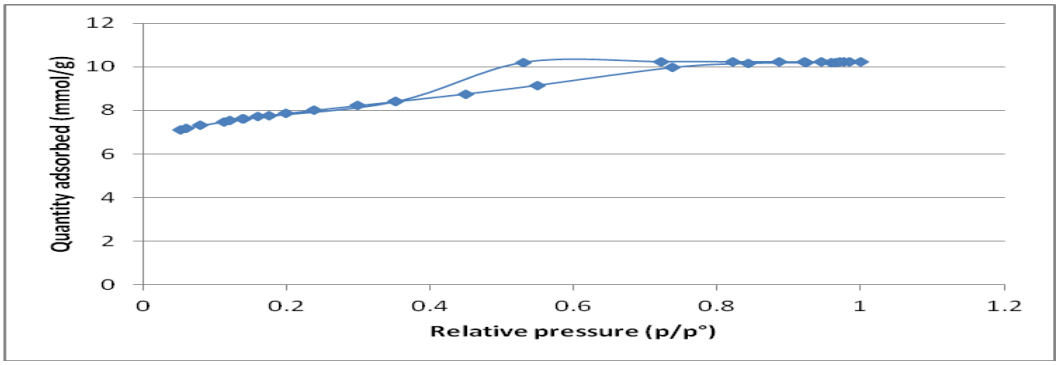

Fig. 1: Adsorption-desorption isotherm of porous carbon synthesized by carbonization of smoked cigarette filter at 900 °C and 5 °C/min for 1 hour.

As it is shown in Fig.,by increasing the temperature from 700 °C to 800 °C and then to 900 °C , the pore area increases. This can be due to the fact that an increase in the temperature will result in the decomposition of more carbon matter and maybe unblocking the blocked pores by tar which will eventually provide a higher degree of surface area. However, interestingly by further increase in temperature from 900 °C to 1000 °C, BET surface area slightly decreases. Therefore, the optimized carbonization temperature could be estimated to be 900 °C. By allowing the carbonization hold time to increase from 30 minutes to 1 hour, the BET surface area increases accrodingly. This can be well justified by the fact that longer carbonization time would provide a longer time for the carbon matter to get decomposed and create a larger surface area. However, there is also an optimum of hold time which is 1 hour. Elevating pyrolysis time further (2 and 3 hours) surprisingly decreased the BET pore surface area. On the other hand, it is expected that by decreasing the heating rate, carbonaceous matter would find a better opportunity to decompose. This is seen as in the results (10,7 and 5 °C/min). However, further reduction (less that 5 °C/min) could lead to a decline in the porous area of the final product.

Scanning Electron Microscopy. The surface morphology and pore structures on the surface of the carbonized carbon samples at three different temperatures are shown in Figs. 2,3 and 4. It is seen that by an increase in the temperature, the surface mprphology also changes. At higher temperatures it seems that the macro pores start to deteriorate and this may result in the creation of smaller pores and an increase in BET surface area.

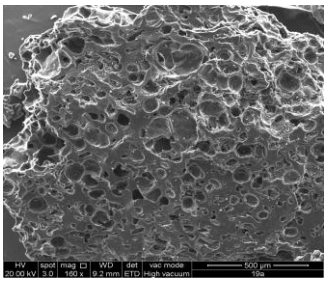

Fig. 2: Carbonized filter at 800 °C for for 1 hr at 5 °C/min

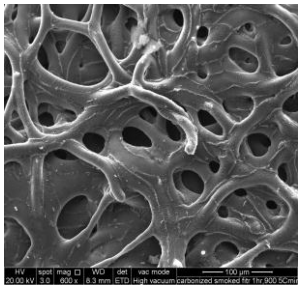

Fig. 3: Carbonized filter at 900 °C for 1 hr at 5 °C/min

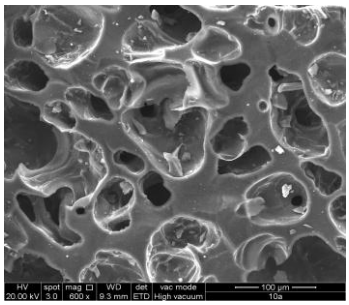

Fig. 4: Carbonized filter at 1000 °C for 1 hr at 5 °C/min

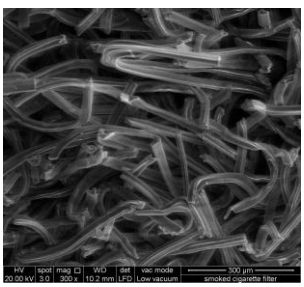

Fig. 5: Smoked cigarette filter

Thermal gravimetric analysis (TGA) Fig. 6. shows the TGA results obtained by the thermal decomposition of smoked cigarette filters in an inert atmosphere. When ramping starts, a mass loss of around 10% is seen until 280 °C is reached. This could be due to the evaporation of the water content in the used cigarette filters. The sample shows a sharp weight-loss which begins at about 280 °C and is ended at 370 °C. This weight-loss can be due to dehydration and acetic acid removal and corresponds to a mass loss of 70 % [6]. By increasing the temperature to 900 °C another weight-loss of 9% is observed. This may be due to the incomplete degree of carbonization (C_xH_y species) [6]. The final weight-loss shows a final carbon yield of around 11% which is almost in good agreement with our synthesized carbon [6].

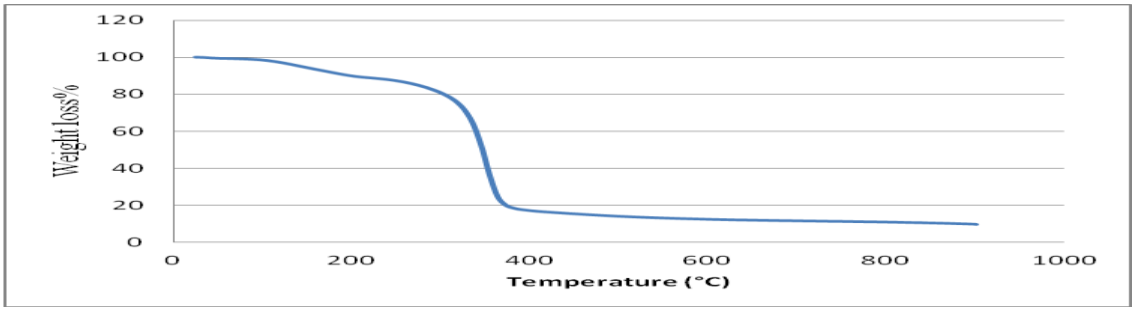

Fig. 6: TGA graph of cigarette filter (at 900 °C at 5 °C/min for 1 hr)

Energy-dispersive X-ray spectroscopy (EDX)

EDX was used to investigate the elemental composition of the carbonized cigarette filter. The EDX spectrum is shown in Fig. 7. It is observed that more than 94% (by weight) of the porous matter is made of carbon. Oxygen contributes most to the remaining weight balance which is possibly found among the surface groups.

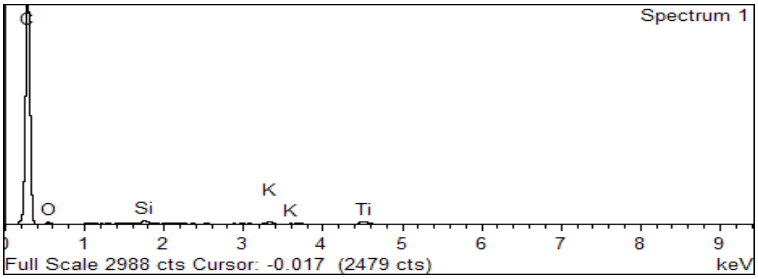

Fig. 7: EDX spectrum of carbonized filters at 900 °C for 1 hr at 5 °C/min

Conclusions

This work finds the optimum carbonization conditions among a series of operational parameters which include pyrolysis temperature, heating rate and hold time resulting in the maximum BET surface area of the porous carbon synthesized from the pyrolysis of cigarette filters. The resulted carbon could be further investigated by post activation through chemical or physical methods. Also, since cigarette filters are made up of cellulose acetate, other cellulose acetate and cellulosic wastes can consequently be considered to be recycled for the production of porous carbons.

Acknowledgements

The authors would like to thank the University of Nottingham Malaysia Campus (UNMC) for providing us with the required facilities to conduct this research. Also, special thanks to the laboratory technicians, Mr. Andrew Yakin Sinit and Ms. Farrawahida Mohtar for their professional supports.

References

[1] M. B.Vazquez-Santos, A. Castro-Muniz, A. Martinez-Alonso and J.M. Tascon: Microporous and mesoporous materials. Vol. 116 (2008) , p.622

[2] E.A. Smith and T.E. Novotny: Tobacco journal. Vol. 20 (2011), p. i2

[3] R. Barnes: Tobacco control. Vol. 20 (2011), p. i45

[4] Information on http://www.longwood.edu/cleanva/cigbuttfilters.htm

[5] S. Polarz, B. Smarsly and J.H. Schattka: Chem. Mater. Vol. 4 (2002), p. 2940

[6] K. Laszlo, A. Bota and L.G. Nagy: *Carbon. Vol. 38* (2000), p. 1965

[7] R.C. Bansal and M. Goyal: *Activated carbon adsorption* (Taylor & Francis Group, 2005).

doi:10.4028/www.scientific.net/AMR.587.93

Pavement Subgrade Improvement by Lime

Bazid Khan[1,a], Abdus Siraj[2,b] and Riaz A. Khattak[3,c]

[1]Department of Civil Engineering, CECOS University of IT and Emerging Sciences, Peshawar- PAKISTAN

[2]Site Engineer, western by Pass Road Project, Mardan- PAKISTAN

[3]Research & Development / VC, CECOS University of IT and Emerging Sciences, Peshawar- PAKISTAN

[a]bmarwat@yahoo.com, [b]Engrsiraj86@yahoo.com, [c]ra_khattak@yahoo.com

Keywords: Pavement, Subgrade, Lime, Stabilization, CBR.

Abstract. The subgrade soil of western by Pass Road Mardan, Pakistan consists of silty clay belonging to A-6(14) group of the AASHTO soil classification system. The average natural moisture content of the soil is more than 18% which makes it susceptible to water logging and problematic for pavement construction. The aim of this research is to improve the supporting power of the existing subgrade material to carry the proposed traffic safely. For this purpose, lime was incorporated into the soil. Soil samples were prepared containing 0, 4, 6, 8, 10 and 12% lime by weight of the soil. Laboratory tests were conducted for determining particle size distribution, Atterberg limits, optimum moisture contents and maximum dry density and California Bearing Ratio (CBR). From this study it was found that the CBR initially increased with increase in lime content, reaching to a maximum value (35.50 %) at 6% lime content and then decreased with further increase in lime content. The optimum lime content for CBR was found as 6.50% (w/w), which enhanced CBR value by 337% compared to control. A consistent decrease from 1.92 at 0 to 1.763 (g/cm^3) at 12% lime was observed suggesting compaction in the material. Results suggested that liming subgrade material is a viable option for improving pavement.

Introduction

The development of a country depends on the quality of infrastructure which depends on transportation-structural and geotechnical engineering. All these fields are directly concerned with soil and its engineering properties. The term soil according to engineering point of view is defined as the unconsolidated material by means of which and upon which engineers build their structures [1]. According to AASHTO soil classification system, soil is divided into seven groups from A-1 to A-7 and the performance of soil as a subgrade material depends upon its Group Index (GI), which is given by the following equation [2]:

$$GI = (F_{200} - 35)[0.2 + 0.005\,(LL - 40)] + 0.01(F_{200} - 15)(PI - 10) \quad (1)$$

Where, F_{200} = % passing No.200 sieve, expressed as a positive whole number, LL = Liquid limit and PI = Plasticity Index,

The higher the GI of a soil, inferior will be its performance as a subgrade material.

Roadway is a main mean of communication within a country as well as with other neighbouring countries. The roadway alignment passes over several locations with changing subsoil conditions. In many locations, the engineering properties of soil in its natural state are so unfavourable for engineering construction especially for pavement construction that some method / measure must be used for its improvement before the pavement construction.

The concept of soil improvement by using some additives has been developed several thousand years ago [3]. Many materials have been used as additives to stabilize soils, including chlorides, lignin, molasses and several of the synthetic resins. However, the only materials now used on large scale are cement, bitumen and lime [4]. Raw materials such as cement kiln dust and ashes of

different materials are becoming more popular to be used as soil stabilizer. Cement kiln dust was mixed with dune sand and California Bearing Ratio (CBR) values were determined after 96 hours soaking. Incorporation of 30 and 50% cement kiln dust should enhanced CBR value from 29% to 206 and 317% respectively while 100% CKD should 288% CBR [5].

Calcium Carbide Residue (CCR) and Fly Ash (FA) have been used to improve the strength of problematic silty clay in the northern Thailand[6]. Both strength and micro structural investigation showed that the input CCR reduced specific gravity and soil plasticity, resulting in maximum dry unit weight and water sensitivity. The maximum strength of the stabilized silty clay is dependent on the OMC for different binder contents, CCR: FA and curing times.

The use of cement kiln dust, rise husk and their combinations as stabilizer for clayey soils have been reported[7]. Their stabilizing effect were judged by determining Atterberg's limits, standard proctor compaction, unconfined compressive strength, splitting tensile strength, modulus of elasticity and CBR. It was concluded that soils stabilized by these stabilizers showed satisfactory strength and durability characteristics and may be used for low cost construction to build houses and road infrastructure.

A mixture of soil cement and arcyclic resin has been used for improving the engineering properties of soil for construction[8]. This study suggested it was found that the strength of soil-cement increased considerably by adding arcyclic resin as an additive material, however the increase in strength for a given cement content was a function of curing time and percentage of resin. It has been found by field and laboratory investigation that incorporation of lime in pavement subgrade soil brings much improvement in the properties of soil. The addition of lime decreases the plasticity of the soil and increases CBR, however, the construction quality determined from the field tests was highly variable [9]. It has been indicated that Gelincik pumice waste may be used to improve the properties of clayey subgrade of pavement [10].

Problem Statement

In the Khyber Pukhtunkhuwa Province of Pakistan, Western by Pass Road Mardan of about 12 km is to be constructed. The water table in the area is at shallow depth and the subgrade soil has high moisture content which made it prone to waterlogging and problematic for placement of pavement over it. Several alternatives were suggested to improve the existing soil. Lime stabilization is also one of the techniques for improving the engineering properties of the soil. For this purpose, this experimental study was conducted.

Experimental Program

Sample Collection and Classification of the Soil. Natural moisture content of the soil was determined and an average value was found as more than 16%. Samples were collected from several sections of the pavement and were mixed to have a representative sample. After oven drying at 105 C^0, the sample was passed through sieve NO.200 and percent passing was found as 98.30%. Liquid limit and plastic limit of the soil were also determined and were found as 34.10% and 19.90% respectively. ASTM D 4318 Test procedure was followed for Atterberge limits determination. According to the equation-1, GI is calculated as 14 and according to the AASHTO soil classification system the soil is A-6(14)-silty clay.

Stabilizing Agent Mixing. Hydrated lime $\{Ca(OH)_2\}$ was added as the stabilizing agent@ 0,4,6,8,10 and 12% (w/w) to soil and mix thoroughly.

Tests Performed. The following laboratory tests were performed on these samples: Compaction tests were done and optimum moisture content (OMC) and maximum dry density ($\Upsilon_{d\text{-}max}$) were determined. The ASTM D 698 test method was followed. California Bearing Ratio (CBR) tests were done according to the AASHTO NO. T 193

Results and Discussion

The results of compaction tests and CBR tests are shown in Table 1 and Fig. 1 to 3.

Table 1: Compaction Test and CBR Test Results

% Lime added	OMC [%]	$\Upsilon_{d\text{-}max}$ [g/cm^3]	CBR [%]
0	12.30	1.915	8
4	14.80	1.837	31
6	16.80	1.810	33.5
8	16.20	1.814	35
10	16.80	1.795	25
12	16.80	1.763	17

The results given in Table 1 are plotted in Fig.1, Fig.2 and Fig.3 which shows variation of OMC, $\Upsilon_{d\text{-}max}$ and CBR with lime contents respectively. Best fitted Trend lines were drawn and correlation equations are displayed on the trend lines.

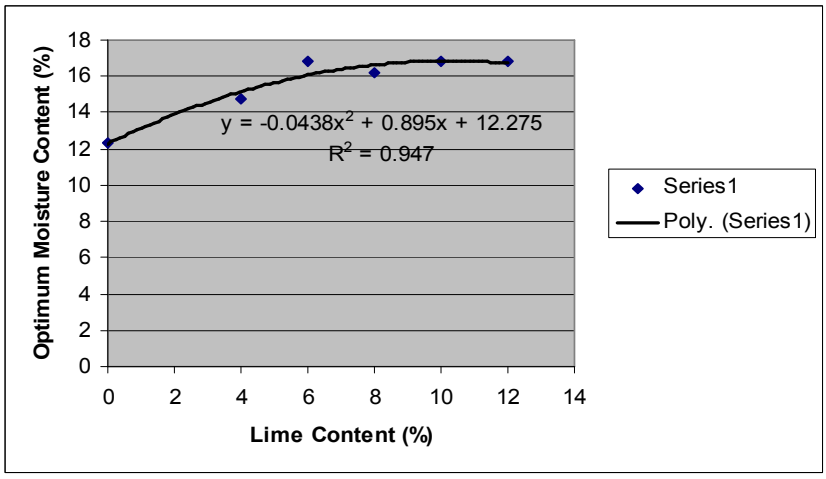

Fig. 1 Variation of OMC with Lime Contents

Fig. 1 indicates that OMC initially increases with increase in lime content up to 6% but beyond this level of lime, it becomes nearly constant for all higher lime contents. This may be due to larger specific surface of lime as it is relatively fine than the soil.

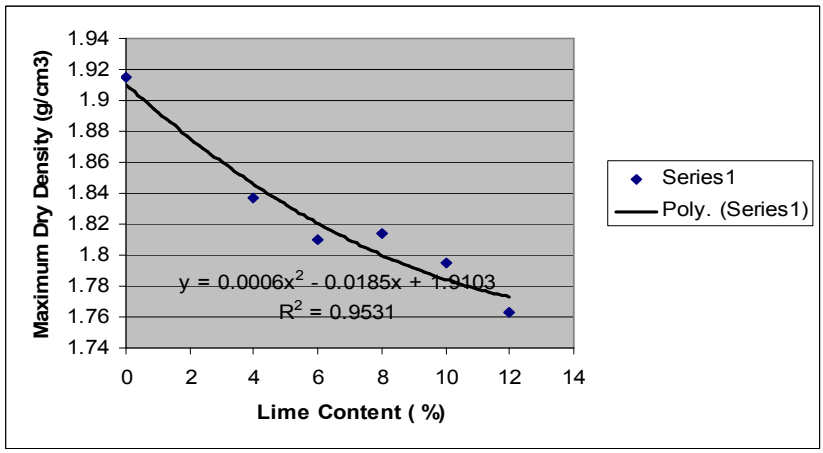

Fig. 2 Variation of Ɣd-max with Lime Contents

Fig. 2 indicates that maximum dry density decreased by 8% lime content. This may be due to the compaction and subsequent increases in mass per unit with increase in lime content as compared to soil.

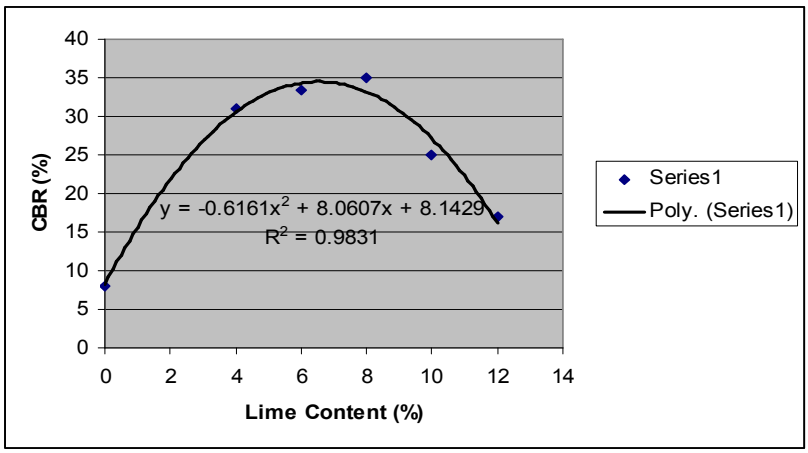

Fig. 3 Variation of CBR with Lime Contents

Fig. 3 indicates that CBR values increased with increase in lime contents, reaching to a maximum value of 35.50% at 6% lime content and then decreased with further increase in lime contents, suggesting 6.50 % lime for optimum CBR.

Conclusions

From this study, it is concluded that clayey subgrade material can be effectively and economically stabilized by incorporation of lime into it. The CBR values can be improved by incorporation of lime, however; the rate of improvement is a function of the lime content and type of material. A lime content of 6.50 % by weight of soil is recommended as an optimum content for CBR improvement, which enhanced CBR by 337 % as compared to control.

Reference

[1] A.K. Shaukat: Soil Mechanics, HEC Islamabad Pakistan (2006)

[2] B.M. Das: Principles of Geotechnical Engineering, 5th Edition, Pashupati Printers Limited New Delhi India.

[3] J.K. Mitchell: Soil Improvement-State of The Art Report, Proc, 10th ICSMFE, Vol. 4 (1981). p. 509.

[4] C.R. Scott: Soil Mechanics and Foundation, 3rd Edition, Applied Science Publishers limited London (1980).

[5] Z.A Baghdadi, M.M. Fortari and N.A. Sabban: Soil Modification by Cement Kiln Dust, Journal of Materials in Engineering, Vol. 7, No. 4 (1996). p. 218.

[6] S. Horpibulsak, C. phetchuag, and Chin A. kulkiniwat: soil stabilization by calcium carbide residue and fly ash, journal of material in Civil Engineering (2011).

[7] K.M. Anwar hussain: Stabilized soils incorporating combinations of Rice Husk Ashe and Cement Kiln Dust, Journal of Civil Engineering Materials Vol.23 (2011).

[8] A.R. Estabragh, I. Beytoluhpour and A.A. Javadi: Effect of resin on the strength of soil-cement mixture, Journal of materials in Civil Engineering. Vol.23, (2011).

[9] C. Jung, A. Bobet, N.Z. Siddiqui and D. Kim: Postconstruct evaluation of subgrades chemically treated with Lime Kiln Dust, Journal of materials in Civil Engineering. Vol.23, (2011).

[10] M. Saltan, U. Kavlak and F.S. Ertern: Utilization of pumice waste for clayey subgrade of pavement, Journal of materials in Civil Engineering (2011).

doi:10.4028/www.scientific.net/AMR.587.97

Microstructural Study of Cement Composites Produced by Hazardous Waste Stabilization/Solidification

Bozena Vacenovska[a], Rostislav Drochytka[b] , Vit Cerny[c]

Brno University of Technology, Faculty of Civil Engineering, Department of Buildings Materials Technology and Components, Veveri 95, Brno, Czech Republic

[a]vacenovska.b@fce.vutbr.cz, [b]drochytka.r@fce.vutbr.cz, [c]cerny.v@fce.vutbr.cz

Keywords: Hazardous waste, solidification/stabilization, fluid fly ash, classic fly ash, cement, composite, microstructure, X- Ray diffraction, electron microscopy.

Abstract. This paper deals with the chosen hazardous waste solidification/stabilisation (S/S) under the catalogue code 190811 using cement matrix with addition of classic fly ash and fluid fly ash as secondary raw binders. The main task of the research works was a microstructural study of the most successful S/S formula that will be used for development of new reclamation material. The S/S process product was subject to X-Ray analysis and to the electron microscopy analysis two years after its production to evaluate the possibility of degradation of the cement composite and releasing the contaminants into environment.

Introduction

A technology which is very often used for hazardous waste disposal is a S/S technology representing a wide variety of methods differing in types of used binders, ratios of their mixing or in process temperature. S/S processes are characterized by the decrease of the waste surface, but the content of hazardous substances remains. A barrier is being formed between the hazardous substances and surrounding environment and the contaminants are chemically bounded to the matrix consisting of organic or inorganic inert substances [1].

This paper represents one part of the research that is in a progress at Brno University of Technology. This research deals with hazardous wastes S/S with the aim to develop a new reclamation material as cement composites produced by hazardous waste S/S/stabilization. This paper is devoted to the microstructural study of cement composites.

Before the microstructural study a basic laboratory testing was realized to verify whether the selected type of hazardous waste is appropriate for development of new reclamation material or not. These basic laboratory testing was provided by subjecting the S/S product to leaching tests and to compressive strength testing. Consequently after the composite testing is proved to be successful in these tests, then there were next and more intensive laboratory tests and pilot plant testing that proved the possibility of S/S product to be used as a reclamation material. Next step was a microstructural study.

Hazardous waste (HW)

Selected type of hazardous waste is listed in European Waste catalogue under the catalogue code 190811. This hazardous waste is a sludge that comes from biological industrial waste water treatment and has a definite content of hazardous substances. For better handling a waste producer provides a preliminary treatment of sludge mediated by its drying to a content of 15 % dry residue. The selected HW was subjected to leaching tests according to the valid Czech legislation. The most critical was the content of indicator dissolved organic carbon.

S/S binders and S/S formulas

Low-cost binders – secondary raw materials – were used as S/S binders, especially fluid and classic fly-ash. These are Pozzolanic materials and they set and harden after addition of activator – Portland cement was used as an activator. S/S formulas were de-signed in such way that the amount of HW was a constant value – as well as the content of classic fly ash.

Laboratory testing

Among the analytical methods that are used for the verification of S/S process success are the most important the batch tests. These tests are based on the extraction process and determine the S/S product ability to release the pollutants into the environment. The principle of this test is to expose the S/S product to action of leaching medium and after definite time interval to determine pollutant`s concentration in this medium [2]. Methods for leachate analysis are laid down by Czech Annex No. 12 of Decree No. 294/2005 Coll.

Among the physical tests there are important tests of strength that are deter-mined to verify the S/S product ability to resist the mechanical stress by overloading. Czech legislation does not set any limiting value of the minimum unconfined compressive strength (UCS); however, the solidified waste must have a definite minimum strength to ensure its safe use. A correlation between S/S product strength and a degree of pollutants stabilization was not detected, but it is generally assumed that higher values of strength provide better physical barrier and thus it leads to a reduction of the risk of pollutants leaching into the environment. Solidificates were subjected to compressive strength tests according to standard CSN EN 12390-3 Testing hardened concrete - Part 3: Compressive strength.

After this laboratory testing it was found out that the content of almost all contaminants (except sulphates) were decreased after S/S process. Content of contaminants was decreased even after two years of solidificate maturing. The most successful formula was proved to be formula with the content of hazardous waste 30 % and with the content of fluidized bed combustion fly ash (FBC-A), classic fly ash and content of cement. By this formula there was achieved the lowest values of all contaminants and the highest values of UCS. This formula has the best potential to be further tested for use as reclamation material. This S/S formula was subjected to microstructural study in the next laboratory testing.

The microstructure study

The aim of this research was to look into the S/S product`s microstructure and to try to understand the physical and chemical processes those taken place in S/S product two years after their production. The study of the microstructure helps to clarify and to understand the way of contaminants interception in structure of S/S product. The test samples were subjected to X-ray diffraction analysis that provides information about the internal structure and crystallography of tested S/S product and it was completed by electron microscopy (SEM). This analysis was performed on a Philips PW machine 1130.

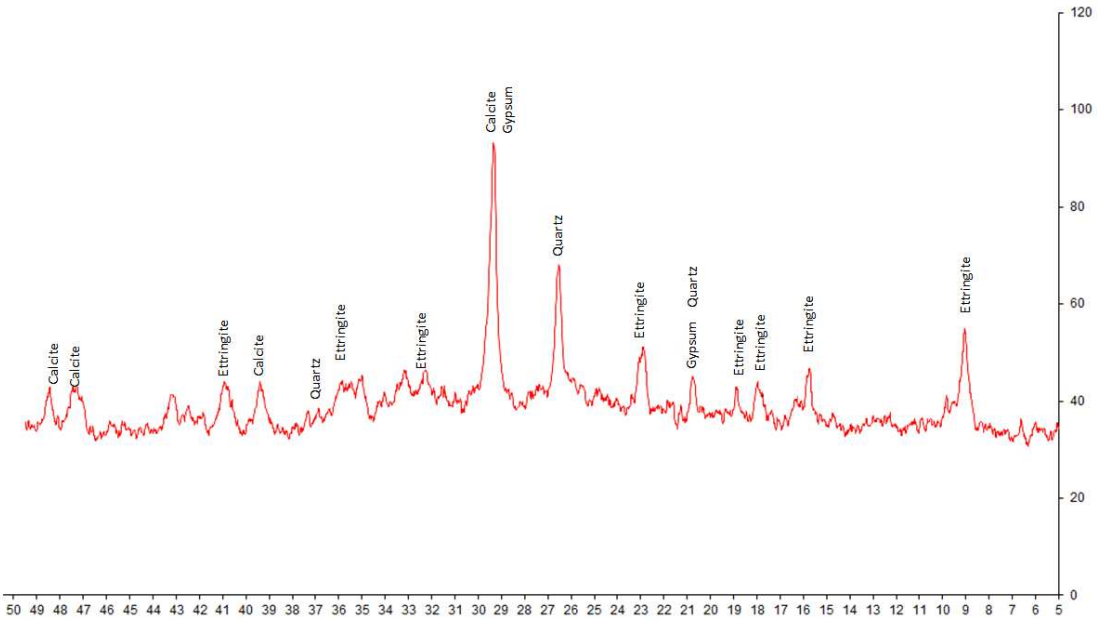

Fig. 1: The results of X-Ray analysis.

With the help of X-Ray analysis the presence of calcite, quartz, ettringite, gypsum and feldspar was detected in S/S product structure (Fig. 1). The ettringite was created as the product of degradation processes and it was presented in the S/S product in paragenesis with calcite and gypsum. The advantage of the ettringite is its flexible structure that allows easy incorporation of toxic elements into a stable structure that is almost insoluble in water [3]. This is an undeniable benefit for disposal of hazardous wastes containing various contaminants. The results of X-ray analysis also proved the presence of SiO_2 in the form of quartz. The sources of SiO_2 are mainly fly ashes; these were used in all S/S formulas.

During the microstructure study with the use of electron microscopy method at the low magnification a dense microstructure without pores and cracks of the S/S process product was detected. According to the results of X-ray diffraction analysis and according to electron microscopy method outputs the ettringite was proved to be the main hydration product.

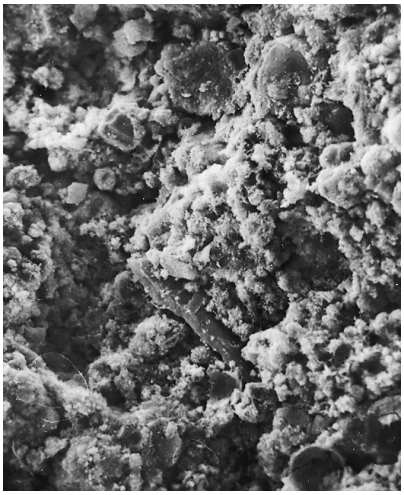

Fig. 2: SEM at magnification 600 times.

Fig. 3: SEM at magnification 2000 times.

The Fig. 2 shows the overall morphology of S/S process product. There are the remnants of sewage sludge observable on the Fig. 2. We can also observe a visible light coating of C-S-H gel. Also a dense structure of S/S process product without cracks and pores is apparent on the picture at the low magnification.

The Fig. 3 shows a detailed view of the rest of the impurities from the waste sludge – probably with metallic character – that is covered with a thin layer of corrosion. There is also observable a light layer of C-S-H gel covered with needle-like shaped ettringite crystals. When using this magnification a micro porosity of S/S product is obvious (dark areas on the picture).

Fig. 4: SEM at magnification 2500 times.

Well-developed crystals of non-expansive ettringite with different dimensions are shown on the Fig. 4; these crystals fill the S/S product micro pores. No cracks caused by the formation of expansive ettringite were observed in final S/S process product.

The presence of ettringite in S/S product microstructure was also confirmed by the use of X-ray diffraction. Ettringite is stable at a pH of 10.7 and in reducing to 9.5 it leads to a gradual disintegration of the ettringite to gypsum and aluminum hydroxides. Ettringite can be presented also at value of pH lower than 10.7, but only in association with gypsum and Al-hydroxides [4,5], which is this case, since the chemical analyzes showed the values of pH 10.5 and the presence of gypsum was also confirmed during the X-ray analysis. The complete dissolution of ettringite can be expected at values of pH close to neutral pH value [5].

Fig. 5: SEM at magnification 800 times.

Fig. 6: SEM at magnification 3000-times.

The Fig. 5 shows the macrostructure at low magnification. A spherical grain of fly ash with observable surface reactions is dominant on the picture. Except of the grain of fly ash also a layer of C-S-H gel is observable on the SEM image.

The Fig. 6 shows in detail a grain of fly ash from the previous figure (Fig. 5). Even at the age of 2 years of the sample unreacted grains not affected by the pozzolanic reaction of fly ash were observable – smooth surface of the grain – these grains of fly ash acted only as filler in the S/S process product.

Conclusion

The presence of calcite, quartz, ettringite, gypsum and feldspar was detected by XRD analysis during the microstructure study of S/S product. The SEM images showed the micro structure of S/S product without pores and cracks and with the ettringite as main hydration product. In conclusion, any causes of potential degradation were not detected during the microstructure analysis of the most successful S/S formula, therefore the possibility of contaminant releasing into environment was confirmed not only by laboratory testing, but also by microstructural analysis two years after S/S production.

Acknowledgement

This paper has been developed under the support of the project FR-TI2/341 „Development of progressive S/S technology for transformation of hazardous waste into new materials".

References

[1] B. Vacenovská: *Verification of possibility of industrial waste sludges disposal by using solidification method*, In XII. International Research Conference, Brno, Czech Republic, 2009. Brno University of Technology, Faculty of Civil Engineering, 2008, ISBN 978-80-7204-629-4, 195 – 198.

[2] Z. Kafka, J. Vošický: *Chemická stabilizace nebezpečných složek v průmyslových odpadech (Chemical stabilization of hazardous substances in industrial wastes)*, Chemické listy 92, Institute of Chemical Technology Prague, Department of Chemistry, www.chemicke-listy.cz/docs/full/1998_10_789-793.pdf>

[3] M. Karfíková, J. Havlica: *Imobilizace odpadních iontů ve struktuře ettringitu (Waste immobilization of ions in the structure of ettringite),* Department of Material Chemistry, Faculty of Chemistry, Brno University of Technology, In Chemistry,Biology, Physics and Technology Bulletin of the Czech and Slovak Crystallographic Association RPDK 98,1998, pp 47 – 48.

[4] L. Stratilová: *Identifikace novotvořených minerálních fází v betonu dlažebních kostek (Identification of new mineral phases in the concrete paving)*, Masaryk University, Faculty of Science, Brno 2010.

[5] S.C.B. Myeneni, S.J.Traina, T.J. Logan: *Ettringite solubility and geochemistry of the $Ca(OH)_2$ – $Al_2(SO_4)_3$ – H_2O system at 1 atm pressure and 298 K*, Chemical Geology 148, 1998, pp 1–19.

[6] Decree No. 294/2005 Coll. on the conditions of depositing waste in landfill and its use on the surface of the ground and amendments to Decree no./2001 Coll., on details of waste management.

doi:10.4028/www.scientific.net/AMR.587.102

Effects of Interface Condition on Performance of Road Pavements with Non-linear Granular Materials

B.Tiliouine[1,a], K.Sandjak[1,b], C.Y.Ali-Haimoud[1,c], M. Hammoutène[1, d]

[1]Ecole Nationale Polytechnique, Laboratoire LGSDS, Algiers, Algeria

[a]boualem.tiliouine@g.enp.edu.dz,[b]khaled.sandjak@g.enp.edu.dz,
[c]chouaib-yassine.ali-haimoud@g.enp.edu.dz, [d]malek.hammoutène@g.enp.edu.dz

Keywords: flexible pavements, design criteria, cracking fatigue, rutting, design life, interface condition, unbound granular materials, non-linear elastic models, Asphalt Institute distress models.

Abstract. The main results of a numerical investigation into the effects of interface condition on the critical response and predicted performance of flexible pavements with granular bases are presented. In addition, the influence of using linear elastic and non-linear elastic models for granular base characterization, on the design life of typical road structures with granular bases under various combinations of layer interface conditions is examined. Repeated load triaxial tests are carried out and non-linear regression analyses on tests results are performed to determine the constitutive model parameters. The Asphalt Institute distress models for fatigue cracking and rutting using both linear and non-linear analyses are utilized to estimate the pavement design life. It is shown, among others, that interface condition affects significantly the critical response of pavement structures and hence their predicted performance. Furthermore, the results indicate that the use of linear assumption to characterize granular base and sub-base behaviour, grossly over-estimates the design life of pavement structures. This effect strongly depends on interface conditions used between the pavements layers.

Introduction

Existing design procedures of flexible pavements are essentially based on the common assumption that their constitutive layers are fully bonded to one another. However, experimental evidence indicates that inadequate interface contact condition affects pavement performance and often leads to premature failure of road-structures. Only a few studies have focused on developing testing methodologies and constitutive interface models for interlayer interface. However, characterization of pavement layer interface is difficult because there is no standard test procedure to determine it [1,2].

Furthermore, numerical models based on linear hypotheses are commonly used in engineering practice to simulate flexible pavement response and therefore may not realistically account for non-linear aggregate behaviour in the base and sub-base layers of pavement structures. In such a case, it should be expected that computed strains and displacements will become important and inter-layer slip or debonding will eventually take place. Thus, proper modelling of non-linear characterization of granular base behavior and interface bonding condition is of crucial importance for better understanding the real behavior of road structures.

In the present work, interface conditions influence on pavement design criteria and predicted performance of road pavements taking into account both linear and non-linear modeling behavior of local unbound granular materials (UGM) is investigated.

Several simulations are carried out on a typical pavement structure with local UGM commonly used in Algerian pavement network. Simulation results show that interface conditions play an essential role in road structures in terms of design criteria and predicted performance. In addition, it is found that the predicted design life of flexible pavements using non-linear resilient behavior of UGM is substantially shorter than that based on the assumption of UGM linear behaviour. This effect is strongly dependent on interface conditions existing between the constitutive pavement layers.

Pavement structure and materials characterisation

To examine the influence of interface condition on the structural performance of road structures with granular bases, a typical pavement structure (see Table 1 below)with layers thicknesses and material properties commonly used in Algeria [3,4]is considered in the present study. Pavement section is subjected to a circular load with radius of 17.5cm and uniform static pressure of 675.6 KPa.

Table 1:Layers thicknesses and material properties of typical pavement structure

Layer	E [MPa]	Thickness[cm]	ν	Material type
1	4000	6	0.35	Asphalt
2	500	20	0.25	Granular base
3	312.5	15	0.25	Granular sub-base
4	125	-	0.35	Subgrade Soil

where: E,ν are Young modulus and Poisson's ratio respectively. To further examine interface condition effects on pavement critical response and performance when using a constitutive model other than the linear elastic model, the K-theta model is selected herein to simulate the non-linear resilient behaviour of the unbound granular base. In this model, the resilient modulus M_r is expressed as follows: $M_r = K1.\theta^{K2}$, where $K1$ and $K2$ arematerial constants determined from regression analysis, and θ isthe first invariant of stress tensor. The values of material constants $K1$ and $K2$ for the non-linear characterization of base layer were established by fitting the K-theta model to resilient modulus test data obtained from RLT tests, using a non-linear least-square curve fitting technique. For UGM taken from the CAP Djenet quarry, it was found that $K1 = 24496$and$K2 = 0.4472$.

Four cases, A to D as indicated in Table 2,below were used to compute the strain, and displacement with fields in the pavement structure for a combination of four interface conditions.

Table 2: Interface conditions used in this study

Case	Interface between asphalt and UGM	Interface between UGM and subgrade soil
A(T-T)	Tied	Tied
B(U-T)	Untied	Tied
C(T-U)	Tied	Untied
D(U-U)	Untied	Untied

Interface condition A (T-T) and D (U-U) correspond respectively to the beginning and the end of pavement serviceability life. Interface condition B(U-T) is associated to an intermediate state between cases A (T-T) and D(U-U) i.e. partial pavement deterioration due to unfavourable traffic conditions or inadequate application of construction specifications (e.q. inadequate selection of proper asphaltic seal coat materials and quantities requirements). In what follows interface condition C (T-U) will be discarded as it is considered unrealistic from a practical viewpoint.

Pavementmodelling

A four layer model was developed to analyse the strain and stress fields in the selected pavement structure using Kenlayer computer software [5].The backbone of this program is Burmister solution for homogenous linear elastic multilayer half space under a circular loaded area. The solutions are superimposed for multiple wheels, applied iteratively for non - linear layers, and collocated at various times for viscoelastic layers. As a result, Kenlayer software can be applied to layered systems under single, dual, dual-tandem, or dual-tridem wheels with each layer behaving differently, either linear elastic, nonlinear elastic, or viscoelastic. For frictionless interface, the continuity of shear stress and radial displacement is replaced by zero shear stress at each side of the

interface. Computed pavement design criteria and design life using both linear and non-linear elastic analysis assuming different interface conditions are presented and discussed in the following section.

Numerical results and discussion:

The main results of the numerical analyses are summarized in terms of values of the design criteria generally used in pavement engineering:

- The horizontal tensile strain (ε_t) at the bottom of the bituminous layer usually related to risks of asphalt layer cracking by tensile fatigue failure.
- The vertical strain (ε_v) at the top of the subgrade usually related to risks of rutting .
- The deflection at the surface (W), which is to some extent, an indication of the structure ability to bear repeated traffic loads.

With the strain values, the Asphalt Institute transfer functions [6] were used to compute pavement life based on two computing failure mechanisms associated to the fatigue cracking and the rutting models as per the following equations:

$$N_c = f_1 \times \varepsilon_t^{f_2} \times E_1^{f_3} \quad (1)$$

$$N_r = f_4 \times \varepsilon_v^{f_5} \quad (2)$$

Where:

N*c*: Allowable number of load repetitions to prevent cracking fatigue of the asphalt layer

N*r*: Allowable number of load repetitions to prevent the rutting at the top of subgrade soil due to accumulated pavement deformation

ε_t: The maximum tensile strain at the bottom of asphalt layer

ε_v: Compressive vertical strain at the top of subgrade soil

f_i : i = 1,2,3,4 regression distress model parameters depending on material type, definitions used to identify failure limits specified by the agency, climatic and traffic conditions. Asphalt Institute suggest the following f_i values for the regression coefficients:

f_1 = 0.0796, f_2 = 3.291, f_3 = 0.854, f_4 = 1.365E-09, and f_5 = 4.477.

The design life of a flexible pavement is given by the lower of the number of load repetitions to failure obtained from either the fatigue cracking or the rutting distress model. Computed responses under different interface conditions, in term of critical values of design criteria and allowable number of load repetitions N*c*, N*r* and N assuming linear elastic behaviour of granular base and sub-base layers, are presented in Table 3.

Table 3: Results from Linear analysis of pavement structure undervarious interface conditions

Parameters	A(T-T)	B(U-T)	D(U-U)
W (mm)	0. 5994	0. 7644	0. 8705
$\varepsilon_{t\,(10^{-6})}$	-155.1	-363.9	-382.0
$\varepsilon_{v\,(10^{-6})}$	639.4	929.3	390.8
N_c (Cracking)	630160	38068	32448
N_r (Rutting)	272700	51133	2471500
N(Design life)	272700	38068	32448

It is clearly observed that values of the design criteria and pavement lives are very sensitive to changes in interfaces conditions. In particular, when both the asphalt layer-UGM base and the UGM-subgrade soil interface are fully bonded (A (T-T) condition), the maximum tensile strain is minimum and failure by fatigue cracking is unlikely when compared to the other cases. However, if the asphalt-UGM interface is untied but the UGM-subgrade interface remains bounded (B(U-T) condition) the compressive vertical strain at the top of subgrade soil is significantly increased and failure by rutting is

highly likely as compared to the other cases. Finally, when the bond is lost for both asphalt-UGM and UGM-subgrade soil interfaces (D(U-U) condition), the maximum tensile strain at the bottom of asphalt layer is maximum and failure by fatigue is most likely as compared to the other cases.

Table 5 below, presents the results of non-linear analyses using the (k-θ) model for the studied pavement structure under various interface conditions:

Table 4: Results from Non-linear analysis of pavement structure under various interface conditions

Parameters	A(T-T)	B(U-T)	D(U-U)
W (mm)	0.7235	0.8105	0.9395
$\varepsilon_{t\,(10^{-6})}$	-233.8	-389.3	-416.9
$\varepsilon_{v\,(10^{-6})}$	715.1	955.9	410.4
N_c (Cracking)	163260	30488	24335
N_r (Rutting)	165250	45064	1985200
N(Design life)	163260	30488	24335

Similar trends to results obtained from linear analysis are observed. As expected values of design criteria are larger than in the linear case, leading to shorter design life of pavement structure regardless of the nature of interface condition. These observations are best illustrated in Figures 1, 2 and 3, using 3-D representation plots of the main results.

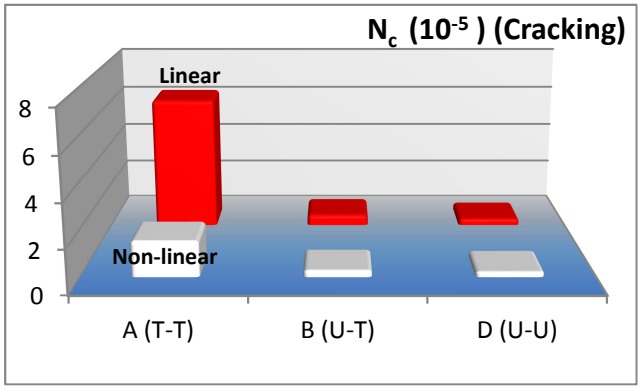

Fig.1: ComputedN*c*usingboth linear and non-linearanalyses for various interface conditions

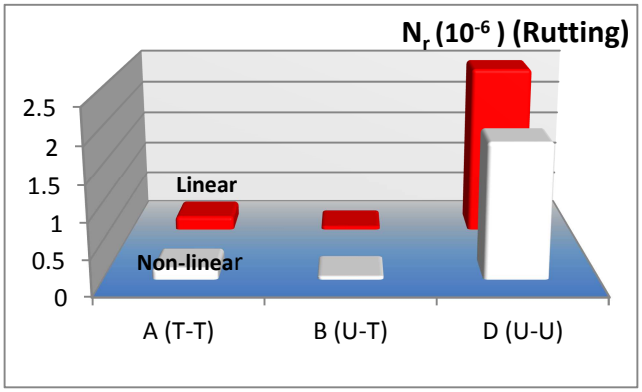

Fig.2: ComputedN*r*using both linear and non-linear analyses for various interface conditions

Concluding remarks

In the present study, the effect of interface condition in on the critical response and predicted performance of flexible pavements with granular bases have been investigated. In addition, the influence of using linear elastic and non-linear elastic models for granular base characterization on the design life of a typical road structure with local UGM commonly used in Algerian pavement network, has been examined under various combinations of layer interface conditions.

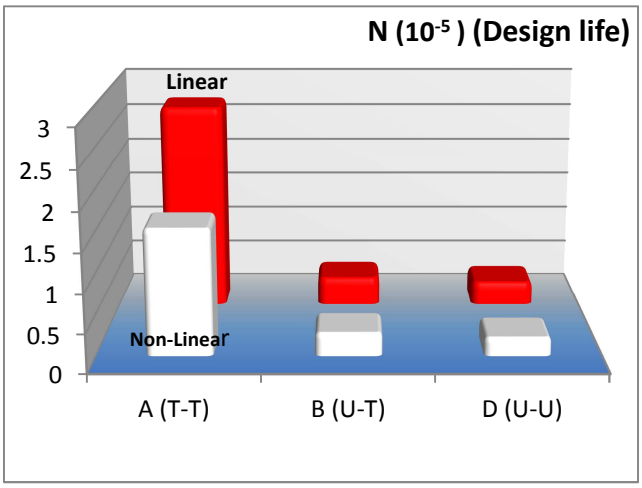

Fig.3: Computed design life using both linear and non-linear analyses for various interface conditions

Simulation results indicate that values of design criteria and design life of pavement structures are very sensitive to changes in interface condition. It follows that in order to ensure an accurate prediction of structural performance of flexible pavements under given traffic and environmental conditions, due consideration should be given to utilization of a reliable interface condition model as well as a proper characterization of the non-linear resilient behaviour of granular base and sub-base materials on at the design stage.

Moreover, strict control and follow-up of construction specifications in terms of selection of proper asphaltic seal coat material and quantity requirements to promote bond behaviour of pavement layers and to prevent slippage should be implemented during the pavement construction process.

Acknowledgements

This study is partially supported by funds from MESRS-DGRST through sub-contract to Ecole Nationale Polytechnique (Contract PNR N° 17/E164/5235; Project Monitor: B. Tiliouine). The support is gratefully acknowledged.

References

[1] H. Ziari and M.M. Khabiri: *Interface condition influence on prediction of flexible pavement life*: Journal of Civil Engineering and Management, Vol.13, No 1 (2007), p.71–76

[2] S.A.Romanoschi: *Characterization of pavement layer interface*: PhD dissertation, Louisiana State University, Baton Rouge, USA(1999).

[3] B. Tiliouine and K. Sandjak, in: *Mechanical Behaviour Simulation of Unbound Aggregates Used in Algerian Pavements:* Proceedings of 4th International Congress on Design and Modeling of Mechanical Systems (Tunisia 2011).

[4] CTTP-Direction des Routes, in: *Catalogue de Dimensionnement des Chaussées Neuves,* Algerie, (2000).

[5] Y. H. Huang, in: *Pavement Design and Analysis*, edited by Prentice Hall, Englewood Cliffs, NJ (2004).

[6] Asphalt Institute, in: *Research and Development of the Asphalt Institute Thickness Design Manual (MS-1)*, Research Report 82-2, Asphalt Institute, Kentucky, (1982).

doi:10.4028/www.scientific.net/AMR.587.107

Optimal Carbon NanoTubes concentration incorporated in mortar and concrete

R. Hamzaoui [1,*], A. Bennabi[1], S.Guessasma [2], M.R. Khelifa [3,4], N. Leklou[5]

[1]Université Paris-Est, Institut de Recherche en Constructibilité, ESTP, 28 avenue du Président Wilson- 94234 Cachan, France

.[2] INRA, rue de la Géraudière 44300 Nantes, France

[3] Département LMD Sciences et Techniques, Faculté de Technologie de l'Université de Batna & Laboratoire Habitat et Environnement de l'Université de Sétif, Algérie

[4] Département Sciences de la Terre et de l'Univers & Laboratoire Géosciences et Environnement de l'Université de Cergy-Pontoise, France

[5] LUNAM Université, Université de Nantes – IUT Saint-Nazaire, GeM, CNRS UMR 6183, Research Institute in Civil Engineering and Mechanics, France

rhamzaoui@adm.estp.fr

Keywords: Carbon nanotubes (CNT), mechanical properties, microstructure, mortar, concrete.

Abstract. The mechanical properties and microstructure of modified mortar and concrete using Carbon NanoTubes (CNT) are experimentally studied at 7, 14, 28 and 90 curing days. Part of the formulation, CNT are dispersed in a liquid solution. Different concentrations ranging from 0.01% to 0.06% and 0.003% up to 0.01% are used for mortar and concrete, respectively. Mechanical testing of the modified materials reveals that maximum compressive strength is obtained for CNT concentrations close to 0.01%wt and 0.003%wt for mortar and concrete, respectively. The microstructural characterisation of the modified materials suggests that CNT act as bridges between pores and cracks leading to a reduction in porosity and in turn an increase of compressive strength.

Introduction

Most crystalline solids are composed of a collection of many small crystals or grains; termed polycrystalline. The term of nanomaterials or nanocrystalline materials (also known as nanostructured or nanophase materials) is used to describe those materials that have a majority of grain size in the typical range from ~1 to 60 nm. Whether it can be called a revolution or simply evolution, the nanomaterials have received much attention as advanced engineering materials with unique physical, chemical and mechanical properties. Generally nanomaterials have exceptional properties in comparison than to those of coarse-grained ones [1-5]. Since invented by Iijima [6] in 1991, carbon nanotubes have been widely used in a wide spectrum of applications such as in electronics technology, biomaterials design, chemical compounding and multifunctional composites. Carbon nanotubes (CNT) are allotropes of carbon with a cylindrical nanostructure and members of the fullerene structural family [7-8]. One of the most important properties achieved by CNT, in civil engineering applications, is their capability to confer a mechanical reinforcement to cement based structural materials [9-10]. The aim of this work is to study the effect of addition of different amounts of CNT varying from 0.01% to 0.06% and from 0.003% to 0.01% on the compressive strength and microstructure of mortar and concrete respectively

Materials and methods

The ordinary Portland cement used in our work is CEMII 32.5R from Colas company and classified in NF P15-301 norm. The carbon nanotubes are delivered by Arkema Company as a liquid solution. The scientific name is Graphistrength CL1-020. Carbon nanotubes multiwall developed by Arkema is an allotrope of carbon and appear as small concentric cylinders of graphite. Table.1 summarizes CNT properties. Different concentrations namely 0.01%, 0.02%, 0.03%, 0.04%, 0.05%, 0.06% for mortar and 0.003%, 0.004%, 0.006%, 0.01% for concrete are prepared and added to the standard

formulation like mixing water. The procedure of mortar preparation follows the classified European Standard EN 169-1. The mixed mortar is poured into molds to form prisms of typical dimensions 4x4x16 cm. The mixed concrete is poured into molds to form cylindrical samples with a height of 11 cm and diameter of 22 cm. The cylinderical concrete samples are finished to have a smooth surface before mechanical testing. Table.2 summarizes the selected concrete formulation used. Compressive testing for the strength at the 7th, 28th and 90th days is performed using a mechanical testing system (MTS) under constant speed for mortar and hydraulic mechanical testing system (3R) under load control for concrete. Mortar and concrete samples are characterized by Scanning electron microscopy (SEM) (stereo scan 120, Leo 120), with IDIFIX program coupled with energy dispersive spectrometer (EDS).

Table.1 Properties of carbon nanotubes (CNT).

Electric conductivity	$10^2 – 10^4$ [s/cm]
PH	11
Density	1000-1100 [kg/m^3]
Liquid solution concentration	2%wt of CNT
Liquid solution color at 20°C	Black
Liquid solution odor	Slight
Liquid solution	Solubility in other solvents

Table.2 Modified Concrete formulations used with CNT.

Constituents	Aggregates Percentage	Formulation (en kg/m3)
0/4 (Sand)	38 %	704.90
4/8	17 %	315.35
8/16	40 %	742.00
16/20	5 %	92.75
Total Aggregates	100 %	1855
Cement		310
Water		1600

Results and discussions

In order to find an optimal concentration of CNT which exhibits the maximum improvement in compressive strength, different weight percentages of CNT are used. For mortar, test conditions are: 0.01wt%, 0.02%, 0.03%, 0.06% whereas for concrete we use rather 0.003%, 0.006%, 0.01%.

Figure.1a shows the evolution of the mortar compressive strength as function CNT percentage for 90 days. It is observed that the largest compressive strength is found when adding 0.01% of CNT. Also, it is remarked that the compressive strength for the optimal CNT percentage is 21.2% higher than the reference mortar. However, further increasing of CNT degrades the compressive strength of mortar.

At 90 days of concrete curing time, the effect of CNT percentage on compressive strength is shown in Figure.1b. Again, the observed maximum compressive strength is reached for a CNT percentage of 0.003%. The gain in compressive strength is 17.65% with regards to the reference condition. We observe the same trend of strength degradation using a larger amount of CNT.

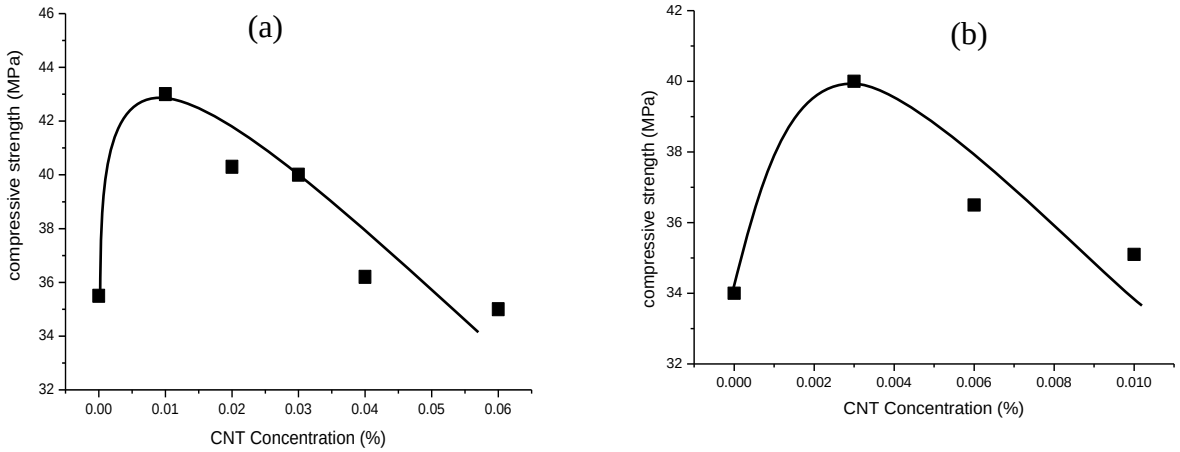

Fig.1 Evolution of the compressive strength as function CNT percentages for 90 days for (a) mortar, (b) concrete

In order to understand the microstructural implications of the observed mechanical behaviour we carried out a morphology analysis using SEM on 90 days concrete samples as presented in Figure 2 (a, b). Figure.2 (a) shows the SEM micrographs of reference concrete for 90 curing days. The microstructure corresponding to the reference condition well highlights the existence of microcrystalline and nearly amorphous phases. The presences of calcium silicate hydrates (C-S-H), calcium hydroxide (C-H) crystals, voids between the hydrated phases are all evidenced. The calcium silicate hydrates (C-S-H) exist in the form of stand-alone clusters, lapped and joined together by many needle-like hydrates. Furthermore, $CaOH_2$ crystals are distributed among the cement paste. The morphology of concrete with optimal concentration (0.003%) of CNT for 90 curing days is shown in Figure.2 (b). We qualitatively observe particular positioning of assemblies of CNT around pores and micro-crackes in a way to provide solid bridges. As the mechanical behaviour is negatively affected by the pore content, we suggest that improvement of strength is due to a reduction of the porosity role. Porosity and mostly microcracks act as preferential sites for stress localisation. Thus, the bridging provided here by CNT increases locally the intrinsic strength of the material as these handle more stress than the matrix.

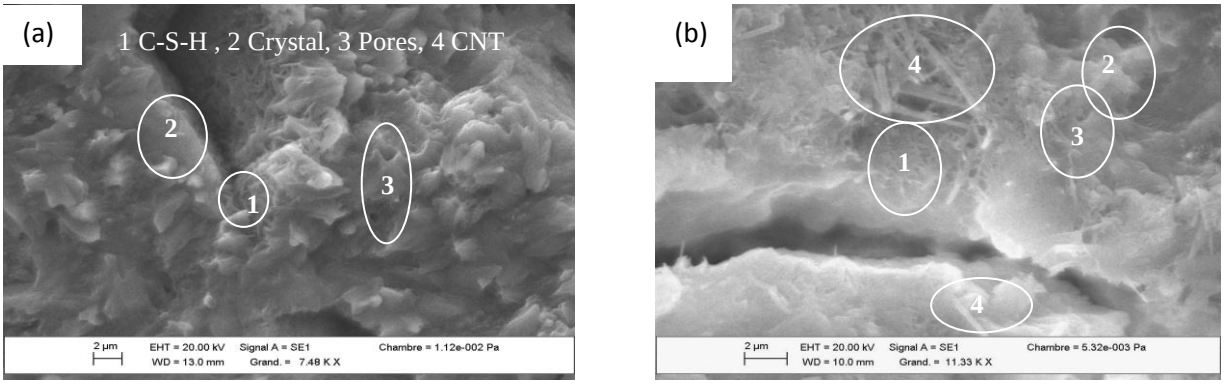

Fig.2 Morphology analysis by scanning electronic microscopy is performed for concrete samples aged of 90 days: (a) reference concrete, (b) concrete + 0.003% CNT

Summary

The aim of the present research work is to study the mechanical properties and microstructure of different CNT concentrations 0.01%, 0.02%, 0.03%, 0.06% for mortar and.003%, 0.004%, and 0.006% for concrete. The following main results are obtained:

1) Optimal concentrations of CNT which give the best compressive strength improvement is 0.01%wt and 0.003%wt for mortar and concrete, respectively.
2) The factor of compressive strength improvement is 1.2 for mortar and 1.17 for concrete compared to the reference condition free of CNT.

Acknowledgements

We thank Margarita Walferdein from IRC/ ESTP, Cachan, France, for her technical assistance concerning mechanical measurements. We thank Arkema Company for providing us with the carbon nanotubes in liquid solution.

References

[1] E. Gaffet, G.Le Caër, "Mechanical processing for Nanomaterials", Encyclopedia of Nanosciences and Nanotechnology. V 5, (2004) 91-129.

[2] M. S. El-Eskandarany, "Mechanical alloying for fabrication of advanced engineering materials", ISBN: 0-8155-1462-X Printed in the United States (2001).

[3] Hui Li, Hui-gang Xiao, Jie Yuan, Jinping Ou, Microstructure of cement mortar with nano-particles, Composites: Part B 35 (2004) 185–189

[4] R.Hamzaoui, O.Elkedim, N.Fenineche, E.Gaffet and J.Craven, "Structure and magnetic properties of nanocrystalline mechanically alloyed Fe-10%Ni and Fe-20%Ni". Materials Sciences and Engineering A 360 (2003) 299-305.

[5] S. Tria, O.Elkedim, R. Hamzaoui, X. Guo, F. Bernard, N. Millot and O.Rapaud "Deposition and characterization of cold sprayed nanocrystalline NiTi" Powder Technology Vol210, (2011) 181-188.

[6] S. Iijiman, "Helical microtubes of graphitic carbon", Nature 354(7), (1991), 8-56.

[7] M. S .Dresselhaus, G. Dresselhaus, Ph. Avouris, "Carbon nanotubes synthesis, structure, properties and applications", ISSN print edition: 0303-4216, Spriner-Verlag Berlin Heideberge, printed in Germany (2001).

[8] S. Reich, C. Thomsen, J. Maultzsch, "Carbon nanotubes, basic concepts and physical properties", 1st edition, WILEY-VCH Verlag GmbH&Co.KGaH, (2004)

[9] Geng Ying Li, Pei Ming Wang, Xiaohua Zhao, Mechanical behavior and microstructure of cement composites incorporating surface-treated multi-walled carbon nanotubes, Carbon 43 (2005) 1239–1245.

[10] Pudov P.A, Pislegina A.V, Lshnikova A.A Pervushin, Yakovlev G.I, Challenges in carbon nanotube dispersion during the modification of fine cement concretes. International conference on nano-Technology for green and sustainable construction, Cairo-Egypt 14-17 March (2010).

doi:10.4028/www.scientific.net/AMR.587.111

Zero Valent Iron Particles for the Degradation of Polycyclic Aromatic Hydrocarbons in Contaminated Soil

Salina Alias[1,a], Megawati Omar[2,b], Noor-Hana Hussain[3,c] and Suhaimi Abdul-Talib[1,d]

[1]myBioREC,Institute for Infrastructure Engineering & Sustainable Management, Faculty of Civil Engineering, Universiti Teknologi MARA, 40450 Shah Alam, Selangor, Malaysia

[2]Research Management Institute, Universiti Teknologi MARA, 40450 Shah Alam, Malaysia

[3]Institute of Science, Universiti Teknologi MARA, 40450 Shah Alam, Malaysia

[a]salina346@ppinang.uitm.edu.my, [b]megawati@salam.uitm.edu.my, [c]noorhana@salam.uitm.edu.my, [d]ecsuhaimi@salam.uitm.edu.my

Keywords: Contaminated Soil; Degradation; Polycyclic Aromatic Hydrocarbon; Zero Valent Iron

Abstract. The removal of polycyclic aromatic hydrocarbons (PAHs) from contaminated soil through oxidative degradation by zero valent iron (ZVI) has been investigated in this study. The results showed a fast decrease of PAHs within the first 30 minutes of treatment followed by a slow degradation. The degradation rates coefficient (k) of PAHs analysed using pseudo first-order rate model showed the rate of reaction increased with the increase of ZVI concentrations from 0.003 min^{-1} at 1% ZVI concentration to 0.011 min^{-1} at 3% ZVI. However, the normalized surface area constant (k_{SA}) decreased when the ZVI dosage above 3% was applied.

Introduction

Currently, deploying zero valent iron (ZVI) to remove organic and inorganic pollutants from the environment has gained popularity among researchers. ZVI (Fe^0) can replace the conventional oxidizing agents, ozone and hydrogen peroxide, as ZVI has shown the potential to generate hydrogen peroxide and Fenton reagent through series of reduction/oxidation (redox reaction) process on ZVI surfaces as depicted in Eq. 1 to Eq. 3. ZVI which can be obtained as waste material of iron scrap from the iron manufacturing sectors can be an economical and effective materials in treating pollutants.

$$Fe^0 \rightarrow Fe^{2+} + 2e, \quad O_2 + 2e \rightarrow 2O^{2-}, \quad H_2O \rightarrow H^+ + OH^- \tag{1}$$

$$Fe^0 + O_2 + 2H^+ \rightarrow Fe^{2+} + H_2O_2 \tag{2}$$

$$Fe^{2+} + H_2O_2 \rightarrow Fe^{3+} + OH^- + {}^{\cdot}OH \tag{3}$$

Although many studies have investigated the ability of ZVI to degrade organic pollutants such as halogenated hydrocarbon [1, 2], the effect of ZVI on the polycyclic aromatic hydrocarbon (PAHs) seems to have been overlooked. At present, most studies on PAH reduction by ZVI do not use ZVI bare particles; instead the ZVI is coated with other metals such as nickel, cobalt and palladium to form bimetal particles [3, 4]. These catalyzed ZVI-metals will enhance the PAH reduction as they provide more electron donors to mediate in electron transfer and preserve the reactivity of ZVI particles from fast corrosion in the redox process. Secondly, most of these studies only focused on experiments in liquid condition under anaerobic environment. Only Chang et al. [5] investigated the removal of pyrene which is a 4-ring PAH in contaminated soil under aerobic condition. To the authors best of knowledge, there is no study on the remediation PAH such as phenanthrene (PHE), anthracene (ANT) and benzo(a)pyrene (BaP) in contaminated soil using ZVI bare particles. Besides, the PAHs degradation under a non-limited oxygen condition with ZVI has not been reported. Thus, this study may offer a new reference in the field of PAHs treatment in contaminated soil using ZVI.

Materials and Methods

Preparation of Artificially PAH Contaminated Sand. Artificially PAH contaminated sand was prepared by spiking benzo(a)pyrene (100 mg/kg), phenanthrene and antracene (350 mg/kg) into flasks containing 20 g of cleaned and sterilized silica sand. Each flask was capped with non-absorbent cotton wool to prevent contamination by atmospheric microorganisms and covered with aluminum foil to prevent photolysis of PAHs. The initial concentration of PAHs in spiked soil was analyzed prior the experiment.

Preparation of ZVI Particles. ZVI was synthesized using a method developed by Wang and Zhang [6]. A one liter volume of Ferric(III)chloride solution (0.11M) was prepared using ethanol:deoxygenated Ultra-Pure-Water (UPW) solution (volume ratio of 3:7). Borohydride solution ($NaBH_4$) at concentration of 1.0M was prepared at the volume of 220 mL using UPW and titrated at the rate of 40-50 drops per minutes into $FeCl_3.6H_20$ solution. The ZVI particles were formed immediately at the first drop of borohydride solution as the ferric ion (Fe^{3+}) oxidized as depicted in Eq. 4. The precipitate of ZVI particles was separated from the solution by centrifuging at a speed of 5000 rpm for 10 minutes. The particles were washed with 99% absolute ethanol and dried in an oven at 105^0C for 2 hours.

$$FeCl_3 + 3NaBH_4 + 10H_2O \rightarrow Fe^0 + 3H_2BO_3 + 3NaCl + 12H_2 + H_2O \quad (4)$$

Properties of ZVI. The particle size distribution of ZVI was analysed using Zeta-Sizer Nano ZS Instrument (Malvern, USA) while specific surface area was determined using BET-201A Soptometer (Porous Materials, Inc., USA). Through the X-ray Diffraction (XRD) analysis using D8 Advance Bruker Instrument (German), the presence of ZVI particle produced in the synthesized process was verified.

Kinetic of PAH Removal from Contaminated Sand. The synthesized ZVI particles at the percentage weight ratio of 1, 3, 5, 7 and 10% to the total weight of soil (i.e. g of ZVI/ 20 g of sand) were added into flasks containing sterilized PAHs contaminated sand. This was followed by the addition of 15 mL sterilized deoxygenated UPW. The flasks were then incubated in an incubator shaker at 30^0C and 150 rpm. At predetermined duration, 1 g of sand from flask was sampled by spatula. Flasks with non-added ZVI were prepared as control samples. The degradation kinetics of PAHs was determined using the typical pseudo first-order rate model (Eq. 5) and described in term of ZVI surface area and ZVI concentration as in Eq. 6 [2]:

$$\frac{dC}{dt} = -k_{obs} C \quad (5)$$

$$\frac{dC}{dt} = -k_{SA}\alpha_s \rho_m C \quad , \; k_{SA} = \frac{k_{obs}}{\alpha_s \rho_m} \quad (6)$$

where C is the PAH concentration in the soil medium at time, t, k_{obs} is the observed first order rate constants of degradation process (min^{-1}), k_{SA} is normalized surface area rate constant (L $m^{-2}h^{-1}$), α_s is specific surface area of ZVI (m^2/g) and ρ_m is the ZVI concentration in liquid (g/L).

PAH Analyses. The PAH compounds from the sampled sand were extracted using a Microwave-Assisted Extraction (MAE) system (Multiwave 3000, AntonPaar). The sand of 0.5 g was weighed, placed into a Teflon liner cup and dissolved in 25 mL n-hexane and acetone (7:3 v/v). The MAE system was set to operate at 120^0C and 1000 W where the pressure was increased 0.5bar/s and then maintained at 10 bars for 45 minutes. The volume of the extracted supernatants reduced to 1 mL in a rotary evaporator (Buchi) at 43^0C was then transferred into a clean HPLC vial.

The PAH compounds from the extracts were analysed using High Performance Liquid Chromatograph (HPLC), which was equipped with reverse phase Kinetex column C18, 2.6 μm 100A (Phenomenex, USA) at a set UV/VIS wavelength of 254 nm. Acetonitrile and water were used as the mobile phase to carry the PAH samples which was set to flow at rate of 0.5mL/min in a gradient mode. The concentration of PAH was analysed by comparing the area of the peak based on retention time with a standard calibration curve.

Results and Discussion

Properties of Zero Valent Iron Particles. The particle size analysis showed the size of ZVI particles obtained in this study was not homogenous with diameter in the range of nano to micrometer (Fig. 1a). The particle size instrument produced a graph showed that the lowest and the highest mean diameter were at 22 nm and 6.3µm respectively, with the most represented mean diameter of 221.5 nm. In addition, the result of BET analysis measured the ZVI surface area was 12.8 m^2g^{-1}. Meanwhile, the analysis of XRD as shown in Fig. 1b confirmed that the ZVI (Fe) was produced in the synthesize process. However, the time taken to perform the XRD analysis has oxidized the ZVI and this can be seen with the presence of magnetite compound (Fe_3O_4) in the analysis (Fig. 1b).

Degradation Kinetic of PAH. The degradation kinetics of PAH at different concentration of ZVI were investigated in this study. A very fast removal of PAHs was exhibited in ZVI-sand water system at all ZVI concentrations (Fig. 2). The PAHs was removed at a high rate within 30 minutes and turned almost constant after 1 h at ZVI concentrations of 3, 5, 7 and 10%. More than 36% of PHE was removed in the first 30 minutes of reaction time for all ZVI concentrations as previously mention (Fig. 2a). However, only 14.5% of PHE was removed at 1% ZVI concentration. At the end of 48 hours reaction time, 39-54% of PHE was removed. On the other hand, degradation of ANT by ZVI was slightly slower than the PHE, at all ZVI concentrations (Fig. 2b). During the first 30 minutes reaction time, approximately 9% of ANT was removed at 1% ZVI, while more than 28% of ANT was removed at other concentrations. The final removal of this PAH at 1% ZVI was 35.9%, while at 3, 5, 7 and 10% ZVI, more than 40% of ANT was removed. At the same time, the finding on BaP (Fig. 2c) revealed significant difference between the 1% ZVI concentration and the rest. In the same vein (30 minutes reaction), there was only 7.7% of BaP removed in 1% ZVI compared to more than 30% in the other concentrations. At the end of 48 hours, 39, 48, 52, 53 and 54% of BaP were removed at ZVI concentrations of 1, 3, 5, 7 and 10%. The finding in this study is almost similar as reported by Chang et al. [5] where approximately 30% of pyrene (4-ring PAH) was removed at 2.5% nanoscale ZVI concentration in 30 minutes reaction time. Meanwhile, at 5% and 10% ZVI concentrations the study reported more than 45% and 70% of pyrene was removed [5].

The correlation between the observed pseudo-first order degradation rates coefficients of PAHs (k_{obs}) at linear data (in 30 minutes reaction time) and ZVI concentration is shown in Fig. 3. The reaction rates increase significantly from 1% (0.01g/g) to 3% ZVI concentration and then increase steadily up to 10% ZVI concentration. This can be seen where at 3, 5, 7 and 10% ZVI concentrations, almost similar values of the reaction rate coefficient (k) were observed for all PAHs which were within the range of 0.011-0.019 min^{-1}. The removal rate becomes constant when the binding sites reach maximum capacity or point of saturation. The saturation point for BaP removal was attained at 7% ZVI concentration, while for the PHE and ANT, the sign of saturation was observed at 10% ZVI. However, when the ZVI at 5% to 10% concentration were applied to contaminated soil containing pyrene, slower degradation rate of this PAH was depicted as it reach it's almost saturation point [5].

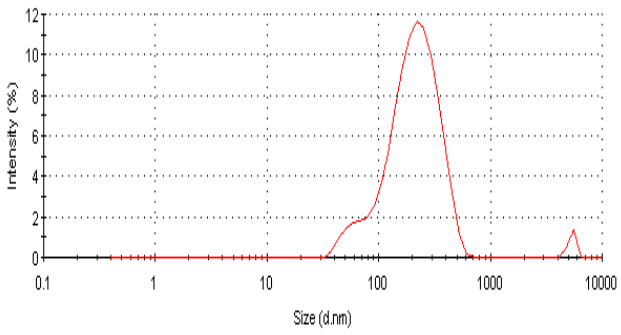

Fig. 1a: Particles size distribution of ZVI

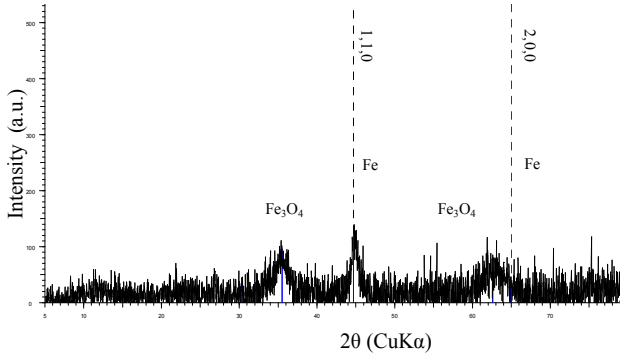

Fig. 1b: Image of XRD analysis

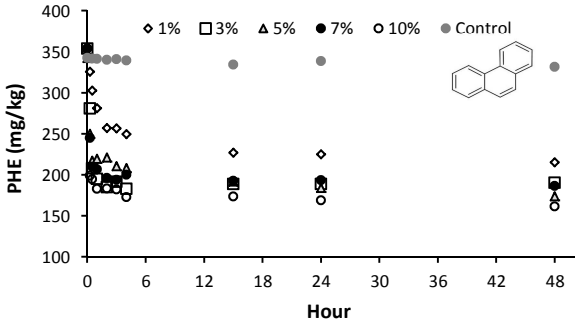

Fig. 2a: Phenanthrene degradation at different ZVI concentration. Data are mean of triplicate samples

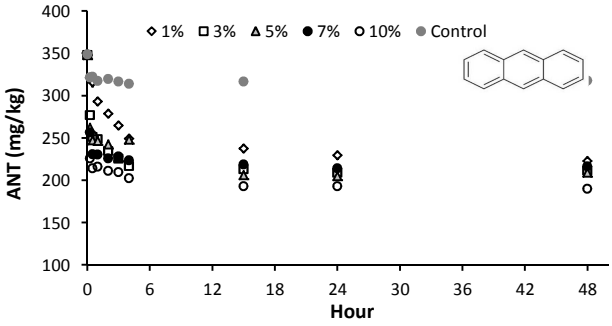

Fig. 2b: Anthracene degradation at different ZVI concentration. Data are mean of triplicate samples

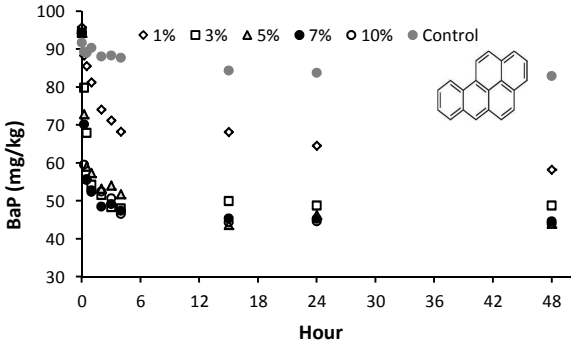

Fig. 2c: Benzo(a)pyrene degradation at different ZVI concentration. Data are mean of triplicate samples

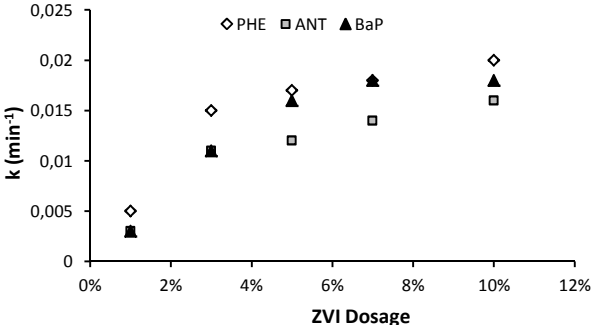

Fig. 3: Effect of ZVI concentrations on the degradation rates coefficient in different PAHs

The normalized surface area rates constant (k_{SA}) were determined (Table 1) in order to identify the actual reactivity of PAHs degradation per unit surface area of ZVI. Higher surface area which is resulted from the presence of ZVI in large quantities and smaller individual particle size, will promote higher removal of PAHs. In other word, the greater the k_{SA} value the higher the ZVI surface reactivity to degrade PAHs. From the current study, the k_{SA} values increased 2-fold when the sand-water system was introduced with ZVI at 1% to 3% concentrations. However, these values were found to decrease when the higher specific surface area was applied or ZVI concentration was above 3%. It has been hypothesized that pollutants will reduce as the ZVI concentration and surface area increases. These results are however not in agreement with the hypothesis but in agreement with finding by Tratnyek et al. [7], where the purity of ZVI or the presence of a wider reactive surface of ZVI is more important than the nano size of metal particle to remove the pollutants. In this study, when ZVI is excess, this metal has a tendency to be oxidized rather than involved in PAHs degradation. Thus for economical reason, the 3% of ZVI concentration is proposed to be used to treat soils contaminated by PAHs.

The fast decrease of PAHs in the early stage in this test is consistent with the findings by Feitz et al. [8] who explained that the reaction is as such was due to the catalytic reaction. The study indicated the high production of hydrogen peroxide (H_2O_2) and hydroxyl radical ($^{\cdot}OH$) from catalytic reaction between the ferrous and oxygen ions (Eq. 2 to Eq. 3) at early stage influenced the fast degradation rate of pollutants by ZVI. The oxidation of ZVI particles with time, lead to passivation of ZVI surface which prevents the redox reaction, thus slowed the rate of the PAH removal. In the present work, ZVI has been found capable of removing PHE, ANT and BaP. The degradation rate of BaP (5-ring PAH) was found higher than that of ANT (3-ring PAH). This finding is in contrast with the norms of the removal of higher ring PAH (more than 3-ring) by biodegradation experiments which are harder to remove. However, the result of this study agrees with the finding by Kulik et al. [9] where the degradation of 4-ring PAH by ozone was higher than 3-ring PAH. The reaction rate of ANT however is lower than phenanthrene's and benzo(a)pyrene's at all ZVI concentrations. This difference could have been due to the structure arrangement between ANT and PHE (upper right sides in Fig. 2a and 2b) where the linear structure of ANT is harder to be broken than the chemical bond of the angular arrangement of PHE.

Table 1: Pseudo first-order reaction rates coefficient (k) and specific reaction rate (k_{SA}) for the degradation of PAHs at different concentrations of ZVI within the first 30 minutes of reaction time

Treatment	PHE			ANT			BaP		
	$k_{[min^{-1}]}$	R^2	K_{SA} $[Lm^{-2}h^{-1}]$	$k_{[min^{-1}]}$	R^2	K_{SA} $[Lm^{-2}h^{-1}]$	$k_{[min^{-1}]}$	R^2	K_{SA} $[Lm^{-2}h^{-1}]$
1%	0.005	0.9988	1.76×10^{-3}	0.003	0.8771	1.1×10^{-3}	0.003	0.9263	1.06×10^{-3}
3%	0.015	0.9540	1.76×10^{-3}	0.011	0.9490	1.3×10^{-3}	0.011	0.9999	1.29×10^{-3}
5%	0.017	0.948	1.19×10^{-3}	0.012	0.8714	0.85×10^{-3}	0.016	0.9968	1.12×10^{-3}
7%	0.018	0.9943	0.91×10^{-3}	0.014	0.9270	0.70×10^{-3}	0.018	0.9948	0.91×10^{-3}
10%	0.019	0.7776	0.67×10^{-3}	0.016	0.8328	0.56×10^{-3}	0.018	0.8483	0.63×10^{-3}

Conclusion

ZVI is capable of removing PHE, ANT and BaP from contaminated soil. The removal capability of PAH is dependent on ZVI concentration where the more concentrated the ZVI is, the higher the removal of PAH. The k_{SA} values increase to 2-fold when ZVI concentrations were increased from 1% to 3%. However, there is no significant effect on PAHs removal above the 3% of ZVI concentration. ZVI concentration at 3% is thus proposed to be used to treat soil contaminated by PAHs. The utilization of ZVI to remove PAH in contaminated soil will encourage on the reuse of waste materials. This practice is in line with sustainable resource management policies that can help to safeguard the environment, human health and quality of life.

Acknowledgements

This research was funded by the Fundamental Research Grant Scheme (FRGS) from the Ministry of Higher Education, Malaysia and the Vice Chancellor Special Project (VSCP) Grant, Universiti Teknologi MARA (UiTM) Malaysia.

References

[1] Y. Shih, C. Hsu, Y. Su. Reduction of hexachlorobenzene by nanoscale zero-valent iron: Kinetics, pH effect, and degradation mechanism. *Separation and Purification Technology*. 2011, **76**: 268–274.

[2] T.L. Johnson, M.M. Scherer, P.G. Tratnyek. Kinetics of halogenated organic compound degradation by iron metal. *Environ. Sci. and Technol.* 1996, **30**:2634–2640.

[3] Y. Kim, W.S. Shin, S. Ko, M. Kim. Reduction of aromatic hydrocarbons by zero valent iron and palladium catalyst. 227th American Chemical Society Meeting, Anaheim, 2004.

[4] E. Nelkenbaum, I. Dror, B. Berkowitz. Reductive hydrogenation of polycyclic aromatic hydrocarbons catalyzed by metalloporphyrins. *Chemosphere*. 2007, **68**: 210–217.

[5] M. Chang, H. Shu, W. Hsieh, M. Wang. Remediation of soil contaminated with pyrene using ground nanoscale zero-valent iron. *J. of the Air & Waste Manage. Assoc*. 2007, **57**: 221-227.

[6] C.B. Wang, and W.X. Zhang. Synthesizing nanoscale iron particles for rapid and complete dechlorination of TCE and PCBs. *Environ. Sci. Technol*. 1997, **31**: 2154–2156.

[7] P.G. Tratnyek, V. Sarathy, J.H. Kim, Y.S. Chang, B. Bae. Effects of particle size on the kinetics of degradation of contaminants. *International Environmental Nanotechnology Conference, Applications and Implications.* 2009, Chicago, IL. EPA 905-R09-032, 67-72.

[8] A.J. Feitz, S. H. Joo, J. Guan, Q. Sun, D.L. Sedlak, T. D. Waite. Oxidative transformation of contaminants using colloidal zero-valent iron. *Colloids and Surfaces A:Physicochem. Eng. Aspects*. 2005, **265**: 88–94.

[9] N. Kulik, A. Goi, M. Trapido, T. Tuhkanen. Degradation of polycyclic aromatic hydrocarbons by combined chemical pre-oxidation and bioremediation in creosote contaminated soil. *J. Environ. Manage*. 2006, **78**:382–391.

doi:10.4028/www.scientific.net/AMR.587.116

Evaluation of the Geo-Mechanical Parameters of the Interface Between Asphalt Concrete and Sand with Applying Direct Shear Test and Numerical Modeling

Milad Tajdini[1, a], Ali Rostami[2, b], Mohammad M.Karimi[3, c], Hasan Taherkhani[4, d]

[1]Deparment of Civil Engineering, University of Zanjan, IRAN

[2]Department of Civil Engineering, Sharif University of Technology, Tehran, IRAN

[3]Department of Civil Engineering, Sharif University of Technology, Tehran, IRAN

[4]Department of Civil Engineering, Faculty of engineering, University of Zanjan, IRAN

[a]milad_tajdini@alum.sharif.edu, [b]alirostami@mehr.sharif.ir, [c]mohammadkarimi@mehr.sharif.ir, [d]taherkhani.hasan@znu.ac.ir

Keywords: Asphalt concrete; Sand; Direct shear test; Marshal test; Interface; Numerical modeling

Abstract. Asphaltic concrete has been used as waterproofing core in embankment dams, since 1948. In this application, the asphaltic core is surrounded by granular filter materials. The interaction of the asphaltic concrete and the granular materials has not been sufficiently investigated. In this paper the mechanical behavior of the interface between a natural smooth sand filter and asphaltic concrete at different levels of normal stresses and a constant shear strain rate has been studied. Small scale direct shear test has been conducted in this study, in which the shear surface is considered as the interface. Asphalt concrete specimens used in the shear test were cut in square shape (10×10×2.5 cm) from cylindrical specimen compacted by modified marshal compaction method. According to the direct shear test the interface constitutive parameters (cohesion, friction angle and shear stiffness) have been obtained. Using the parameters obtained from the direct shear tests, the numerical model of the test by applying FLAC3D Finite Difference software has been made, for which the Mohr-Coulomb constitutive parameters of the asphalt concrete have been obtained from back analysis using ABAQUS Finite Element software according to the conducted Marshal Test results on the asphalt. Utilizing the obtained parameters for both asphalt and interface, the normal stiffness of the interface has been extracted by back analysis with applying FLAC3D. It is shown that the shear stiffness and shear yield strength of the interface between sand and asphalt concrete, and the normal stiffness of the interface increase with increasing the normal stress level since driving direct shear test. The results of this study can help solving numerical problems of the interaction of asphaltic core and surrounding soil with considering more precise interface constitutive value, especially in the embankment dams with asphaltic core, which normal stress distribution on the asphaltic core varies through the different depths in the dam due to the hydrostatic pressure.

Introduction:

The large majority of embankment dams' central core is made of clay worldwide. However, as clay is increasingly difficult to access at new construction sites, asphalt concrete has been used as a replacement core material. Cores made of clay has also some other disadvantages such as, low shear strength, potential of compressibility, long construction time, requiring higher amount of material and accurate controls needed during construction, etc. These are in favor of using asphalt concrete, which has advantages such as less sensitivity to weather conditions, less width of core, healing behavior of bitumen, high shear strength etc. In this application, granular materials are used around the asphaltic concrete as a filter, which makes a complicated behavior in the interface and needs to be researched by experiments and modeling. The interaction of asphaltic materials and unbound aggregates and soil has attracted the attention of pavement technologists and researchers since the asphaltic materials have been used in highway pavements, and has been investigated in different

ways. The frictional and interlocking parameters are the major parameters of the interface between asphaltic material and soil [1, 2]. In the embankment dams with asphaltic concrete core, the interaction of asphaltic concrete and soil plays a vital role in the stability of dam, especially during earthquakes [3]. However, it has not been sufficiently investigated. Previous experiments on the interaction have showed that the interface parameters variably depends on factors such as the type of bitumen and soil, stress level, temperature, time etc, [1, 4, 5].

Mariana et al. studied the effects of interlocking conditions on the pavement performance using Finite Elements method. They showed that the stress state of the interface is highly effective on the cohesion of pavement layers. It was demonstrated that the bearing capacity of pavement decreases with increasing the stress level, [1]. Using a nonlinear analysis, they found that the optimum interlocking strength is achieved at a friction coefficient ranged between 0.3 to 1.5. Investigating the interlocking strength in another research project, Mariana et al. showed that the properties of interface materials is more effective than the amount of bitumen used for tacking two layers, [5]. They used Nottingham shear tester, in which the relation between shear stress and shear stiffness follows Goodman law. They used cobbles coated with asphalt as base layer and two asphaltic mixtures with different air voids content as surface layer, and demonstrated that the mixture with less air voids has a higher interlock, and stated that, for achieving an appropriate interlock, a high compaction level is needed.

In this paper, the results of an experimental work and its numerical modeling for investigating the interaction between an unbound compacted sand and asphaltic concrete are described.

Experimental Work:

The materials used in this study were sand and asphalt concrete. The sand used in this research was a graded and washed natural sand with a particle size ranging from 1 to 5 mm, and the asphaltic concrete, was made of a B60 grade of bitumen and a dense graded aggregates with a maximum nominal size of 16 mm. The hot mixture was compacted using a modified Marshal compaction mold, which is 6 in. in diameter. After compaction, the cylindrical specimens were trimmed and square shape specimens, 10 cm in each side and 1.5 cm in thickness were cut. Small scale direct shear test equipment has been used in this study. The equipment includes a fixed box at the top and a moving box at the bottom, which its rate of movement is controlled by a digital system. After preparing the materials, they were placed in the boxes; then, a certain normal stress was applied followed by applying a shear displacement at a constant rate.

The tests in this study were performed in the dry condition of the interface. A specimen of the sand was prepared at a relative density of 65%, and placed in the shear box. The tests were started by applying three different normal stresses of 0.8, 2.8 and 4.8 kg/cm^2. After applying the normal stress, a horizontal rate of displacement of 0.1 mm/min was selected for shearing the specimen, which was continued until the rupture of specimen. For investigating the interaction of asphalt and sand, the same conditions was utilized, except for using the asphalt briquette in the lower box and the sand in the top box. Using the shear stress at failure for each normal stress (Fig. 1), and considering the Mohr-Coulomb failure criterion, (Fig. 2), the cohesion and friction angle of the interface were obtained, (Table 1). The shear stiffness of the interface was calculated using the slope of the tangent line of the curve of shear stress versus shear strain at the initial stage, (Fig. 1). The values are shown in Table 3.

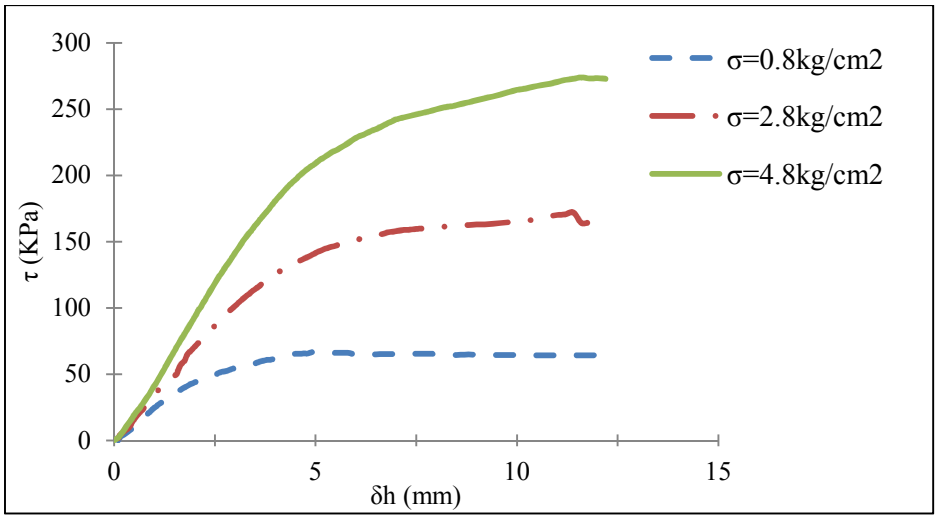

Fig. 1.Shear stress versus shear strain at different normal stress levels obtained from direct shear test

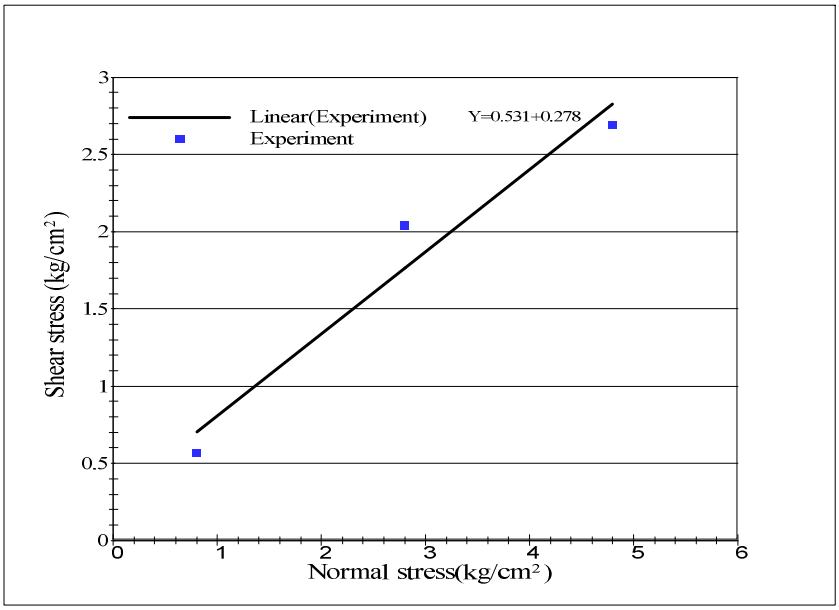

Fig. 2.Mohr-Coulomb failure criterion for the interface material (fictitious layer between Asphalt and sand)

Table 1: Shear strength parameters of the interface materials obtained from direct shear tests

Type	Cohesion (kg/cm^2)	Friction angle
Interface	0.278	27.97

Numerical Modeling of Marshal Test:

A back analysis was carried out for obtaining the Mohr-Coulomb parameters of asphalt concrete. To do this, the results of a Marshal test (ASTM D6927-06) were compared with the numerical modeling results, [6]. Using the load-displacement results of the Marshal test at the failure stage, and the Mohr-Coulomb constitutive model [7], the back analysis was conducted in order to extract mechanical parameters of asphaltic concrete. The ABAQUS Finite Element Software has been applied for numerical modeling of the Marshal test. The standard dimensions have been used for the modeling. Figure 3 shows the finite element model of the Marshal test. The results of analysis and

tests are shown in Figure 4. The single variable optimization method of back analysis has been implemented for the three parameters of elastic modulus, cohesion and internal friction angle. The values of the parameters obtained from analysis are shown in Table 2.

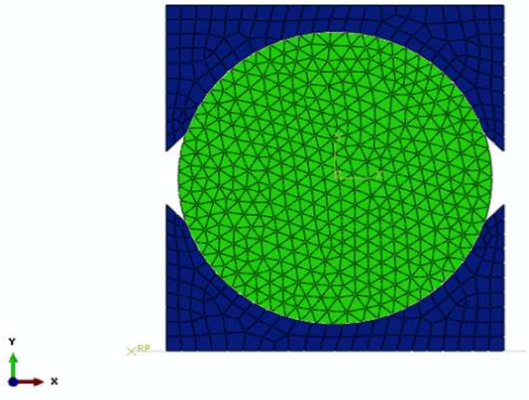

Fig. 3.Finite Element model of Marshal test

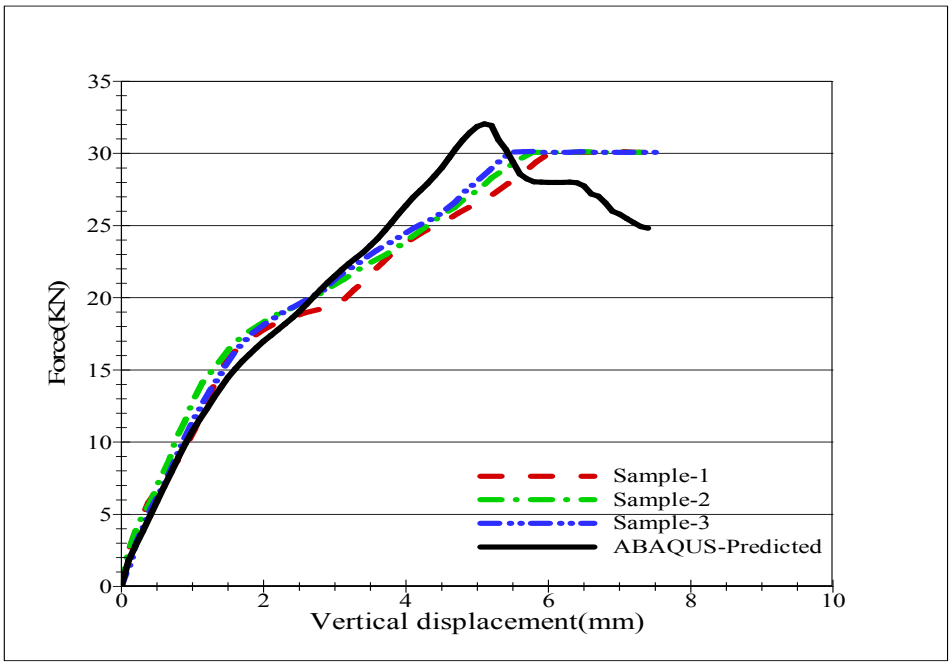

Fig. 4.Comparison of load-displacement results of Marshal test and back analysis using numerical modeling

Numerical Modeling of Direct Shear Test:

FLAC3D Software was used for modeling the direct shear test for the specimens of sand, asphalt concrete and their interface, (Fig. 5). The interface parameters and Mohr-Coulomb parameters of the materials, required for the numerical modeling, were as shown in Table 1 and 2, respectively. Different normal stresses of 0.8, 2.8 and 4.8 kg/cm2 were used in back analysis for obtaining the normal stiffness of the interface between two materials. For numerical modeling in FLAC3D, first, it is required to create an initial equilibrium state in the model for balancing the initial stress distribution before applying the horizontal velocity. Then, in order to simulate the applied rate of velocity of the bottom box of direct shear test, a displacement rate of 1×10-5m/sec, for the convergence of the numerical solution was uniformly applied to the asphalt zone. The back analysis, using the single variable optimization method, was performed. The main objective in the back analysis was to reduce the error value in comparison between the value of failure shear stress of the test and numerical modeling. The results of the analysis are shown in Figure 6. Table 3 shows the evaluated normal stiffness of the interface.

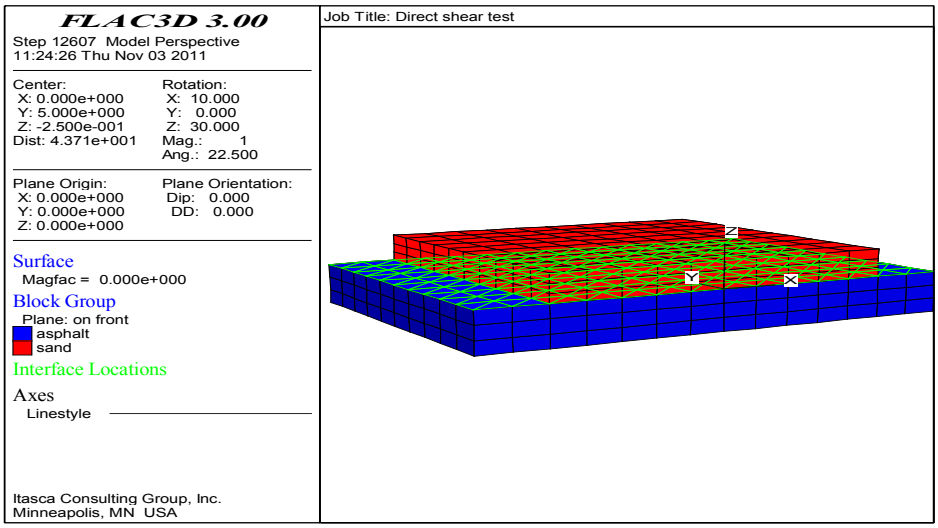

Fig. 5.Direct shear test model in FLAC3D

Table 2: Geo-mechanical parameters of asphalt concrete and sand in direct shear test model

Type	Cohesion (kg/cm^2)	Friction angle	Elastic modulus (kg/cm^2)	Dilation angle	Poisson's ratio
Sand (experiment)	0	32.9	3000	7	0.3
Asphalt (evaluated)	6.78	10.3	1800	3	0.35

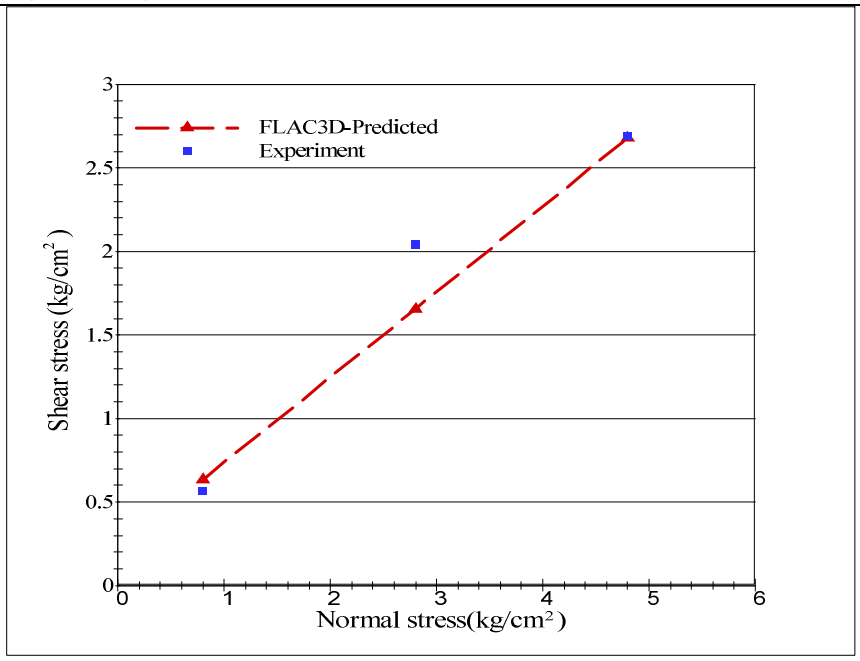

Fig. 6.Comparison between the yielding shear stress obtained from numerical modeling and direct shear test

Table 3: The normal stiffness of the interface evaluated by the back analysis in different levels of normal stress

Normal stress kg/cm^2	Shear stiffness (experiment) $kg/cm^2/cm$	Normal stiffness (evaluated) $kg/cm^2/cm$
0.8	0.69	2.2
2.8	1.79	6
4.8	2.84	8

Conclusions:

Based on the direct shear tests on the sand compacted at a relative density of 65% and asphalt concrete, it was demonstrated that increasing the normal stress increases the shear stiffness and shear yielding strength. The back analysis conducted with applying FLAC3D, showed that the normal stiffness of the interface is also increased by increasing the normal stress.

According to the technique introduced for evaluation of the constitutive parameters for the interface between sand and asphalt concrete, the obtained results could be useful in numerical modeling of embankment dam to apply more precise value for the interface parameters instead of improper and risky assumption.

References

[1] Mariana, R., Kruntcheva, Andrew, C., Collop and Nicholas H., Thom, (2005), " Effect of Bond Condition on Flexible Pavement Performance".ASCE0733-974, pp. 880-886.

[2] MahinRoosta, R., (2007), "Seismic Response of an Asphaltic Concrete Core Embankment Dam." 4th International Conference on Earthquake Geotechnical Engineering.

[3] Feizi-Khankandi, S., Mirghasemi and A., Ghanooni, S., 2004, “Behavior of Asphaltic Concrete Core Rock Fill Dams”, Published International Conference on Geotechnical Engineering.

[4] Arnevik, A., Kjarnsli, B. and Walbo, S., (1988), "The Storvatn Dam A Rock Fill Dam with a Central Core of Asphaltic Concrete."

[5] Mariana, R. Kruntcheva, Andrew, C., Collop and Nicholas H. Thom, (2006), "Properties of Asphalt Concrete Layer Interfaces", ASCE0899-1561, pp. 467-471.

[6] Standard Test Method for Marshall Stability and Flow of Bituminous Mixture, (D 6927) ASTM, 2006.

[7] Fwa, T.F., Tan, S.F., 2005, "C-φ Characterization Model for Design of Asphalt Mixtures and Asphalt Pavement", Journal of ASTM International, Vol.2, No.3.

doi:10.4028/www.scientific.net/AMR.587.122

A Solution for Corrosion Effect of Durable Concrete Structures

JAGATH KUMARI.DUNGI [1,a], Dr. K.SRINIVASA RAO [2,b]

[1] Assistant Professor, Department of Architecture, School of Planning and Architecture (V), Vijayawada, Andhra Pradesh, India.

[2]Associate Professor, Department of Civil Engineering, College of Engineering, Andhra University, Visakhapatnam, Andhra Pradesh, India.

[a]kumari_stru@yahoo.co.in, [b]killamsetti@yahoo.com

Keywords: Reinforced cement concrete, corrosion, high volume fly ash cement concrete, Epoxy coating on rebar.

Abstract. Corrosion of reinforcements has been one of the major challenges that the civil engineers have been facing. Corrosion leads to the formation of rust which results in the spalling of concrete which in turn leads to the exposure of rebars to the aggressive environment. This will accelerate the ill effects and ultimately leads to the breakdown of the structure. Corrosion mainly occurs in areas of aggressive environment such as coastal regions. It was discovered that structures such as highways, bridge decks, parking ramps and marine installations, designed to last from 50 to 100 years, required replacement or extensive repairs in just 10 years. The problem was found to be the absorption of airborne pollutants, acids and chloride salts through the surface which eventually found their way to the reinforcing steel, causing it to corrode.

It is very important that corrosion of reinforcement must be prevented in order to have a durable structure. Even though there are many methods to prevent corrosion, most of them are uneconomical and requires great skill. Studies on corrosion of reinforcement in various parts of the world have revealed that High Volume Fly Ash (HVFA) concrete can protect the steel reinforcement effectively, so that it can resist corrosion, and thus the structure as a whole. Similarly coating of rebars is the best and cheapest solution for corrosion attack, because prevention is better than cure.

Epoxy coated reinforcement rebar can be used in construction to protect steel more efficiently from corrosion. Epoxy coating works by preventing chlorides and moisture reaching the surface of the steel. So, it is the most practical and scientific way for protecting the steel reinforcement against corrosion effect. This paper reviews the HVFA concrete with fusion bonded epoxy coated rebars is the solution for corrosion effect.

Introduction

Reinforced concrete structures have the potential to be very durable and capable of withstanding a variety of adverse environmental conditions. However, failures in the structures do still occur as a result of premature reinforcement corrosion.

Corrosion of reinforcement has been established as the predominant factor causing widespread premature deterioration of concrete construction worldwide, especially of the structures located in the coastal marine environment [1]. The most important causes of corrosion initiation of reinforcing steel are the entry of chloride ions and carbon dioxide to the steel surface. After initiation of the corrosion process, the corrosion products (iron oxides and hydroxides) are usually deposited in the restricted space in the concrete around the steel. Their formation within this restricted space sets up expansive stresses, which crack and spall the concrete cover. This in turn results in progressive deterioration of the concrete. As a result, the repair costs nowadays constitute a major part of the current spending on infrastructure. Quality control, maintenance and planning for the restoration of these structures need non-destructive inspections and monitoring techniques that detect the corrosion at an early stage.

The maintenance and repair of bridges and buildings for their safety requires effective inspection and monitoring techniques for assessing the reinforcement corrosion. Engineers need better techniques for assessing the condition of the structure when the maintenance or repair is required. These methods need to be able to identify any possible durability problems within structures before they become serious.

During the last century, while emerging as the principal hydraulic binder, Portland cement is undergoing several modifications to suit to the ever changing construction needs. In the last few decades, for example, the concern for sustainability along with the need for durability is making researchers look more closely at the use of such industrial wastes as fly ash. In this regard, High volume fly ash (HVFA) concrete, developed by Malhotra and his associates at CANMET, Ontario, Canada in 1980's, is a pioneering effort addressing such issues as sustainability, CO_2 emissions, improved durability and economy [2]. Based on the numerous research efforts, HVFA concrete is now getting accepted in a number of structural applications including structures exposed to elevated temperatures.

How to Prevent Corrosion?

Quality Concrete and Concrete Practices: The first defense against corrosion of steel in concrete is quality concrete and sufficient concrete cover over the reinforcing bars. Quality concrete has a water-to-cementitious material ratio (w/c) that is low enough to slow down the penetration of chloride salts and the development of carbonation. The w/c ratio should be less than 0.50 to slow the rate of carbonation and less than 0.40 to minimize chloride penetration. Concretes with low w/c ratios can be produced by (1) increasing the cement content; (2) reducing the water content by using water reducers and superplasticizer; or (3) by using larger amounts of fly ash, slag, or other cementitious materials. Additionally, the use of concrete ingredients containing chlorides should be limited. The ACI 318 Building Code provides limits on the maximum amount of soluble chlorides in the concrete mix.

Another ingredient for good quality concrete is air entrainment. It is necessary to protect the concrete from freezing and thawing damage. Air entrainment also reduces bleeding and the corresponding increased permeability due to the bleed channels. Spalling and scaling can accelerate corrosion damage of the embedded reinforcing bars. Proper scheduling of finishing operations is needed to ensure that the concrete does not scale, spall, or crack excessively.

Methods of prevention of corrosion are

- High performance concrete
- Corrosion inhibitors
- Coatings on concrete surface
- Cathode protection
- Corrosion resistant steel bars
- Coatings on rebar's

Concrete Barrier: Increasing concrete depth has proven effective in slowing the ingress of chloride to the steel. The biggest problem with progress, besides high cost, is an increase in cracking propensity.

Corrosion Inhibitors: Corrosion Inhibitors are materials added in small amounts to the concrete mix or injected into the concrete element to reduce or stop corrosion. These materials function on the anodic surface of the reinforcing steel by reforming the passive film on the reinforcing steel and converting ferrous oxide to ferric oxide. This ferric oxide Fe_2O_3 serves as a barrier which prevents ions from leaving the reinforcing steel.

Coatings on concrete surface: Surface Sealers include membrane and materials such as silanes, siloxanes, and methacrylates that function by providing an impervious layer on or in the concrete between external coregents and the steel. The practical problems are that they are site applied and

preparation of the existing concrete can be an important factor. A key element to the successful implementation of the sealer is to prevent the ingress of water but allow the passage of water vapors to prevent blistering and peeling.

Cathode protection: Electro chemical Cathode protection works by imposing an electric potential to oppose the corrosion cell. It requires an anode current distribution system and a power supply. The major drawback is that is a technically sophisticated, expensive system that requires trained engineer site visits. It also requires high maintenance expenditures and an external power supply, often in remote areas. The long-term effect of cathode protection treatment is not well defined.

Corrosion resistant steel bars: Stainless steels have excellent resistance to corrosion. All true stainless steels contain a minimum of about 12% Cr (chromium) which permits a thin protective surface layer of chromium oxide to form when the steel is exposed to oxygen. The presence of oxide layer formation which is a poor conductor of electrons there by reducing the corrosion rate. But the cost of which is very high, prohibits its use on large scale in the construction industry.

Besides all these methods**,** the increased interest in sustainable design and construction has created a renewed interest in fly ash and other coal combustion products. This trend has been accelerated by the emergence of agencies like the U.S. Green Building Council (USGBC), Leadership in Energy and Environmental Design (LEED), and Coal Combustion Products Partnership (C2P2) of the USEPA. Their primary goal is environmentally and socially focused towards overall sustainable development.

Mineral admixtures can be used to enhance the corrosion-control potential of concrete by reducing permeability. Fly ash is one of the most common admixtures used in concrete but **rarely thought of to mitigate corrosion**. Fly ash concrete is substantially more impermeable compared to conventional concrete mix CCM from the age of 56 days on wards [5].

Keith Bargaheiser1 et al [6] Longer-term chloride ion permeability tests were carried out on samples of concrete containing 0, 15, 30, and 50% Class F fly ash replacing cement. The chloride ion permeability of the fly ash mixes was significantly lower than that of the no fly ash mix. The permeability reduced with increase in percent fly ash. Increase in curing time from 6 months to 1 year led to about 4.75% reduction in the permeability of the no fly ash mix, while the permeability of the fly ash mixes reduced 30% to 40% over the same time period. Even at one year of curing, the no fly ash concrete sample had moderate chloride ion penetrability while all the fly ash concrete samples had very low penetrability values. The high-volume fly ash mixes would be the most durable concrete mixes for preventing corrosion in reinforced concrete structures.

Strength wise also, It is proved that the HVFA concrete showed almost equal ultimate strengths with OPC concrete columns. J. kumari et al [7] investigated the behavior and load carrying capacities of columns made of HVFA cement concrete, exposed to fire and compare the results with those of the companion OPC concrete columns. HVFA cement concrete columns showed comparable ultimate strengths with OPC concrete columns. The better performance of HVFA concrete in comparison to the conventional concrete can be attributed to the fact that the fly ash reacts with lime and offers mineralogy to OPC that is conducive to strength development. The crystalline matter of fly ash which is not reactive gives a packing effect to concrete, filling up pores and thus contributing to the load carrying capacity of HVFA cement concrete.

Coatings on rebars are

- Galvanizing
- Cement slurry coating
- Cement polymer composite coating
- Various polymer based brush applied coatings and
- Fusion Bonded Epoxy coating

Various corrosion protection technologies have been developed to arrest and control the chlorides-induced corrosion of the reinforcing steel. Out of those technologies, some will post pone the problem of corrosion, some will control the corrosion phenomenon and the use of corrosion resistance materials as reinforcing steel will eliminate this problem. However, each of these technologies has its own limitations which should be considered during the selection of the measures.

Fusion Bonded Epoxy coating: This is one of the most popular corrosion protection strategies to combat rebar corrosion is to coat rebar with Fusion Bonded Epoxy. FBECR was first introduced in the United States in a Pennsylvania bridge in 1973 in response to the corrosion problems in the bridges caused by deicing salts. Since that time, the use has increased steadily into other structures such as water cooling towers, sewage treatment plants, parking garages and marine structures.

The Fusion Bonded Epoxy coating is a process where epoxy powder is applied by electrostatic spray on hot steel at pre-set temperature level. Epoxy coating works by preventing chlorides and moisture from reaching the surface of the steel. Its greatest advantage lies in its applicability to existing designs without changes in load capacity or section size the only change is in the development length slightly. The U.S government agencies have placed a great deal of emphasis on the careful handling and storage of epoxy coated reinforcement to minimize abrasion and mechanical damage. Touch-up of damaged areas of the coating is usually required. Ideally, the rebar should be prefabricated prior to coating which will minimize the need for the touch-ups. This process is much more expensive, but the final product is more likely to be more effective against corrosion.

Corrosion resistance activity in FBEC rebar: FBE coated rebar, the coating restricts the availability of surrounding cathode areas (as FBE coated areas are electrically insulated) and therefore restricts the corrosion activity, alleviating its severity. **Process of** coating of epoxy on rebar

- Bare rebar stacking
- Blast Cleaning
- Preheating
- Applying of Epoxy coating
- Cooling of bars
- Tests

BARE REBAR STACKING: The reinforcement bars are for which the coating is to be done is called as Bare rebar. If the diameter of rebar is less, than 3 to 4 bars are tied and sent to further processing.

BLAST CLEANING: Reinforcing bars are blast-cleaned to a near white metal finish using abrasive grit. This cleans the steel of contaminants, mill scale and rust. It also roughens the surface to give it a textured anchor profile. During this process, salt contamination is also removed. Roughness test is to be performed to the blasted bars (it should be between 40 microns to 100microns)

PREHEATING: Induction heaters are used to heat the bars to a temperature of 210 to 220 degrees (Thermo chalks or Infra Red Temperature Gauges are used to measure the temperature)

APPLYING OF EPOXY COATING: Electrically charged particles are attracted to the grounded-steel surface providing even coating coverage. When the dry powder hits the hot steel, it melts and flows into the anchor profile (i.e., the microscopic peaks and the valleys on the surface) and conforms to the ribs and deformations of the bar. The heat also initiates a chemical reaction that causes the powder molecules to form complex cross-linked polymers which give the material its beneficial properties.

COOLING OF BARS: The coating is allowed to cure for a short period (approximately 30 seconds) during which time it hardens to a solid. In some plants, the curing is often followed by an air or water quench that quickly reduces the bar temperature to facilitate handling.

TESTS

(To be performed as per **IS 13620: 1993**)To ensure the quality of coating on the bars

- Adhesion test
- Thickness test
- Holiday test

ADHESION TEST: The adhesion of the test is checked by bending the coated bar to 120degrees around a mandril or a manual bending equipment. No cracks, fracture in coating should be observed.

THICKNESS TEST: Code specifies for acceptance purpose at least 90% of all the coating thickness measuring shall be 0.1 mm to 0.3 mm after curing. Thickness gauge is used to measure the thickness.

HOLIDAY TEST: A 67.5volts is to be applied to the coated rebars. A holiday detector shall be used to detect the pinholes on the bars. Code allows 2 holidays per every 300 cm of bar.

THE TESTS TO BE PERFORMED ON ORGANIC COATINGS

- Cathodic disbondment test
- Salt spray test
- Resistance to applied voltage
- Chemical resistance
- Abrasion resistance
- Impact test

CATHODIC DISBONDMENT: This test provides acceleration conditions for loosing of coating. These are placed in 3% NaCl solution and potential of -1.5 V measured against the calomel electrode is applied. This test is conducted for 168 hours. The coating disbondment radius should not exceed 4mm when measured from the edge of intentional coating defect.

RESISTANCE TO APPLIED VOLTAGE TEST: Immerse 23,200 sq. mm of coated specimen in 7% NaCl solution and apply a potential of 2V. if no holiday is developed in 30days, a intentional holiday of 6 mm diameter is made and placed in the electrolyte. After 24hours no undercutting shall develop from the edge of intentional hole

CHEMICAL RESISTANCE TEST: Coated specimens with 6 mm diameter intentional holes are placed in the following solutions:

- Distilled water -- 3M Calcium chloride
- 3M sodium hydroxide -- Saturated calcium Hydroxide

It is retained for 45days. No blistering, softening, lose bonding, holiday should be developed on the coating.

ABRASION RESISTANCE: A panel as per specifications is prepared. Weigh the coated panel and place in the table abrasion having CS-10 wheels and apply 1 kg and run the table. Post weighs the coated panel. After 1000 cycles the weight loss shall not exceed 100 mg/1000cycles.

IMPACT TEST: A 1.8 kg mass with approximately 16 mm diameter top nose is dropped from height to make a 9 Nm impact. No cracking, shuttering or bond loss of coating should occur.

ADVANTAGES: Advantages of FBE application over conventional liquid coating application are Ease of application, Less waste of material

- Rapid application and cure schedules, which mean faster production rates
- Finished coated pieces can be moved to the storage area within minutes after the application

AREAS OF APPLICATION: Is the structure is expected to be exposed to chloride attack ordinary rebars gets corroded soon, hence FBEC rebars finds its application necessary

- Highway Bridges, Flyovers, Road over bridges, Marine works. Power plants, Chimneys, Cooling towers, Swimming pools and many other works.

S.H AI-Idi et al [8] the field and laboratory performance over the past 20 years has been very good. A field study of 22 bridges decks in Pennsylvania indicates good performance over ten years. None of the 11 decks reinforced with epoxy coated bars showed any visual signs of deterioration. Four of the 11 decks with uncoated bars showed concrete deterioration caused by corrosion of the reinforcement.

Conclusion

"Prevention is better than cure" So, For long lasting structures especially in coastal areas and aggressive environments Fly ash concrete mix with FBEC rebars are advisable than for the conventional reinforced concrete. For other than coastal and marine structures FBEC rebars are only advisable than for the ordinary uncoated rebars.

References

[1] Aging port infrastructure gains new life june2009 world port development 57

[2] Malhotra, V.M. and Kumar Mehtha,P., Guest editorial comments HVFA concrete for sustainable development , *The Indian concrete Journal*, November 2004,Vol. 78, pp.3-4.

[3] P. Garcés, Martínez C. Andrade Galvanic currents and corrosion rates of reinforcements measured in cells simulating different pitting areas caused by chloride attack in sodium hydroxide

[4] Rasheeduzzafar, Fahd H. Dakhil, Maher A. Bader, and Mohammed Mukarram Khan Performance of Corrosion-Resisting Chloride-Bearing Concrete

[5] prabir C Basu and Subhajit saraswathi High volume fly ash concretes with Indian ingredients *The Indian concrete Journal*, March 2006

[6] Keith Bargaheiser, Tarunjit S. Butalia Prevention of Corrosion in Concrete Using Fly Ash Concrete Mixes

[7] Kode VenkataRamesh, D. Jagath Kumari, M.Potha Raju, and D. Sree Ramachandra Murty Behavior of high volume fly ash cement concrete columns subjected to elevated temperatures *The Indian concrete Journal*, may2012,Vol. 78, pp.3-4.

[8] Application of available technologies for production of durable concrete S.H AI-Idi and M.H Al-Mehtal fourth soudi engineering conference Nov. 1995 volume-II

[9] Gustfson, D.P 'Epoxy update' civil Engineering ASCE,October 1988 pp38-40

[10] J.C. Ball, D.W. Whitmore, P.Eng Galvanic Protection for Reinforced Concrete Bridge Structures: Case Studies and Performance Assessment. Vector Corrosion Technologies

[11] Non Destructive Detection of Fractures in Prestressed and Post-tensioned Cables Garth Fallis P.Eng. and Matt Peeler EIT Vector Corrosion Technologies

[12] Hoff, G.C., Bilodeaua and Malhotra,V.M., Elevated temperature effects on HSC residual strength, *Concrete International*, 2000,April,41-47

[13] IS 8112-1989, Specification for 43 grade ordinary Portland cement(First Revision), Bureau of Indian Standards, New Delhi.

[14] IS 383-1970, Specification for coarse and fine aggregates from natural sources for concrete(Second Revision), Bureau of Indian Standards, New Delhi.

[15] IS 1786-1985, Spcification for High strength deformaed steel bars and wires for concrete reinforcement(Third Revision), Bureau of Indian Standards, New Delhi.

doi:10.4028/www.scientific.net/AMR.587.129

Cure Time Effect on Compressibility Characteristics of Expansive Soils Treated with Eco-Cement

Aniculaesi Mircea[1, a], Lungu Irina[2, b] and Stanciu Anghel[3,c]

[1, 2, 3]Faculty of Civil Engineering and Building Services, 43 Dimitrie Mangeron Blvd.,Iasi 700050, Romania,

[a]aniculaesi.mircea@gmail.com, [b]ilungu@ce.tuiasi.ro, [c]anghel.stanciu@yahoo.com

Keywords: expansive soils, eco-cement, consolidation test, curing time

Abstract. The objective of this paper is to investigate the influence of curing time on expansive soil as a construction material when treated with eco-cement stabilizer, as partly substituting the Portland cement. Standard consolidation samples were prepared from treated soils with 10 % cement (5% eco-cement and 5% Portland cement), reported to the dry unit weight of soil, and cured for 1, 7 and 14 days. After this period the soil samples were then socked in water and standard consolidation tests were performed on them. The compressibility characteristics, for the improved soil with 10% cement, Eoed, mv and Cv have shown a significant improvement during the first 7 days. After 7 days curing time the variation of compressibility characteristics is less pronounced.

Introduction

In the past, soft soils with poor engineering properties such as high plasticity, low bearing capacity, large settlement etc. were improved with classical stabilizers such as Portland cement or lime. The key factor in choosing the stabilizer was the proximity of them and the economic impact, disregarding the environmental issue. Nowadays, there is a mandatory responsibility in civil engineering that created a new trend in developing and using new materials with low impact on the environment.

This study investigates the capability of eco-cement to replace the traditional Portland cement used as a stabilizing agent in soils, in this particular situation to control the compressibility of one expansive/active soil. The research is focused on the stabilization solution of the soil named the Bahlui clay that is present in the city of Iasi, situated in North-East of Romania. Many geotechnical problems in constructions on the expansive Bahlui clay are triggered by the possibility of heavy soil expansion and shrinkage with wetting and drying cycles. Therefore, the research results will have an important benefit in the cost-effective design of various infrastructure facilities.

Materials and experimental methods

Soils. The basic properties of the expansive Bahlui clay used in this research are given in Table 1. The experiments were conducted to determine the Atterberg's limits, compaction characteristics and unconfined compressive strength.

From the particle size analysis resulted that the clay fraction is the major constituent (Fig. 2a), with the group symbol CH. According to IS 1498 [1], STAS 1913/12-88, USCS Classification, based on the physical proprieties from Table 1, the investigated clay displays a very high degree of expansion, leading to serious problems in geotechnical design [2].

Specification of cement used. Eco-cement is made from a by-product of the production of iron in a blast furnace where iron ore, limestone and coke are heated to about 1500°C. Eco-cement comprises mainly of CaO, SiO_2, Al_2O_3, MgO, contains less than 1% crystalline silica [3]. It has the same main chemical constituents as ordinary Portland cement, but in different proportions.

Because of these chemical similarities, Portland cement can be replaced by eco-cement in soil stabilization. A small amount of Portland cement is still needed to activate the eco-cement. In this study the Portland cement and the eco-cement are used in a ratio of 1:1 (50% Portland cement replacement).

Specimen preparation. The Bahlui clay samples were first dried in the oven at 110^0C, then milled and sieved through sieve No.14 (AASTO M145) [4]. The dry material was mixed with cement (1:1 ratio) thoroughly until a uniform colour was observed. Samples were prepared following a Standard Proctor Test at optimum water content and maximum dry density. Cement treated samples for 1, 7 and 14 days were kept in an air tight container at constant humidity.

Results and discussions

Effect of stabilization on physical proprieties. Fig. 1b shows that the liquid limit (LL) of soil decreases gradually with the increases of cement content. The plastic limit on the other hand, increases with the increase of cement content.

This improvement is attributed to the puzzolanic reaction of the cement with the soil and therefore, cement treated soil significantly reduces the plasticity index (PI).

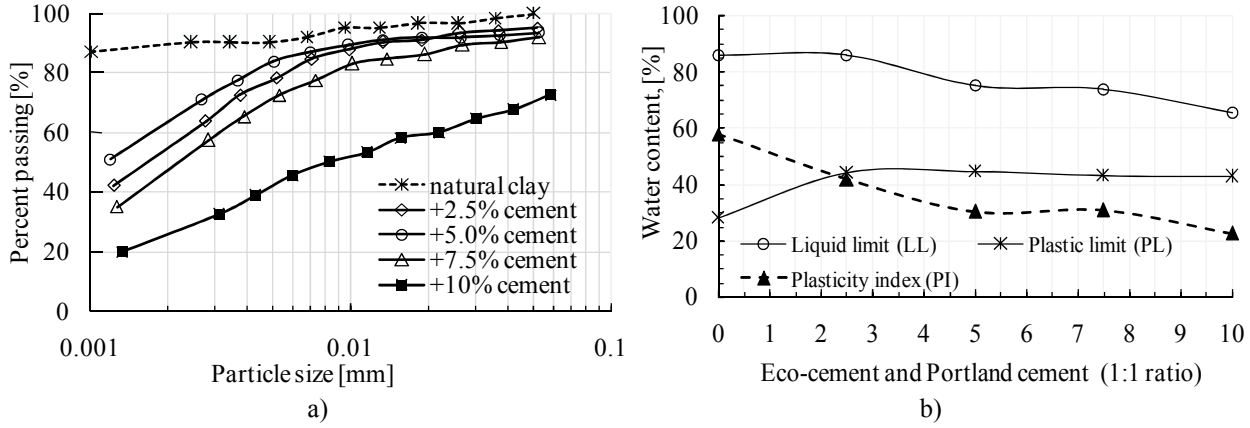

Fig. 1 Physical properties of the Bahlui clay treated with cement (1:1 Portland to eco-cement ratio); a) particle size distribution; b) the Atterberg's limits

Table 1 describes the indices and engineering properties of the untreated soil and treated soil with cement in different proportions.

Table 1. Properties of the treated Bahlui clay samples with cement

Properties		Bahlui clay with cement in proportion of [%]				
		0	2.5	5	7.5	10
Colloidal clay content	$C_{2\mu}$ [%]	89	63	55	48	26
Liquid limit	LL [%]	86.03	86.2	75.1	74	65.6
Plastic limit	PL [%]	28.2	44.33	44.72	43.16	43
Plasticity index	PI [%]	57.83	41.87	30.40	30.84	22.59

Fig. 2 shows that the Bahlui clay was classified into CH which is primarily inorganic clay of high plasticity, fat clay [2], that based on the USCS Classification belongs to the category with high volume change [5].

After improvement with 10% cement the plasticity decreases gradually (Fig. 1b) and the new soil structure is classified into OH which is organic clay with medium plasticity [6].

The swelling potential of stabilized clay, can be estimated indirectly based on the plasticity chart proposed by Cassagrande (Fig. 2a), results as high value.

In a graphical correlation of the activity and the percent of colloidal clay content (<0.002mm), proposed by Seed, after mixing the expansive clay with cement in different proportion, the swelling potential decreases from very high (25%) in natural state of the clay to medium swelling potential (1.5% to 5%) for treated clay with10% cement.

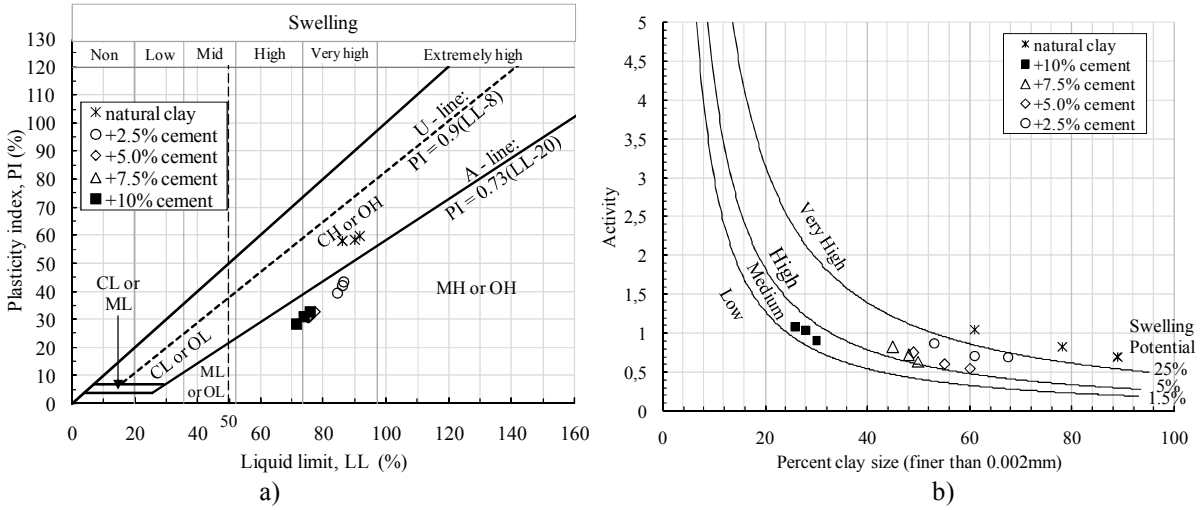

Fig. 2 Swelling potential classification based on: a) plasticity chart proposed by Cassagrande and b) classification chart proposed by Seed et al. (1962)

Effect of stabilization on the unconfined compressive strength. Unconfined compression tests were performed to determine the influence of the clay treatment with eco-cement and Portland cement on the soil strength. The experiments were conducted with the contribution of 10% cement content (5% eco-cement and 5% Portland cement) having curing periods of 1, 7 and 14 days. Figure 3 illustrates the variation of unconfined compressive strength with the curing time. Strength values of the cement treated samples increase from a 171.56kPa (1day cured samples) to a value of 458.2kPa (14 days cured samples). These increase of strength with time is related to the puzzolanic reaction and consequently on the cement hardness.

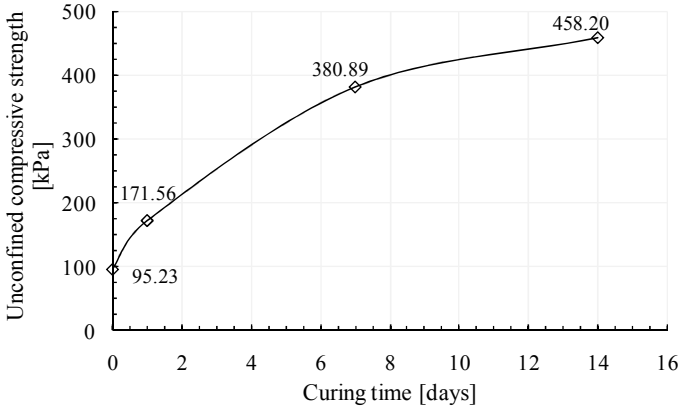

Fig. 3 Increase of the unconfined compressive strength for 10% cement mix with time

Compressibility characteristics of eco-cement clay treated samples. Fig. 4a and 4b show the variation of the oedometer modulus (E_{oed}) and the coefficient of compressibility (m_v) for 10% cement (1:1 Portland cement and eco-cement ratio) at different curing days.The coefficient of volume compressibility (m_v) [5] (Fig. 4b) gradually decreases by increasing the consolidation pressure. The variation of the coefficient of volume compressibility with time indicates that this parameter has an important variation during the first 7 days curing time, after this time the variation is less pronounced. Approximately the same trend can be seen for the oedometer modulus (Fig. 4a) with the curing time and the applied pressure.

The stabilized soil can be classified according to compressibility based on oedometer modulus E_{oed} for the interval of pressure between (200 ÷ 300) kPa [7]. Based on these classification the stabilized soil with 10% (5% eco-cement and 5% Portland cement) develops low compressibility (E_{oed} = 20000 ÷ 50000 kPa).

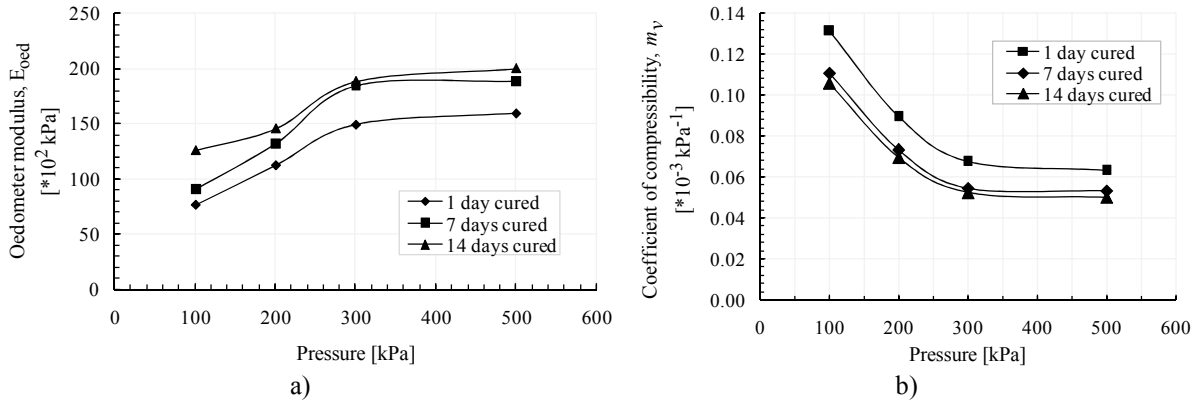

Fig. 4 Variation of compressibility indices: a) oedometer modulus and b) coefficient of volume compressibility with time and the consolidation pressure

Fig. 5a, shows the variation of coefficient of consolidation with time of curing. This variation is less pronounced for consolidation pressure below 100kPa. The curing time for treated expansive clay with 10% cement (eco-cement and Portland cement in 1:1 ratio) decrease the value of hydraulic conductivity, k (Fig. 5 b) [5], from (2.50 x 10^{-7} ÷ 0.96 x 10^{-7}) cm/sec for 1 day curing time to (0.98 x 10^{-7} ÷ 0.72 x 10^{-7}) cm/sec for 14 days curing time for the consolidation pressure between (100 ÷ 500) kPa.

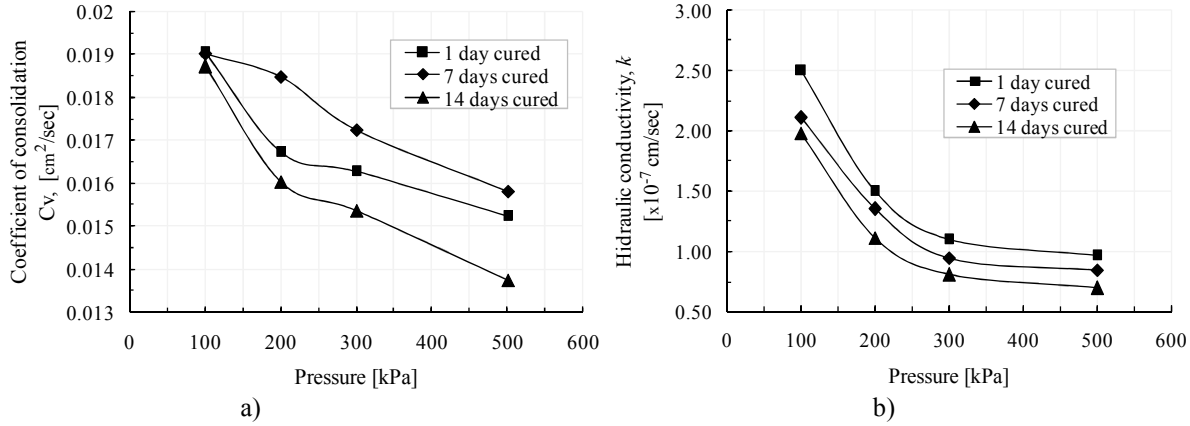

Fig. 5 Variation of relevant geotechnical indices: a) coefficient of consolidation and b) hydraulic conductivity, with time and the consolidation pressure

Conclusions

The effect of using eco-cement as a stabilizing agent in expansive soil treatment was investigated in this paper and the concluding remarks are based on the data and discussions presented previously. The compressibility characteristics, for the improved soil with 10% cement, E_{oed}, m_v and C_v have shown a significant improvement during the first 7 days. The coefficient of volume compressibility (m_v) is in the range of (0.13 x 10^{-3} ÷ 0.06 x 10^{-3}) kPa^{-1} for 1 day curing time and (0.11 x 10^{-3} ÷ 0.05 x 10^{-3}) kPa^{-1} for 14 days curing time for the consolidation pressure between (100 ÷ 500) kPa.

The coefficient of consolidation (C_v) is in the range of (0.018 ÷ 0.015) cm^2/sec for 1 day curing time and (0.019 ÷ 0.005) cm^2/sec for 14 days curing time for consolidation pressure between (100 ÷ 500) kPa. The results of the tested soil compressibility characteristics stabilized with 10 % eco-cement and Portland cement show that the values of these characteristics varies greatly during the first 7 days and after this period the variation is only slightly recorded.

Acknowledgment: This paper was supported by the project "Develop and support multidisciplinary postdoctoral programs in primordial technical areas of national strategy of the research - development - innovation" 4D-POSTDOC, contract nr. POSDRU/89/1.5/S/52603, project co-funded from European Social Fund through Sectorial Operational Program Human Resources 2007-2013.

Acknowledgment: Thank to ECOCEM Ireland, for the eco-cement support provided during the research study.

References

[1] BUREAU OF INDIAN Standard: *Classification and Identification of Soils for General Engineering Purposes*. BIS, New Delhi, (1970), (Reaffirmed 1987), IS 1498.

[2] R.G. McKeen: *Design and construction of airport pavements on expansive soils*, Report No. FAA – RD -76-77, (June 1976)

[3] http://www.ecocem.ie: Ecocem (GGBS) cement

[4] R.M. Brooks: *Soil stabilization with flyash and rice husk as*, submitted to International Journal of Research and Reviews in Applied Sciences, Vol. I, Issue 3 (December 2009)

[5] J.T. Germaine; A.V. Germaine: *Geotechnical Laboratory Measurements for Engineers*, edited by John Wiley & Sons, Inc, (2009)

[6] A.A. Al-Rawas, M.F.A. Goosen: *Expansive soils – Recent advances in characterization and treatment*. Taylor & Francis Group, London, UK, (2006)

[7] A. Stanciu and I. Lungu: *Foundation*, Technical Editure, Bucharest [2006], in Romanian

doi:10.4028/www.scientific.net/AMR.587.134

Sustainable Building Finishes: Use of Renewable Standardized Wood-Based Material in Nigeria

Adedeji, Y.M.D. [a] and Taiwo, A.A. [b]

Department of Architecture, Federal University of Technology, Akure, Nigeria

[a] yomi_adedejiy2k@yahoo.com ; [b] abraham_taiwo@yahoo.com

Keywords: building finishes, Nigeria, renewable, sustainability, wood-based material

Abstract. This paper reports a research on sustainable building finishes in Nigeria. Because the building industry consumes a substantial percentage of the materials entering the global economy, and is responsible for the emission of almost half of the global greenhouse gases, it is important to consider the aspect of material efficiency as a component of achieving sustainability. This paper critically appraises this development as the use of the renewable wood-based materials has impacted remarkable success towards achieving sustainable building finishes in the country. It reports findings on the authors' research through case studies, observations and structured questionnaire on the influence of use of renewable wood-based materials on the building industry in Nigeria. Findings of empirical survey conducted among professionals such like Architects, Engineers, Quantity Surveyors, Builders and Contractors practising in some selected cities in Nigeria on the use of the material were analysed along side with personal interviews of these professionals to obtain their views on the subject, revealing that the industrial production of standardised wood-based material to a finished stage makes building operation faster, reduces labour and wastages and enhances modular designs and construction thus aligning production with the current global trend. Timber material used for finishes was also observed to have good aesthetic value in building construction. The paper recommends that the material should be made available in the market in finished standard sizes for users to assemble on sites.

Introduction

Wood has been used throughout the history of mankind as one of the most common and oldest forms of building material. It is easy to work with, structurally strong construction material suitable for numerous applications such as framing, flooring, roofing and finishing [1]. From the very first housing, bridges and tools, timber has provided man with a broad range of building products and materials for construction. The forest has always been man's resort for major raw materials needed for constructional, recreational and technological designs and fabrication. This is due to the uniqueness of the major product of the forest (that is timber) in terms of its ability to naturally regenerate itself, its durability, its workability and adaptability to different environmental conditions. This has eventually resulted in increased demand for building materials and wood fibre products. Reports Forest & Wood Products Development Corporation Germany [2] and National Timber Development Council [3] confirmed that wood being an environmentally friendly housing material is suitable for construction and building finishes.

However, the conventional methods of using timber in construction of buildings in Nigeria are plagued with enormous waste, which can be avoided with intelligent applications. Also, timber usage in piecemeal sourcing adds to the building cost when compared with prefabricated components produced on industrial level [4]. In recent development, man has gradually improved the technologies adopted in wood processing in order to achieve better products in terms of utilisation for constructional works up till this age. Timber can be developed to standard sizes in finished forms and used as partition walls or finishing as done in some developed nations of the world. Such timber panels should be produced at industrial level for the public to enhance quality, aesthetic output and yet cost-effective, rather than the current piecemeal efforts of sourcing the material [5]. The focus of this paper is to provide information for standardization of wood-based materials for usage as finishes in buildings. This method would save time and resources and enhance sustainability in the building industry.

Wood-Based Building Materials and Sustainability

Wood is usually of different varieties and sources. Sun *et al.*[6] classified 82 types of wood into four groups on the basis of magnitude of their environmental impacts (eco-indicators). The use of timber in construction has gained increasing support, especially in the regions with vast forest resources (such as Southern Nigeria), because it can reduce both the energy demands of the buildings and the concentration of greenhouse gases in the atmosphere. Generally, this can be achieved by making use of wood instead of either fossil fuels or non-wood materials, such as steel, aluminium and concrete materials. This is not the case in Western and Central Europe, where the use timber is rather at low level [7]. In achieving sustainability, production of materials must use resources and energy from renewable sources instead of non-renewable ones. Calkins [8] opined that sustainable building materials should pose no or very minimal environmental and human health risks.

Joseph [1] posited that a sustainable building should be designed, built, renovated, operated or reused in an ecological and resource efficient approach, with a minimal negative impact on built and natural environment. Goals of a sustainable building should include: resource and energy efficiency [9]; carbon dioxide (CO2) and greenhouse gas emissions reduction[9]; pollution prevention; mitigation of noise; improved indoor air quality; harmonisation with the environment; low construction cost, modest maintenance, but return completely to the earth when abandoned [10]. Others include materials efficiency, elimination or reduction of generated waste; low toxicity; water conservation; affordability. González and Navarro [11] estimated that selection of building materials with low environmental impacts can reduce CO2 emissions by up to 30% [8]. Merits of sustainable building materials to owners of such buildings include greater flexibility in design, low maintenance and replacement costs, energy conservation, improved occupant's health and productivity and lower costs associated with changing space configurations [12].

Research Methodology

The data presented in this report were obtained from research conducted by the authors on building materials in Nigeria. A well-structured questionnaire, designed to investigate variables on preference for the use of standardized wood-based materials for finishes over the conventional type was used to collect primary data. The variables, structured in question form, written in English language, and responses required in pre-coded alternatives given were targeted to elicit opinions of professional on the use of these materials. Research assistants, who had earlier been trained by the author, administered the questionnaire to selected professionals (Architects, Engineers and Quantity Surveyors) distributed over four out the six geo-political zones in Nigeria. One hundred and twenty (120) respondents were randomly selected equally from the two hundred administered in the four geo-political zones as shown in Table 1. The cities were purposively selected as places with high concentration of these professionals practicing in Nigeria.

Table 1: Distribution of Questionnaire within the Study Area

S/No	Geopolitical zone	Town	No of Questionnaire	No of Responses
1	South West	Akure	50	28
2	North	Abuja	50	32
3	South South	Port Harcourt	50	40
4	South East	Enugu	50	20
Total			**200**	**120**

Source: Field survey, 2007

Besides, additional data for the study were obtained through case studies and observations carried out in these selected cities. Cases studied include Soft Designs outfit in Akure; Yar Adua Centre, Abuja; IBB Gulf centre, Abuja; Queen's Shopping Complex, Mary Avenue, Port-Harcourt and

Ebeano Housing Estate, Enugu. Buildings raging from residential to institutional and commercial types that exhibited the use of timber as finishes were purposively selected, carefully observed and analysed below.

Findings and Discussion of Results

Preference for the use of standardised timber by the respondents. The frequency table revealed that 81% of the respondents favoured the use of timber in buildings as finishes as well as the mass production of the product as shown in Table 2. The availability of timber and other wood-based materials locally in large quantity, particularly in the Southern part of Nigeria facilitates high preference for the choice of these materials for finishes.

Table 2: Willingness to use timber for building finishes in the Study Area

S/N	Use timber for finishes	Frequency	Percentage
1	Not willing at all	2	2
2	Rarely willing	9	8
3	Moderate	10	8
4	Willing	53	43
5	Very willing	46	38
	Total	**120**	**100**

Source: Researcher's field survey (2007), obtained from the four selected cities.

This implies that the application of timber for finishes in buildings will be a good substitute for other imported materials used as building finishes in the country. This will promote local building materials content in the building industry and encourage sustainability in the sector.

Standard components such as ceiling, roof tiles, wall panels, floor, partitions, doors and windows as well as skirting observed in cases studied can be mass-produced and marketed in standard sizes. This will facilitate the efficiency of the materials when used in building finishes as corroborated by earlier studies observed by Apu[12] and Ogunsote & Adedeji[13]. Timber is widely used in numerous developed and developing nations of the world for high quality building construction. Its advantages as a modern building material include flexibility of space arrangement as shown in Figures 1-3, workability, dry construction, industrial production and comparative cost effectiveness.

Fig.1: Use of timber for moveable partitions and Finishes in Soft Designs, Akure, Nigeria. *Source: Authors' Field survey (2011).*

Fig. 2: Standardised timber finishes used for ceiling at Thomas Laniyan housing estate, Lagos, Nigeria. *Source: Authors' Field survey (2011).*

Such timber panels should be produced at industrial level for the public to enhance quality, aesthetic output and yet cost-effective, rather than the current individual efforts of sourcing the material. This method would save time and resources in the industry.

Fig. 3: Standardised timber finishes used in the reception hall, Yar Adua Centre, Abuja, Nigeria.
Source: Authors' Field survey (2011)

Conclusion

This paper discusses sustainable building finishes in Nigeria. It looks at the use of renewable standardised wood-based material as building finishes in selected cities in Nigeria. Although, the paper shows that the tendency for the use of prefabricated timber is high coupled with relative advantages of the material if sourced industrially, the use of standardised timber for finishes in Nigeria is still low and proffers suggestions to improve it.

References

[1] P. Joseph; Sustainable non-metallic building material. *Sustainability Review* 2, (2010). www.mdpi.com/journal/sustainability.

[2] Forest & Wood Products Development Corporation; Environmental properties of timber. Forest & Wood Products Development Corporation, Germany, (3); 4-9. (1997).

[3] National Timber Development Council; Environmentally friendly housing using timber.NSW: FWPRDC, (2001).

[4] Y.M.D. Adedeji; Materials preference options for sustainable low-income housing in selected cities in Nigeria. Ph. D Thesis, Department of Architecture, Federal University of Technology, Akure, (2007).

[5] Y.M.D. Adedeji; C. Arum, & B. Ajayi; Affordable housing initiative in Nigeria: use of composite panels. Proceedings of West Africa Built Environment Research, July 19-21 Accra (2011), pp 79-86.

[6] M. Sun, C.J. Rydh, & H. Kaebernick; Material grouping for simplified product life cycle assessment. *J. Sustain. Product Des*., *3*(2003), 45-58.

[7] European Commission, Enterprise & Industry Construction; *Overview*. Available online: http://ec.europa.eu/enterprise/construction/index_en.htm (accessed on 30 September 2009).

[8] M. Calkins; *Materials for Sustainable Sites*: *A Complete Guide to the Evaluation*, *Selection*, *and Use of Sustainable Construction Materials*; John Wiley & Sons: Hoboken, NJ, USA (2009).

[9] G. John, D. Clements-Croome; G. Jeronimidis; Sustainable building solutions: A review of lessons from natural world. *Building Environment, 40* (2005), 319-328.

[10] D. A. Bainbridge; Sustainable building as appropriate technology. In *Building without Borders*: *Sustainable Construction for the Global Village*; Kennedy, J., Ed.; New Society Publishers: Gabriola Island, Canada (2004), pp. 55-84.

[11] M. J. González, & J. G. Navarro; Assessment of the decrease of CO2 emissions in the construction field through the selection of materials: Practical case study of three houses of low environmental impact. *Building Environment 41*(2006), 902-909.

[12] S. S. Apu, Wood structure and construction method for low-cost housing. International Seminar / Workshop on Building Materials for Low-Cost Housing, Indonesia, September, 17-28. (2003).

[13] O.O. Ogunsote, & Y.M.D. Adedeji; Modern techniques of using timber in building structures and components in Nigeria. A Paper Presented at International Conference on Science and Technology at The Federal University of Technology, Akure (2005). http://www.futa.edu.ng/PDF/Internationalconference_PDF/sectiond.pdf pp. 705-711.9.

doi:10.4028/www.scientific.net/AMR.587.139

Shear Resistance of Non-Reinforced Oil Palm Shell Concrete Beams

Mei Yun Chin[a] and Teck Leong Lau[b]

Department of Civil Engineering, University of Nottingham (Malaysia Campus), Jalan Broga, 43500,Semenyih, Selangor Darul Ehsan, Malaysia.
[a]MeiYun.Chin@nottingham.edu.my, [b]TeckLeong.Lau@nottingham.edu.my

Keywords: Shear strength, Oil palm shell reinforced concrete beams.

Abstract. The test results of reinforced concrete beams cast with Oil Palm Shell (OPS) in shear mechanism are presented. It was found that the shear mechanism in Oil Palm Shell Concrete (OPSC) beams is similar in nature to those found in normal weight concrete (NWC) beams. Comparative studies carried out on variables affecting the shear mechanism indicate OPSC beamsproduce similar shear strength to NWC beams.

Introduction

Oil palm shell (OPS) is one of the bi-products derives from Palm Oil production and it is mostly left to decay. As part of the efforts to minimize the environmental impacts, the idea of using OPS in concrete was initiated in the last decade. Since then, some amount works [1-5] have carried out to study the potential use of OPS as coarse aggregate in normal strength concrete. The use of OPS as coarse aggregate in concrete results in the reduction of concrete density, 1800 kg/m^3, and hence, considered as lightweight concrete.

It was observed from tests that by varying the content of OPS the compressive strength of Oil Palm Shell Concrete (OPSC) can achieved up to 40 N/mm^2. Recent researches [1-3] have been focusing on the material properties of oil palm shell concrete (OPSC), such as, compressive strength, effect of curing condition, bond, and durability. Up to now, only a limited amount of works [4, 5] have been carried out to study the structural performance, bending,and shear of the OPSC beams. As a result, no guidance has been provided in the current codes of practice [7, 8]with regards to the shear design procedures of OPSC beams. In view of the importance of the shear failure mechanism with respect to the overall structural performance of a reinforced concrete structure, it is believed that more research has to be carried out to aid the current understandings.

In this paper, the test results of non-shear reinforced OPSC beams are presented and compared to the normal weight concrete (NWC) beams [6]. The variables considered in the current paper consist of concrete compressive strength, reinforcement ratio, effective depth, and shear span.

Mix Design of OPS Concrete and Beam Details

The oil palm shell concrete (OPSC) constitutes of ordinary Portland cement, sand as fine aggregate, oil palm shell as coarse aggregate, and water. The adopted mixes (measure in volume) were 3:1:3, 4:1:3 and 5:1:3 (Cement: Sand: OPS). The OPSC beams presented in current paper were rectangular in cross section and non-shear reinforced. Details of the OPSC beams are presented in Table 1.

Four series of OPSC beam specimens were tested to take account of the considering the variables; effective depth, steel ratio, concrete strength, and shear span. All beams were loaded with two point loads on the top surface and supported at both ends (Figure.1).

Experimental Setup

Figure 1 shows the setup of the experimental works. Four number of steel rods were used during the tests, of which two were positioned under the spreader beam to transfer vertical load from the load hydraulic jack, and the other two were used as roller supports at both ends. The load was applied using hand operated hydraulic jack. The load increments were limited to 10 bars (4.21 kN) until failure occurred. Tests on OPSC beams were conducted at an age range from 30 to 60 days.

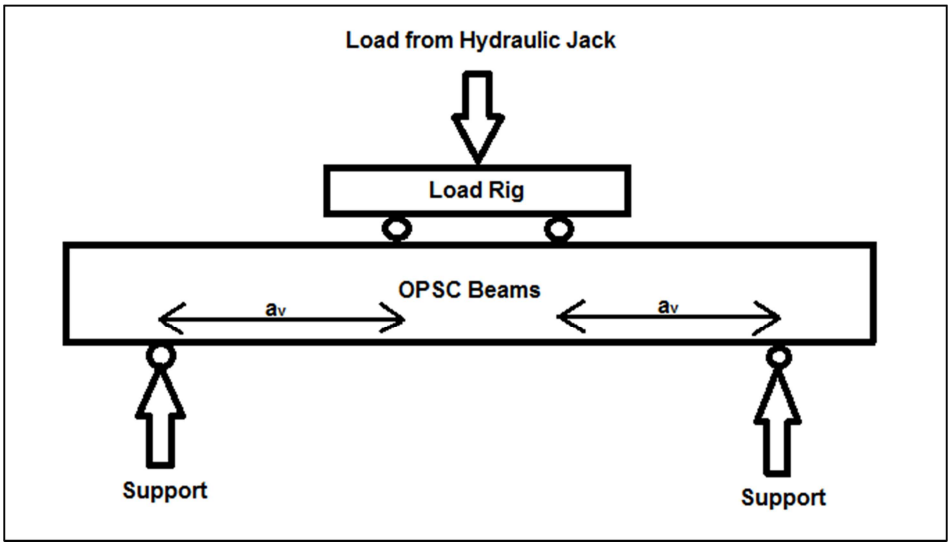

Fig. 1 Experimental Setup For OPSC Beams Experiment

Results and Discussion

The test results as well as its comparisons with the predictions from code of practice [7, 8] are presented in Table 1. The codes' predictions (V_{EC2}& V_{BS8110}) shown in Table 1 were derived so as for a non-shear reinforced NWC beam with the material factor taken as unity.

Table 1 Beam Details and Test Results of Non-shear Reinforced OPSC Beams

Specimen	ρ (%)	b (mm)	h (mm)	d (mm)	a_v/d	f_{ck} (N/mm^2)	V_{Test}	V_{EC2}	V_{BS8110}	V_{Test}/V_{BS8110}	V_{Test}/V_{EC2}
S1	0.91	102	200	170	2.50	27.86	21.05	12.85	18.33	1.15	1.64
S2	2.36	102	200	167	2.50	28.96	36.64	15.45	25.22	1.45	2.37
H1	2.49	102	153	121	2.64	25.97	38.95	11.98	19.45	2.00	3.25
H2	2.22	102	313	278	2.10	25.97	52.53	26.29	34.90	1.51	2.00
AD1	2.36	102	200	167	1.00	25.60	58.19	12.11	48.41	1.20	4.81
AD2	2.36	102	200	167	3.00	25.60	32.33	16.15	24.20	1.34	2.00
F1	2.36	102	200	167	2.50	25.97	32.67	16.23	24.32	1.34	2.01
F2	2.36	102	200	167	2.50	32.08	47.41	17.41	26.09	1.82	2.72

Notation:

b =Breadth of beam
h = Height of beam
d = Effective depth of beam
a_v/d = Shear span to effective depth ratio
ρ(%) = Longitudinal steel ratio in percentage
f_{ck}= Concrete cylinder compressive strength
V_{Test} = Shear strength test results from OPSC beams
V_{EC2} = Shear strength Predictions from Eurocode 2
V_{BS8110} = Shear strength Predictions from BS8110

In general, it was observed that beam specimens having $a_v/d<2.5$ failed in a sudden rapture mode of shear failure (Figure2) while those having $a_v/d >2.5$ (AD2) failed in diagonal tension shear failure taken place in a mode with some signs of failure (Figure 3).

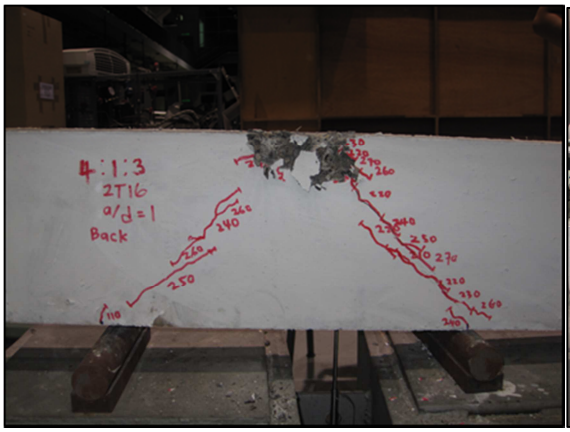

Fig. 2 Beam AD1 (Beam of av/d=1.0)

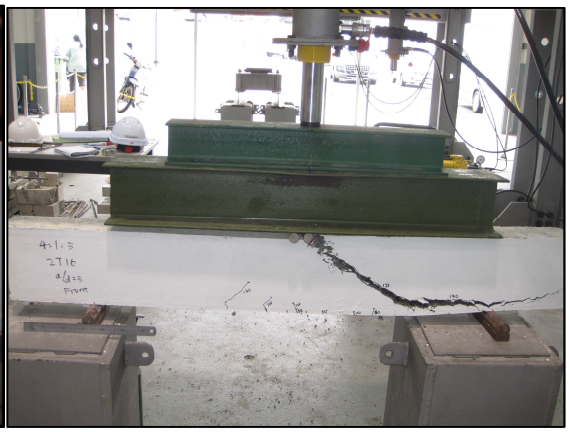

Fig. 3 Beam AD2 (Beam of av/d=3)

It was observed that shear compression failure mechanism occurs in beam specimens having applied loads positioned closely to the supports (Figure 2). This type of shear failure consist of diagonal shear cracks that couple with crushing of concrete in the top of the compression zone.

For diagonal tension shear failure, it was observed that the shear cracks usually propagated from the tensile zone to compressive zone within the shear span. The formation of fine diagonal shear cracks was observed at about 75% of the failure loads; these cracks initiated from very fine cracks, widen as the applying loads increases, and became dominant prior to failure.

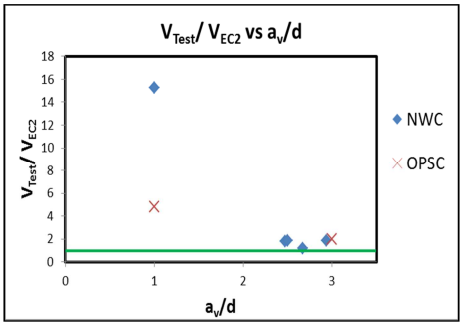

Fig. 4 VTest/VEC2 vs av/d

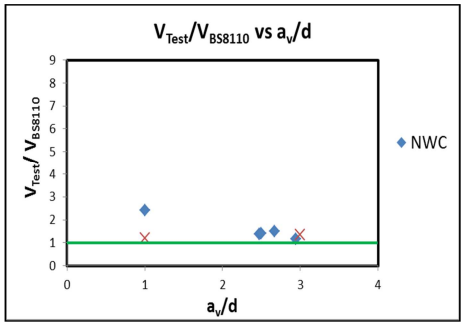

Fig. 5VTest/VBS8110 vs av/d

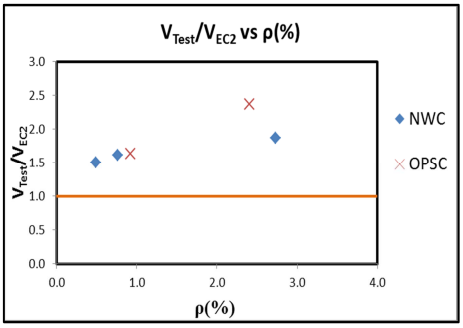

Fig. 6 VTest/VEC2 vs ρ(%)

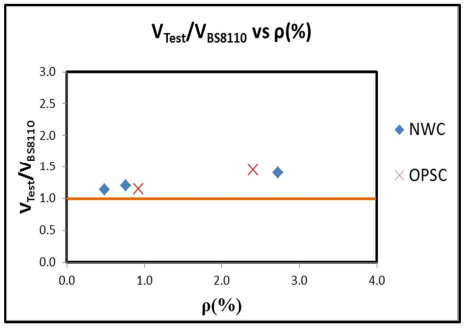

Figure 7:VTest/VBS8110 vs ρ(%)

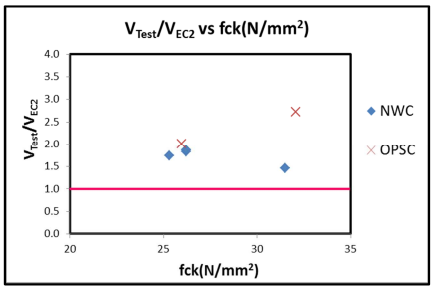

Fig. 8 V_{Test}/V_{EC2} vs fck(N/mm^2)

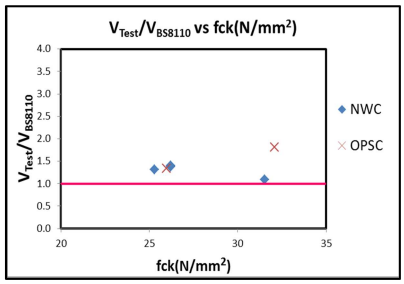

Fig. 9 V_{Test}/V_{BS8110} vsfck(N/mm^2)

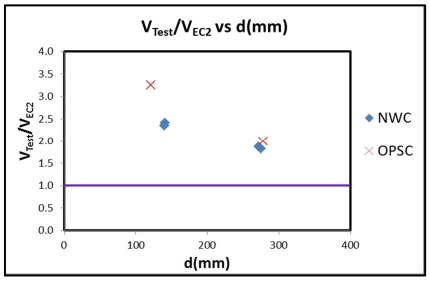

Fig. 10: V_{Test}/V_{EC2} vs d(mm)

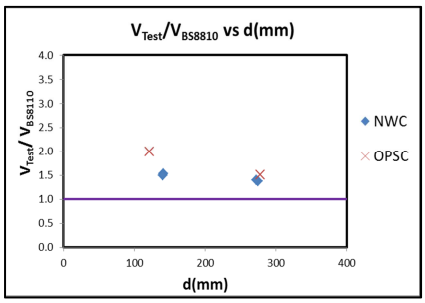

Fig. 11:V_{Test}/V_{BS8110} vs d(mm)

Comparisons between NWC beams [6] and OPSC beams with respect to various variables are presented in the current paper (Figures 4 to 11). The NWC beams [6] were chosen because of its similarity indetails to the specimens used in the current research; beam size, compressive strength, steel ratio, and shear span. Although the shear strengths of the OPSC beams are similar in nature to those of NWC beams [6], some variations were foundto be evidenced from these comparisons. Further comparisons between the codes of practice [7, 8] indicating the prediction derives from EC2 [7] are conservative with respect to those derives from BS8110 [8].

In Figures 4 &5, comparisons between the test results of OPSC beams and NWC beams were carried out to study the effects of shear span, a_v/d, to the ultimate shear resistance. It can be noted that EC2 [7] underestimate the increase of shear strengths resulting from the decrease of shear span. However, it is also observed that the increments in shear strength are more profound in NWC beams than that of OPSC beams.

In Figures 6 &7, emphasis was on the effects of flexural reinforcement, ρ, to shear strengths. It can be noted that both codes [7, 8] underestimate the increase of shear strength resulting from the increase of flexural reinforcement. Comparisons between the codes [7, 8] indicate the conservativeness being more profound in EC2 [7] with respect to BS8110 [8].

In Figures8 &9, emphasis was on the effects of concrete strength, f_{ck}, to shear strengths. It can be noted that both codes [7, 8] are conservative, with the conservativeness being more profound in EC2 [7]. Further comparisons indicate the OPSC beams can produce higher shear strength resulting from the increase of concrete strength with respect to those found in NWC beams [6].

In Figures10 &11, emphasis was on the effects of effective depth, d, to shear strengths. It can be noted that both codes [7, 8] are conservative and underestimate the increase of shear strength resulting from the decrease of effective depth. Comparisons between the codes [7, 8] indicate the conservativeness being more profound in EC2 [7] with respect to BS8110 [8].

Conclusions

The findings from current research indicate positive results for the use of OPS as coarse aggregate in reinforced concrete beams with respect to shear mechanism. Test results confirmed the shear strength of OPSC beamsare comparable to that found in the NWC beams [6]. Comparative studies with the current design clauses [7, 8]indicateconservativeness in the prediction of shear resistances for OPSC beam. In general, it is concluded that OPS can be used as an alternative to replace the conventional coarse aggregates in reinforced concrete construction.

References

[1] H.B.Basri, M.A.Mannan, M.F.M Zain,"*Concrete Using Waste OPS as Aggregates"*, Cement and Concrete Research, 29, 619-622, 1999.

[2] M.A.Mannan, C. Ganapathy, "*Mix Design of Oil Palm Shell Concrete"*, Cement and Concrete Research, 31, 1323-1325, 2001.

[3] M.A.Mannan, C. Ganapathy,"*Engineering Properties of Concrete with OPS as Coarse Aggregate"*, Construction and Building Materials,16, 29-34, 2001.

[4] D.C.L. Teo,M.A.Mannan, V.J. Kurian,"*Structural Concrete Using Oil Palm Shell as Lightweight Aggregate",* Turkish J. Eng. Env. Sci, 251-257, 2006.

[5] U.J. Alengaram, M.Z. Jumaat, H.Mahmud,"*Shear behaviour of reinforced palm kernel concrete beams",* Construction and Building Materials, 25, 2918-2927, 2011.

[6] Kani, G.N.J,"*How safe are our large reinforced concrete beams*?", ACI J, 64(3), 129-141, 1967.

[7] Eurocode 2: "*Design of Concrete Structure, Part 1-1 General Rules and Rules for Buildings"*, 85-86, 2004.

[8] British Standard 8110: *Part 1-Structural Use of Concrete,"Code of Practice for Design and Construction"*, 28-30, 1997.

doi:10.4028/www.scientific.net/AMR.587.144

Effects of Fibre on Drying Shrinkage, Compressive and Flexural Strength of Lightweight Foamed Concrete

Hanizam Awang[1,a], Md Azree Othuman Mydin[2,b] and Ahmad Farhan Roslan[3,c]

[1,2,3]School of Housing, Building and Planning, Universiti Sains Malaysia, 11800 Penang, Malaysia.

[a]hanizam@usm.my, [b]azree@usm.my, cafr11_hbp118@student.usm.my

Keywords: Lightweight foamed concrete; fibre; compressive strength; flexural strength; drying shrinkage.

Abstract. The present study covers the use of fibre in lightweight foamed concrete (LFC) to produce the lightweight concrete for use in construction of non-load bearing elements. LFC with 600, 1000 and 1400 kg/m^3 density were cast and tested. Polypropylene fibres with different percentage were used into LFC and the resulting products were compared to normal LFC. Compressive strength, flexural strength and drying shrinkage tests were carried out to evaluate the mechanical properties up to 180 days. The addition of fibres in LFC showed no contribution on compressive strength but improvement in the flexural and shrinkage test results.

Introduction

Lightweight foamed concrete (LFC) is usually made from mixing stable foam to slurry of mortar. This action incorporates small-enclosed air bubbles within the mortar thereby making it lighter and possessing special properties such as low thermal conductivity and high fire resistance. In foamed concrete mortar, the bubbles (typically 0.3-0.4 mm in diameter) provide the stability of the LFC. LFC may have densities ranging from as low as 500 kg/m^3 to as high as 1600 kg/m^3. The application of LFC is limited to lightweight partition and secondary structural elements [1].

The compressive strength of LFC is moderately low and it would be beneficial if this property can be improved. One possibility is by way of addition of fibers in the mix. Fiber offers very promising technical and economical possibilities in fiber optimization. It is known from the previous studies that the inclusion of fibers in a cement mortar can result in increased of compressive strength [2]. Raju et al. [3] also found that the cube compressive strength of concrete increased linearly with the addition of fibers.

Normal concrete reinforced with less than 2% of volume content of steel fibres provides better properties compared to normal concrete, especially the improvement of toughness [4,5]. Similarly applied to LFC it is expected that the fiber would contribute to the enhancement of load carrying capacity of the material by shear deformation at the fiber - matrix interface thereby contributing to increased strength. It was also reported by Sanjuan and Moragues [6] that shrinkage and differential settlement can be inhibited or prevented effectively by using fiber reinforcement.

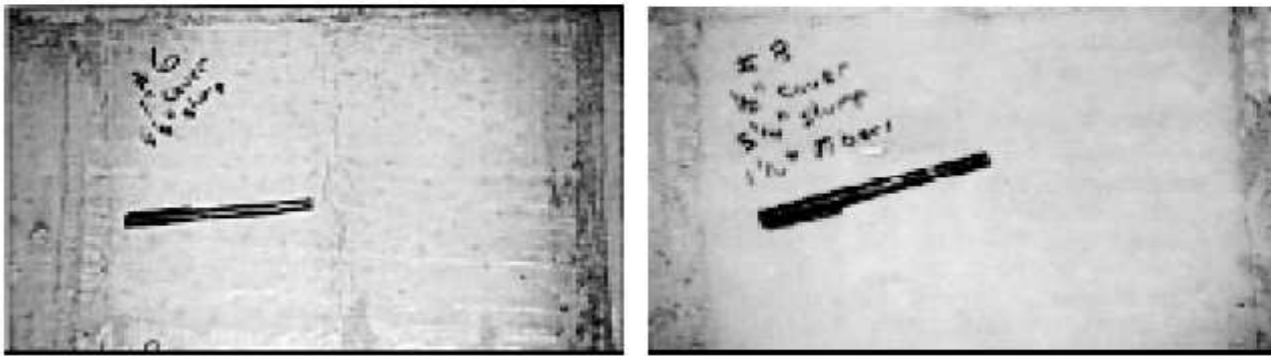

(a) fibre-free concrete (b) fibres concrete

Figure 1. Effect of fibre in concrete on crack progression

Chopped polypropylene fibers of 12 mm length in the dosage range of 1–3 kg/m^3 has been reported to enhance the shear behaviour of LFC equivalent to that of normal concrete. In addition, the usage of fibers is reported to alleviate brittleness, whilst reducing its weight and cost as well [7]. Research conducted by Parikh [8[shown that the inclusion of polypropylene fibres in concrete can stop the crack progression. Figure 1(a) shows a typical subsidence crack in fibre-free concrete. All specimens that didn't contain synthetic fibres cracked in this manner. But there were no subsidence cracks in the fibres concrete specimens as shown in Figure 1(b).

This study will focus on the effects of the fibre not only on the compressive strength but also on flexural and shrinkage of LFC of different densities.

Materials and Mixture Proportions

i) Portland Cement SEM1 and Fine Aggregates.

Portland Cement SEM1 was used for the experiment. The fine aggregate used was natural sand that was obtained from a local riverbed. A sieve analysis was carried out to see the suitability of the sand to be used and the percentage passing 5 mm sieve size. The sand falls in zone 3 in accordance with British Standard BS 882: Part 2: 1973. Norizal [9] mentioned that the appropriate size of fine aggregate used should be between 0 to 2 mm. In addition, 20% of the total quantity of sand used should preferably be of size less than 0.5 mm. Figure 2 shows the particles sizes distribution of the river sand used in this study. A constant of cement to sand ratio of 1: 1.6 was used for all bathes of LFC. The dry mix (cement and sand) was blended with water which had been fixed using a water-to-cement ratio of 0.45. The 0.45 water cement ratio was found acceptable to achieve adequate workability [10].

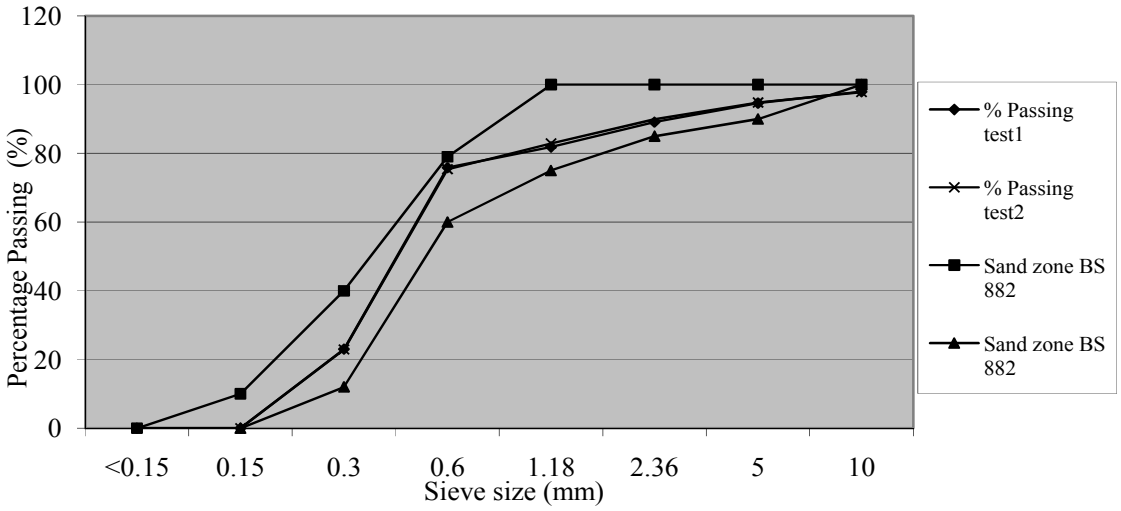

Figure 1 : Particles Size Distribution of Sand

ii) Stable Foam.

The stable foam used was protein-based (Noraite PA-1) surfactant with unit weight of between 70 to 80 gram/litre. The stable foam was produced using foam generator portafoam (Portafoam PM-2) system. A foam generator is used to generate stable aqueous foam for the production of foam concrete. The air pores are introduced by agitating air with a foaming agent diluted with water. Dilution rate for Noraite PA-1 has been set to 1:33 (one part of surfactant to 33 parts of water) by its manufacturer and has to adhere strictly in order to obtain the desired quality of foam output.

iii) Mega Mesh Polypropylene Fibre.

The fibre used in this study was Mega Mesh polypropylene fibre. Polypropylene fibre is a fibrillated fibre made of polypropylene specifically engineered and manufactured in accordance to ISO9001 certified facility. Each fibre provides maximum anchorage to increase their resistance to pull-out with its specific three dimensional planes. Properties of the fibres are shown in Table 1.

Table 1: Physical and Mechanical Properties of Mega Mesh polypropylene fibre

Characteristic	**Material Properties**
Material	Polypropylene
Colour	White
Length	12 mm
Thermal Conductivity	Low
Electrical Conductiviry	Low
Chemical Stability	Non-reactive
Absorption	None
Tensile Strength	45-60 ksi (0.31-0.42kN/mm^2)
Modulus of Elesticity	0.5 x 10 ksi (3.5kN/mm^2)
Specific Gravity	0.9
Youngs Modulus	8.2 GPa
Melt Point	160-170°C
Ignition Point	590° C

Experimental Programs

Nine different LFC mixes were prepared. The mixture proportions and fresh properties of the concrete mixtures produced in experimental are shown in Table 2. LFC samples of three densities of 600, 1000 and 1400 kg/m^3 were cast and tested for fresh and mechanical properties test. The types of mixtures produced, which were normal LFC, with fibre contents of 0.2% and 0.4%, An average of three samples was used for each mix to test the named parameters. From each LFC mixture, tests were conducted on the fresh concrete to determine slump. The information in table 3 shows the result of the slump test. It is important to achieve slump in a range of 23 to 27mm. 100 mm cubic specimens were cast for the determination of compressive strength, 100mm x 100mm x 500mm for flexural strength and drying shrinkage tests. The test specimens were left to stand for 24 hours, after which they were demould and immersed in the water for curing purpose.

Table 2: Specimens and mix proportions

Sample	Sample reference	Composition of mixture			Dry density (kg/m^3)	Wet density (kg/m^3)	Foam volume (m^3)	Slump (mm)	Percentage of porosity (%)
		Cement (kg)	Sand (kg)	Water (kg)					
Normal LFC	NF-A	15.32	22.97	6.89	600	700	0.050	25	69.49
0.20 % fiber	PF20-A	15.32	22.97	6.89	600	700	0.048	25	69.81
0.40 % fiber	PF40-A	15.32	22.97	6.89	600	710	0.046	25	70.52
Normal LFC	NF-B	25.15	37.73	11.32	1000	1105	0.037	23	49.02
0.20 % fiber	PF20-B	25.15	37.73	11.32	1000	1085	0.035	26	54.14
0.40 % fiber	PF40-B	25.15	37.73	11.32	1000	1070	0.032	25	56.60
Normal LFC	NF-C	42.49	63.73	19.12	1400	1500	0.029	25	35.82
0.20 % fiber	PF20-C	42.49	63.73	19.12	1400	1480	0.028	25	35.62
0.40 % fiber	PF40-C	42.49	63.73	19.12	1400	1510	0.029	25	35.34

Test Results and Discussion

i. Compression Strength.

Figure 3 shows the results of compressive strength with different densities. The compressive strength tests were carried out up to 180 days. It was shown that, the present of fibres does not contribute to the strength development of the LFC at higher density. Based on the results,

polypropylene fibre gives good results in compressive strength for low density of LFC. Adding polypropylene fiber to the LFC of lower densities (600 kg/m^3) gives good results in compressive strength compared to the higher densities (1000 kg/m^3 and 1400 kg/m^3 respectively). The compressive strength of LFC (density of 600 kg/m^3) with 0.2% and 0.4% fibre has increased by 17% and 35% respectively at 28 days. The compressive strength continuously increased by 44% and 54% at 60 days, after which there is a tendency for the strength to be reduced at 180 days. On the other hand, at the higher densities, fibres do not contribute to the strength of LFC. The compressive strength obtained has been observed to decrease by 15-25%, due to the characteristics of polypropylene fibre as hydrophobic material, which retains water. Water that has been retained in the mix will affect the strength as it will create more voids. Amount of fiber will obstruct the voids which will cause weak bonding between the matrix. More addition of fiber will increase porosity and voids thus lowered the density of LFC slightly. This will affect the strength of LFC at the same time.

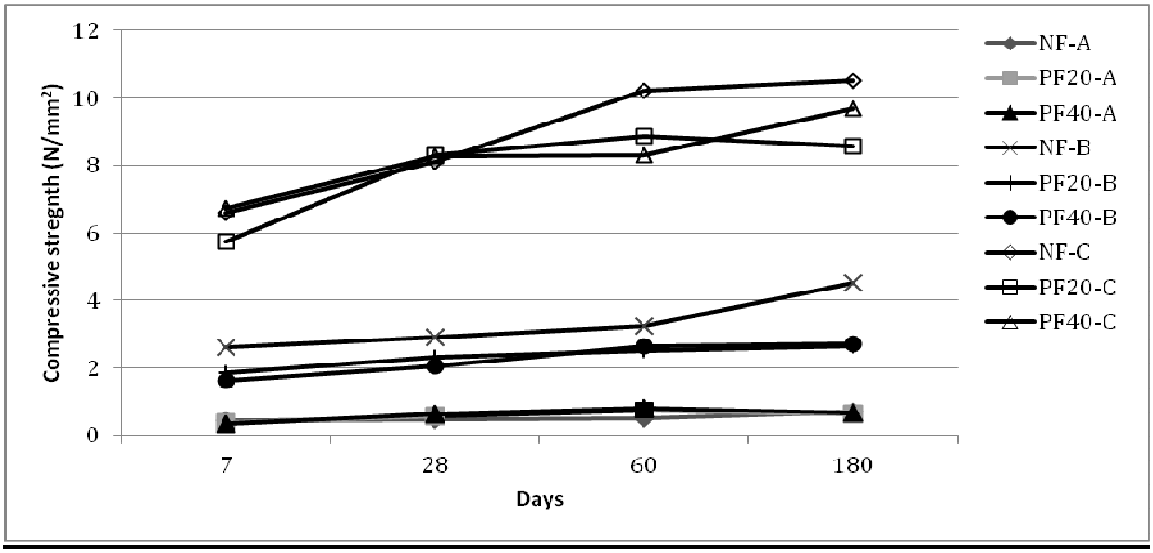

Figure 3: Compressive strength at different densities

ii. Flexural Strength.

The flexural strength development from day-7 to day-180 for all the mixes having densities of 1000 kg/m^3 and 1400 kg/m^3. Flexural strength tests indicated that the fibres are capable to resist bending stress, which was influenced by inter-particle bonding characteristics in the microstructures. Figure 4 shows mixes that obtained ultimate flexural strength in the vicinity of 0.7 MPa to 2.71 MPa. It is observed that flexural strength development is generally similar with the compressive strength development for most mixes.

Flexural strength tests at 28 days showed that PF20-B and PF40-B obtained 0.85 MPa and 0.95 MPa respectively, an achievement of 18% and 32% higher than that of the control mix. Similar flexural strength development pattern also was noticed for the samples NF-C, PF20-C and PF40-C. The test results revealed that higher rate of enhancement achieved in the first 7 days and from 28 days to 60 days. The percentage increased was between 15-25%. However, from Figure 4, there are evidences of strength retardation in the periods after 60 days onwards. It could therefore be deduced that, apart from inter-particle bonding, dry density could also affect flexural strength performances.

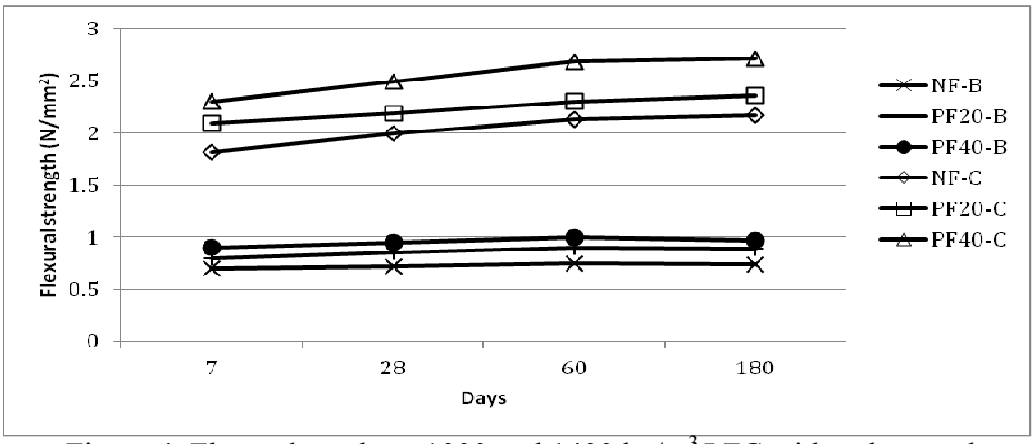

Figure 4: Flexural result on 1000 and 1400 kg/m^3 LFC with polypropylene fiber

iii. Shrinkage.

The drying shrinkage tests were carried out under air-curing conditions of 31± 3^{0}C and 55 ± 5 % humidity. The expansions of all test specimens, during first days, are due to the curing and immersing in water to saturate the specimens. After the LFC leaves the water curing, it has very higher content of water, and most voids are completely filled with water. This contributes the LFC to expand. The variation in weight or moisture content of the specimens is due to the variations in the relative humidity in the local climate. It can be seen in Figure 5, the addition of polypropylene fibers to the foam concrete also has a significant effect on the shrinkage of foam concrete. The effect of polypropylene fibers increases significantly with the increase of density of LFC.

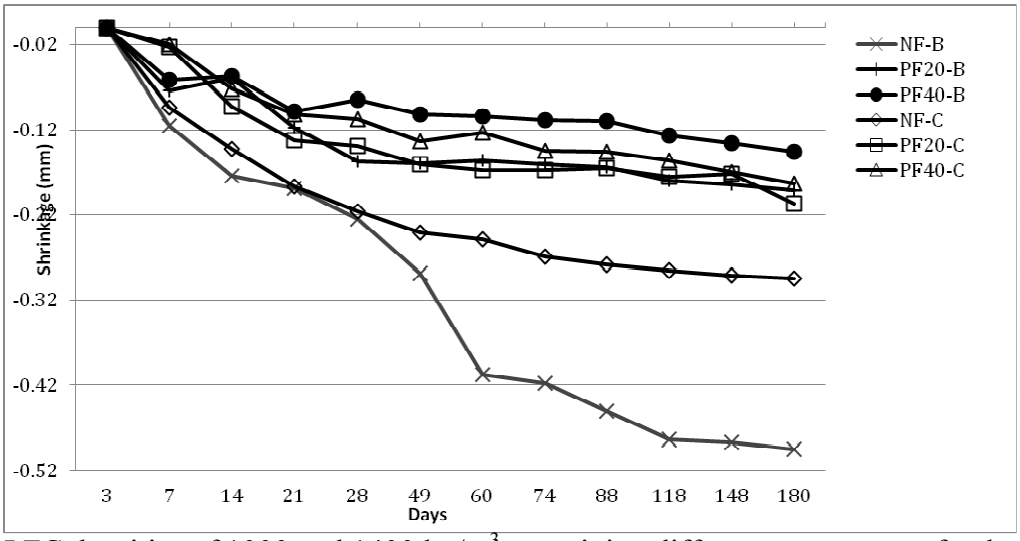

Figure 5: LFC densities of 1000 and 1400 kg/m^3 containing different percentage of polypropylene fiber on shrinkage

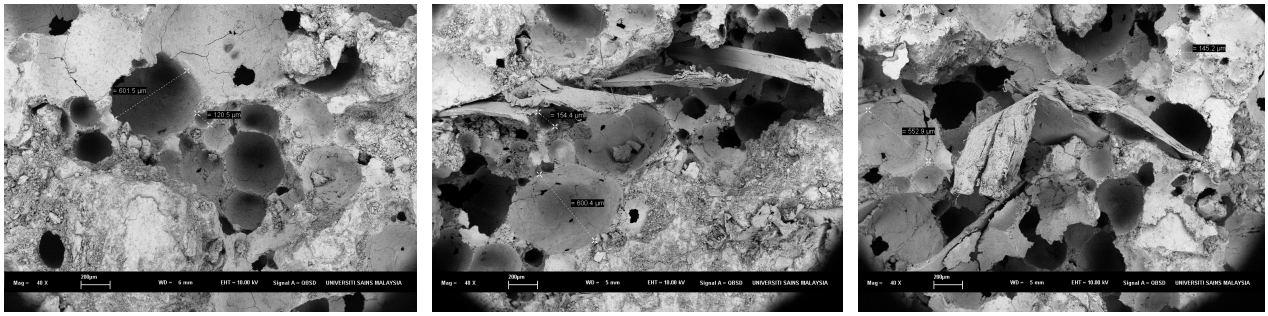

(a) normal LFC (b) LFC with 0.2% fibre (c) LFC with 0.4% fibre

Figure 6: Addition of fibers result in production of pore and cavities that surround area of fibre

iv. Microstructure.

Based on the observations done using the light microscope, the formation of the microstructure can be obviously seen for comparison in different percentage. Each percentage has a different type of microstructure formation. Figure 6 shows the formation of microstructure with a density of 1000 kg/m^3. It can be seen that, the higher percentage of fibre (0.4%) produces more pores and voids compared to concrete with 0.2 % of fibre and normal LFC. The pores produced with higher percentage of fibre were larger than those found in 0.2% fibre and normal LFC. It can be suggested that area of matrix surface will influence the connection between each pore. The size of the pores has also been affected as a large amount of the pores merged with each other thus creating larger sized pores. Inadequate surface area connects the pores and voids leading to a weak cell structure in the LFC. Therefore, the surface area of the matrix becomes stiff and the connection of pores and voids becomes weak.

Conclusion

The use of polypropylene fibre gives good results in strength for low density when compared to high density LFC. As polypropylene fibre will produce more pores and voids, it will affect the strength of high density concrete. Compared to low density concrete, more pores are produced than high density concrete. Therefore, the production of pores by adding fibre inside the mix is limited due to existing formation of pores inside low density LFC. Fiber has less influence on the compressive strength but resulted in an increase in the tensile strength of LFC.

Acknowledgements

The authors thankfully acknowledge financial support for this research granted by Universiti Sains Malaysia under USM RU Grant (Ref. No. 1001 / PPBGN / 814073).

References

[1] Sabarudin,M., Chee, K.W., and Lim, P.Y. Development of Artificial Lightweight Aggregates, *Annual Bulletin*, Institution of Engineers Malaysia. (2000)

[2] Swamy, R.N. and Mangat, P.S. *Cem. Concr. Res*. 4(3), (1974), p.451

[3] Raju,N.K., Basavarajaiah, B.S. and Rao, K.J. *Indian Concr. J*. 51(6), (1977), p.183 -191

[4] Chen, B., Liu, J. Contribution Of Hybrid Fibers On The Properties Of The High Strength Lightweight Concrete Having Good Workability. Cement and Material Research. 35 (2005). 913 – 917.

[5] Jones, M. R. & Mccarthy, A. Preliminary views on the potential of foamed concrete as a structural material. *Magazine of concrete research* 57**,** (2005), 21-31.

[6] Sanjuán, M.A and Moragues, A, Polypropylene-fibre-reinforced mortar mixes: optimization to control plastic shrinkage, Composites Science and Technology 57, Issue 6, (1997), Pages 655-660

[7] Ramamurthy, K., Kunhanandan Nambiar, E.K. and Indu Siva Ranjani, G. A classification of studies on properties of foam concrete. Cement & Concrete Composites (**31**), (2009). 388-396.

[8] Parikh, K., Fibres in concrete, The Indian Concrete Journal. (2003)

[9] Noordin, M.N., Development of a lightweight concrete wall panel system. PhD Thesis, Universiti Sains Malaysia. (2000)

[10] Awang, H., Noordin, M.N., Ismail, M.R., Hussein Al-Haidary, M.H.M. Properties of Hardened foam concrete. Proceeding of 4th. International Conference on Built Environment in Developing Countries 2010. (2010), pp 1013-1021

Keywords Index

Authors Index